


University of Alberta

Nucleoside Dicarboxylates as Mimics of Diphosphates and Disulfide Bond Replacement
in Pediocin PA-1

by

Marc A. Boudreau 

A thesis submitted to the Faculty of Graduate Studies and Research in partial fulfillment
of the requirements for the degree of
Doctor of Philosophy

Department of Chemistry

Edmonton, Alberta

Fall 2007



Library and
Archives Canada

Bibliothèque et
Archives Canada

Published Heritage
Branch

Direction du
Patrimoine de l'édition

395 Wellington Street
Ottawa ON K1A 0N4
Canada

395, rue Wellington
Ottawa ON K1A 0N4
Canada

Your file *Votre référence*
ISBN: 978-0-494-32923-8
Our file *Notre référence*
ISBN: 978-0-494-32923-8

NOTICE:

The author has granted a non-exclusive license allowing Library and Archives Canada to reproduce, publish, archive, preserve, conserve, communicate to the public by telecommunication or on the Internet, loan, distribute and sell theses worldwide, for commercial or non-commercial purposes, in microform, paper, electronic and/or any other formats.

The author retains copyright ownership and moral rights in this thesis. Neither the thesis nor substantial extracts from it may be printed or otherwise reproduced without the author's permission.

AVIS:

L'auteur a accordé une licence non exclusive permettant à la Bibliothèque et Archives Canada de reproduire, publier, archiver, sauvegarder, conserver, transmettre au public par télécommunication ou par l'Internet, prêter, distribuer et vendre des thèses partout dans le monde, à des fins commerciales ou autres, sur support microforme, papier, électronique et/ou autres formats.

L'auteur conserve la propriété du droit d'auteur et des droits moraux qui protègent cette thèse. Ni la thèse ni des extraits substantiels de celle-ci ne doivent être imprimés ou autrement reproduits sans son autorisation.

In compliance with the Canadian Privacy Act some supporting forms may have been removed from this thesis.

Conformément à la loi canadienne sur la protection de la vie privée, quelques formulaires secondaires ont été enlevés de cette thèse.

While these forms may be included in the document page count, their removal does not represent any loss of content from the thesis.

Bien que ces formulaires aient inclus dans la pagination, il n'y aura aucun contenu manquant.


Canada

ABSTRACT

The synthesis of a series of nucleoside dicarboxylates (maleates and succinates) and their biological evaluation against nucleoside diphosphate (NDP) kinase, the enzyme responsible for the phosphorylation of nucleoside diphosphates to their corresponding triphosphates, is first described. Efforts towards preparing analogues with an ether or a thioether linkage to the dicarboxylate moiety focused on the 1,4-addition to various esters of acetylenedicarboxylic acid. In all cases, the final step involving several different deprotection strategies failed to afford any of the desired products.

Various strategies were explored for the synthesis of the analogues containing methylene spacers. Approaches involving the treatment of dimethyl acetylenedicarboxylate (**46**) with nucleoside-derived organocuprates were unsuccessful. Other strategies employing modified Stille conditions for alkyl bromides containing β -hydrogens, or the photolysis of diacyl peroxides, also failed to provide any of the desired products.

The final approach involved olefin cross metathesis to attach the dicarboxylate portion to the nucleoside. Although access to dimethyl 2-(3-((3*aR*,4*R*,6*R*,6*aR*)-6-(2,4-dioxo-3,4-dihydropyrimidin-1(2*H*)-yl)-2,2-dimethyltetrahydrofuro[3,4-*d*][1,3]dioxol-4-yl)allyl)maleate (**148**) was possible using this methodology, selective reduction of its 5',6'-double bond could not be achieved.

In a revised strategy, the 5',6'-double bond was reduced prior to formation of the maleate, which was later accessed *via* a Horner-Emmons-Wadsworth (HEW) reaction between methyl diethylphosphonoacetate (**163**) and an α -keto ester. Using this approach, the uridine maleates lithium 1-((2*R*,3*R*,4*S*,5*R*)-5-((*Z*)-3,4-dicarboxylatobut-3-enyl)-3,4-

dihydroxytetrahydrofuran-2-yl)-2,4-dioxo-2,4-dihydro-1*H*-pyrimidin-3-ide (**182**), lithium 1-((2*R*,3*R*,4*S*,5*R*)-5-((*Z*)-4,5-dicarboxylatopent-4-enyl)-3,4-dihydroxytetrahydrofuran-2-yl)-2,4-dioxo-2,4-dihydro-1*H*-pyrimidin-3-ide (**188**), and lithium 1-((2*R*,3*R*,4*S*,5*R*)-5-((*Z*)-5,6-dicarboxylatohex-5-enyl)-3,4-dihydroxytetrahydrofuran-2-yl)-2,4-dioxo-2,4-dihydro-1*H*-pyrimidin-3-ide (**193**) were obtained. Reduction of the maleates after the HEW reaction followed by deprotection gave the corresponding uridine succinates lithium 1-((2*R*,3*R*,4*S*,5*R*)-5-(3,4-dicarboxylatobutyl)-3,4-dihydroxytetrahydrofuran-2-yl)-2,4-dioxo-2,4-dihydro-1*H*-pyrimidin-3-ide (**200**), lithium 1-((2*R*,3*R*,4*S*,5*R*)-5-(4,5-dicarboxylatopentyl)-3,4-dihydroxytetrahydrofuran-2-yl)-2,4-dioxo-2,4-dihydro-1*H*-pyrimidin-3-ide (**201**), and lithium 1-((2*R*,3*R*,4*S*,5*R*)-5-(5,6-dicarboxylatohexyl)-3,4-dihydroxytetrahydrofuran-2-yl)-2,4-dioxo-2,4-dihydro-1*H*-pyrimidin-3-ide (**202**). None of the analogues inhibited NDP kinase at a concentration of 1 mM. The six dicarboxylate salts and their corresponding dimethyl diesters **180**, **186**, **191**, **196**, **197**, and **198** also exhibited no antimicrobial activity against several pathogenic bacteria at 20 µg/mL.

Several analogues of the type IIa bacteriocin pediocin PA-1 in which one of the disulfide bonds was replaced with amino acids capable of hydrophobic interactions were synthesized on solid phase and tested for their antimicrobial activity against *Listeria monocytogenes* ATCC 43256 and *Carnobacterium divergens* LV13. The analogues, 9,14-diallyl 31-butyl pediocin PA-1 (**211**), 9,14-dibenzyl 31-butyl pediocin PA-1 (**212**), 9,14-dipropyl 31-butyl pediocin PA-1 (**213**), and 24,44-diallyl 31-butyl pediocin PA-1 (**214**), were inactive against these strains.

ACKNOWLEDGEMENTS

I would like to acknowledge my research supervisor, Professor John C. Vederas, for his constant guidance, encouragement, and understanding. His enthusiasm for science, his commitment to promoting independent thought, and his role as an excellent mentor and teacher, command him the utmost respect and provide an environment in which scientific curiosity can thrive. The time spent in his group has undoubtedly prepared me for the journey ahead.

I would like to thank Drs. Steven Cobb and Viji Moorthie for their careful proofreading of this manuscript. I am thankful to past and present members of the Vederas group who have contributed to a positive work environment, and who have been an inspiration through their enthusiasm and dedication. In particular, I would like to thank Mike Pollard, Hanna Pettersson, and Steven Cobb for their friendship and for teaching me a bit about science, about life, and about myself. To all my other friends both in and out of the Chemistry Department, thank you for making my time here memorable. Thanks to Zhendong Li (summer student, 2006) for his assistance on the pediocin project. The dedicated support staff in the Department of Chemistry, especially those in analytical and spectral services, are acknowledged for their technical assistance.

I am grateful to Edward Ishiguro, Professor of Microbiology at the University of Victoria, for his constant belief in my abilities. Finally, I would like to thank my family, especially my parents, John and Brenda, for their love and encouragement. From a young age, they instilled in me the virtues of perseverance, independence, respect, and understanding. Without them, none of this would have been possible.

TABLE OF CONTENTS

CHAPTER 1. Synthesis and Biological Evaluation of Nucleoside Dicarboxylates as Potential Mimics of Nucleoside Diphosphates

INTRODUCTION	1
1. Nucleoside Diphosphate Kinase	1
1.1 Inhibitors of NDP Kinase	4
2. Replacement of Monophosphates and Diphosphates in the Design of Enzyme Inhibitors	6
2.1 Non-Hydrolyzable Mimics of Monophosphates	7
2.2 Non-Hydrolyzable Mimics of Diphosphates	10
2.3 Maleates and Succinates as Diphosphate Mimics	13
3. Project Objectives: Synthesis and Biological Evaluation of Nucleoside Dicarboxylates as NDP Kinase Inhibitors	18
RESULTS AND DISCUSSION	19
1. Synthesis of Nucleoside Dicarboxylates	20
1.1 Nucleoside Dicarboxylates Containing an Ether Linkage	21
1.2 Adenosine Dicarboxylates Containing a Thioether Linkage	26
1.3 Nucleoside Dicarboxylates Containing Methylene Spacers	30
2. Biological Evaluation of Uridine Dicarboxylates	63
2.1 NDP Kinase Inhibition Assay	63
2.2 Antimicrobial Assays	66

3. Conclusions and Future Work	66
CHAPTER 2. Replacement of the Cysteine Residues of Pediocin PA-1 with Amino Acids Capable of Hydrophobic Interactions	
INTRODUCTION	69
1. Bacteriocins as Alternatives to Conventional Antibiotics	69
1.1 Classification of Bacteriocins	70
2. Secondary Structure and Mechanism of Action of Class IIa Bacteriocins	71
2.1 Role of Disulfide Bonds in Class IIa Bacteriocins	76
3. Project Objectives: Synthesis and Biological Evaluation of Analogues of Pediocin PA-1 with Cysteine Residues Replaced by Amino Acids Capable of Hydrophobic Interactions	79
RESULTS AND DISCUSSION	82
1. General Strategy for Solid Phase Synthesis of Pediocin PA-1 Analogues	82
1.1 Choice of Resin	82
1.2 Use of Pseudoproline Dipeptides	84
2. Solid Phase Peptide Synthesis (SPPS) of Pediocin PA-1 Analogues	85
2.1 Synthesis of 9,14-Diallyl 31-Butyl Pediocin PA-1 (210)	85
2.2 Synthesis of 9,14-Dibenzyl 31-Butyl Pediocin PA-1 (211)	91
2.3 Synthesis of 9,14-Dipropyl 31-Butyl Pediocin PA-1 (212)	92
2.4 Synthesis of 24,44-Diallyl 31-Butyl Pediocin PA-1 (213)	93
3. Biological Evaluation of Pediocin PA-1 Analogues	95

CHAPTER 3. Experimental Procedures

1. General Procedures	100
1.1 Reagents, Solvents, and Solutions	100
1.2 Purification Techniques	101
1.3 Instrumentation for Compound Characterization	102
2. Nucleoside Dicarboxylates	103
2.1 Experimental Data for Compounds	103
Dimethyl 2-(((3 <i>aR</i> ,4 <i>R</i> ,6 <i>R</i> ,6 <i>aR</i>)-6-(2,4-dioxo-3,4-dihydropyrimidin-1(2 <i>H</i>)-yl)-2,2-dimethyltetrahydrofuro[3,4- <i>d</i>][1,3]dioxol-4-yl)methoxy)-fumarate (48a)	104
Dimethyl 2-(((3 <i>aR</i> ,4 <i>R</i> ,6 <i>R</i> ,6 <i>aR</i>)-6-(2,4-dioxo-3,4-dihydropyrimidin-1(2 <i>H</i>)-yl)-2,2-dimethyltetrahydrofuro[3,4- <i>d</i>][1,3]dioxol-4-yl)methoxy)-maleate (48b)	104
Dimethyl 2-(((2 <i>R</i> ,3 <i>S</i> ,4 <i>R</i> ,5 <i>R</i>)-5-(2,4-dioxo-3,4-dihydropyrimidin-1(2 <i>H</i>)-yl)-3,4-dihydroxytetrahydrofuran-2-yl)methoxy)maleate (50b)	105
Dibenzyl acetylenedicarboxylate (52)	106
Dibenzyl 2-(((3 <i>aR</i> ,4 <i>R</i> ,6 <i>R</i> ,6 <i>aR</i>)-6-(2,4-dioxo-3,4-dihydropyrimidin-1(2 <i>H</i>)-yl)-2,2-dimethyltetrahydrofuro[3,4- <i>d</i>][1,3]dioxol-4-yl)methoxy)-fumarate (53a)	107
Dibenzyl 2-(((3 <i>aR</i> ,4 <i>R</i> ,6 <i>R</i> ,6 <i>aR</i>)-6-(2,4-dioxo-3,4-dihydropyrimidin-1(2 <i>H</i>)-yl)-2,2-dimethyltetrahydrofuro[3,4- <i>d</i>][1,3]dioxol-4-yl)methoxy)-	

maleate (53b)	107
Dibenzyl 2-(((2 <i>R</i> ,3 <i>S</i> ,4 <i>R</i> ,5 <i>R</i>)-5-(2,4-dioxo-3,4-dihydropyrimidin-1(2 <i>H</i>)-yl)-3,4-dihydroxytetrahydrofuran-2-yl)methoxy)maleate (54b)	108
Di- <i>tert</i> -butyl 2-(((3 <i>aR</i> ,4 <i>R</i> ,6 <i>R</i> ,6 <i>aR</i>)-6-(2,4-dioxo-3,4-dihydropyrimidin-1(2 <i>H</i>)-yl)-2,2-dimethyltetrahydrofuro[3,4- <i>d</i>][1,3]dioxol-4-yl)methoxy)-fumarate (58a)	109
Di- <i>tert</i> -butyl 2-(((3 <i>aR</i> ,4 <i>R</i> ,6 <i>R</i> ,6 <i>aR</i>)-6-(2,4-dioxo-3,4-dihydropyrimidin-1(2 <i>H</i>)-yl)-2,2-dimethyltetrahydrofuro[3,4- <i>d</i>][1,3]dioxol-4-yl)methoxy)-maleate (58b)	109
<i>S</i> -(((3 <i>aS</i> ,4 <i>S</i> ,6 <i>R</i> ,6 <i>aR</i>)-6-(6-Amino-9 <i>H</i> -purin-9-yl)-2,2-dimethyltetrahydrofuro[3,4- <i>d</i>][1,3]dioxol-4-yl)methyl ethanethioate (63)	111
(((3 <i>aS</i> ,4 <i>S</i> ,6 <i>R</i> ,6 <i>aR</i>)-6-(6-Amino-9 <i>H</i> -purin-9-yl)-2,2-dimethyltetrahydrofuro[3,4- <i>d</i>][1,3]dioxol-4-yl)methyl methanethiol (64)	112
Dimethyl 2-(((3 <i>aS</i> ,4 <i>S</i> ,6 <i>R</i> ,6 <i>aR</i>)-6-(6-amino-9 <i>H</i> -purin-9-yl)-2,2-dimethyltetrahydrofuro[3,4- <i>d</i>][1,3]dioxol-4-yl)methylthio)but-2-enedioate (65)	113
Dimethyl 2-(((2 <i>S</i> ,3 <i>S</i> ,4 <i>R</i> ,5 <i>R</i>)-5-(6-amino-9 <i>H</i> -purin-9-yl)-3,4-dihydroxytetrahydrofuran-2-yl)methylthio)but-2-enedioate (66)	114
Dibenzyl 2-(((3 <i>aS</i> ,4 <i>S</i> ,6 <i>R</i> ,6 <i>aR</i>)-6-(6-amino-9 <i>H</i> -purin-9-yl)-2,2-dimethyltetrahydrofuro[3,4- <i>d</i>][1,3]dioxol-4-yl)methylthio)but-2-enedioate (67)	115
Dibenzyl 2-(((2 <i>S</i> ,3 <i>S</i> ,4 <i>R</i> ,5 <i>R</i>)-5-(6-amino-9 <i>H</i> -purin-9-yl)-3,4-dihydroxytetrahydrofuran-2-yl)methylthio)fumarate (68a)	117
Dibenzyl 2-(((2 <i>S</i> ,3 <i>S</i> ,4 <i>R</i> ,5 <i>R</i>)-5-(6-amino-9 <i>H</i> -purin-9-yl)-3,4-dihydroxytetrahydrofuran-2-yl)methylthio)maleate (68b)	117

(3a <i>S</i> ,4 <i>S</i> ,6 <i>R</i> ,6a <i>R</i>)-6-(2,4-Dioxo-3,4-dihydropyrimidin-1(2 <i>H</i>)-yl)-2,2-dimethyltetrahydrofuro[3,4- <i>d</i>][1,3]dioxole-4-carbaldehyde (72)	118
<i>N</i> -Phenyltriphenylphosphoranylidenesuccinimide (73)	119
1-((3a <i>R</i> ,4 <i>R</i> ,6 <i>R</i> ,6a <i>R</i>)-6-((<i>E</i>)-2,5-Dioxo-1-phenylpyrrolidin-3-ylidene)-methyl)-2,2-dimethyltetrahydrofuro[3,4- <i>d</i>][1,3]dioxol-4-yl)pyrimidine-2,4(1 <i>H</i> ,3 <i>H</i>)-dione (74)	120
(<i>E</i>)-Ethyl 3-((3a <i>R</i> ,4 <i>R</i> ,6 <i>R</i> ,6a <i>R</i>)-6-(6-amino-9 <i>H</i> -purin-9-yl)-2,2-dimethyltetrahydrofuro[3,4- <i>d</i>][1,3]dioxol-4-yl)acrylate (80)	121
Ethyl 3-((3a <i>R</i> ,4 <i>R</i> ,6 <i>R</i> ,6a <i>R</i>)-6-(6-amino-9 <i>H</i> -purin-9-yl)-2,2-dimethyltetrahydrofuro[3,4- <i>d</i>][1,3]dioxol-4-yl)propanoate (81)	122
3-((3a <i>R</i> ,4 <i>R</i> ,6 <i>R</i> ,6a <i>R</i>)-6-(6-Amino-9 <i>H</i> -purin-9-yl)-2,2-dimethyltetrahydrofuro[3,4- <i>d</i>][1,3]dioxol-4-yl)propan-1-ol (82)	122
<i>N</i> -Benzoyl- <i>N</i> -(9-((3a <i>R</i> ,4 <i>R</i> ,6 <i>R</i> ,6a <i>R</i>)-6-(3-hydroxypropyl)-2,2-dimethyltetrahydrofuro[3,4- <i>d</i>][1,3]dioxol-4-yl)-9 <i>H</i> -purin-6-yl)benzamide (83)	123
<i>N</i> -Benzoyl- <i>N</i> -(9-((3a <i>R</i> ,4 <i>R</i> ,6 <i>R</i> ,6a <i>R</i>)-6-(3-bromopropyl)-2,2-dimethyltetrahydrofuro[3,4- <i>d</i>][1,3]dioxol-4-yl)-9 <i>H</i> -purin-6-yl)benzamide (84)	124
(<i>E</i>)- 3-((3a <i>R</i> ,4 <i>R</i> ,6 <i>R</i> ,6a <i>R</i>)-6-(2,4-Dioxo-3,4-dihydropyrimidin-1(2 <i>H</i>)-yl)-2,2-dimethyltetrahydrofuro[3,4- <i>d</i>][1,3]dioxol-4-yl)acrylaldehyde (87)	125
3-((3a <i>R</i> ,4 <i>R</i> ,6 <i>R</i> ,6a <i>R</i>)-6-(2,4-Dioxo-3,4-dihydropyrimidin-1(2 <i>H</i>)-yl)-2,2-dimethyltetrahydrofuro[3,4- <i>d</i>][1,3]dioxol-4-yl)propanal (88)	126
3-((3a <i>R</i> ,4 <i>R</i> ,6 <i>R</i> ,6a <i>R</i>)-6-(2,4-Dioxo-3,4-dihydropyrimidin-1(2 <i>H</i>)-yl)-2,2-dimethyltetrahydrofuro[3,4- <i>d</i>][1,3]dioxol-4-yl)propanol (89)	127
3-((3a <i>R</i> ,4 <i>R</i> ,6 <i>R</i> ,6a <i>R</i>)-6-(3-(4-Methoxybenzyl)-2,4-Dioxo-3,4-dihydro-	

pyrimidin-1(2 <i>H</i>)-yl)-2,2-dimethyltetrahydrofuro[3,4- <i>d</i>][1,3]dioxol-4-yl)propanol (90)	128
1-((3 <i>aR</i> ,4 <i>R</i> ,6 <i>R</i> ,6 <i>aR</i>)-6-(3-Bromopropyl)-2,2-dimethyltetrahydrofuro[3,4- <i>d</i>][1,3]dioxol-4-yl)-3-(4-methoxybenzyl)pyrimidine-2,4(1 <i>H</i> ,3 <i>H</i>)-dione (91)	129
(<i>E</i>)-Methyl 3-((3 <i>aR</i> ,4 <i>R</i> ,6 <i>R</i> ,6 <i>aR</i>)-6-(6-amino-9 <i>H</i> -purin-9-yl)-2,2-dimethyltetrahydrofuro[3,4- <i>d</i>][1,3]dioxol-4-yl)acrylate (94)	130
Methyl 3-((3 <i>aR</i> ,4 <i>R</i> ,6 <i>R</i> ,6 <i>aR</i>)-6-(6-amino-9 <i>H</i> -purin-9-yl)-2,2-dimethyltetrahydrofuro[3,4- <i>d</i>][1,3]dioxol-4-yl)propanoate (95)	130
Methyl 3-((3 <i>aR</i> ,4 <i>R</i> ,6 <i>R</i> ,6 <i>aR</i>)-6-(6-(<i>tert</i> -butoxycarbonylamino)-9 <i>H</i> -purin-9-yl)-2,2-dimethyltetrahydrofuro[3,4- <i>d</i>][1,3]dioxol-4-yl)propanoate (96)	131
3-((3 <i>aR</i> ,4 <i>R</i> ,6 <i>R</i> ,6 <i>aR</i>)-6-(6-(<i>tert</i> -Butoxycarbonylamino)-9 <i>H</i> -purin-9-yl)-2,2-dimethyltetrahydrofuro[3,4- <i>d</i>][1,3]dioxol-4-yl)propanoic acid (97)	132
<i>tert</i> -Butyl 9-((3 <i>aR</i> ,4 <i>R</i> ,6 <i>R</i> ,6 <i>aR</i>)-6-(3-hydroxypropyl)-2,2-dimethyltetrahydrofuro[3,4- <i>d</i>][1,3]dioxol-4-yl)-9 <i>H</i> -purin-6-ylcarbamate (98)	133
<i>tert</i> -Butyl 9-((3 <i>aR</i> ,4 <i>R</i> ,6 <i>R</i> ,6 <i>aR</i>)-6-(3-bromopropyl)-2,2-dimethyltetrahydrofuro[3,4- <i>d</i>][1,3]dioxol-4-yl)-9 <i>H</i> -purin-6-ylcarbamate (99)	134
Dimethyl 2-(tributylstannyl)maleate (100)	135
1-((3 <i>aR</i> ,4 <i>R</i> ,6 <i>R</i> ,6 <i>aR</i>)-6-(3-Iodopropyl)-2,2-dimethyltetrahydrofuro[3,4- <i>d</i>][1,3]dioxol-4-yl)-3-(4-methoxybenzyl)pyrimidine-2,4(1 <i>H</i> ,3 <i>H</i>)-dione (108)	136
<i>tert</i> -Butyl 9-((3 <i>aR</i> ,4 <i>R</i> ,6 <i>R</i> ,6 <i>aR</i>)-6-(3-iodopropyl)-2,2-dimethyltetrahydrofuro[3,4- <i>d</i>][1,3]dioxol-4-yl)-9 <i>H</i> -purin-6-ylcarbamate (110)	137

3-((3 <i>aR</i> ,4 <i>R</i> ,6 <i>R</i> ,6 <i>aR</i>)-6-(3-(4-Methoxybenzyl)-2,4-dioxo-3,4-dihydro- pyrimidin-1(2 <i>H</i>)-yl)-2,2-dimethyltetrahydrofuro[3,4- <i>d</i>][1,3]dioxol- 4-yl)propanoic acid (117)	138
(<i>Z</i>)-5-Methoxy-3-(methoxycarbonyl)-5-oxopent-3-enoic acid (118)	139
Dimethyl 2-allylmalate (120)	139
(<i>E</i>)-Methyl 3-((3 <i>aR</i> ,4 <i>R</i> ,6 <i>R</i> ,6 <i>aR</i>)-6-(2,4-dioxo-3,4-dihydropyrimidin-1(2 <i>H</i>)- yl)-2,2-dimethyltetrahydrofuro[3,4- <i>d</i>][1,3]dioxol-4-yl)acrylate (121)	140
Methyl 3-((3 <i>aR</i> ,4 <i>R</i> ,6 <i>R</i> ,6 <i>aR</i>)-6-(2,4-dioxo-3,4-dihydropyrimidin-1(2 <i>H</i>)-yl)- 2,2-dimethyltetrahydrofuro[3,4- <i>d</i>][1,3]dioxol-4-yl)propanoate (122)	141
Methyl 3-((3 <i>aR</i> ,4 <i>R</i> ,6 <i>R</i> ,6 <i>aR</i>)-6-(3-(4-methoxybenzyl)-2,4-dioxo-3,4- dihydropyrimidin-1(2 <i>H</i>)-yl)-2,2-dimethyltetrahydrofuro[3,4- <i>d</i>][1,3]dioxol- 4-yl)propanoate (123)	142
2-Methoxypropan-2-yl peroxy-3-((3 <i>aR</i> ,4 <i>R</i> ,6 <i>R</i> ,6 <i>aR</i>)-6-(3-(4-methoxybenzyl)- 2,4-dioxo-3,4-dihydropyrimidin-1(2 <i>H</i>)-yl)-2,2-dimethyltetrahydrofuro- [3,4- <i>d</i>][1,3]dioxol-4-yl)propanoate (125)	143
3-((3 <i>aR</i> ,4 <i>R</i> ,6 <i>R</i> ,6 <i>aR</i>)-6-(3-(4-Methoxybenzyl)-2,4-dioxo-3,4-dihydro- pyrimidin-1(2 <i>H</i>)-yl)-2,2-dimethyltetrahydrofuro[3,4- <i>d</i>][1,3]dioxol-4- yl)peroxypropanoic acid (126)	144
3-((3 <i>aR</i> ,4 <i>R</i> ,6 <i>R</i> ,6 <i>aR</i>)-6-(3-(4-Methoxybenzyl)-2,4-dioxo-3,4-dihydro- pyrimidin-1(2 <i>H</i>)-yl)-2,2-dimethyltetrahydrofuro[3,4- <i>d</i>][1,3]dioxol-4- yl)propanoic pentanoic peroxyanhydride (129)	145
Dimethyl 2-(but-3-enyl)maleate (131)	146
Dimethyl-2-(3-oxopropyl)maleate (132)	147

(<i>Z</i>)-6-Methoxy-4-(methoxycarbonyl)-6-oxohex-4-enoic acid (133)	148
(<i>Z</i>)-6-Methoxy-4-(methoxycarbonyl)-6-oxohex-4-enoic 3-((3 <i>aR</i> ,4 <i>R</i> ,6 <i>R</i> ,6 <i>aR</i>)-6-(3-(4-methoxybenzyl)-2,4-dioxo-3,4-dihydropyrimidin-1(2 <i>H</i>)-yl)-2,2-dimethyltetrahydrofuro[3,4- <i>d</i>][1,3]dioxol-4-yl)propanoic peroxyanhydride (134)	149
Methyl 3-((3 <i>aR</i> ,4 <i>R</i> ,6 <i>R</i> ,6 <i>aR</i>)-6-(2,4-dioxo-3-((2-(trimethylsilyl)ethoxy)methyl)-3,4-dihydropyrimidin-1(2 <i>H</i>)-yl)-2,2-dimethyltetrahydrofuro[3,4- <i>d</i>][1,3]dioxol-4-yl)propanoate (136)	150
3-((3 <i>aR</i> ,4 <i>R</i> ,6 <i>R</i> ,6 <i>aR</i>)-6-(2,4-Dioxo-3-((2-(trimethylsilyl)ethoxy)methyl)-3,4-dihydropyrimidin-1(2 <i>H</i>)-yl)-2,2-dimethyltetrahydrofuro[3,4- <i>d</i>][1,3]dioxol-4-yl)propanoic acid (137)	151
2-Methoxypropan-2-yl peroxy-3-((3 <i>aR</i> ,4 <i>R</i> ,6 <i>R</i> ,6 <i>aR</i>)-6-(2,4-dioxo-3-((2-(trimethylsilyl)ethoxy)methyl)-3,4-dihydropyrimidin-1(2 <i>H</i>)-yl)-2,2-dimethyltetrahydrofuro[3,4- <i>d</i>][1,3]dioxol-4-yl)propanoate (138)	152
3-((3 <i>aR</i> ,4 <i>R</i> ,6 <i>R</i> ,6 <i>aR</i>)-6-(2,4-Dioxo-3-((2-(trimethylsilyl)ethoxy)methyl)-3,4-dihydropyrimidin-1(2 <i>H</i>)-yl)-2,2-dimethyltetrahydrofuro[3,4- <i>d</i>][1,3]dioxol-4-yl)peroxypropanoic acid (139)	153
(<i>Z</i>)-6-Methoxy-4-(methoxycarbonyl)-6-oxohex-4-enoic 3-((3 <i>aR</i> ,4 <i>R</i> ,6 <i>R</i> ,6 <i>aR</i>)-6-(2,4-dioxo-3-((2-(trimethylsilyl)ethoxy)methyl)-3,4-dihydropyrimidin-1(2 <i>H</i>)-yl)-2,2-dimethyltetrahydrofuro[3,4- <i>d</i>][1,3]dioxol-4-yl)propanoic peroxyanhydride (140)	154

1-((3a <i>R</i> ,4 <i>R</i> ,6 <i>R</i> ,6a <i>R</i>)-2,2-Dimethyl-6-vinyltetrahydrofuro[3,4- <i>d</i>][1,3]dioxol-4-yl)pyrimidine-2,4(1 <i>H</i> ,3 <i>H</i>)-dione (144)	155
Dimethyl 2-(3-((3a <i>R</i> ,4 <i>R</i> ,6 <i>R</i> ,6a <i>R</i>)-6-(2,4-dioxo-3,4-dihydropyrimidin-1(2 <i>H</i>)-yl)-2,2-dimethyltetrahydrofuro[3,4- <i>d</i>][1,3]dioxol-4-yl)allyl)maleate (147)	156
Dimethyl 2-(3-((2 <i>R</i> ,3 <i>S</i> ,4 <i>R</i> ,5 <i>R</i>)-5-(2,4-dioxo-3,4-dihydropyrimidin-1(2 <i>H</i>)-yl)-3,4-dihydroxytetrahydrofuran-2-yl)allyl)maleate (150)	157
<i>tert</i> -Butyl 3-((3a <i>R</i> ,4 <i>R</i> ,6 <i>R</i> ,6a <i>R</i>)-2,2-dimethyl-6-vinyltetrahydrofuro[3,4- <i>d</i>]-[1,3]dioxol-4-yl)-2,6-dioxo-2,3-dihydropyrimidine-1(6 <i>H</i>)-carboxylate (164)	157
Methyl 2-hydroxy-but-3-enoate (168)	158
Methyl 2-hydroxy-pent-4-enoate (170)	159
Methyl 2-benzyloxypent-4-enoate (171)	160
Methyl 2-oxohex-5-enoate (174)	161
<i>tert</i> -Butyl 3-((3a <i>R</i> ,4 <i>R</i> ,6 <i>R</i> ,6a <i>R</i>)-6-((<i>E</i>)-3-hydroxy-4-methoxy-4-oxobut-1-enyl)-2,2-dimethyltetrahydrofuro[3,4- <i>d</i>][1,3]dioxol-4-yl)-2,6-dioxo-2,3-dihydropyrimidine-1(6 <i>H</i>)-carboxylate (176)	161
<i>tert</i> -Butyl 3-((3a <i>R</i> ,4 <i>R</i> ,6 <i>R</i> ,6a <i>R</i>)-6-(3-hydroxy-4-methoxy-4-oxobutyl)-2,2-dimethyltetrahydrofuro[3,4- <i>d</i>][1,3]dioxol-4-yl)-2,6-dioxo-2,3-dihydropyrimidine-1(6 <i>H</i>)-carboxylate (177)	162
<i>tert</i> -Butyl 3-((3a <i>R</i> ,4 <i>R</i> ,6 <i>R</i> ,6a <i>R</i>)-6-(4-methoxy-3,4-dioxobutyl)-2,2-dimethyltetrahydrofuro[3,4- <i>d</i>][1,3]dioxol-4-yl)-2,6-dioxo-2,3-dihydropyrimidine-1(6 <i>H</i>)-carboxylate (178)	163
Dimethyl 2-(2-((3a <i>R</i> ,4 <i>R</i> ,6 <i>R</i> ,6a <i>R</i>)-6-(3-(<i>tert</i> -butoxycarbonyl)-2,4-dioxo-3,4-	

dihydropyrimidin-1(2 <i>H</i>)-yl)-2,2-dimethyltetrahydrofuro[3,4- <i>d</i>][1,3]dioxol-4-yl)ethyl)maleate (179)	164
Dimethyl 2-(2-((2 <i>R</i> ,3 <i>S</i> ,4 <i>R</i> ,5 <i>R</i>)-5-(2,4-dioxo-3,4-dihydropyrimidin-1(2 <i>H</i>)-yl)-3,4-dihydroxytetrahydrofuran-2-yl)ethyl)maleate (180)	165
Lithium 1-((2 <i>R</i> ,3 <i>R</i> ,4 <i>S</i> ,5 <i>R</i>)-5-((<i>Z</i>)-3,4-dicarboxylatobut-3-enyl)-3,4-dihydroxytetrahydrofuran-2-yl)-2,4-dioxo-2,4-dihydro-1 <i>H</i> -pyrimidin-3-ide (181)	166
<i>tert</i> -Butyl 3-((3 <i>aR</i> ,4 <i>R</i> ,6 <i>R</i> ,6 <i>aR</i>)-6-((<i>E</i>)-4-(benzyloxy)-5-methoxy-5-oxopent-1-enyl)-2,2-dimethyltetrahydrofuro[3,4- <i>d</i>][1,3]dioxol-4-yl)-2,6-dioxo-2,3-dihydropyrimidine-1(6 <i>H</i>)-carboxylate (182)	167
<i>tert</i> -Butyl 3-((3 <i>aR</i> ,4 <i>R</i> ,6 <i>R</i> ,6 <i>aR</i>)-6-(4-hydroxy)-5-methoxy-5-oxopentyl)-2,2-dimethyltetrahydrofuro[3,4- <i>d</i>][1,3]dioxol-4-yl)-2,6-dioxo-2,3-dihydropyrimidine-1(6 <i>H</i>)-carboxylate (183)	168
<i>tert</i> -Butyl 3-((3 <i>aR</i> ,4 <i>R</i> ,6 <i>R</i> ,6 <i>aR</i>)-6-(5-methoxy-4,5-dioxopentyl)-2,2-dimethyltetrahydrofuro[3,4- <i>d</i>][1,3]dioxol-4-yl)-2,6-dioxo-2,3-dihydropyrimidine-1(6 <i>H</i>)-carboxylate (184)	169
Dimethyl 2-(3-((3 <i>aR</i> ,4 <i>R</i> ,6 <i>R</i> ,6 <i>aR</i>)-6-(3-(<i>tert</i> -butoxycarbonyl)-2,4-dioxo-3,4-dihydropyrimidin-1(2 <i>H</i>)-yl)-2,2-dimethyltetrahydrofuro[3,4- <i>d</i>][1,3]dioxol-4-yl)propyl)maleate (185)	170
Dimethyl 2-(3-((2 <i>R</i> ,3 <i>S</i> ,4 <i>R</i> ,5 <i>R</i>)-5-(2,4-dioxo-3,4-dihydropyrimidin-1(2 <i>H</i>)-yl)-3,4-dihydroxytetrahydrofuran-2-yl)propyl)maleate (186)	171
Lithium 1-((2 <i>R</i> ,3 <i>R</i> ,4 <i>S</i> ,5 <i>R</i>)-5-((<i>Z</i>)-4,5-dicarboxylatopent-4-enyl)-3,4-	

dihydroxytetrahydrofuran-2-yl)-2,4-dioxo-2,4-dihydro-1 <i>H</i> -pyrimidin-3-ide (187)	172
<i>tert</i> -Butyl 3-((3 <i>aR</i> ,4 <i>R</i> ,6 <i>R</i> ,6 <i>aR</i>)-6-((<i>E</i>)-6-methoxy-5,6-dioxohex-1-enyl)-2,2- dimethyltetrahydrofuro[3,4- <i>d</i>][1,3]dioxol-4-yl)-2,6-dioxo-2,3- dihydropyrimidine-1(6 <i>H</i>)-carboxylate (188)	173
<i>tert</i> -Butyl 3-((3 <i>aR</i> ,4 <i>R</i> ,6 <i>R</i> ,6 <i>aR</i>)-6-(6-methoxy-5,6-dioxohexyl)-2,2- dimethyltetrahydrofuro[3,4- <i>d</i>][1,3]dioxol-4-yl)-2,6-dioxo-2,3- dihydropyrimidine-1(6 <i>H</i>)-carboxylate (189)	174
Dimethyl 2-(4-((3 <i>aR</i> ,4 <i>R</i> ,6 <i>R</i> ,6 <i>aR</i>)-6-(3-(<i>tert</i> -butoxycarbonyl)-2,4-dioxo-3,4- dihydropyrimidin-1(2 <i>H</i>)-yl)-2,2-dimethyltetrahydrofuro[3,4- <i>d</i>][1,3]dioxol- 4-yl)butyl)maleate (190)	175
Dimethyl 2-(4-((2 <i>R</i> ,3 <i>S</i> ,4 <i>R</i> ,5 <i>R</i>)-5-(2,4-dioxo-3,4-dihydropyrimidin-1(2 <i>H</i>)- yl)-3,4-dihydroxytetrahydrofuran-2-yl)butyl)maleate (191)	176
Lithium 1-((2 <i>R</i> ,3 <i>R</i> ,4 <i>S</i> ,5 <i>R</i>)-5-((<i>Z</i>)-5,6-dicarboxylatohex-5-enyl)-3,4- dihydroxytetrahydrofuran-2-yl)-2,4-dioxo-2,4-dihydro-1 <i>H</i> -pyrimidin-3-ide (192)	177
Dimethyl 2-(2-((3 <i>aR</i> ,4 <i>R</i> ,6 <i>R</i> ,6 <i>aR</i>)-6-(3-(<i>tert</i> -butoxycarbonyl)-2,4-dioxo-3,4- dihydropyrimidin-1(2 <i>H</i>)-yl)-2,2-dimethyltetrahydrofuro[3,4- <i>d</i>][1,3]dioxol- 4-yl)ethyl)succinate (193)	178
Dimethyl 2-(3-((3 <i>aR</i> ,4 <i>R</i> ,6 <i>R</i> ,6 <i>aR</i>)-6-(3-(<i>tert</i> -butoxycarbonyl)-2,4-dioxo-3,4- dihydropyrimidin-1(2 <i>H</i>)-yl)-2,2-dimethyltetrahydrofuro[3,4- <i>d</i>][1,3]dioxol- 4-yl)propyl)succinate (194)	179
Dimethyl 2-(4-((3 <i>aR</i> ,4 <i>R</i> ,6 <i>R</i> ,6 <i>aR</i>)-6-(3-(<i>tert</i> -butoxycarbonyl)-2,4-dioxo-3,4-	

dihydropyrimidin-1(2 <i>H</i>)-yl)-2,2-dimethyltetrahydrofuro[3,4- <i>d</i>][1,3]dioxol-4-yl)butyl)succinate (195)	180
Dimethyl 2-(2-((2 <i>R</i> ,3 <i>S</i> ,4 <i>R</i> ,5 <i>R</i>)-5-(2,4-dioxo-3,4-dihydropyrimidin-1(2 <i>H</i>)-yl)-3,4-dihydroxytetrahydrofuran-2-yl)ethyl)succinate (196)	181
Dimethyl 2-(3-((2 <i>R</i> ,3 <i>S</i> ,4 <i>R</i> ,5 <i>R</i>)-5-(2,4-dioxo-3,4-dihydropyrimidin-1(2 <i>H</i>)-yl)-3,4-dihydroxytetrahydrofuran-2-yl)propyl)succinate (197)	181
Dimethyl 2-(4-((2 <i>R</i> ,3 <i>S</i> ,4 <i>R</i> ,5 <i>R</i>)-5-(2,4-dioxo-3,4-dihydropyrimidin-1(2 <i>H</i>)-yl)-3,4-dihydroxytetrahydrofuran-2-yl)butyl)succinate (198)	182
Lithium 1-((2 <i>R</i> ,3 <i>R</i> ,4 <i>S</i> ,5 <i>R</i>)-5-(3,4-dicarboxylatobutyl)-3,4-dihydroxytetrahydrofuran-2-yl)-2,4-dioxo-2,4-dihydro-1 <i>H</i> -pyrimidin-3-ide (199)	183
Lithium 1-((2 <i>R</i> ,3 <i>R</i> ,4 <i>S</i> ,5 <i>R</i>)-5-(4,5-dicarboxylatopentyl)-3,4-dihydroxytetrahydrofuran-2-yl)-2,4-dioxo-2,4-dihydro-1 <i>H</i> -pyrimidin-3-ide (200)	184
Lithium 1-((2 <i>R</i> ,3 <i>R</i> ,4 <i>S</i> ,5 <i>R</i>)-5-(5,6-dicarboxylatohexyl)-3,4-dihydroxytetrahydrofuran-2-yl)-2,4-dioxo-2,4-dihydro-1 <i>H</i> -pyrimidin-3-ide (201)	185
2.2 NDP Kinase Assay	186
2.3 Antimicrobial Assays	186
3. Pediocin PA-1 Analogues	187
3.1 General Method for Solid Phase Peptide Syntheses (SPPS)	187
3.2 Purification Techniques	188
3.3 Instrumentation for Characterization	189
3.4 Experimental Data for Compounds	190
9,14-Diallyl 31-butyl pediocin PA-1 (210)	190
MS/MS analysis of residues 1-20 of 210	192

MS/MS analysis of residues 12-20 of transamidation product 230	193
9,14-Dibenzyl 31-butyl pediocin PA-1 (211)	194
9,14-Dipropyl 31-butyl pediocin PA-1 (212)	195
24,44-Diallyl 31-butyl pediocin PA-1 (213)	196
3.5 Antimicrobial Assays	198
APPENDIX <i>Sciadopitys verticillata</i> as a Potential Botanical Source of Baltic	
Amber: Summary of Extraction, Methanolysis, and GC-MS	
Studies	199
REFERENCES	207

LIST OF SCHEMES

Scheme 1. Catalytic cycle of NDP kinase.	2
Scheme 2. Inhibition of the GlcNAc phosphotransferase reaction by tunicamycin (25).	12
Scheme 3. Retrosynthetic analysis of target compounds.	20
Scheme 4. Attempted synthesis of uridine maleate 51b using 46 .	22
Scheme 5. Attempted synthesis of uridine maleic acid 55b using 52 .	23
Scheme 6. Attempted synthesis of uridine maleic anhydride 59b using 57 .	24
Scheme 7. LaCl ₃ -mediated nucleophilic addition of 60 to di-lithium salt of maleic acid (61).	25
Scheme 8. Synthesis of 66 as an inseparable mixture of <i>E</i> and <i>Z</i> isomers.	27
Scheme 9. Synthesis thioether-linked fumarate 68a and maleate 68b .	28
Scheme 10. Attempted removal of benzyl groups from 68b .	28
Scheme 11. Attempted synthesis of uridine maleimide 75 .	31
Scheme 12. Possible mechanism for degradation of uridine maleimide 74 .	32
Scheme 13. Attempted synthesis of adenosine dimethyl maleate 85 <i>via</i> organocuprate addition.	33
Scheme 14. Attempted synthesis of uridine dimethyl maleate 92 <i>via</i> organocuprate addition.	35
Scheme 15. Conditions of Fu and co-workers for Stille coupling of β -hydrogen-containing alkyl bromides.	36
Scheme 16. Synthesis of carboxylic acid 97 .	36

Scheme 17. Attempted synthesis of adenosine dimethyl maleate 101 using conditions of Fu.	38
Scheme 18. Selected examples of 1,4-addition to 46 using organocuprates derived from organozinc reagents.	39
Scheme 19. Attempted synthesis of 92 <i>via</i> an organocuprate derived from an organozinc reagent.	40
Scheme 20. Attempted synthesis of 101 <i>via</i> an organocuprate derived from an organozinc reagent.	41
Scheme 21. Decomposition of diacyl peroxides with radical coupling.	42
Scheme 22. Synthesis of functionalized amino acids by photolysis of diacyl peroxides.	43
Scheme 23. Retrosynthetic analysis of 92 based on photolysis of diacyl peroxides.	44
Scheme 24. Synthesis of carboxylic acid 118 .	44
Scheme 25. Synthesis of carboxylic acid 117 .	45
Scheme 26. Attempted synthesis of diacyl peroxide 116 .	46
Scheme 27. Coupling of 126 and 128 to give diacyl peroxide 129 .	47
Scheme 28. Synthesis of carboxylic acid 133 .	47
Scheme 29. Attempted synthesis of 135 by photolysis of diacyl peroxide 134 .	48
Scheme 30. Attempted synthesis of 141 by photolysis of diacyl peroxide 140 .	49
Scheme 31. Olefin CM approach for synthesis of uridine dicarboxylates.	50
Scheme 32. Formation of 147 by olefin CM.	51
Scheme 33. Attempted selective reduction of 5',6'-double bond of 147 .	53

Scheme 34. Attempted selective reduction of 5',6'-alkene of 150 using Crabtree's catalyst.	55
Scheme 35. Explanation of the high Z-selectivity in the HEW reaction with α -keto esters.	57
Scheme 36. Revised olefin CM approach for synthesis of uridine analogues 141 .	58
Scheme 37. Synthesis of alkenes for olefin CM.	59
Scheme 38. Synthesis of uridine maleate analogue containing a two-carbon spacer. 181 .	60
Scheme 39. Synthesis of uridine maleate analogue containing a three-carbon spacer 187 .	61
Scheme 40. Synthesis of uridine maleate analogue containing a four-carbon spacer 192 .	62
Scheme 41. Synthesis of uridine succinate analogues 199-201 .	63
Scheme 42. Coupled assay used for NDP kinase inhibition studies.	64
Scheme 43. Deprotonation of a C-terminal cysteine attached via a hydroxymethyl linker, leading to epimerization (a) or piperidine adduct formation (b).	83
Scheme 44. Incorporation of a pseudoproline dipeptide (222) during SPPS.	84
Scheme 45. Attempted synthesis of pediocin analogue using NovaSyn™ TGT resin.	87
Scheme 46. Synthesis of resin-bound 9,14-diallyl 31-butyl pediocin PA-1 (229).	89
Scheme 47. Final steps in the synthesis of 210 .	90
Scheme 48. Synthesis of 9,14-dibenzyl 31-butyl pediocin PA-1 (211).	92
Scheme 49. Synthesis of 9,14-dipropyl 31-butyl pediocin PA-1 (212).	93
Scheme 50. Synthesis of 24,44-diallyl 31-butyl pediocin PA-1 (213).	95

LIST OF TABLES

Table 1. Nucleophilic addition reactions attempted between 60 and 61 .	26
Table 2. Reactions attempted for removal of benzyl groups from 68b .	29
Table 3. Reactions attempted to selectively reduce the 5',6'-double bond of 148 .	53
Table 4. Reactions attempted to selectively reduce the 5',6'-double bond of 150 .	55
Table 5. Amino acid sequence alignment of several type IIa bacteriocins.	71
Table 6. Percent identity with selected β -turn consensus sequences of positions 10-13 in pediocin PA-1 and leucocin A.	98

LIST OF FIGURES

Figure 1. Co-crystal structure of <i>D. discoideum</i> NDP kinase monomer with ADP in the active site. carbon: grey; oxygen: red; nitrogen: purple; phosphorus: mauve.	4
Figure 2. Nucleotide-based inhibitors of NDP kinase.	5
Figure 3. Selected non-nucleotide-based inhibitors of NDP kinase.	6
Figure 4. Selected monophosphates and their phosphonate and sulfonamide analogues.	8
Figure 5. Selected monocarboxylate and malonate analogues of monophosphates.	9
Figure 6. Structures of alendronate (19) and IPP (20).	10
Figure 7. Selected bisphosphonate analogues of UDP-GlcNAc (21).	11
Figure 8. Analogues of UDP-GlcNAc containing a monosaccharide as a replacement for the diphosphate.	13
Figure 9. Structures of chaetomelic acids A (32) and B (33) and farnesyl diphosphate (34).	14
Figure 10. Structures of actinoplanic acids A (35) and B (36).	15
Figure 11. Selected natural products containing a maleyl or succinyl group.	17
Figure 12. Selected synthetic dicarboxylates.	18
Figure 13. Nucleoside dicarboxylate target compounds.	19
Figure 14. Comparison of PAPS (40) with ADP•AlF ₃ (202) in the active site of NDP kinase (adapted from references 59 and 60).	66
Figure 15. Proposed 3'-phosphate derivatives of UDP analogues.	67
Figure 16. Schematic representation of a class IIa bacteriocin.	72

Figure 17. Mechanism of action of class IIa bacteriocins.	76
Figure 18. Leucocin A (206) and non-cysteine-containing analogues.	78
Figure 19. Structure of pediocin PA-1 (209).	80
Figure 20. Proposed pediocin PA-1 analogues.	80
Figure 21. The bulky trityl groups of the NovaSyn™ TGT (220) and 2-chlorotriyl (221) resins prevent deprotonation at the α -centre of C-terminal cysteine.	83
Figure 22. Pediocin PA-1, with the positions of the threonine and serine residues highlighted.	85
Figure 23. Structure of 230 , arising from transamidation at Asp17 during SPPS.	91
Figure 24. Structure of proposed 9,14-dicarba 31-butyl pediocin PA-1 (231).	99

LIST OF ABBREVIATIONS

$[\alpha]_D^{20}$	specific rotation
A or Ala	alanine
Ac	acetyl
Ac ₂ O	acetic anhydride
AcOH	acetic acid
AcSH	thiolacetic acid
ADP	adenosine 5'-diphosphate
AllGly	allylglycine
app	apparent
Ar	aryl
atm	atmosphere
ATP	adenosine 5'-triphosphate
Bn	benzyl
BnBr	benzyl bromide
Boc	<i>tert</i> -butoxycarbonyl
(Boc) ₂ O	di- <i>tert</i> -butyl dicarbonate
<i>n</i> -Bu	<i>normal</i> butyl
<i>t</i> -Bu	<i>tertiary</i> butyl
<i>t</i> -BuOH	<i>tertiary</i> butanol
br	broad
BrIDP	8-bromoinosine 5'-diphosphate

<i>n</i> -Bu ₄ NI	tetrabutylammonium iodide
Bu ₃ SnH	tri- <i>n</i> -butyltin hydride
Bz	benzoyl
<i>c</i>	concentration
C or Cys	cysteine
calcd	calculated
Cbz	benzyloxycarbonyl
cod	cyclooctadiene
cAMP	adenosine 3',5'-cyclic monophosphate
CM	cross metathesis
COSY	correlation spectroscopy
δ	chemical shift in parts per million downfield from tetramethylsilane
d	doublet
D or Asp	aspartic acid
DBU	1,8-diazabicyclo[5.4.0]undec-7-ene
DCC	1,3-dicyclohexylcarbodiimide
DEAD	diethyl azodicarboxylate
DIBAL-H	diisobutylaluminum hydride
DIPEA	diisopropylethylamine
DMAD	dimethyl acetylenedicarboxylate
DMAP	4-dimethylaminopyridine
DMF	<i>N,N</i> -dimethylformamide
DMSO	dimethylsulfoxide

DNA	deoxyribonucleic acid
dTDP	deoxythymidine 5'-diphosphate
E or Glu	glutamic acid
EI	electron impact
equiv.	equivalents
ES	electrospray
Et	ethyl
EtOCOC1	ethyl chloroformate
Et ₃ N	triethylamine
Et ₂ O	diethyl ether
EtOAc	ethyl acetate
EtOH	ethanol
F or Phe	phenylalanine
Fmoc	9 <i>H</i> -fluorenylmethoxycarbonyl
FPP	farnesyl diphosphate
g	gram
G or Gly	glycine
gCOSY	gradient correlation spectroscopy
GDP	guanosine 5'-diphosphate
gHMBC	gradient heteronuclear multiple bond correlation spectroscopy
gHMQC	gradient heteronuclear multiple quantum correlation spectroscopy
GlcNAc	<i>N</i> -acetylglucosamine
GnT I	UDP- <i>N</i> -acetyl- <i>D</i> -glucosamine:α-3- <i>D</i> -mannoside β-1,2- <i>N</i> -

	acetylglucosaminyltransferase I
GPP	geranyl diphosphate
h	hour
H or His	histidine
HEW	Horner-Emmons-Wadsworth reaction
HPLC	high performance liquid chromatography
HRMS	high resolution mass spectrometry
I or Ile	isoleucine
IBX	<i>o</i> -iodoxybenzoic acid
IC ₅₀	concentration causing 50% inhibition
IPP	isopentenyl diphosphate
IR	infrared
<i>J</i>	coupling constant
K or Lys	lysine
kDa	kilodalton(s)
<i>K_i</i>	inhibition constant
L or Leu	leucine
LC	liquid chromatography
LDA	lithium diisopropylamide
LDH	lactate dehydrogenase
Leu A	leucocin A
lit.	literature reference
m	multiplet

M or Met	methionine
MALDI-TOF	matrix-assisted laser desorption ionization / time of flight
man-PTS	mannose phosphotransferase system
Me	methyl
MeCN	acetonitrile
Me ₄ NF	tetramethylammonium fluoride
MeOH	methanol
Mes	mesityl
min	minute(s)
mL	millilitre
mol	mole
mp	melting point
MHz	megahertz
MS	mass spectrometry
MW	molecular weight
μ	micro
N or Asn	asparagine
NAD	nicotinamide adenine dinucleotide (oxidized form)
NADH	nicotinamide adenine dinucleotide (reduced form)
NaHMDS	sodium <i>bis</i> (trimethylsilyl)amide
NaOMe	sodium methoxide
NaSMe	sodium thiomethoxide
NDP	nucleoside 5'-diphosphate

NDPK	nucleoside diphosphate kinase
NHE	nuclease-hypersensitive element
Nle	norleucine
nm	nanometres
NMM	<i>N</i> -methylmorpholine
NMP	nucleoside 5'-monophosphate
NMR	nuclear magnetic resonance
NOE	nuclear Overhauser effect
NTP	nucleoside 5'-triphosphate
Nva	norvaline
P or Pro	proline
PAP	5'-phosphoadenosine 3'-phosphate
PAPS	3'-phosphate 5'-phosphosulfate
PBP	penicillin-binding protein
Pd(PPh ₃) ₄	tetrakis(triphenylphosphine)palladium
Ped PA-1	pediocin PA-1
PEG	polyethylene glycol
PFTase	protein farnesyltransferase
PGGTase	protein geranylgeranyltransferase
PMF	proton motive force
Ph	phenyl
PK	pyruvate kinase
PMB	<i>para</i> -methoxybenzyl

PMBCl	<i>para</i> -methoxybenzyl chloride
PMe ₃	trimethylphosphine
<i>i</i> -Pr	<i>iso</i> -propyl
PP	protein phosphatase
PPh ₃	triphenylphosphine
PPh ₃ MeBr	methyltriphenylphosphonium bromide
ppm	parts per million
psi	pounds per square inch
py	pyridine
PyBOP	benzotriazole-1-yl-oxy- <i>tris</i> -pyrrolidino-phosphonium hexafluorophosphate
q	quartet
quin	quintet
Q or Gln	glutamine
R or Arg	arginine
RCM	ring closing metathesis
R _f	retention factor
Rm1B	dTDP- α -D-glucose 4,6-dehydratase
RP	reverse phase
rt	room temperature
s	singlet
S or Ser	serine
SEM	2-(trimethylsilyl)ethoxymethyl

SH2	Src homology 2
SMe ₂	dimethyl sulfide
SPPS	solid phase peptide synthesis
t	triplet
T or Thr	threonine
TfO	trifluoromethylsulfonyl
TFA	trifluoroacetic acid
TFE	trifluoroethanol
THF	tetrahydrofuran
TIPSH	triisopropylsilane
TLC	thin layer chromatography
TMS	trimethylsilyl
TMSCl	chlorotrimethylsilane
TMSI	iodotrimethylsilane
TMSOTf	trifluoromethylsulfonyltrimethylsilane
<i>t_R</i>	retention time
Trt	triphenylmethyl
UDP	uridine 5'-diphosphate
UPP	undecaprenyl diphosphate
UV	ultraviolet
V or Val	valine
W or Trp	tryptophan
Y or Tyr	tyrosine

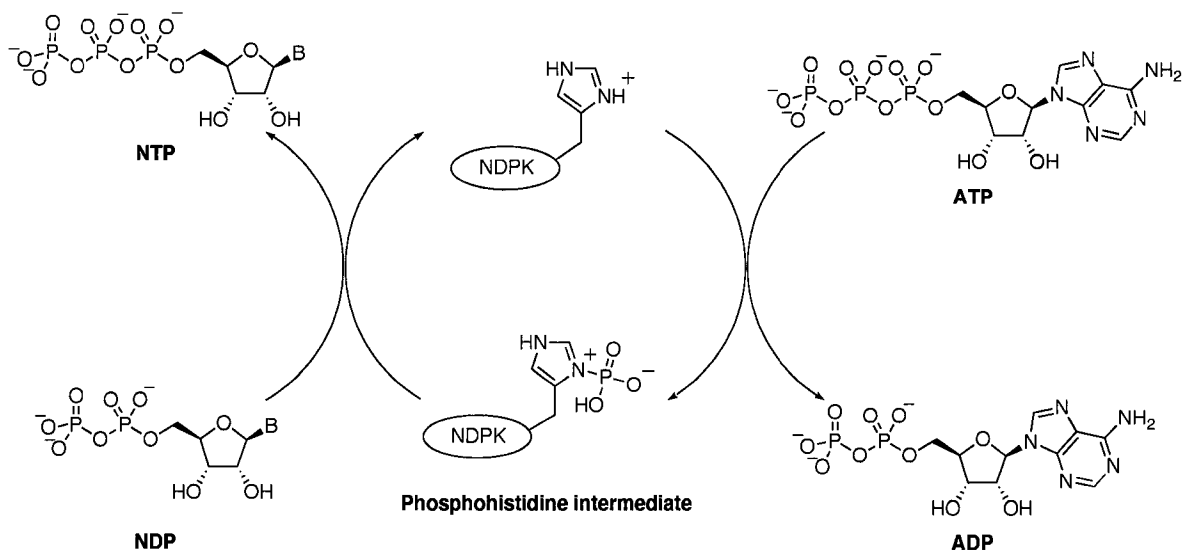
CHAPTER 1: Synthesis and Biological Evaluation of Nucleoside Dicarboxylates as Potential Mimics of Nucleoside Diphosphates

INTRODUCTION

1. Nucleoside Diphosphate Kinase

Nucleoside diphosphate (NDP) kinase is an ubiquitous enzyme that catalyzes the phosphorylation of nonadenine nucleoside diphosphates to their corresponding triphosphates, with a nucleoside triphosphate as the phosphoryl donor.¹ In mammals, adenosine triphosphate (ATP) is the main phosphoryl donor because its cellular concentration is much higher than that of other nucleoside triphosphates. However, this is not the case in lower eukaryotes and prokaryotes. NDP kinase is the main cellular source of nucleoside triphosphates, and thus represents the link between oxidative phosphorylation, nucleic acid, sugar, complex lipid and protein synthesis, and signal transduction. As depicted in Scheme 1, the mechanism of phosphorylation involves formation of a transient covalent N δ -phosphohistidine intermediate at the active site, obtained through γ -phosphate transfer from ATP.¹ The phosphate group is then transferred to a nucleoside diphosphate. Kinetic studies of NDP kinase suggest that either substrate binding or product dissociation may be the rate-limiting step.¹ Phosphate transfer from the phosphohistidine to the nucleoside diphosphate occurs rapidly. NDP kinases accept both nucleotides and 2'-deoxynucleotides as substrates, and show no specificity towards purine-containing (adenosine, guanosine) or pyrimidine-containing (thymidine, cytidine, uridine) nucleotides.

Scheme 1. Catalytic cycle of NDP kinase.

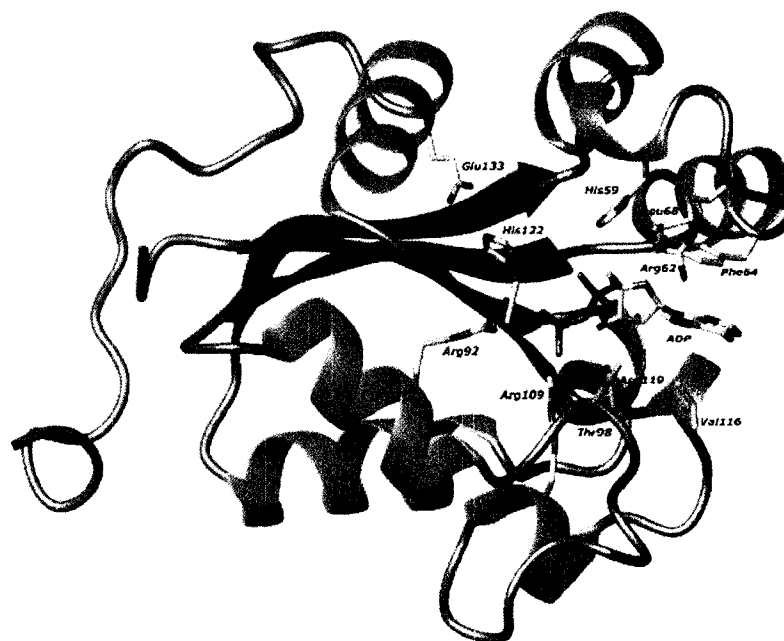


Besides its role in the intermediary metabolism of nucleotides, NDP kinase also plays regulatory roles in a variety of cellular processes. In *Drosophila*, the gene *awd* encoding NDP kinase is involved in development.² The *nm23* family of genes in humans encodes several NDP kinases that play important roles in cell proliferation, tumour metastasis, and transcriptional regulation. For example, *nm23-H1*, which encodes for NDP kinase A, has been shown to be down regulated in some metastatic cell lines,^{3, 4} and transfection of *nm23-H1* into melanoma cell lines reverses the metastatic phenotype, suggesting a role of *nm23* as a metastasis suppressor gene.⁵ Immunohistochemical studies demonstrated an increased level of expression of NDP kinase in a variety of malignant tumours,^{6, 7} neuroblastoma,⁸ and lymphoma.^{9, 10} The gene *nm23-H2*, encoding NDP kinase B,¹¹ was identified as a transcription factor for *c-myc*,¹² a regulator of cell proliferation and differentiation.¹³ NDP kinase B was shown to bind to oligonucleotides representing the nuclease-hypersensitive element (NHE) of the *c-myc* promoter.¹⁴ The *nm23-H2* gene was also found to be one of the 20 genes expressed at the highest level

among 300 000 transcripts analyzed in cells from human gastrointestinal tumours,¹⁵ giving further evidence of its role in oncogenic proliferation.

Eukaryotic NDP kinases are hexamers,¹⁶ with each monomer having a molecular weight of 17 kDa and consisting of a four-stranded anti-parallel β -sheet surrounded by α -helices,¹⁷ as exemplified by the enzyme from the slime mold *Dictyostelium discoideum* (Figure 1).^{18, 19} They are highly conserved, with interspecies sequence identities of at least 40%.²⁰ To date, over 30 NDP kinase crystal structures have been solved. The enzyme from *D. discoideum* is the best understood at the structural level, having been the first NDP kinase for which a three-dimensional structure was determined.²¹ It has 62% structural identity with human NDP kinase, including a completely conserved active site, however it is easier to purify and crystallize than the human enzyme. *D. discoideum* NDP kinase is considered a reliable model of other eukaryotic NDP kinases. Co-crystal structures of this enzyme with adenosine diphosphate (ADP)¹⁸ (Figure 1), deoxythymidine diphosphate (dTDP)²² or guanosine diphosphate (GDP)²³ revealed that the nucleotide binding site of NDP kinase differed from that of other known nucleotide binding domains. An unusual conformation is adopted by the enzyme-bound nucleotide due to an intramolecular hydrogen bond between the 3'-OH of the ribose and the oxygen bridging the β - and γ -phosphate groups. Kinetic experiments showed that the absence of the 3'-OH was detrimental to the enzyme's catalytic efficiency.²⁴⁻²⁶ Another notable conformational feature is the parallel arrangement of the oxygen atoms of the diphosphate of ADP (Figure 1, also observed for dTDP and GDP). This may be relevant in the context of inhibitors based on rigid diphosphate mimics.

Figure 1. Co-crystal structure of *D. discoideum* NDP kinase monomer with ADP in the active site.¹⁹ carbon: grey; oxygen: red; nitrogen: purple; phosphorus: mauve.

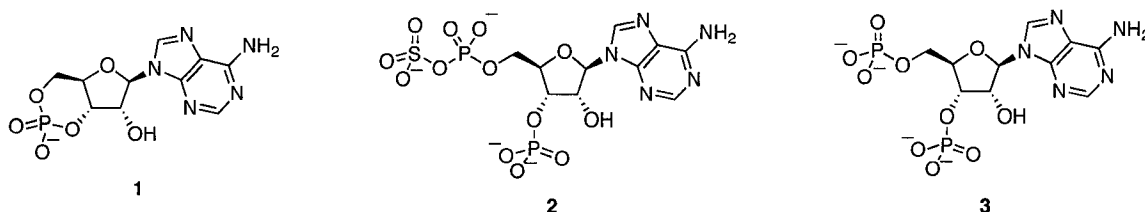


1.1 Inhibitors of NDP Kinase

Despite its role in numerous cellular processes, there are very few known inhibitors of NDP kinase. Those discovered may be divided into nucleotide-based and non-nucleotide-based inhibitors. The nucleotide-based inhibitors (Figure 2) include adenosine 3',5'-cyclic monophosphate (cAMP, **1**), adenosine 3'-phosphate 5'-phosphosulfate (PAPS, **2**), and 5'-phosphoadenosine 3'-phosphate (PAP, **3**). cAMP (**1**) was found to be a weak inhibitor of NDP kinase from *Myxococcus xanthus*, with a K_i value of 550 μM .^{27, 28} PAPS (**2**) is a metabolite involved in sulfonation of a variety of endogenous and exogenous compounds, with **3** being the reaction product.²⁹ With a K_i of 30 μM against *D. discoideum* NDP kinase,²⁸ **2** is the most active of all known nucleotide

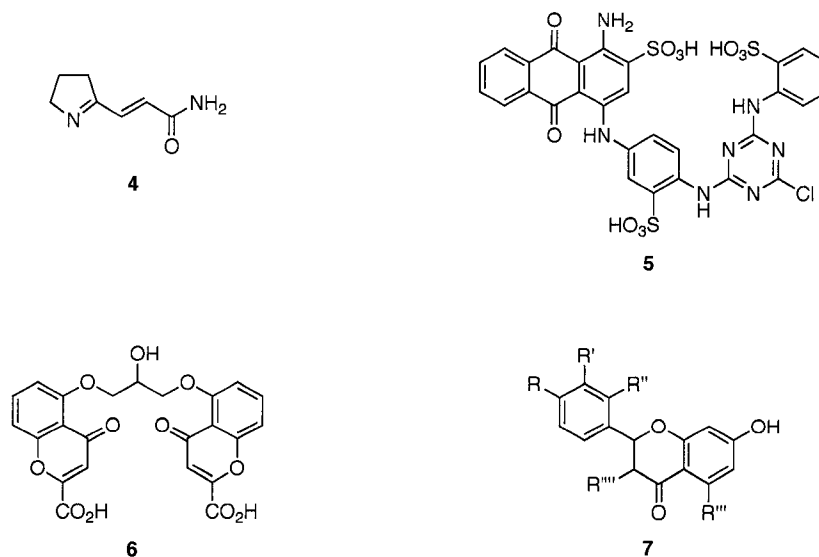
inhibitors of this enzyme. Nucleotide **3** inhibited NDP kinase from *D. discoideum* with a K_i value of 100 μM .²⁸ All three nucleotides are competitive inhibitors of the enzyme.

Figure 2. Nucleotide-based inhibitors of NDP kinase.



The non-nucleotide-based inhibitors of NDP kinase enzymes are comprised of a variety of compound types (Figure 3). The antibiotic desdanine (**4**), produced by *Streptomyces caelestis*, was found to be an irreversible inhibitor of NDP kinase from *E. coli*, but did not inhibit NDP kinase from rat liver.³⁰ Attempts to isolate the ³H-desdanine-enzyme complex were unsuccessful, therefore the binding site of desdanine could not be determined. The polysulfonated anthraquinonic dye Cibacron blue 3GA (**5**) was shown to be a competitive inhibitor of NDP kinase from pig heart with respect to ATP ($K_i = 280$ nM) and an uncompetitive inhibitor with respect to the acceptor nucleotide 8-bromoinosine 5'-diphosphate ($K_i = 310$ nM).³¹ Cromoglycate (**6**), often administered in the prophylactic treatment of bronchial asthma, was found to weakly inhibit NDP kinase from rat mucosal mast cells with an IC_{50} of 2 mM.³² Finally, several flavonoids of the general structure **7** were found to be good inhibitors of NDP kinases from rat mast cells and rabbit muscle.³³ The most potent of these, narigenin ($\text{R} = \text{R}''' = \text{OH}$, $\text{R}' = \text{R}'' = \text{R}'''' = \text{H}$), exhibited an IC_{50} value of 3.89 μM against mast cell NDP kinase and 9.3 μM against rabbit muscle NDP kinase.

Figure 3. Selected non-nucleotide-based inhibitors of NDP kinase.



2. Replacement of Monophosphates and Diphosphates in the Design of Enzyme Inhibitors

The design of inhibitors of enzymes that utilize mono- or diphosphorylated compounds as their natural substrates often involves replacement of the mono- or diphosphate unit by a more hydrolytically stable moiety. This is especially important in the context of *in vivo* studies and drug design, where the limitations of phosphoryl groups become apparent in their lability to cellular phosphatases and in their difficulty in crossing the cell membrane due to their negative charge. Replacement of the natural mono- or diphosphate by a more robust group that has a similar overall charge and 3-dimensional arrangement as the natural unit may give rise to a tight binding inhibitor. In this respect, efforts can either be directed towards slight modifications of the phosphate to

render it more stable, or towards the design of a completely new surrogate that does not contain any characteristics of the phosphate.

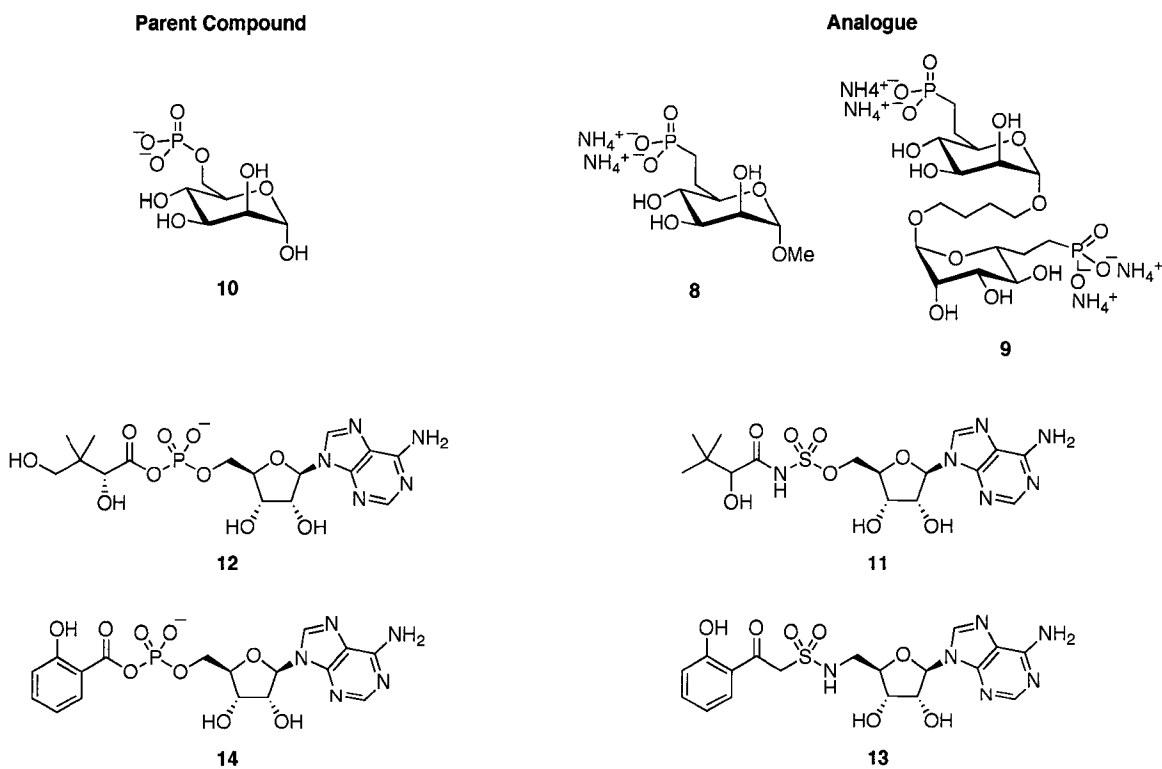
2.1 Non-Hydrolyzable Mimics of Monophosphates

In the context of monophosphates, replacement of the phosphate group with a more stable unit has focused mainly on phosphonates, sulfonamides, and carboxylic acids. The most extensively investigated of all phosphate ester replacements are the phosphonates, which derive their stability from replacement of one or more of the phosphorus-oxygen bonds with hydrolytically inert phosphorus-carbon bonds. Although the second pK_a of a phosphonate can be up to 2 orders of magnitude less than the corresponding phosphate, the two groups have similar bond angles and lengths.³⁴ The literature dealing with the synthesis and biological evaluation of phosphonates is vast, therefore only selected recent examples will be presented here. Monovalent phosphonate **8** and divalent phosphonate **9** were reported as analogues of mannose 6-phosphate (**10**) (Figure 4).³⁵ These compounds exhibited IC_{50} values of 25 and 20 μM , respectively, in binding assays with bovine M6P/IGF2R,³⁶ an enzyme involved in the sorting and transport of lysosomal enzymes, the degradation of non-glycosylated insulin-like growth factor II, and scar formation through transforming growth factor- β . These binding affinities are on the same order of magnitude as the enzyme's natural substrate, mannose 6-phosphate ($IC_{50} = 49 \mu M$).

Sulfonamides contain an N-SO₂ moiety in place of the phosphate, and are thus more stable than the latter. Several sulfonamide-containing analogues of nucleosides have recently been reported, including **11**, a competitive inhibitor of *E. coli* pantothenate

synthase ($K_i = 0.3 \mu\text{M}$) with respect to ATP (Figure 4).³⁷ Compound **11** is an analogue of pantooyl adenylate (**12**), the intermediate which undergoes nucleophilic attack by β -alanine to form pantothenate (vitamin B₅). β -Ketosulfonamide **13** has recently been reported as a good inhibitor ($K_i^{\text{app}} = 3.30 \mu\text{M}$) of MbtA, an enzyme found in *Mycobacterium tuberculosis*.³⁸ MbtA catalyzes the adenylation of salicylic acid, which activates it for ultimate incorporation into the mycobactins,^{39, 40} peptidic siderophores required for growth and virulence of the organism. β -Ketosulfonamide **13** is an analogue of salicyl-adenylate (**14**), the product of salicylic acid adenylation.

Figure 4. Selected monophosphates and their phosphonate and sulfonamide analogues.

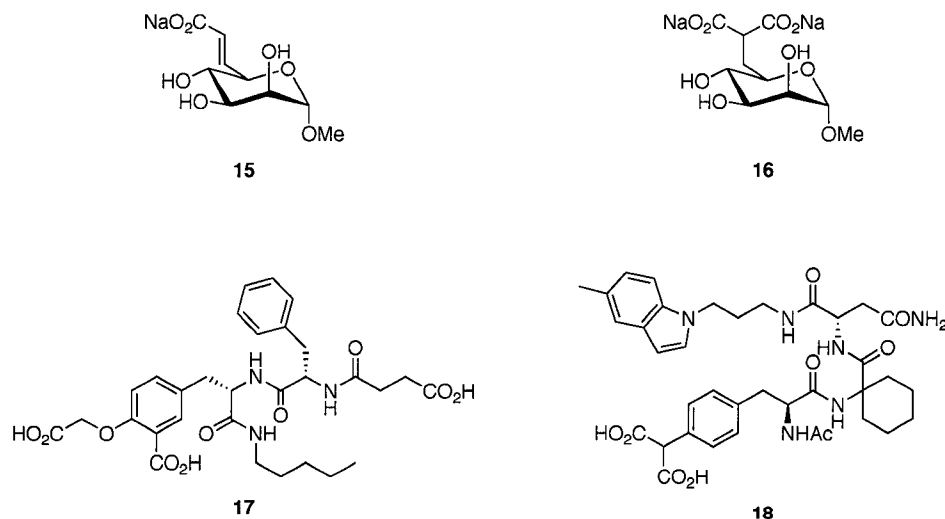


Carboxylic acids have often been introduced as surrogates for monophosphates.

For example, analogous to the phosphonate analogues of **10** discussed above, compounds

were developed wherein the phosphate was replaced by either a carboxylate (**15**) or a malonate (**16**) (Figure 5).⁴¹ As with **8** and **9**, these compounds were found to be inhibitors of M6P/IGF2R, with IC₅₀ values of 39 μM and 12 μM, respectively. Carboxylates and malonates have also been used as monophosphate replacements in the development of phosphotyrosyl mimetics as signal transduction inhibitors.⁴² Carboxylic acid **17** displayed binding towards protein-tyrosine phosphatase 1B, with an IC₅₀ value of 220 nM,⁴³ while malonate **18** exhibited potent affinity towards the phosphotyrosine-binding protein Grb2 Src homology 2 (SH2) domain, for which it was found to have an IC₅₀ of 12 nM.⁴⁴ These proteins play central roles in signal transduction, therefore their inhibition may lead to the development of drugs to treat cancer, type II diabetes, and immune disorders.

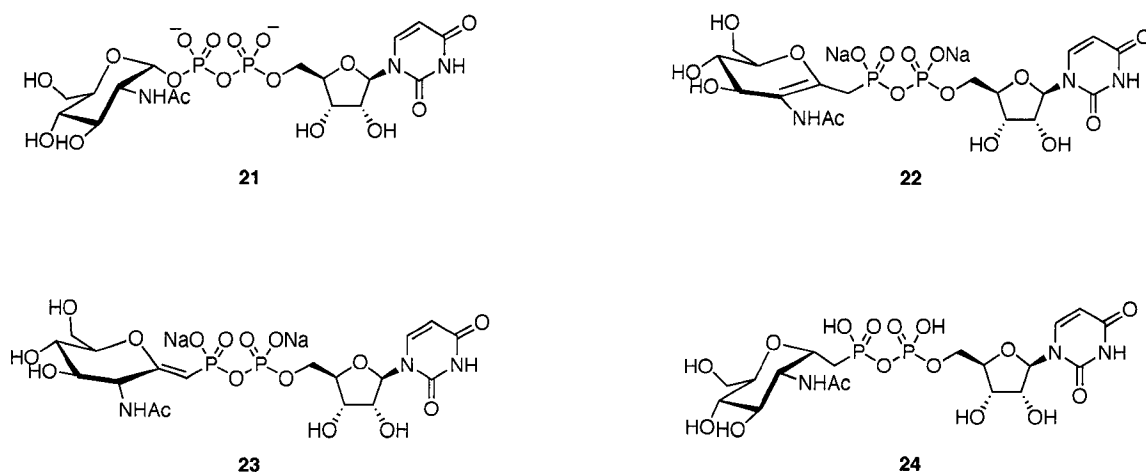
Figure 5. Selected monocarboxylate and malonate analogues of monophosphates.



analogues showed 40-60% inhibition of UDP-GlcNAc 2-epimerase at a concentration of 1.25 mM.

Phosphonate **24**, containing a C-linkage to the anomeric centre of the GlcNAc unit, was found to be a competitive inhibitor of UDP-*N*-acetyl-D-glucosamine:α-3-D-mannoside β-1,2-*N*-acetylglucosaminyltransferase I (GnT I) with respect to UDP-GlcNAc, with a K_i value of 28 μM.⁵³ GnT I catalyzes the initial steps in the conversion of high-mannose oligosaccharides to complex and hybrid structures in the biosynthesis of *N*-linked glycans.^{48, 49} Phosphonate **24** has also been found to be a very weak inhibitor ($K_i > 10$ mM) of chitin synthase from *Saccharomyces cerevisiae*, the enzyme responsible for polymerization of UDP-GlcNAc to form chitin, an essential component of the fungal cell wall.⁵⁴

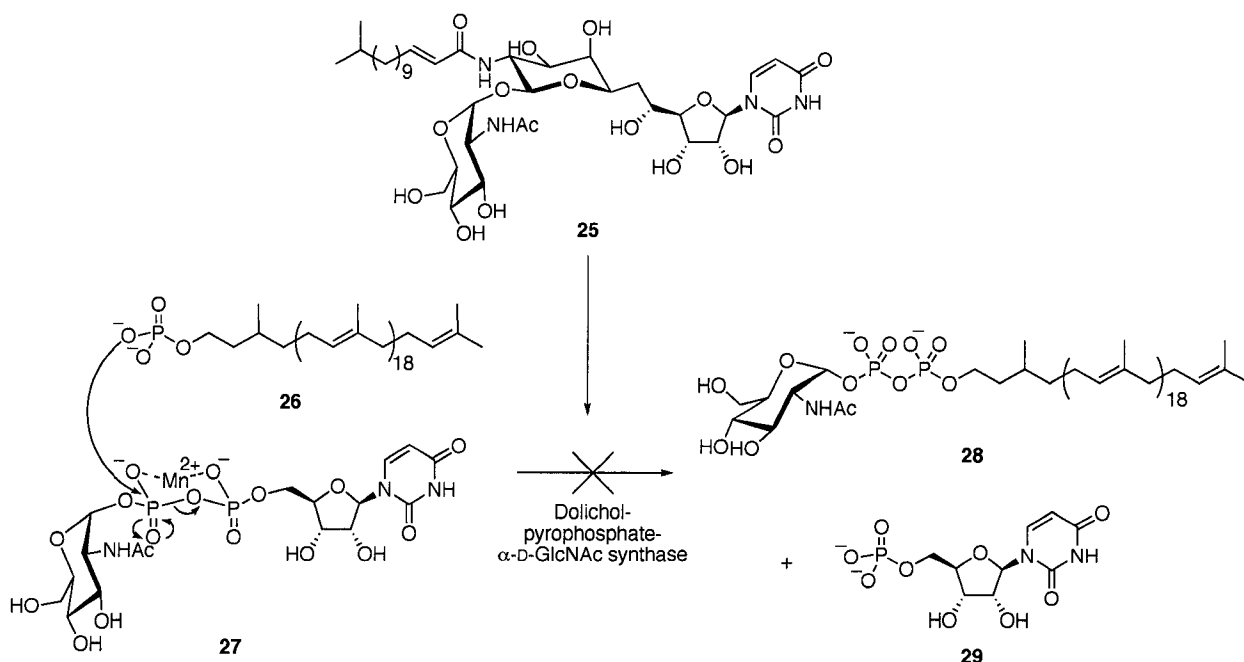
Figure 7. Selected bisphosphonate analogues of UDP-GlcNAc (**21**).



An interesting initiative in the development of stable diphosphate surrogates has been the incorporation of a monosaccharide in the design of glycosyltransferase inhibitors. This hypothesis is based on analogy with the mode of action of several

naturally occurring glycosyltransferase inhibitors. Tunicamycin (**25**)⁵¹ is among the most potent of these inhibitors, with an IC₅₀ value of 7 nM against dolichol-pyrophosphate- α -D-GlcNAc synthase.⁵⁵ It appears to mimic the transition state leading to the formation of dolichol-pyrophosphate- α -D-GlcNAc (**28**), with its monosaccharide adopting a similar conformation as the 6-membered chair of the diphosphate-metal complex **27** in UDP-GlcNAc (Scheme 2).

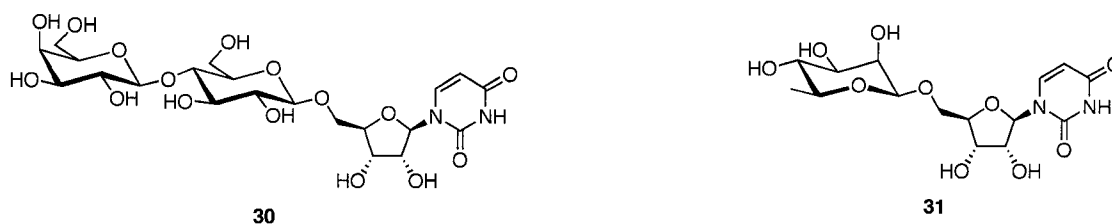
Scheme 2. Inhibition of dolichol-pyrophosphate- α -D-GlcNAc synthase by tunicamycin (**25**).



Some of the analogues developed based on this concept are displayed in Figure 8. UDP-galactose derivative **30**, incorporating a glucosyl moiety in place of the diphosphate, was found to be a moderate inhibitor ($K_i = 119.6 \mu\text{M}$)⁵⁶ of β -1,4-galactosyltransferase, which catalyzes the transfer of galactose from UDP-galactose to an

acceptor sugar. In a separate study, a similar series of UDP and dTDP analogues containing an L-rhamnosyl unit instead of a D-glucosyl unit were synthesized and tested against bovine β -1,4-galactosyltransferase.⁵⁷ The L-rhamnosyl moiety has a similar stereochemistry to that of the monosaccharide found in tunicamycin that is thought to be acting as the diphosphate mimic. Although none of the synthesized compounds showed more than 10% inhibition of the enzyme at 500 mM, moderate inhibition of *Salmonella typhimurium* dTDP- α -D-glucose 4,6-dehydratase (Rm1B) was observed for some. β -L-Rhamnosyl uridine **31** exhibited the highest activity with 47% inhibition at 1 mM.

Figure 8. Analogues of UDP-GlcNAc containing a monosaccharide as a replacement for the diphosphate.

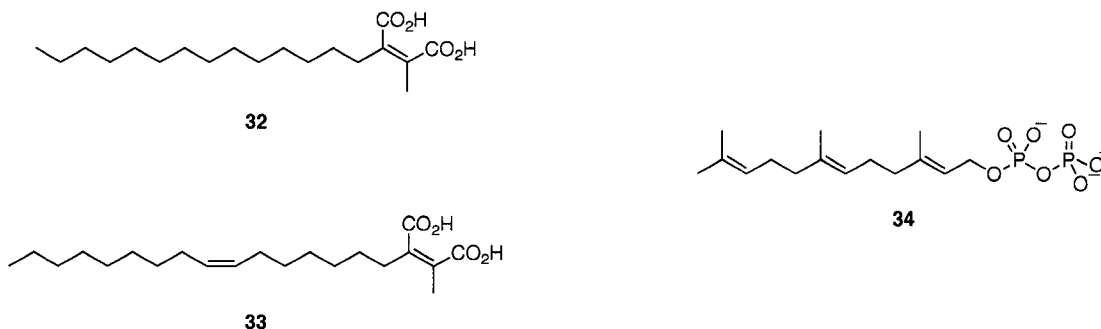


2.3 Maleates and Succinates as Diphosphate Mimics

There is convincing experimental and theoretical evidence suggesting that 1,2-dicarboxylates (*i.e.* maleates or succinates) can act as mimics of diphosphates. The appeal of carboxylic acids lies in the ability to mask them as their corresponding methyl esters, which due to their neutrality can more easily cross the cell membrane and subsequently undergo hydrolysis by esterases once in the cytoplasm. Several dicarboxylate-bearing natural products and their analogues are potent inhibitors of enzymes whose natural

substrates contain a diphosphate group. In 1993, researchers at Merck reported the isolation and characterization of chaetomelic acids A (**32**) and B (**33**) from the coleomycete *Chaetomella acutiseta* (Figure 9).^{58, 59} Both compounds were found to be highly active inhibitors of Ras protein farnesyltransferase (PFTase), an enzyme that catalyzes farnesylation of the oncogenic protein Ras. Farnesylation is required to anchor Ras to the plasma membrane, which is essential for this protein to mediate cell-transforming activity. Compounds **32** and **33** exhibited IC₅₀ values of 55 and 185 nM, respectively, against human PFTase, and further investigation revealed that **32** was competitive with respect to farnesyl diphosphate (**34**). Computer modeling of **32** and **34** using the MM2X force field determined that both compounds overlap very well, with the carboxyl carbons of **32** separated by 3.2 Å and the phosphorus atoms of **34** being 2.8 Å apart.⁵⁸ It was concluded that the maleate unit of the chaetomelic acids was mimicking the diphosphate unit in the enzyme's active site.

Figure 9. Structures of chaetomelic acids A (**32**) and B (**33**) and farnesyl diphosphate (**34**).

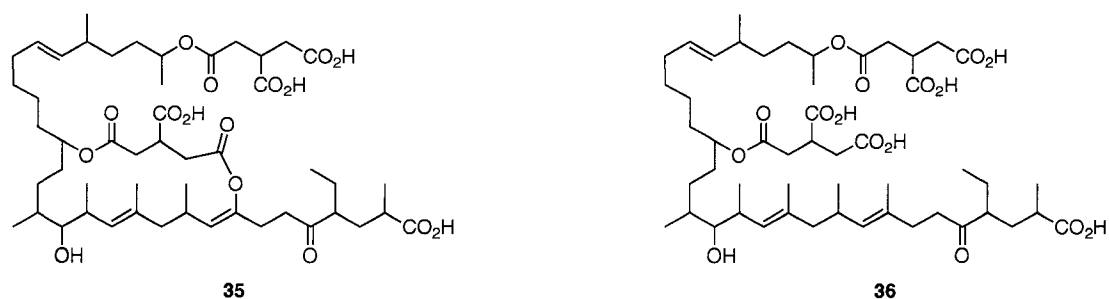


Compound **32** was also found to be an inhibitor of other prenyltransferase enzymes. It was shown to be a moderate inhibitor of protein geranylgeranyltransferase

(PGGTase) from bovine brain ($IC_{50} = 92 \mu\text{M}$),⁶⁰ but did not inhibit PGGTase from yeast. However, replacement of the C_{14} alkyl chain with a geranylgeranyl group resulted in a good inhibitor with an IC_{50} value of $11.5 \mu\text{M}$.⁶¹ Compound **32** was also shown to be a fairly good competitive inhibitor of rubber transferase enzymes from *Hevea brasiliensis* ($K_i = 42 \mu\text{M}$) and *Parthenium argentatum* ($K_i = 8.8 \mu\text{M}$) with respect to **34**.⁶² Rubber transferases utilize **34** as the initiating diphosphate during chain elongation in rubber biosynthesis.

The same research group at Merck also reported the discovery of actinoplanic acids A (**35**) and B (**36**) from an *Actinoplanes* species in 1994 (Figure 10).⁶³⁻⁶⁵ These compounds are also tight binding inhibitors of mammalian Ras PFTase with IC_{50} values of 230 nM and 50 nM and K_i values of 98 nM and 8 nM, respectively. Both compounds contain a succinate unit as part of their structure, and, as in the case of **32** and **33**, were found to be competitive with respect to **34**.

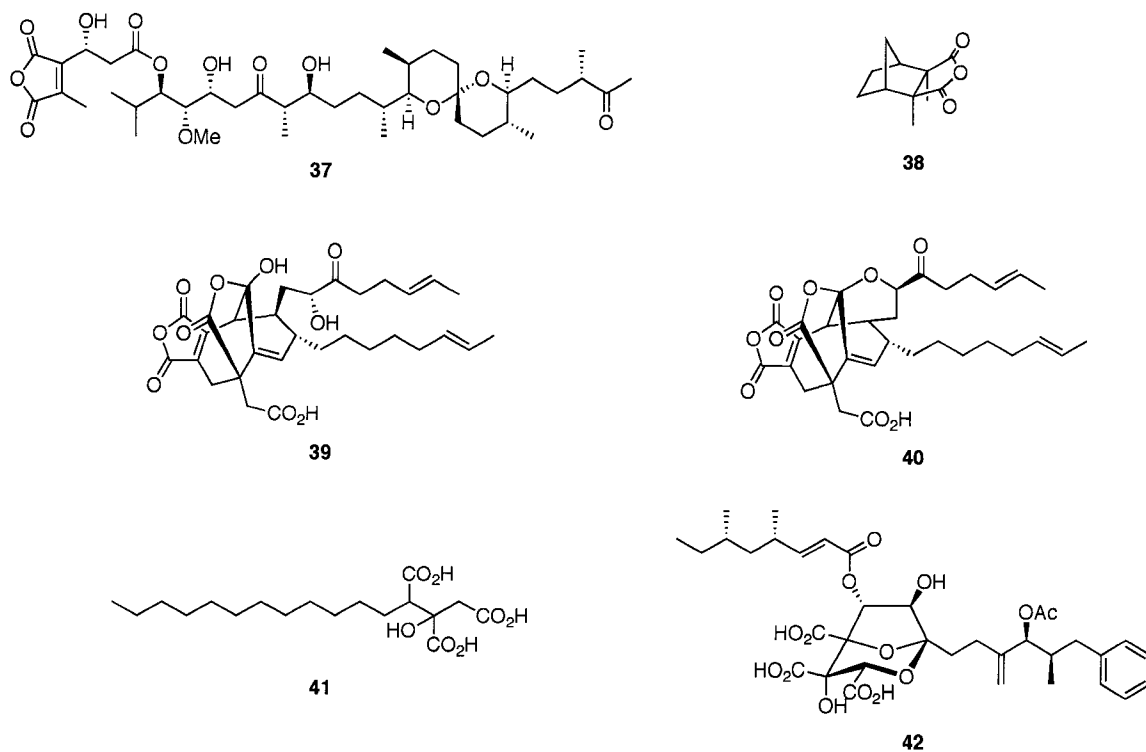
Figure 10. Structures of actinoplanic acids A (**35**) and B (**36**).



There are several other natural products containing a maleate or succinate unit that are good enzyme inhibitors. Selected examples are shown in Figure 11. Tautomycin (**37**),⁶⁶⁻⁶⁸ isolated from *Streptomyces spiroverticillatus*, displays strong antifungal activity

against *Sclerotinia sclerotiorum* and is a potent inhibitor of serine/threonine protein phosphatase 1 (PP1),⁶⁹ with an IC₅₀ value of 22 nM. Although depicted as the anhydride, **37** was shown to be in equilibrium with its diacid in solution, with the diacid being the more active species.⁷⁰ It has been proposed that **37** mimics the phosphorylated form of DARPP-32,⁷¹ an endogenous protein that acts to regulate PP1. In this case, it would appear that the maleate is mimicking a monophosphate. A similar scenario is apparently in effect with cantharidin (**38**), the toxic constituent of blister beetles and the active ingredient of the purported aphrodisiac “Spanish fly”. Anhydride **38** is a potent inhibitor of serine/threonine PP2A (IC₅₀ = 160 nM)^{72, 73} and a good inhibitor of PP1 (IC₅₀ = 1.7 μM).⁷³ It was proposed that the active form dicarboxylate mimics the phosphorylated substrate peptide. In a separate study, several analogues of **38** were synthesized and shown to be selective inhibitors of serine/threonine PP2B (calcineurin) over other serine/threonine protein phosphatases.⁷⁴ Other active compounds isolated as their anhydrides include CP-225,917 (**39**) and CP-263,114 (**40**), isolated from an unidentified fungus by workers at Pfizer.^{75, 76} These complex natural products were found to be inhibitors of Ras PFTase from rat brain, with IC₅₀ values of 6 and 20 μM, respectively. They also inhibited squalene synthase from rat liver, although to a lesser extent, with IC₅₀ values determined to be 43 and 160 μM. Squalene synthase catalyzes the first committed step of cholesterol biosynthesis starting from FPP,⁷⁷ therefore there is significant interest in developing inhibitors of this enzyme.

Figure 11. Selected natural products containing a maleyl or succinyl group.

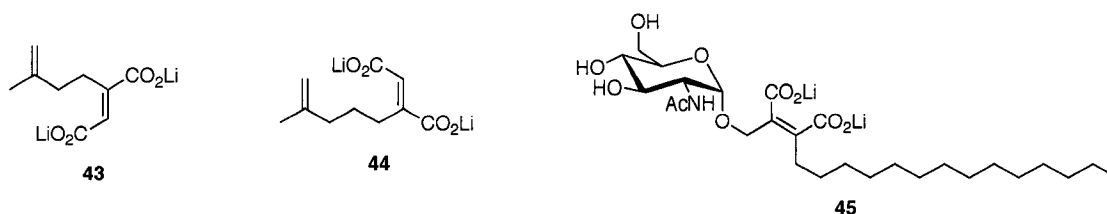


A compound labeled CJ-13,982 (**41**) was the more potent of two products that were also isolated from an unidentified fungus, and it was found to inhibit human liver microsomal squalene synthase with an IC_{50} value of $1.1 \mu\text{M}$.⁷⁸ Despite its similarity in structure to the chaetomelic acids (**32** and **33**), **41** exhibited no inhibitory activity against human brain PFTase. The zaragozic acids,⁷⁹ which contain a 1,2,3-tricarboxylic acid moiety, have also been found to be potent inhibitors of squalene synthase. For example, zaragozic acid A/squalestatin S1 (**42**) exhibited competitive inhibition with respect to FPP (**34**) of squalene synthase from a variety of sources ($IC_{50} = 0.9\text{-}2.1 \text{ nM}$), which was followed by mechanism-based irreversible inactivation.⁸⁰

Our group has reported several synthetic diphosphate analogues containing a dicarboxylate unit, although they proved to be only modest inhibitors. Fumarates **43** and

44 (Figure 12) were synthesized as analogues of IPP and investigated as inhibitors of yeast PFTase and *E. coli* undecaprenyl diphosphate (UPP) synthase.⁸¹ Fumarate **43** was found to inhibit PFTase with an IC₅₀ value of 384 μM and UPP synthase with an IC₅₀ value of 492 μM. Fumarate **44** was more active than **43** towards UPP synthase, with an IC₅₀ value of 135 μM, but showed no inhibition of PFTase. Interestingly, **43** and **44** were more active than their corresponding maleates, which may reflect a specific spatial arrangement required for the diphosphate in the active site of these enzymes. We have also reported the synthesis and evaluation of lipid II analogue **45** as an inhibitor of the transglycosylase activity of *E. coli* penicillin-binding protein 1b (PBP1b).⁸² This compound displayed a very modest inhibition of 28% at 100 μM.

Figure 12. Selected synthetic dicarboxylates.

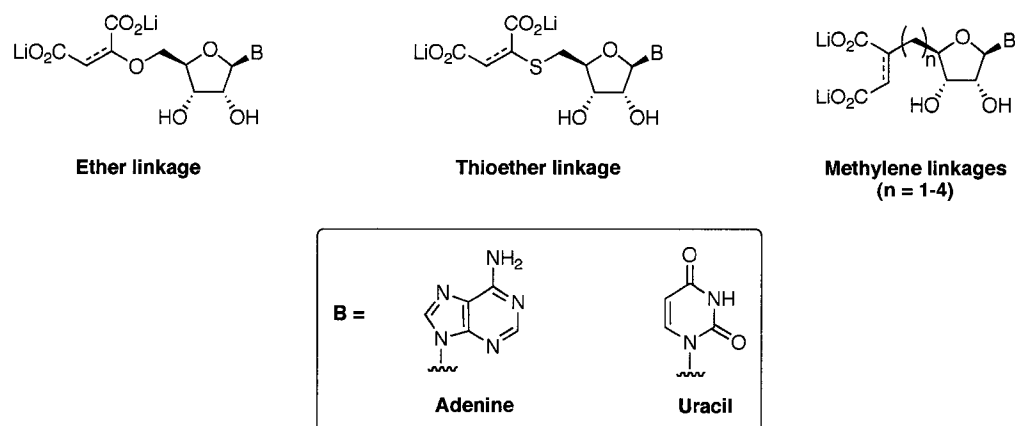


3. Project Objectives: Synthesis and Biological Evaluation of Nucleoside Dicarboxylates as NDP Kinase Inhibitors

The concept of 1,2-dicarboxylates as diphosphate mimics has not been examined in the context of nucleoside diphosphates. Thus, the goal of this project is the synthesis and biological evaluation of a series of nucleoside dicarboxylates as nucleoside diphosphate analogues and evaluation of their activity against NDP kinase. As

previously discussed, the diphosphate of the substrate in the enzyme's active site has a parallel arrangement of the oxygen atoms (Figure 1). Molecular modeling suggests that this arrangement would be required to allow the dicarboxylate oxygens of analogues containing a maleate unit to mimic those of the diphosphate. Initially, we chose to incorporate three different types of spacers into the analogues: an ether linkage, a thioether linkage, and one, two, three, or four methylene linkages (Figure 13). The focus was restricted to nucleosides of adenine and uracil because of the abundance of literature precedent for syntheses involving adenosine and uridine analogues, including numerous protecting group strategies and modifications at the 5' position.

Figure 13. Nucleoside dicarboxylate target compounds.

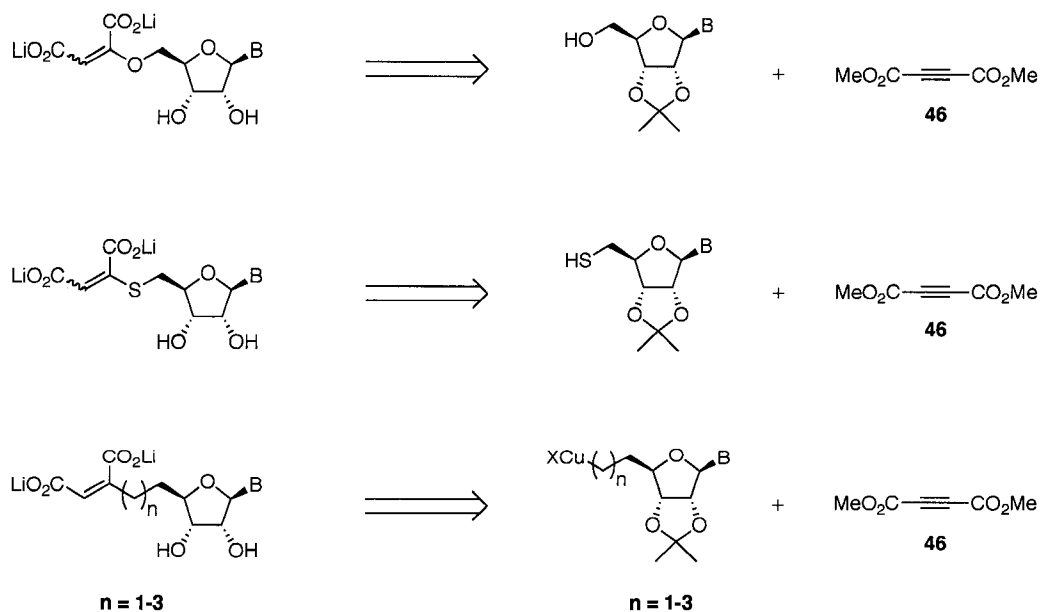


RESULTS AND DISCUSSION

1. Synthesis of Nucleoside Dicarboxylates

The initial strategy envisioned for accessing all target compounds involved nucleophilic 1,4-addition onto commercially available dimethyl acetylenedicarboxylate (DMAD, **46**) (Scheme 3). The 1,4-addition of oxygen,⁸³ sulfur,^{84, 85} and carbon nucleophiles^{61, 86-90} to acetylenic esters is well-documented in the literature. Although alcohol and thiol addition would be expected to generate products as mixtures of *E* and *Z* isomers, we were confident that nucleophilic organocuprate addition would give rise to the methylene-linked analogues with high stereospecificity favouring the *Z* isomers, as we⁶¹ and others⁸⁶⁻⁹⁰ have previously demonstrated.

Scheme 3. Retrosynthetic analysis of target compounds.



1.1 Nucleoside Dicarboxylates Containing an Ether Linkage

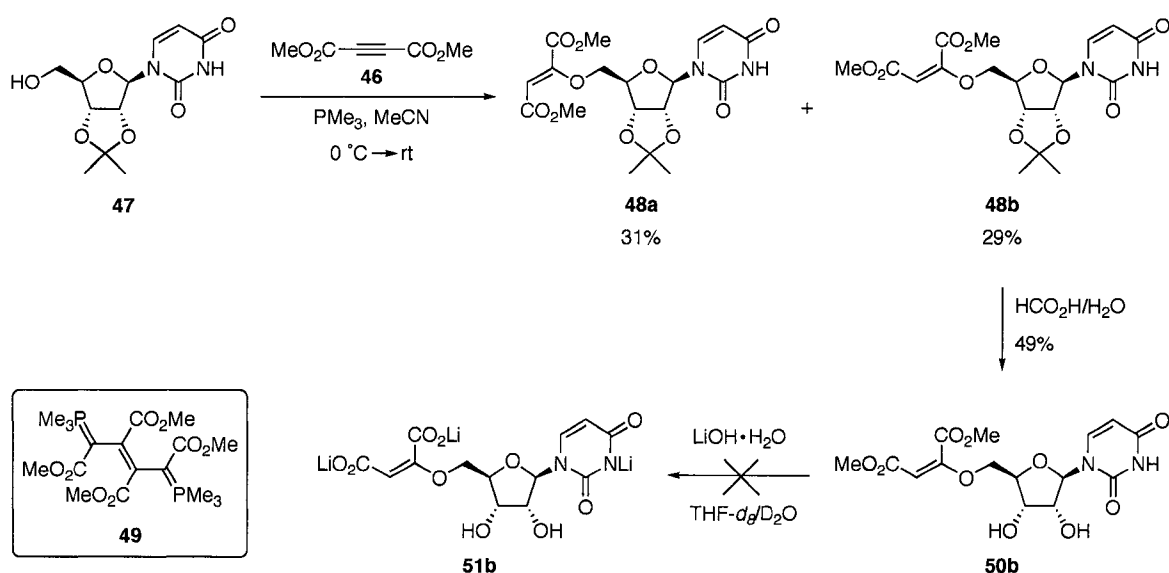
The synthesis of analogues containing an ether linkage began with a survey of various reagents known to promote the reaction between alcohols and DMAD. This was done to determine the optimal conditions for obtaining the highest *E/Z* ratio. Commercially available 2',3'-*O*-isopropylideneuridine (**47**, Scheme 4) was used as the nucleoside because it is more soluble in MeCN than the corresponding adenosine derivative. Trimethylphosphine^{91, 92} was found to give the combination of highest yield and best *E/Z* selectivity, as determined by measuring the relative integration of the maleate and fumarate vinylic hydrogens in the ¹H NMR spectrum. Other promoters gave either traces of product (triphenylphosphine), a very low *E/Z* selectivity (*N*-methylmorpholine, *E/Z* = 1:15.7), a complex mixture of products (dimethylaminopyridine), or no reaction (trifluoromethanesulfonic acid).⁹³

Compound **47** adds to DMAD under catalysis by trimethylphosphine to give dimethyl diesters **48a** and **48b** as a 1.1:1 mixture of *Z* and *E* isomers in 60% overall yield. It is important that DMAD be added slowly to a cooled solution of the alcohol and phosphine to minimize dimerization to the 1,4-diphosphorane **49**, as has been previously observed to occur in polar solvents.^{92, 94} After separation of **48a** and **48b** by column chromatography, the isopropylidene protecting group of **48b** is removed by aqueous formic acid to afford dimethyl maleate derivative **50b**.

Treatment of **50b** with LiOH at rt or at 0 °C does not lead to any evidence of **51b**, and yields only a complex mixture of products. The same fate results during attempted hydrolysis of **48b** using identical or milder conditions (Na₂CO₃), negating the presence of the free 2' and 3' hydroxyl groups as interfering moieties. Monitoring the reaction by ¹H

NMR reveals that the hydrogen signal corresponding to the maleate =CH (~ 6.70 ppm) as well as the signals of the uracil (H-5)-C=C-(H-6) group (~ 5.80 and ~ 8.10 ppm, respectively) disappear immediately upon addition of an aqueous solution of LiOH to **48b** in THF-*d*₈/D₂O. Although the nature of the decomposition pathway is not immediately obvious, it is clear that both **48b** and **50** are unstable to basic conditions.

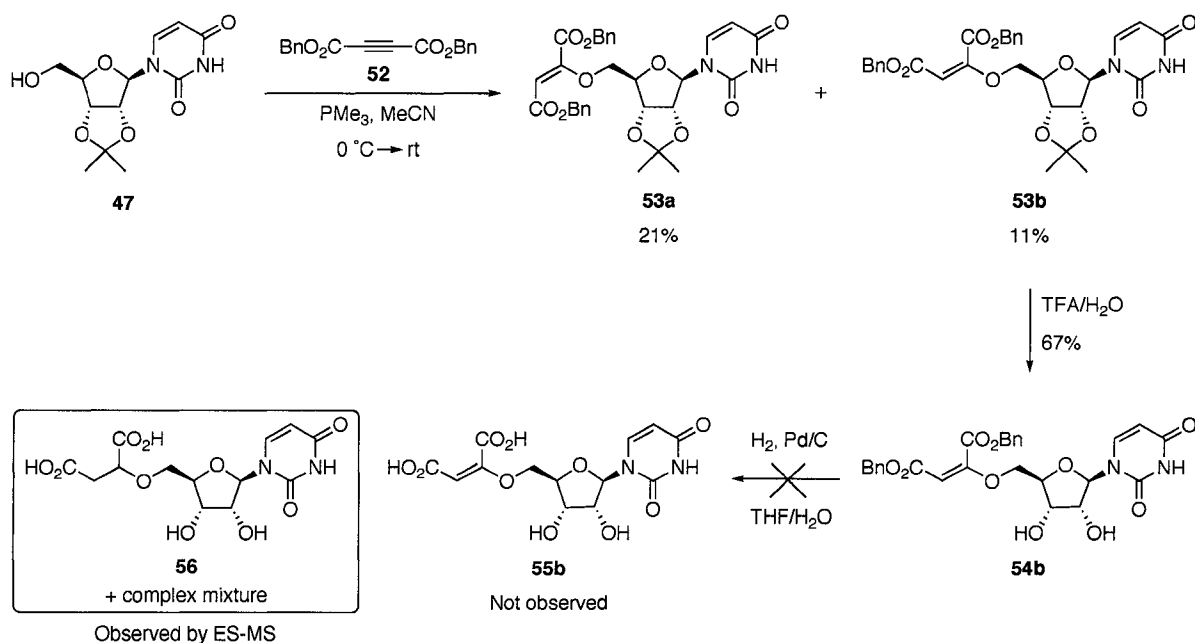
Scheme 4. Attempted synthesis of uridine maleate **51b** using **46**.



The focus was thus shifted to maleates containing esters that could be deprotected under non-basic conditions to give the diacid or the anhydride. Benzyl esters were chosen because of the ready access to dibenzyl acetylenedicarboxylate (**52**) and the ability to remove the benzyl groups under mild conditions (Scheme 5). Diester **52** is prepared in 77% yield from acetylenedicarboxylic acid and benzyl alcohol.⁹⁵ Using identical conditions as described for DMAD, **52** is then treated with 2',3'-*O*-isopropylideneuridine (**47**) in the presence of trimethylphosphine to give dibenzyl

fumarate **53a** and dibenzyl maleate **53b** as a separable 1.9:1 mixture of *Z* and *E* isomers in 32% overall yield (Scheme 5). Deprotection of **53b** with aqueous trifluoroacetic acid (TFA) affords **54b**. Subjection of **54b** to 1 atm H₂ over 10% Pd/C does not generate diacid **55b** but a complex mixture of products, one of which is not surprisingly succinic acid derivative **56**, arising from reduction of the maleate double bond. Although not distinguishable in the ¹H NMR spectrum, the presence of **56** is confirmed by EI-MS (383.1, [MNa]⁺). For the sake of completeness, **54b** was also treated with K₂CO₃, but once again a complex mixture is obtained.

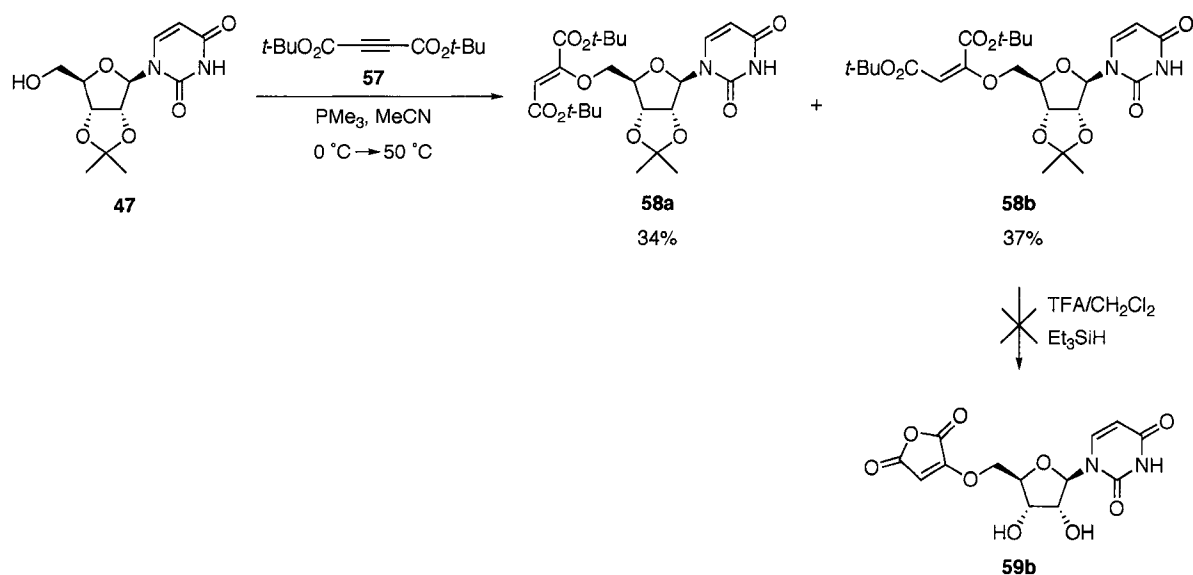
Scheme 5. Attempted synthesis of uridine maleic acid **55b** using **52**.



Attention was finally focused on removal of the ester protecting groups under acidic conditions, which could be achieved with concomitant removal of the isopropylidene group. Reaction of **47** with commercially available di-*tert*-butyl acetylenedicarboxylate (**57**) yields di-*tert*-butyl fumarate **58a** and di-*tert*-butyl maleate

58b as a separable 1:1.1 mixture of *E* and *Z* isomers in 71% overall yield (Scheme 6). In this case, prolonged reaction times (24 h) and heating at 50 °C are required to coerce the reaction between the nucleoside and the sterically hindered acetylenic diester to proceed to completion. Attempted deprotection of **58b** with TFA in CH₂Cl₂ with added triethylsilane as a cation scavenger again leads to a complex mixture of products and none of the expected maleic anhydride **59b**. A peak at 229.2 mass units is evident in the ES-MS of the mixture, which may correspond to the product obtained upon loss of the uracil ring from **59b**.

Scheme 6. Attempted synthesis of uridine maleic anhydride **59b** using **57**.



Due to the difficulties encountered in attempting to synthesize an ether-linked maleate analogue, attention was turned to accessing a succinate. The strategy adopted was the LaCl₃-mediated nucleophilic addition of alcohols to the di-lithium salt of maleic acid to give substituted succinates (Scheme 7).⁹⁶ The reaction must be conducted in water, necessitating the use of a very polar nucleoside as starting material, thus 2',3'-*O*-

isopropylideneadenosine (**60**) was chosen. However, this nucleoside is insoluble in H₂O, therefore the use of co-solvents was examined. The results of addition of **60** to maleic acid di-lithiate (**61**) are summarized in Table 1. The use of co-solvent systems such as dioxane/H₂O or acetone/H₂O results in no reaction (Entries 1 and 2), presumably due to the insolubility of the nucleoside and/or the reagent salts. Reactions conducted in DMF (Entry 3) or DMSO (Entry 4) at 120 °C only result in isolation of maleic anhydride after acidic workup. The elevated temperatures may lead to decomposition of the nucleoside starting material in this case. Finally, when the reaction is conducted in H₂O using adenosine as the starting material, an intractable mixture is obtained (Entry 5). Therefore due to the general insolubility of the reagents and the harsh conditions required, it was decided that this procedure is not compatible with nucleoside chemistry. Concurrent to the synthesis of ether-linked analogues, analogues with a thioether spacer were also being synthesized. The decision was made to focus subsequent efforts on the synthesis of an analogue of the latter type.

Scheme 7. LaCl₃-mediated nucleophilic addition of **60** to di-lithium salt of maleic acid (**61**).

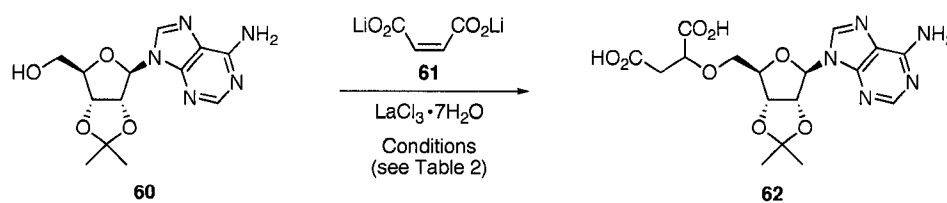


Table 1. Nucleophilic addition reactions attempted between **60** and **61**.

Entry	Conditions	Result ^a
1	Dioxane/H ₂ O (3:1), 100 °C, 5 h	NR
2	1) Acetone/H ₂ O (4.5:1), 120 °C, sealed tube, 24 h 2) HCl	NR
3	1) DMF, 120 °C, 24 h 2) HCl	Maleic anhydride isolated
4	1) DMSO, 120 °C, 24 h 2) HCl	Maleic anhydride isolated
5 ^b	H ₂ O, 120 °C, sealed tube, 12 h	Complex mixture

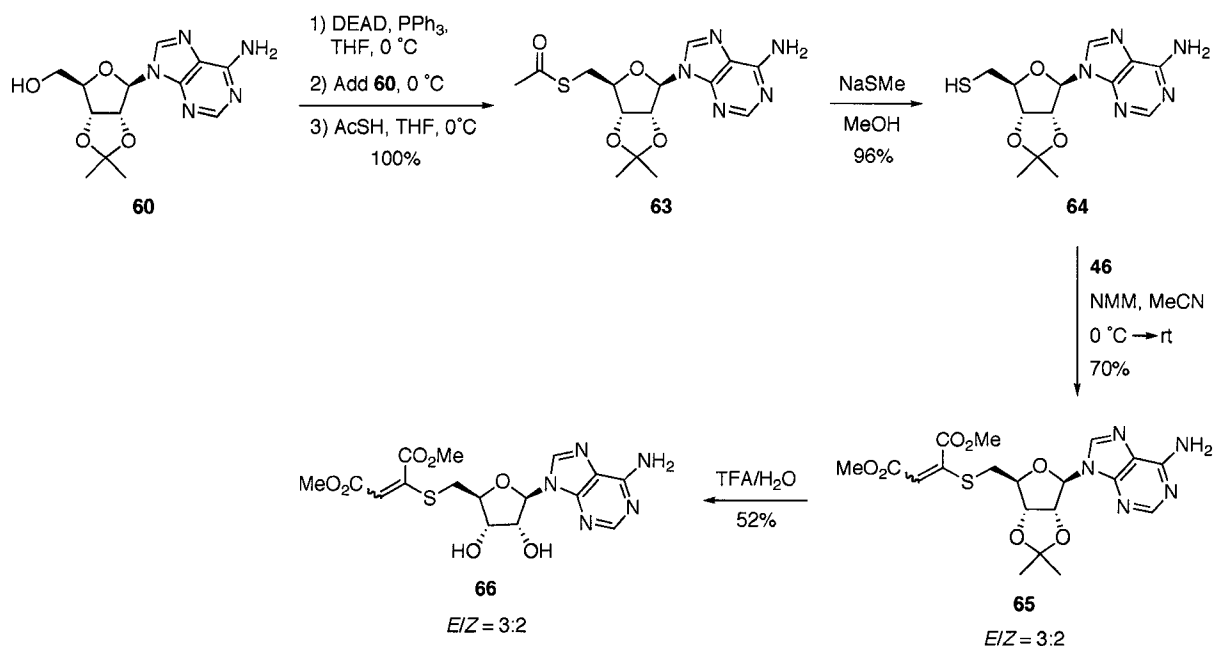
^aNR = no reaction, nucleoside starting material recovered

^badenosine used as starting material

1.2 Adenosine Dicarboxylates Containing a Thioether Linkage

The dicarboxylate analogues containing a thioether linkage are based on adenosine because the 5'-thiol functionality can be conveniently installed *via* Mitsunobu conditions⁹⁷ using thiolacetic acid.⁹⁸ Thus, 2',3'-*O*-isopropylideneadenosine (**60**) reacts with thiolacetic acid in the presence of diethyl azodicarboxylate (DEAD) and triphenylphosphine to quantitatively afford thioacetate **63** (Scheme 8). Removal of the acetyl group is accomplished with sodium thiomethoxide,⁹⁹ giving thiol **64**. Addition of **64** to DMAD (**46**) using an adaptation of a published procedure¹⁰⁰ affords **65** as an inseparable 3:2 mixture of *E* and *Z* isomers. Treatment of mixture **65** with aqueous TFA yields **66**. Unfortunately, all attempts to separate the *E* and *Z* isomers were unsuccessful, therefore it was decided to exchange **46** for the bulkier dibenzyl acetylenedicarboxylate (**52**) in the hopes that the size of the benzyl groups would provide sufficient discrimination between the *E* and *Z* isomers.

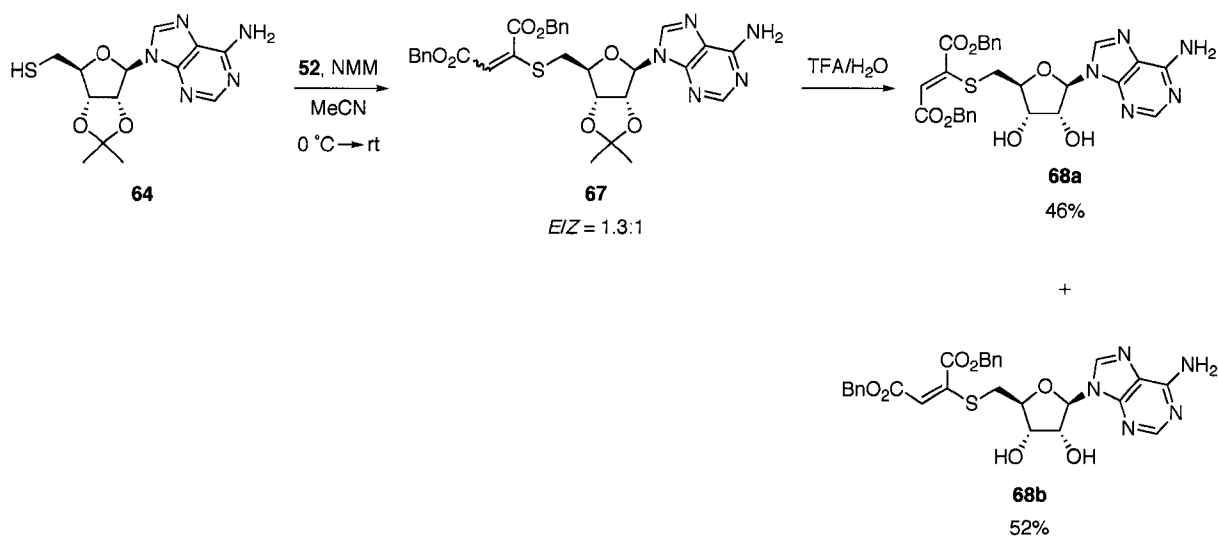
Scheme 8. Synthesis of **66** as an inseparable mixture of *E* and *Z* isomers.



Nucleophilic addition of **64** to **52** in the presence of *N*-methylmorpholine (NMM) gives **67** as an inseparable 1.3:1 mixture of *E* and *Z* isomers (Scheme 9). However, after removal of the isopropylidene protecting group with aqueous TFA, separation can be achieved by careful chromatography using a mixture of CHCl₃/MeOH/TFA (95:4:1) to afford fumarate **68a** in 46% yield and maleate **68b** in 52% yield. Several conditions were explored in an attempt to remove the benzyl groups from **68b** to give maleic acid **69b** or the corresponding dicarboxylate salts **70b** or **71b** (Scheme 10 and Table 2). Use of standard hydrogenation conditions at 1 atm H₂ with either Pd/C (Entry 1) or Pd(OH)₂/C (Entry 2) results in recovered starting material. Similar results are obtained if pressures of 40-50 psi (Entries 3 and 4) or transfer hydrogenation (Entry 5) are employed. An increase in both pressure (50 psi) and temperature (70 °C) results in decomposition with some recovered starting material (Entry 6). It is possible that poisoning of the Pd catalyst by the sulfide functionality in the substrate is occurring. Basic conditions using either

K_2CO_3 (Entry 7) or $LiOH$ (Entry 8) generate a complex mixture, as do Lewis acidic conditions with either TMSOTf (Entry 9) or *in situ* generated TMSI (Entry 10). These conditions are apparently too harsh for the nucleoside.

Scheme 9. Synthesis thioether-linked fumarate **68a** and maleate **68b**.



Scheme 10. Attempted removal of benzyl groups from **68b**.

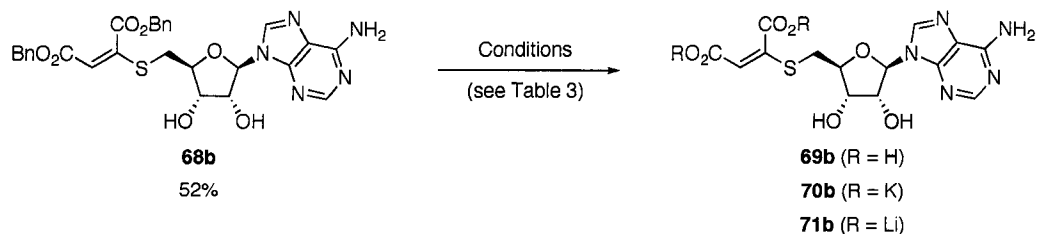


Table 2. Reactions attempted for removal of benzyl groups from **68b**.

Entry	Conditions	Result ^a
1	H ₂ (1 atm), 10% Pd/C, THF/H ₂ O (11:1), 16 h	NR
2	H ₂ (1 atm), Pd(OH) ₂ /C, THF/H ₂ O (10:1), 74 h	NR
3	H ₂ (40 psi), 10% Pd/C, THF/H ₂ O (10:1), 2 h	NR
4	H ₂ (50 psi), Pd(OH) ₂ /C, THF/H ₂ O (10:1), 16 h	SM + decomposition
5	1,4-dicyclohexadiene, 10% Pd/C, DMF, 5 h	NR
6	H ₂ (50 psi), 10% Pd/C, 70 °C, THF/H ₂ O (9:1), 2.5 h	SM + decomposition
7	K ₂ CO ₃ , THF/H ₂ O (1:1), 288 h	Complex mixture
8	LiOH·H ₂ O, THF/H ₂ O (1:1), 8 h	Complex mixture
9	TMSOTf, TFA, 0 °C, 2 h	Complex mixture
10	NaI, TMSCl, MeCN, 5 min	Complex mixture

^aNR = no reaction, starting material recovered

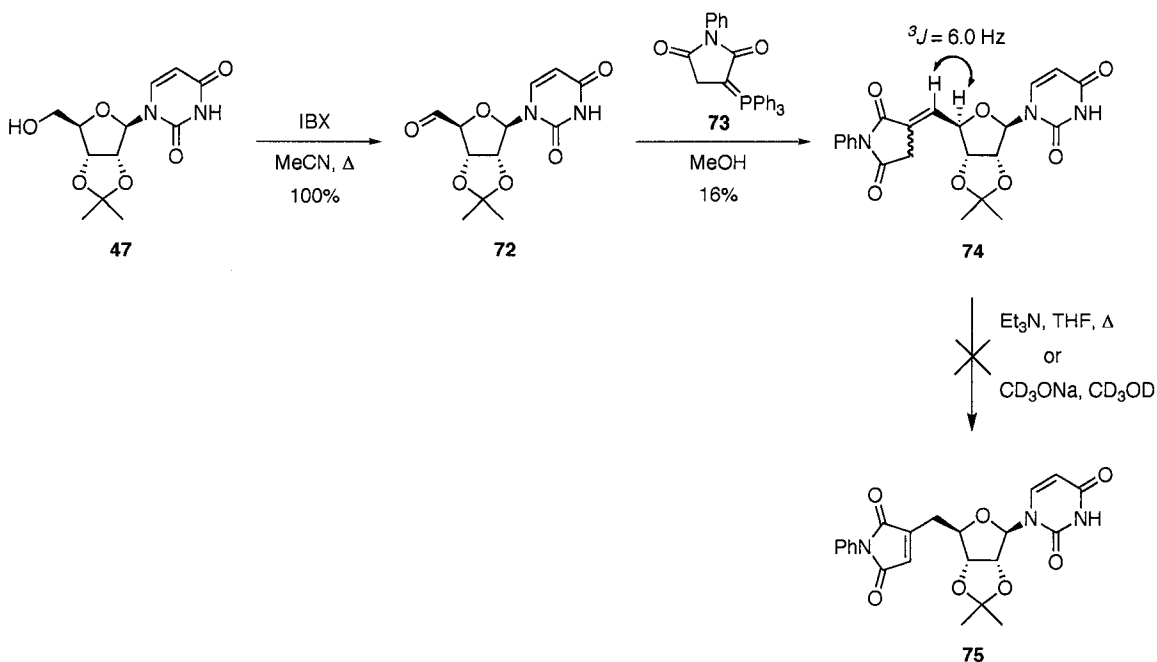
SM = starting material

Presumably, many of the problems encountered during synthetic manipulations of the ether- and thioether-linked analogues are due to the labile vinyl ether or vinyl thioether functionalities. These difficulties, in conjunction with the requirement of tedious separation of *E* and *Z* isomers, made it difficult to justify devoting any more time to these targets. Therefore, the decision was made to focus all efforts on syntheses of the nucleoside dicarboxylates containing methylene spacers. These analogues are devoid of labile functionality adjacent to the dicarboxylate moiety. Furthermore, they can take advantage of the availability of several methods to access the *cis*-dicarboxylate exclusively, eliminating the need for separations of isomers.

1.3 Nucleoside Dicarboxylates Containing Methylene Spacers

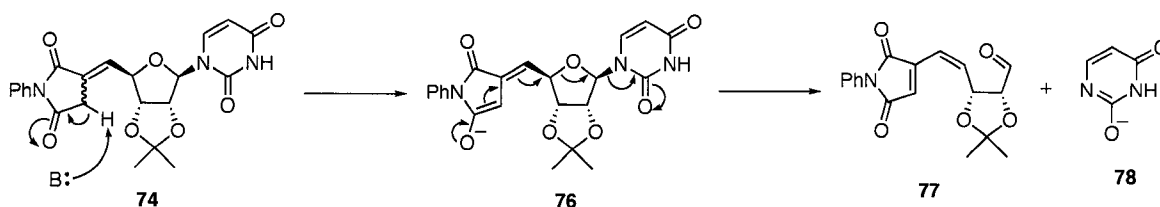
Initial studies into the synthesis of the methylene-linked analogues focused on the synthesis of an analogue containing one methylene spacer. The approach taken was based on a report by Theodoropoulos and co-workers demonstrating that triphenylphosphine-maleimide adducts can undergo Wittig reactions.¹⁰¹ Thus, oxidation of **47** with *o*-iodoxybenzoic acid (IBX) (prepared according to the procedure of Frigerio *et al.*¹⁰²) affords aldehyde **72** in quantitative yield (Scheme 11). This undergoes a Wittig reaction with phosphorane **73**¹⁰¹ in MeOH to provide uridine succinimide derivative **74** in 16% yield after flash chromatography and HPLC. The low yield may be a result of using MeOH as the solvent for the reaction. It was observed by ES-MS that MeOH adds to aldehyde **72** to give the corresponding hemiacetal. Although this hemiacetal is in equilibrium with the aldehyde, the excess MeOH would be expected to shift the equilibrium towards the hemiacetal, leaving little aldehyde to undergo the Wittig reaction. Although at the time the reaction was done, the conditions of Theodoropoulos and co-workers were being followed, in retrospect, CH₂Cl₂ or DMSO would have better choices of solvents for this reaction.

Scheme 11. Attempted synthesis of uridine maleimide **75**.



It was hoped that the double bond in **74** would spontaneously isomerize to give the thermodynamically more stable product **75**; however, this does not appear to be the case. The exocyclic position of the double bond is confirmed by coupling of the H-5' vinylic hydrogen to H-4' of the ribose ring ($J = 6.0$ Hz). Such a large J -value would not be expected between the vinylic hydrogen and H-4' of **75**. Attempts to isomerize **74** to **75** using Et_3N in refluxing THF or CD_3ONa in CD_3OD (monitoring by ^1H NMR) were unsuccessful. In each case, addition of the base to the reaction mixture immediately gives a deep red to purple solution, possibly arising from deprotonation of succinimide **74** and subsequent extrusion of the uracil functionality to give conjugated product **77** (Scheme 12).

Scheme 12. Possible mechanism for degradation of uridine maleimide **74**.

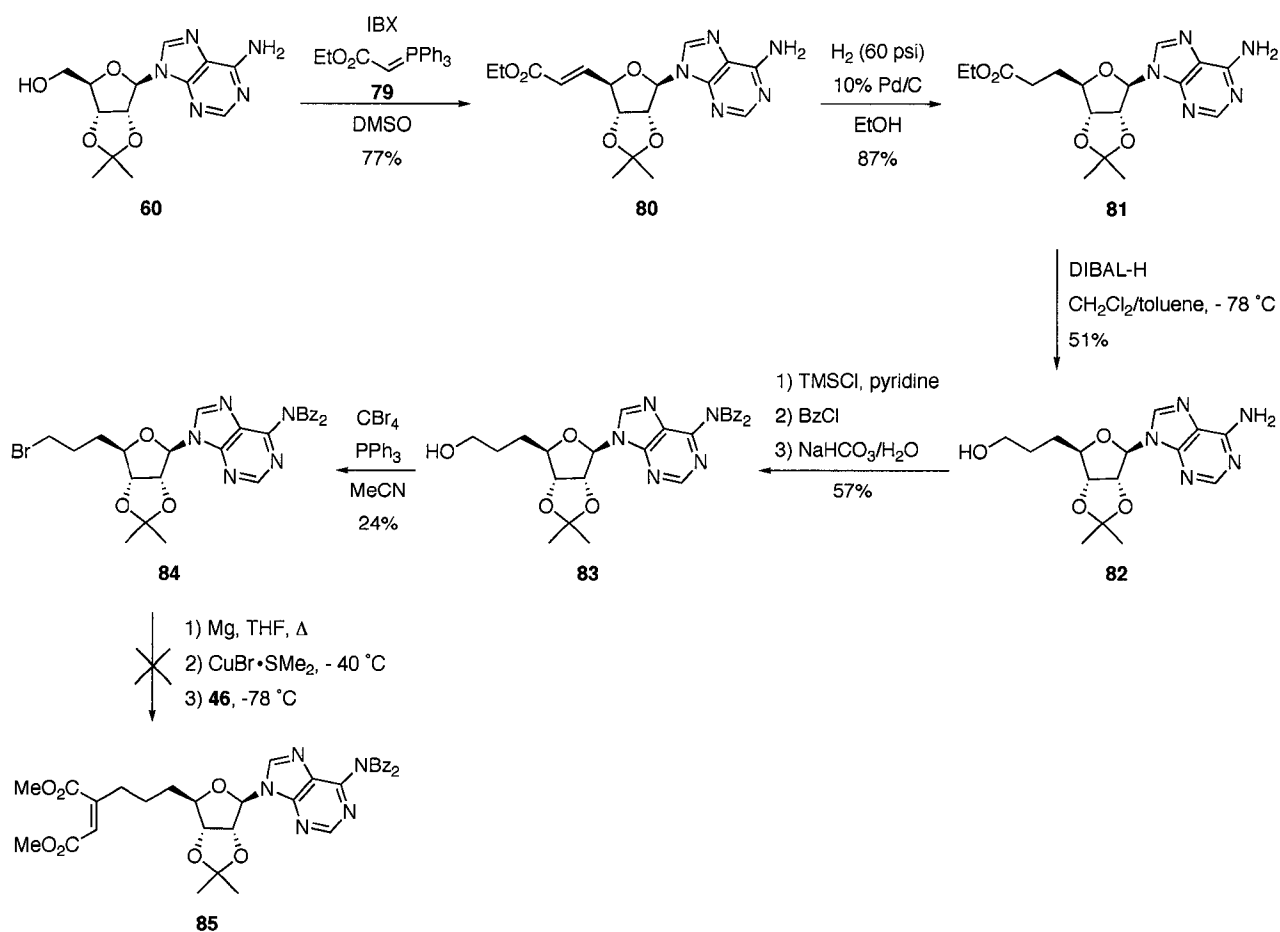


Concurrently with these synthetic studies, some simple modeling studies using Chem3D were done to determine the length of the spacer between the ribose ring and the dicarboxylate that would give optimum overlap of the analogue with its parent nucleoside diphosphate. It was found that a 3-carbon spacer provides the flexibility and length required for the dicarboxylate to achieve the position of the diphosphate of the natural nucleoside while maintaining reasonable overlap of the ribose and heterocyclic base moieties between the two. The decision was made to direct efforts on obtaining a nucleoside diphosphate analogue containing three methylene groups.

The most obvious approach for obtaining a maleate-containing analogue with a three-carbon spacer involves 1,4-organocuprate addition to **46** (Scheme 3). We have shown that this reaction proceeds with greater than 99:1 *Z/E* selectivity using simple cuprates.⁶¹ The requisite spacer consisting of three methylene groups can be conveniently installed *via* a Wittig reaction. Starting with 2',3'-*O*-isopropylideneadenosine (**60**), oxidation with IBX and Wittig olefination with ((ethoxycarbonyl)methylene)-triphenylphosphorane (**79**) in one pot¹⁰³ gives α,β -unsaturated ester **80** (Scheme 13). Hydrogenation over Pd/C affords saturated ester **81**, which is then reduced to alcohol **82** with diisobutylaluminum hydride (DIBAL-H). This reduction is not reproducible, with yields varying from trace amounts to a high of 51%. The reason for this may be that the DIBAL-H is able to coordinate at several points in the nucleoside framework, and this

may act to sequester the nucleoside upon workup, during which insoluble aluminum salts are formed. Transient protection of the alcohol functional group of **82** with TMSCl is then followed by treatment with benzoyl chloride. The TMS group is then removed using aqueous NaHCO₃ to give di-benzoylated product **83**. Upon treatment with carbon tetrabromide and triphenylphosphine, this undergoes conversion to the bromide **84**. Unfortunately, subjecting **84** to Grignard conditions does not result in formation of the Grignard reagent, as observed by TLC.

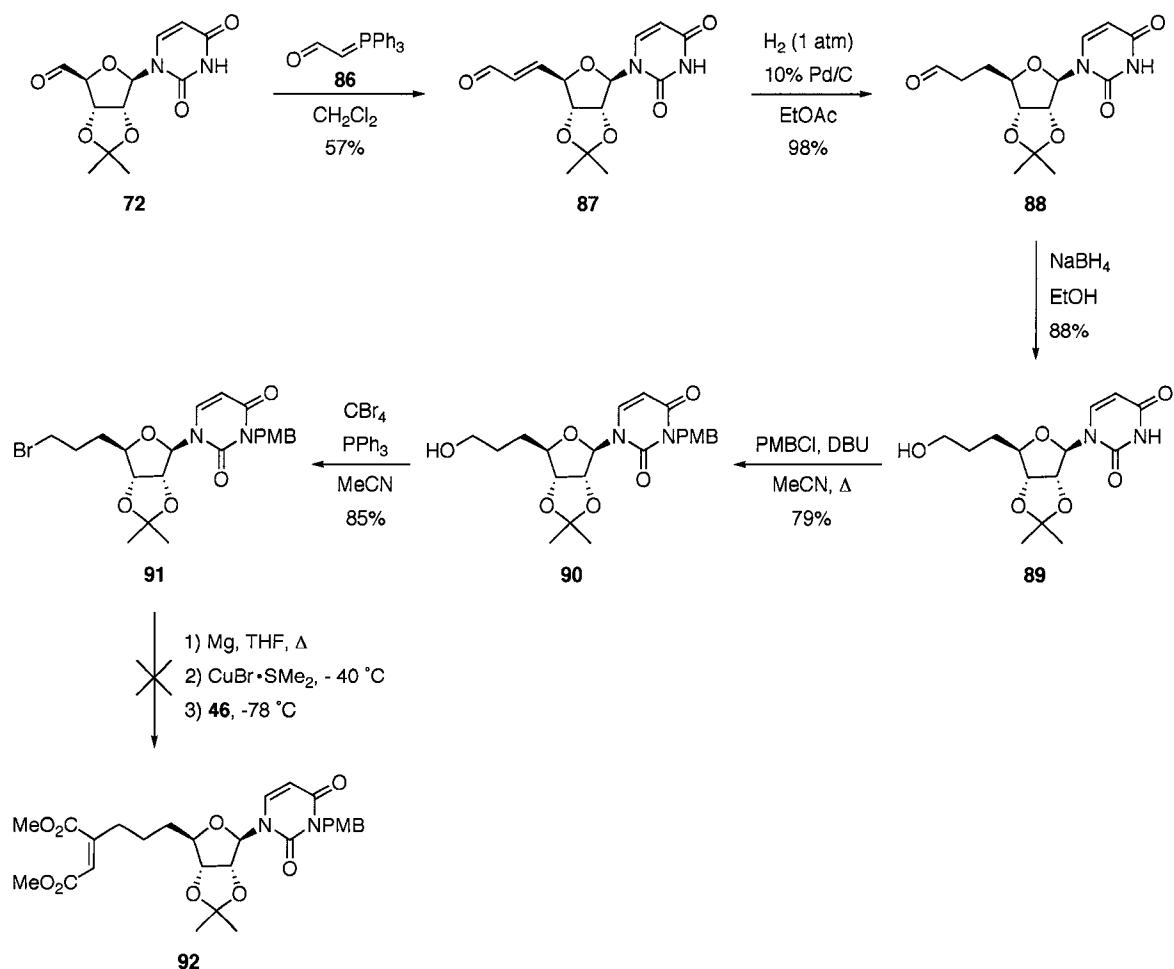
Scheme 13. Attempted synthesis of adenosine dimethyl maleate **85** via organocuprate addition.



At this point, it became clear that the amide protecting groups for the NH₂ functionality on the adenine ring are not suitable for Grignard conditions. As well, the acidity of H-8 in the adenine ring precludes formation of the Grignard reagent at an sp³ centre in this molecule. H-8 is easily abstracted with LDA¹⁰⁴ (pK_a 35.7 in THF).¹⁰⁵ Thus, no attempt was made to recover unreacted **84**, and it was decided to explore this route for a methylene-linked analogue using uridine instead.

The synthesis of the uridine derivative was approached in the same general manner as that of the adenosine analogue, with some modifications. In order to avoid using DIBAL-H, the Wittig reaction was performed with (triphenylphosphoranylidene)acetaldehyde (**86**), allowing the resulting aldehyde to be reduced under mild conditions using NaBH₄. Reaction of **86** with **72** results in α,β -unsaturated aldehyde **87** (Scheme 14). Reduction of the double bond is achieved by hydrogenation over Pd/C to give **88**. This aldehyde is then reduced to alcohol **89** using NaBH₄. The N-3 position of the uracil ring is then protected using PMBCl to give **90**. Bromide **91** is then formed from **90** using the same conditions as previously described. As in the previous attempt at cuprate addition to **46** using the adenosine derivative (Scheme 12), formation of maleate **92** did not occur. Instead, **91** was recovered in impure form.

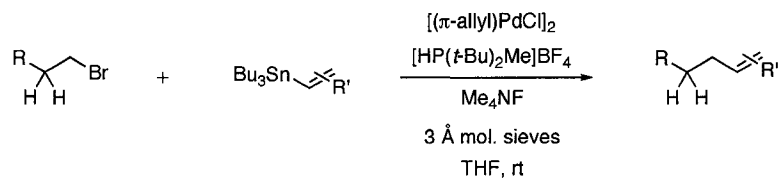
Scheme 14. Attempted synthesis of uridine dimethyl maleate **92** *via* organocuprate addition.



The harsh conditions required for formation of the Grignard reagent and its high reactivity prompted a search for an approach wherein the carbon-bromine bond could be activated under milder conditions. Gratifyingly, Fu and co-workers had recently reported conditions which allowed the Stille cross-coupling of alkyl bromides containing β -hydrogens with alkenyl tin reagents (Scheme 15).¹⁰⁶ The success of the methodology depended on the use of the additive Me_4NF to increase the rate of transmetalation and the

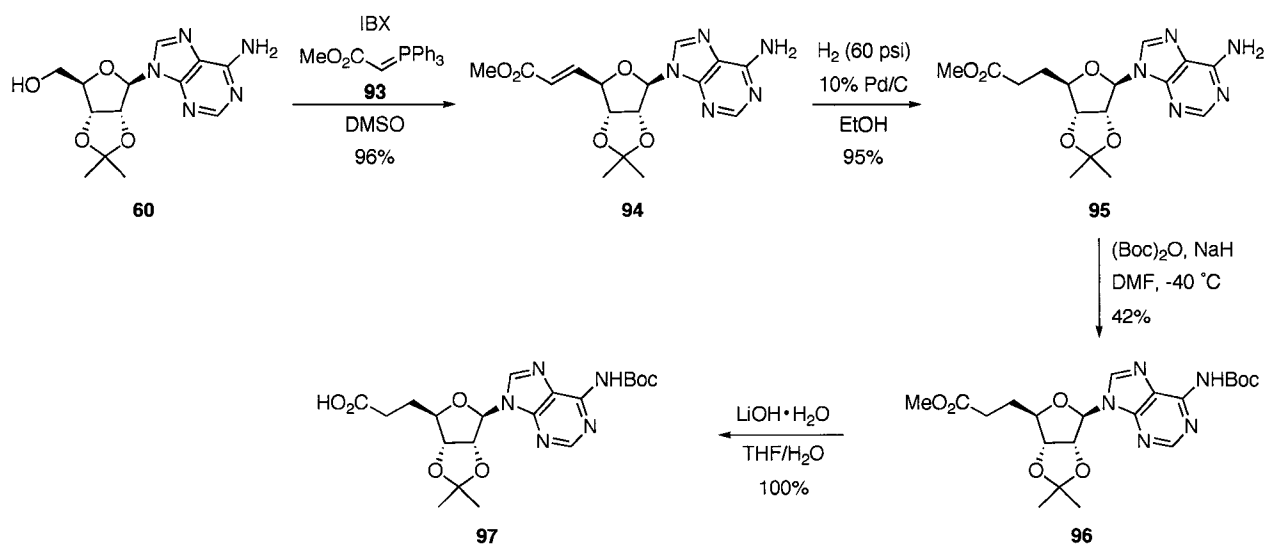
bulky ligand $P(t\text{-Bu})_2\text{Me}$ to prevent β -hydride elimination in the organopalladium complex.

Scheme 15. Conditions of Fu and co-workers for Stille coupling of β -hydrogen-containing alkyl bromides.¹⁰⁶



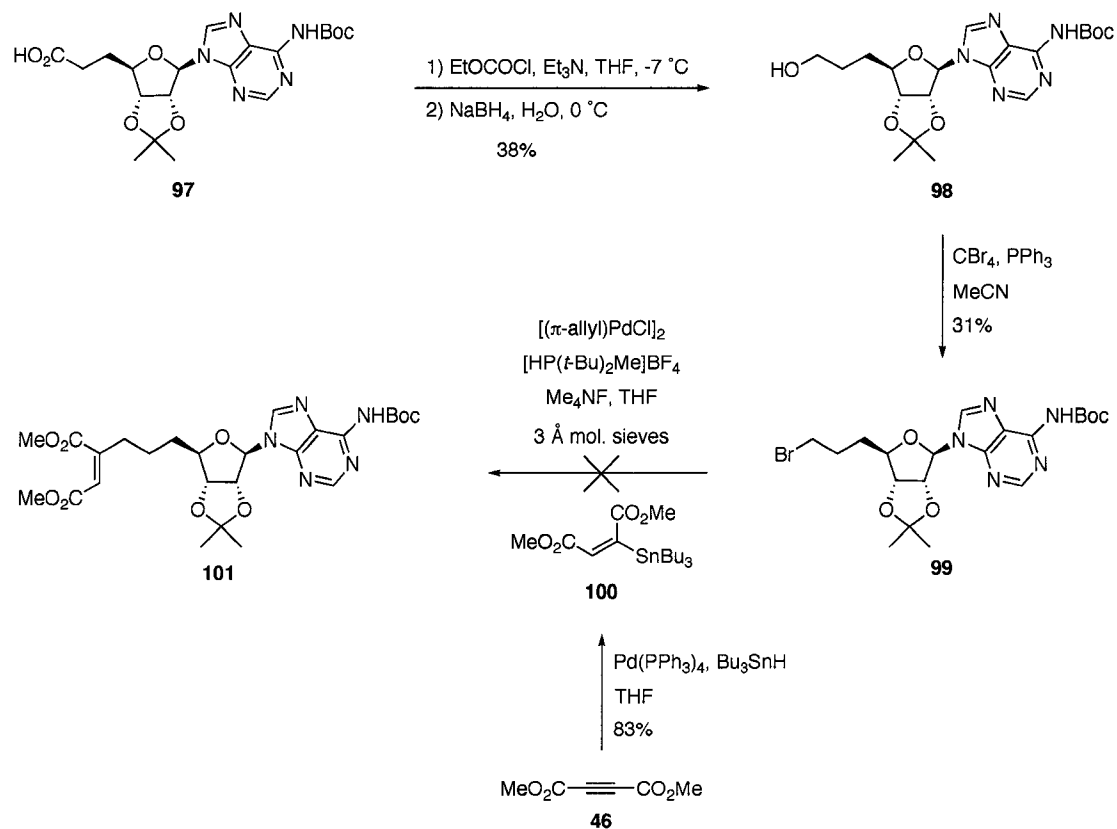
It was decided to apply this methodology to the synthesis of nucleoside dicarboxylates. Starting with **60**, IBX oxidation and Wittig olefination using ((methoxycarbonyl)methylene)triphenylphosphorane (**93**) gives α,β -unsaturated ester **94** (Scheme 16). Hydrogenation over Pd/C yields reduced product **95**. Treatment of this compound with $(\text{Boc})_2\text{O}$ and NaH gives Boc-protected derivative **96**. Hydrolysis of the ester of **96** is achieved with LiOH to give acid **97** quantitatively.

Scheme 16. Synthesis of carboxylic acid **97**.



Reduction of the acid to the alcohol proceeds first with treatment of **97** with ethyl chloroformate to form the mixed anhydride (Scheme 17). This is then reduced with NaBH₄, giving the corresponding alcohol **98**. A significant quantity of unreacted mixed anhydride (22%) is also isolated. The elaboration of **98** to bromide **99** using carbon tetrabromide and triphenylphosphine proceeds in low yield. The requisite vinyl stannane **100** for the Stille coupling can be obtained in one step by palladium-catalyzed hydrostannylation of **46**.¹⁰⁷ The $^3J_{\text{Sn-H}}^{117}$ and $^3J_{\text{Sn-H}}^{119}$ values of 46.8 Hz and 48.0 Hz, respectively, are consistent with a *cis* relationship.¹⁰⁸ The expected values for a *trans* relationship are in the 110-130 Hz range.¹⁰⁹ Upon subjecting **99** and **100** to Fu's conditions for the modified Stille coupling, none of the desired product **101** is obtained. Workup and purification results in recovery of unreacted **99** in ~ 22% yield or of impure stannane **100**, as well as material that upon examination by ¹H NMR appears to have undergone decomposition. The problem may reside in the use of **100**, which is an electron-deficient vinyl stannane, and therefore may be deactivated toward transmetalation. The study by Fu was limited to electron-rich alkenyl tin reagents and simple alkyl bromides.¹⁰⁶ A recent example showed that the cross-coupling of an electron-deficient aryl stannane required the presence CuI and CsF in order to achieve high yields.¹¹⁰ Indeed, the Stille cross-coupling reaction in general is notorious for sometimes presenting difficulties, as the choice of catalyst, ligands, additives, solvent, and temperature can significantly affect the outcome and yield of the reaction.¹¹¹

Scheme 17. Attempted synthesis of adenosine dimethyl maleate **101** using conditions of Fu.¹⁰⁶

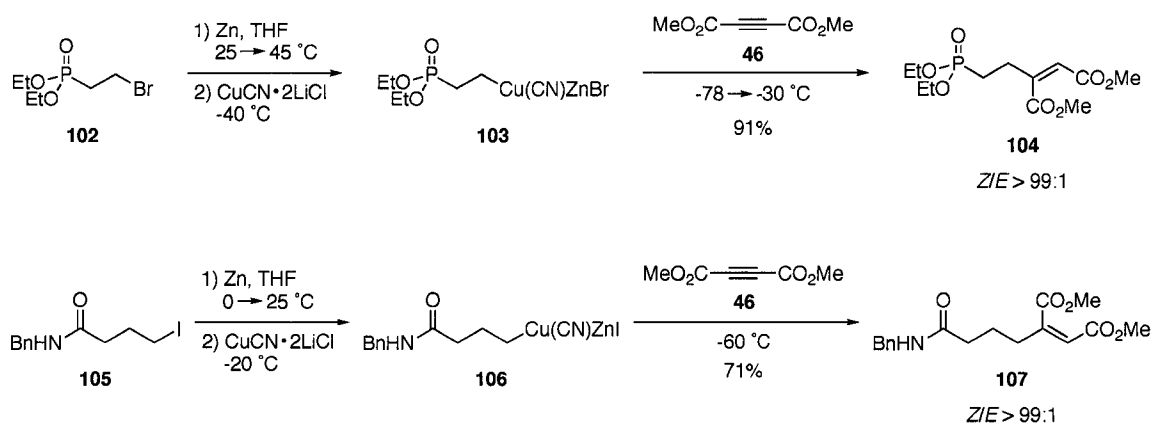


Conjecturing that the alkyl bromide may not be reactive enough to readily undergo oxidative addition of metals into the carbon-bromine bond, it was decided to deviate slightly from this approach. The use of alkyl iodides to form organozinc compounds was especially enticing, as organozinc reagents can be formed under mild conditions from primary alkyl iodides (2-3 h, 35-40 °C).¹¹² Furthermore, their low reactivity stemming from the relatively high covalent character of the carbon-zinc bond makes them especially attractive from the viewpoint of nucleoside chemistry, where synthetic manipulations must often contend with a multitude of functional groups. On the other hand, the low-lying p orbitals of zinc permit many transmetalation reactions

with metallic salts to proceed, including those of Cu, Ti, Pd, Ni, and Pt, giving rise to more reactive organometallic species.¹¹²

Knochel and co-workers have shown that organozinc reagents of the form RZnX (X = Br, I) undergo rapid transmetalation using the THF-soluble copper salt CuCN·2LiCl, giving reagents with the general structure RCu(CN)ZnX. These undergo addition to several electrophiles, including 1,4-addition to α,β -unsaturated carbonyl compounds¹¹³ such as DMAD (**46**). The maleate is obtained in high yield with no detection of the corresponding fumarate, as shown by the examples in Scheme 18.^{114, 115} The mildness of the organozinc reagents is highlighted by the presence of the relatively acidic amide N-H in **105**, which does not interfere with the reaction.

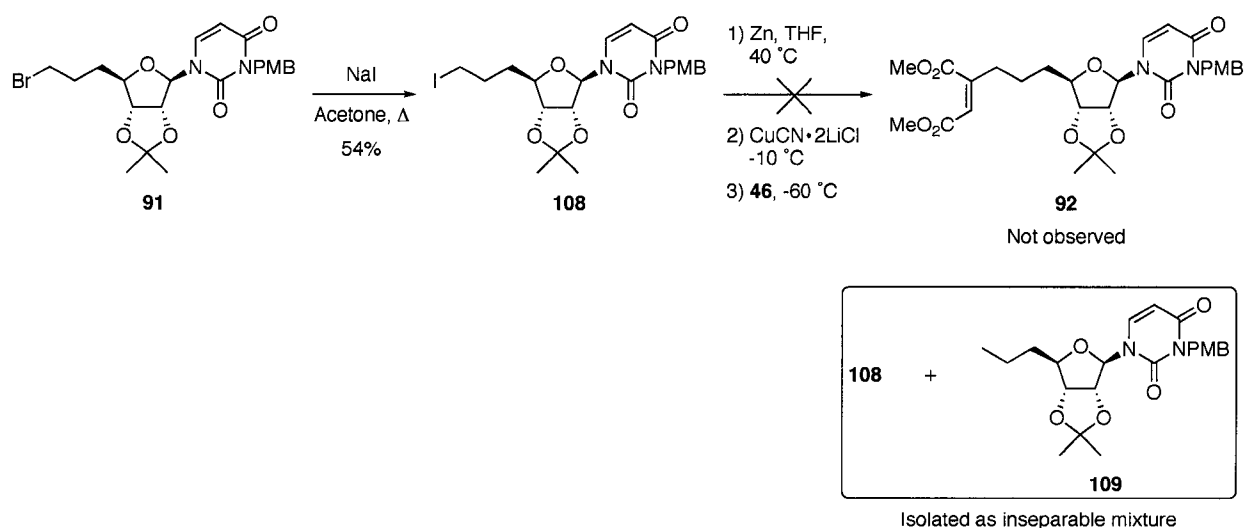
Scheme 18. Selected examples of 1,4-addition to **46** using organocuprates derived from organozinc reagents.^{114, 115}



Iodide **108** can be rapidly obtained from the corresponding bromide **91** via a Finkelstein reaction (Scheme 19). For the organozinc formation, the zinc metal was freshly prepared by lithium reduction of ZnCl₂.¹¹⁶ This results in a zinc powder that is far

more reactive than the metal prepared by potassium or sodium reduction. Upon subjecting **108** to Knochel's conditions¹¹⁵ for organozinc formation, transmetalation to the cuprate, and addition to **46**, none of the expected dimethyl maleate **92** is obtained. Instead, an inseparable mixture of unreacted **108** and quenched organometallic reagent **109** are isolated.

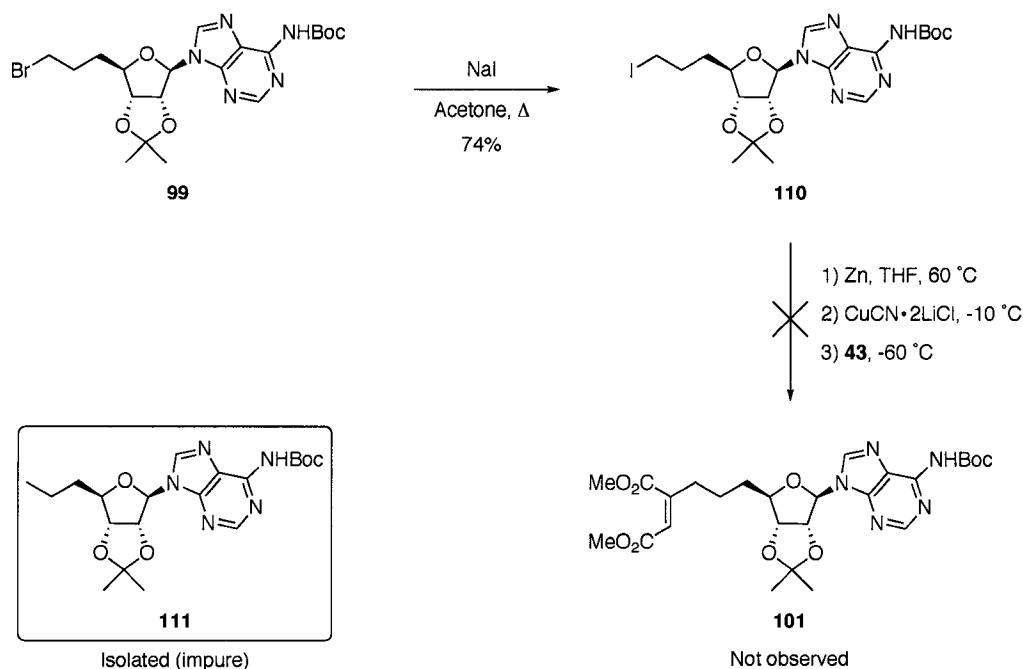
Scheme 19. Attempted synthesis of **92** via an organocuprate derived from an organozinc reagent.



Bromide **99** can also be easily converted to its corresponding iodide **110**, therefore it was investigated concurrently for formation of a dicarboxylate through this methodology (Scheme 20). In this case, the zinc powder was further activated by heating in the presence of 1,2-dibromoethane,¹¹⁷ and the reactivity of the carbonyl moiety of **46** was enhanced through the addition of TMSCl. Furthermore, formation of the organozinc reagent was conducted at 60 °C rather than 40 °C. Despite these modifications, the reaction did not proceed as expected, and quenched organometallic reagent **111** was

isolated in low purity. Although zinc insertion into the carbon-iodine bond occurs to some extent in both cases, transmetalation to the cuprate and/or 1,4-addition to **46** are impeded. The reasons for this are not clear.

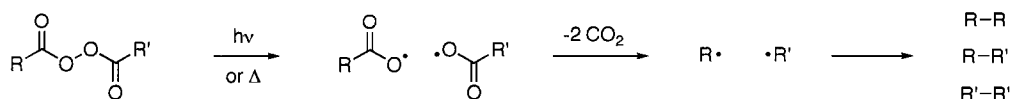
Scheme 20. Attempted synthesis of **101** *via* an organocuprate derived from an organozinc reagent.



The multitude of difficulties encountered with the formation and reaction of nucleoside-derived organometallic reagents called for a paradigm shift in how the nucleoside moiety could be attached to that of the dicarboxylate. In this new approach, it was sought to pre-form the maleate and the 5'-derivatized nucleoside as separate entities such that each would contain an appended functionality that would enable the two ends to be coupled using well-established chemistry. One attractive option is the photochemical decomposition of diacyl peroxides. It has long been known that photolysis (or

thermolysis) of diacyl peroxides proceeds to generate acyloxy radicals that decarboxylate to form alkyl radicals (Scheme 21). These will then either recombine or disproportionate to form stable products. If the R and R' groups are different, a complex mixture is often obtained due to crossover radical coupling. However, in the mid-1980s Schäfer and co-workers reported that photolyses of unsymmetrical aliphatic diacyl peroxides conducted at -78 °C in the absence of solvent lead to radical recombination in good yield without scrambling.¹¹⁸⁻¹²¹ This is due to restricted movement of the reactive partners in the solid state, enhancing cage recombination of the alkyl radicals.

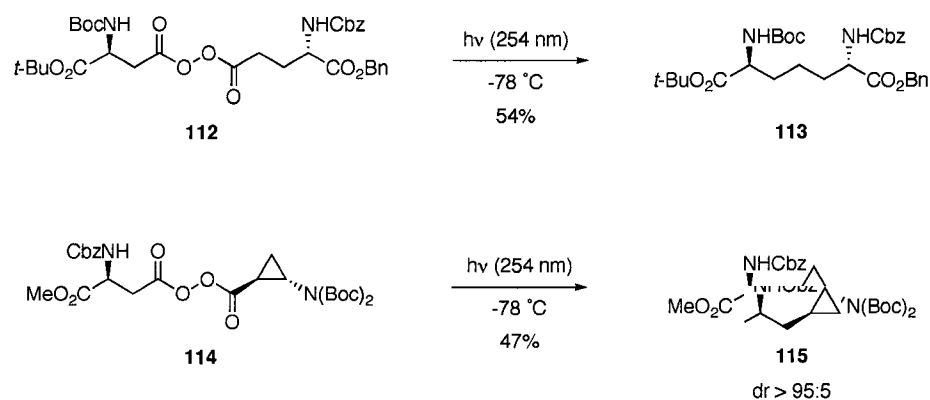
Scheme 21. Decomposition of diacyl peroxides with radical coupling.



We recently expanded on this observation and showed that unsymmetrical diacyl peroxides derived from protected aspartic and/or glutamic acids¹²² (e.g. **112**) as well as cyclopropane carboxylic acids¹²³ (e.g. **114**) could be coupled to give highly functionalized amino acid derivatives (**113** and **115**, respectively) in moderate yields without crossover (Scheme 22).

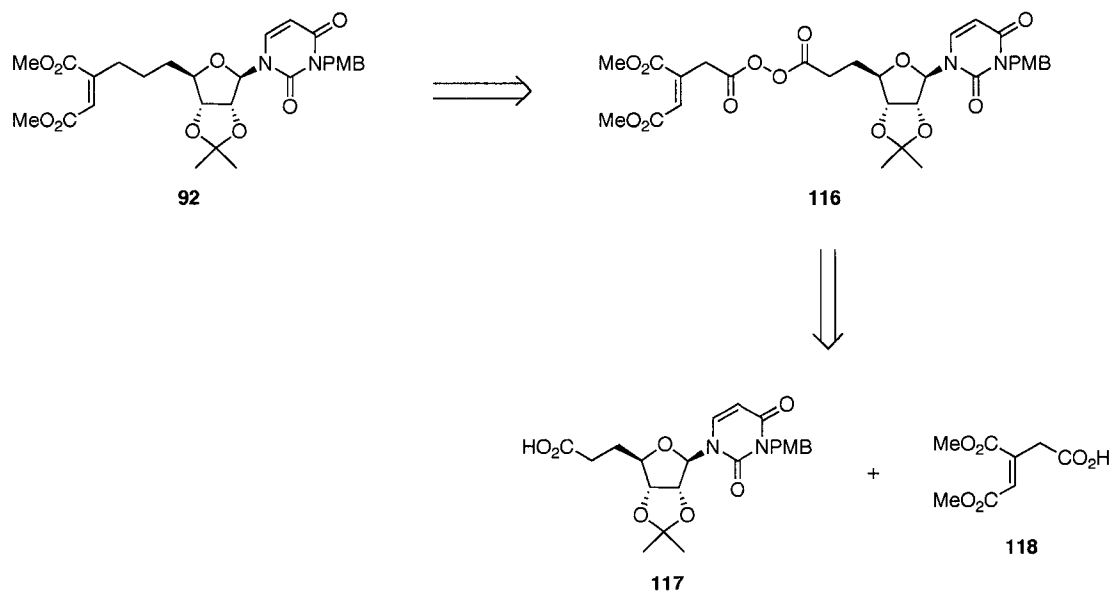
Scheme 22. Synthesis of functionalized amino acids by photolysis of diacyl peroxides.^{122,}

123



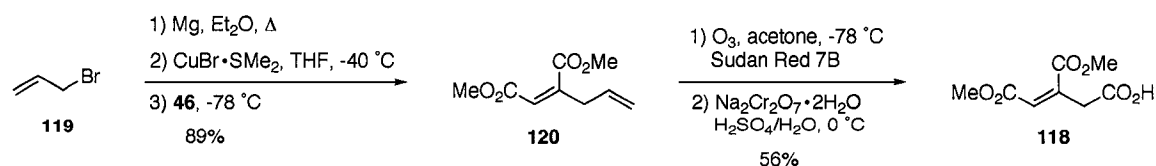
The tolerance of this methodology towards several functional groups provided optimism for its use in the synthesis of nucleoside derivatives. At this point, the decision was made to focus exclusively on analogues of UDP, as uridine derivatives are generally easier to handle than their corresponding adenosine congeners because of their higher stability and lower polarity. Furthermore, they offer a wider range of protecting group strategies for the nucleobase portion. Fully protected uridine dimethyl maleate **92** can thus be envisioned to arise from the photochemical radical coupling of unsymmetrical diacyl peroxide **116**, which in turn can be generated from easily accessible carboxylic acids **117** and **118** (Scheme 23).

Scheme 23. Retrosynthetic analysis of **92** based on photolysis of diacyl peroxides.



To this end, the maleate coupling portion was generated as shown in Scheme 24. Allyl bromide (**119**) is first converted into its corresponding Grignard reagent and transmetalated to the cuprate using copper(I) bromide dimethylsulfide complex. Addition of allyl cuprate to **46** furnishes dimethyl 2-allylmaleate (**120**). Selective ozonolysis¹²⁴ of the electron-rich terminal double bond with oxidative workup¹²⁵ provides carboxylic acid **118**.

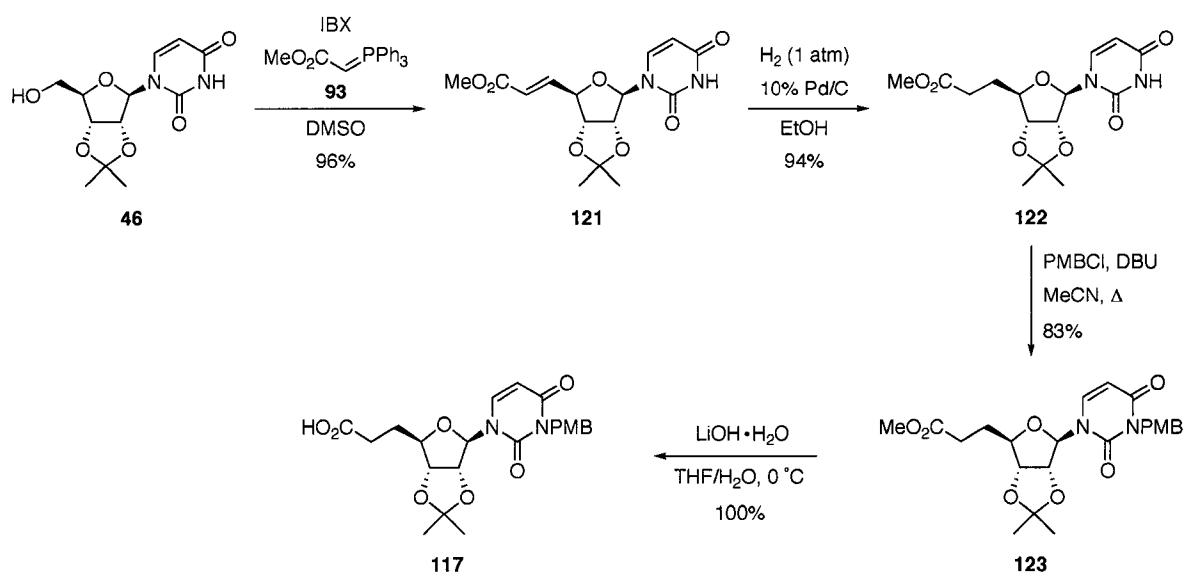
Scheme 24. Synthesis of carboxylic acid **118**.



The synthesis of the nucleoside coupling portion begins with nucleoside **46**. Oxidation with IBX is followed by Wittig reaction with ((methoxycarbonyl)methylene)-

triphenylphosphorane (**93**) in one pot to install the three-carbon extension and give α,β -unsaturated ester **121** (Scheme 25). Reduction of the 5',6'-double bond is done *via* catalytic hydrogenation to give **122**. *p*-Methoxybenzyl (PMB) protection of the N-3 position in the uracil ring is achieved using PMBCl and diazabicyclo[5.4.0]undec-7-ene (DBU) to afford **123**. Hydrolysis of the methyl ester with LiOH then yields carboxylic acid **117** quantitatively.

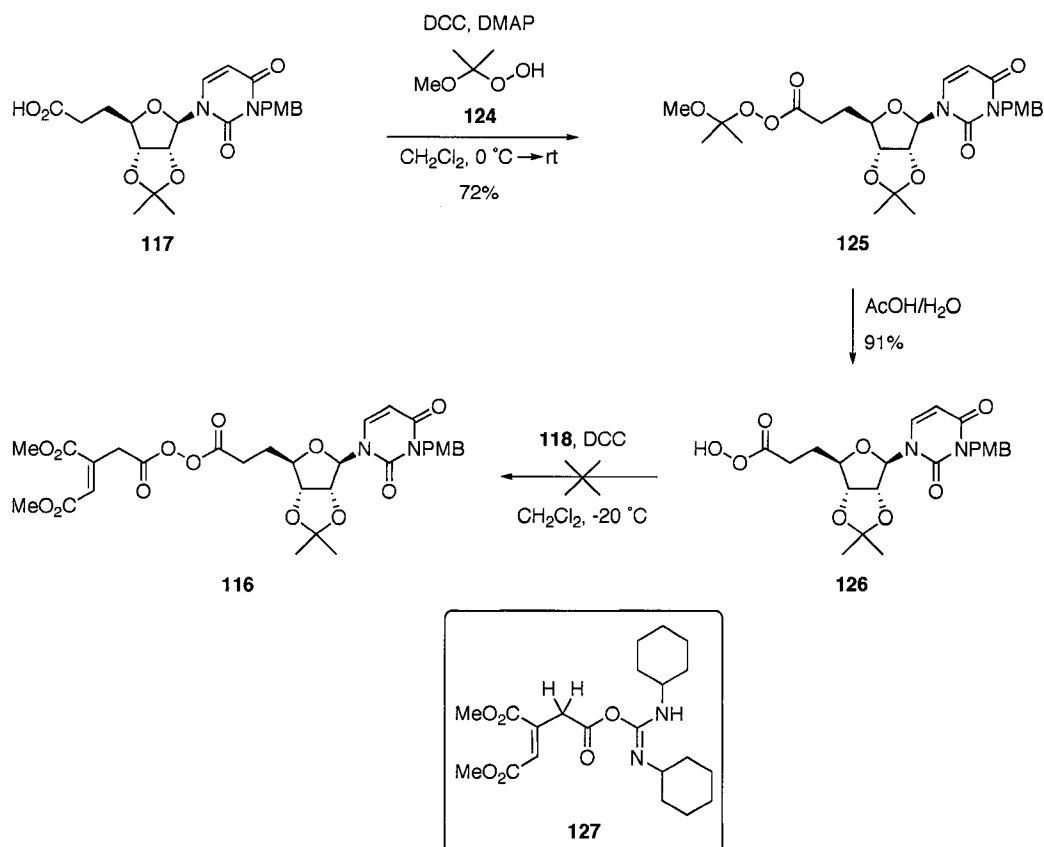
Scheme 25. Synthesis of carboxylic acid **117**.



A dicyclohexylcarbodiimide (DCC)-mediated coupling of this acid with 2-methoxyprop-2-yl hydroperoxide^{126, 127} (**124**) generates perester **125** (Scheme 26). The methoxypropyl group in **125** is hydrolyzed using 50% aqueous acetic acid, leaving the isopropylidene protecting group intact, to afford peracid **126**. All attempts to form diacyl peroxide **116** through coupling of **126** with carboxylic acid **118** result in a complex mixture, with some recovered impure nucleoside starting material. It was thought that the failure of the coupling reaction stems from the enhancement of the acidity of the CH₂

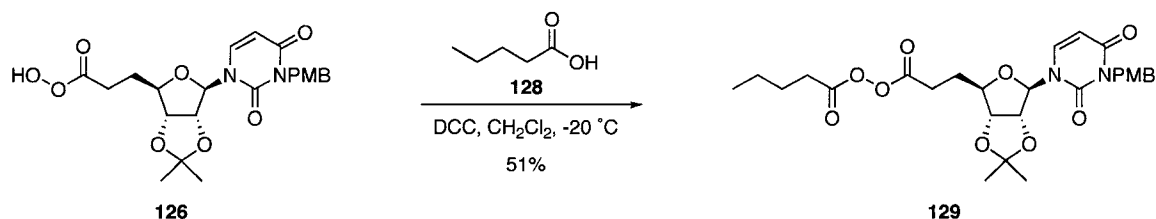
protons upon activation of acid **118** with DCC to give the dicyclohexyl isourea **127** (Scheme 26). Deprotonation at this site gives an anion that is highly resonance-stabilized, and that may subsequently undergo undesired side reactions.

Scheme 26. Attempted synthesis of diacyl peroxide **116**.



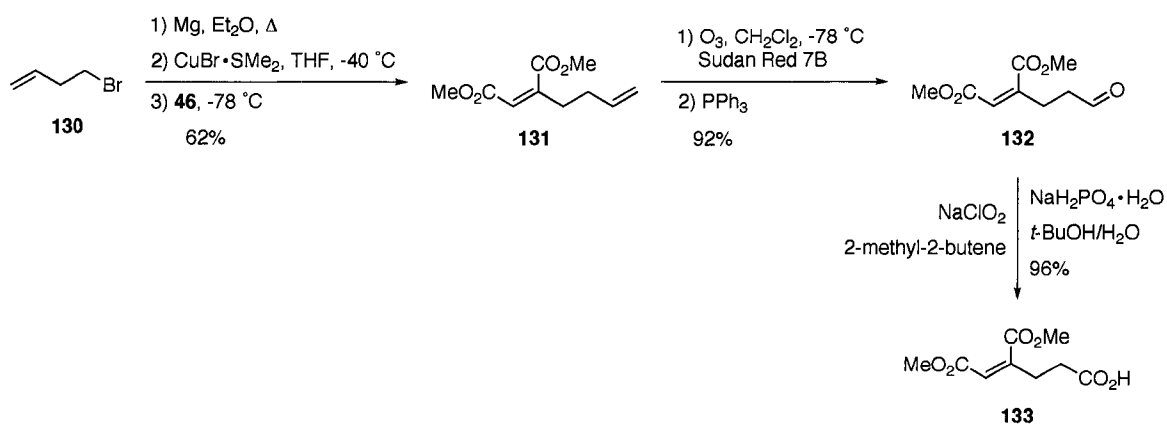
To test this hypothesis, peracid **126** was coupled with the simple carboxylic acid valeric acid (**128**) using the same conditions as described previously. Peracid **126** undergoes DCC-mediated coupling with **128** to cleanly provide diacyl peroxide **129** (Scheme 27), corroborating the hypothesis. Based on these results, it was decided to extend the carbon chain to four methylene groups by adding an extra methylene between the acid and maleate moieties.

Scheme 27. Coupling of **126** and **128** to give diacyl peroxide **129**.



The maleate portion with an extra methylene group was synthesized in a similar manner as for **118**. 3-Butenyl bromide (**130**) is converted into its corresponding Grignard reagent, which is then transmetalated as previous to the cuprate (Scheme 28). The cuprate undergoes 1,4-addition to **46** to give maleate derivative **131**. In this case, ozonolysis of the terminal double bond is followed by a reductive workup using triphenylphosphine to give aldehyde **132**. This is then oxidized with NaClO₂ in a second step to afford carboxylic acid **133**.

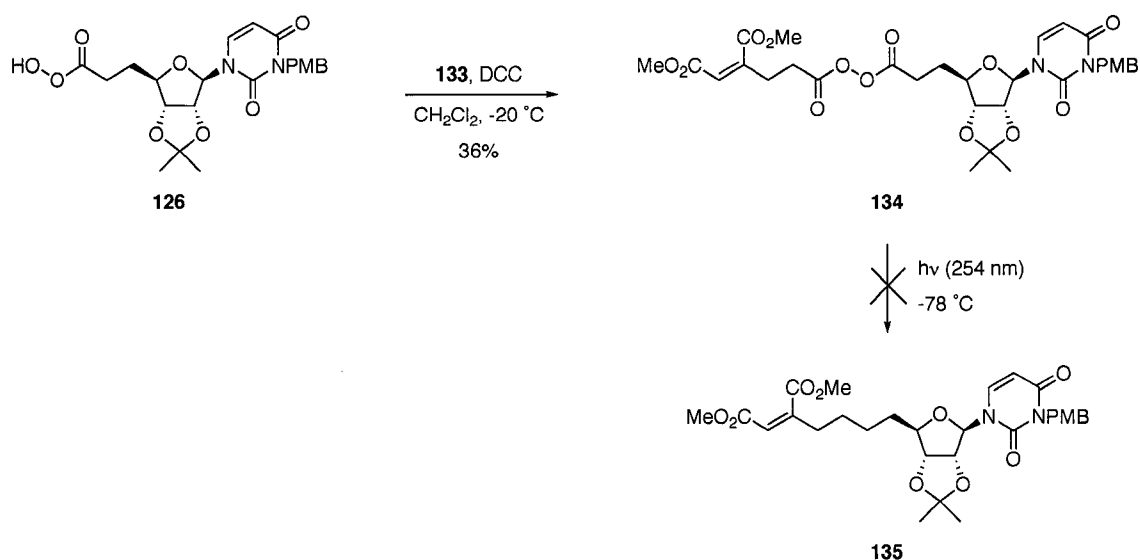
Scheme 28. Synthesis of carboxylic acid **133**.



Carboxylic acid **133** reacts with peracid **126** in the presence of DCC to give diacyl peroxide **134** in a fairly low yield of 36% (Scheme 29). Photolysis of **134** in the solid

state at $-78\text{ }^{\circ}\text{C}$ for 5 days gives only trace amounts of impure uridine maleate **135**, along with 10% unreacted **134**. The mass balance is presumably insoluble polymeric material. The low efficiency of the photolysis may be due to the presence of the PMB protecting group, which is capable of absorbing UV light. It was previously observed that the presence of an Fmoc group hinders facile cleavage of an amino acid-derived diacyl peroxide, ¹²² probably for the same reasons.

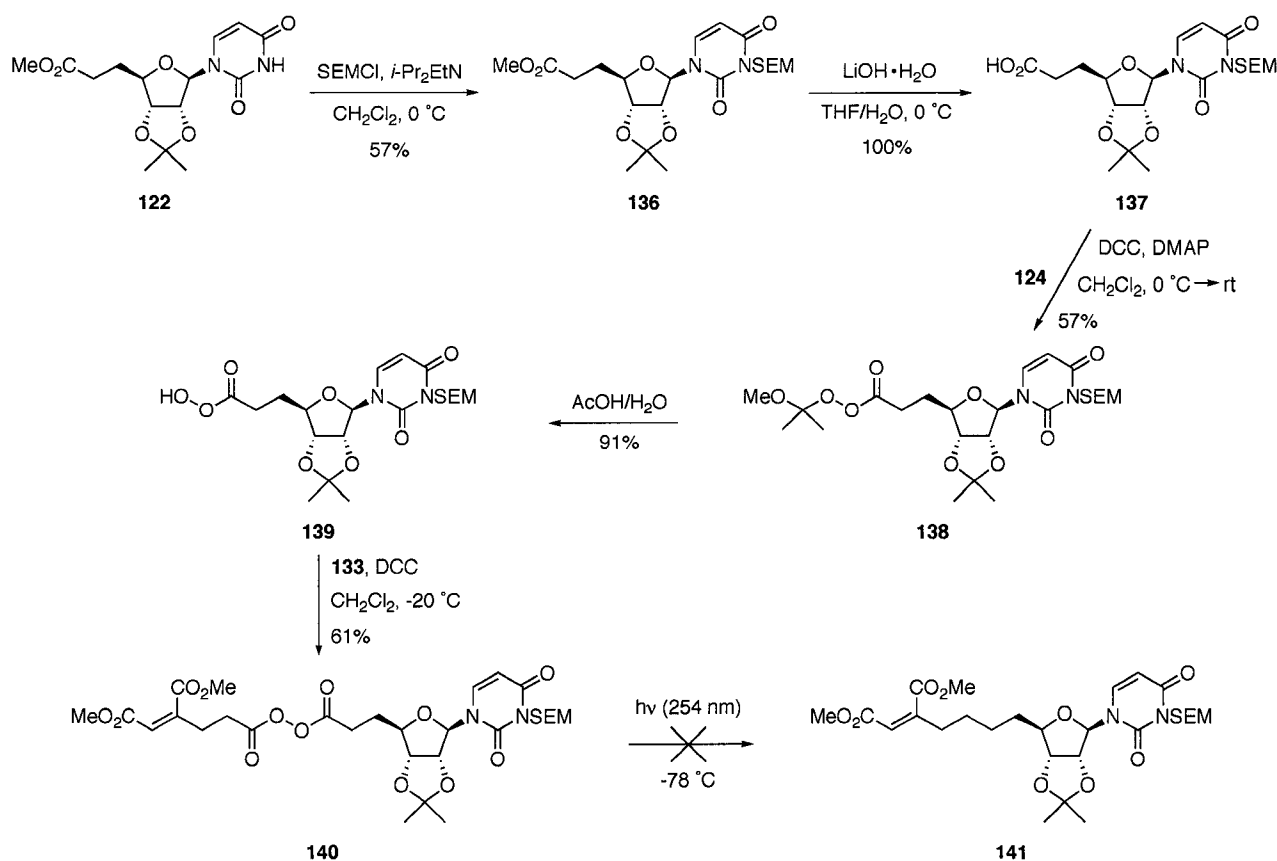
Scheme 29. Attempted synthesis of **135** by photolysis of diacyl peroxide **134**.



To circumvent this problem, the PMB protecting group was changed to the 2-(trimethylsilyl)ethoxymethyl (SEM) group, which is not expected to absorb UV light. Thus, starting from **122**, the SEM group is installed using SEMCl to give protected uridine derivative **136** (Scheme 30). The methyl ester of **136** is hydrolyzed with LiOH to afford carboxylic acid **137** quantitatively. Coupling of **137** with **124** in the presence of DCC gives perester **138**, which is then deprotected with 50% aqueous acetic acid to give peracid **139**. This undergoes reaction with carboxylic acid **133** in the presence of DCC to

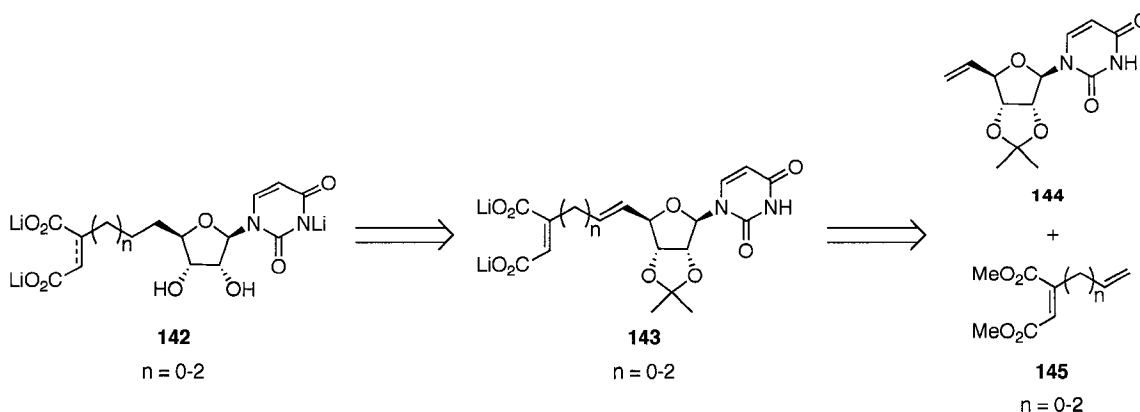
give diacyl peroxide **140**. Photolysis of **140** at $-78\text{ }^{\circ}\text{C}$ for 6 days gives a complex mixture, with none of the desired product **141** detected. The failure of this reaction when applied to these nucleoside derivatives may in part result from the incompatibility of the uracil ring with these conditions. The structurally similar thymine nucleobase in thymidine undergoes radical dimerization under UV light, a process responsible for DNA damage.¹²⁸ Furthermore, the SEM protecting group contains sites where hydrogen abstraction can lead to a radical stabilized either by silicon, oxygen, or nitrogen. Subsequent reactions of these radicals may compete with the desired photolytic pathway. This approach was not explored any further.

Scheme 30. Attempted synthesis of **141** by photolysis of diacyl peroxide **140**.



It was decided to examine olefin cross metathesis (CM) for synthesis of the target molecule(s). Olefin metathesis is one of the most powerful reactions for carbon-carbon bond formation.^{129, 130} The 2005 Nobel Prize in Chemistry was awarded to Yves Chauvin, Robert H. Grubbs, and Richard R. Schrock for its discovery and development into a synthetically useful process. Olefin CM was especially attractive in the context of the syntheses described here because the required starting materials could be readily accessed in three steps or less, and the number of methylene groups in the maleate moiety could potentially be varied by simply changing the nature of the nucleophile used for organocuprate addition to **46**. This allows a range of analogues to be synthesized wherein the number of methylene spacers varies between two and four (Scheme 31), and may give insights as to the effect of the length of the spacer on enzymatic activity. Derivatives **144** and **145** were expected to react selectively under olefin CM conditions and avoid statistical product distributions produced by homodimerization. Olefin **144** should behave as a protected secondary allylic alcohol, a Type II olefin as described by Grubbs and co-workers,¹³¹ and **145**, being a terminal olefin, is designated as Type I.

Scheme 31. Olefin CM approach for synthesis of uridine dicarboxylates.



An important consideration in this route was whether or not selective reduction of the isolated 5',6'-double bond in the presence of the maleate double bond could be achieved after olefin CM, as it was anticipated that a mixture of maleate and succinate products would be difficult to separate. To this end, a three-carbon linked analogue was synthesized and several conditions were evaluated for selective reduction (Scheme 32). Aldehyde **72** undergoes a Wittig reaction with methyltriphenylphosphorane generated *in situ* to give olefin **144**. In the presence of Hoveyda-Grubbs' 2nd generation catalyst (**146**), **144** and olefin **120** undergo olefin CM to afford **147**. Determination of the olefin geometry is difficult because both olefin protons overlap with three other protons in the ¹H NMR spectrum. This is of no consequence, as the ultimate goal is reduction of this double bond.

Scheme 32. Formation of **147** by olefin CM.

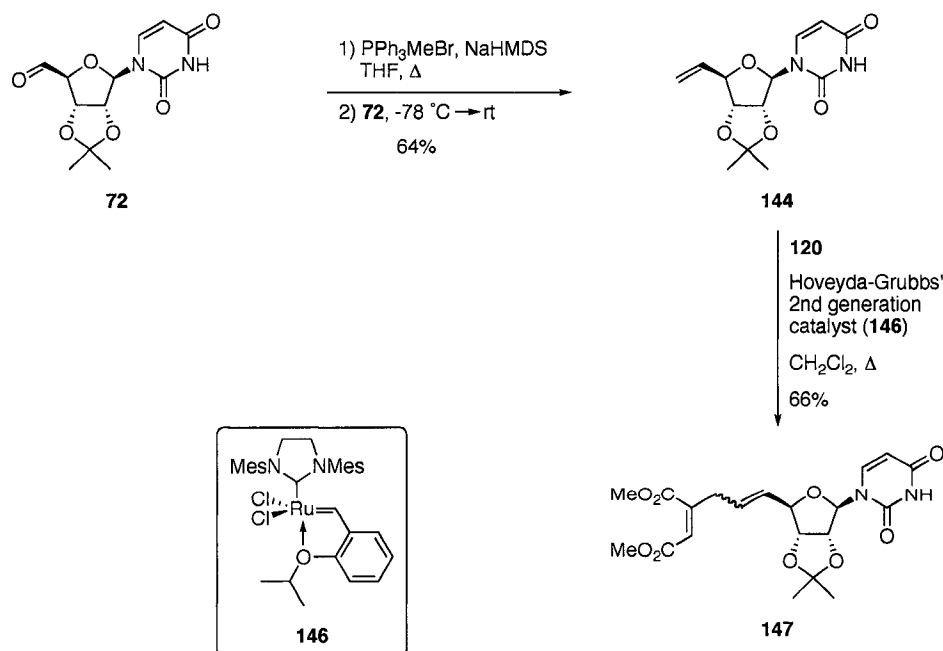


Table 3 contains a summary of results from studies into selective reduction of the 5',6'-double bond (Scheme 33). The reactions were monitored by ^1H NMR spectroscopy of aliquots taken at regular intervals. Standard hydrogenation conditions using 10% Pd/C give only **149** (Entry 1), whereas reducing the Pd loading to 5% gives a 1:1 mixture of products (Entry 2). An attempt to decrease the activity of the catalyst with 2,2'-dipyridyl^{132, 133} completely impedes the reaction (Entry 3). Decreasing the catalyst loading to 1% Pd/C results in a slightly improved selectivity for **148**, however the reaction is sluggish, even at 4 atm H_2 (Entry 5). The very active catalysts $\text{Pd}(\text{OH})_2/\text{C}$ and PtO_2 give predominantly **149** as the product (Entries 6 and 7). Changing the solid support to CaCO_3 ¹³⁴ gives at best a 2:1 ratio of **148:149** (Entry 9).

Since heterogeneous catalysis did not give promising results, attention was turned to homogeneous transition metal catalysis. It was hoped that the metal centre would coordinate to the electron rich 5',6'-double bond over the electron deficient maleate double bond and thus deliver hydrogen to the former. However, use of Wilkinson's catalyst¹³⁵ ($\text{Rh}(\text{PPh}_3)_3\text{Cl}$) affords only a moderate 3:1 ratio of products (Entry 11), whereas Crabtree's catalyst¹³⁶ ($[\text{Ir}(\text{cod})(\text{PCy}_3)\text{py}]\text{PF}_6$) results in an essentially 1:1 mixture of products (Entry 13).

Scheme 33. Attempted selective reduction of the 5',6'-double bond of **147**.

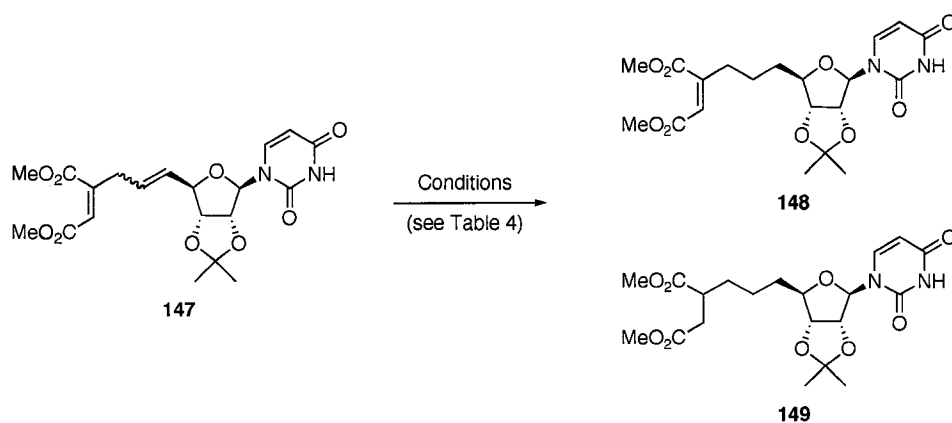


Table 3. Reactions attempted to selectively reduce the 5',6'-double bond of **147**.

Entry	Conditions	148:149
1	H ₂ (1 atm), 10% Pd/C, MeOH, 10 min	100% 149
2	H ₂ (1 atm), 5% Pd/C, MeOH, 30 min	1:1
3	H ₂ (1 atm), 5% Pd/C, 2,2'-dipyridyl, MeOH, 24 h	NR
4	H ₂ (3 atm), 1% Pd/C, EtOAc, 21 h	NR
5	H ₂ (4 atm), 1% Pd/C, EtOAc, 14 h	1.7:1 (76% conversion)
6	H ₂ (1 atm), 20% Pd(OH) ₂ /C, MeOH, 30 min	1:9
7	H ₂ (1 atm), PtO ₂ , MeOH, 1.5 h	100% 149
8	H ₂ (1 atm), 5% Pd/CaCO ₃ , EtOAc, 10 °C, 24 h	NR
9	H ₂ (1 atm), 5% Pd/CaCO ₃ , EtOAc/toluene (98:2), rt, 4 h	2:1 (86% conversion)
10	H ₂ (1 atm), 1% Pd/CaCO ₃ , EtOAc/benzene (98:2), 24 h	NR
11	H ₂ (1 atm), WC ^a (11 mol %), CH ₂ Cl ₂ , 48 h	3:1
12	H ₂ (1 atm), CC ^b (3 mol %), CH ₂ Cl ₂ , 0 °C, 1.5 h	NR
13	H ₂ (1 atm), CC (18 mol %), CH ₂ Cl ₂ , rt, 24 h	1.2:1

^aWC = Wilkinson's catalyst, Rh(PPh₃)₃Cl

^bCC = Crabtree's catalyst, [Ir(cod)(PCy₃)py]PF₆

Although these results were discouraging, it was decided that the reduction with Crabtree's catalyst should be examined further. This catalyst is able to coordinate to the oxygen of carbonyl, ether, and hydroxyl groups, which can direct the reduction of a double bond to one face over the other.¹³⁷ With this in mind, the isopropylidene group of **147** can be removed with aqueous TFA to give diol **150** (Scheme 34). It was hoped that freeing the 3'-hydroxyl would allow the catalyst to coordinate to it, bringing the iridium centre in close proximity to the 5',6'-double bond. Reactions were conducted at low temperature in order to increase selectivity, however at 0 °C, no reaction takes place (Table 4, Entry 1). Raising the temperature to 15 °C gives **151** as the only detectable product (Entry 2), however the reaction is very sluggish, most likely due to catalyst deactivation over the long reaction time. At room temperature, reduction still proceeds slowly, and the selectivity begins to erode (Entry 3). Thus, although it appears that greater selectivity can be achieved using Crabtree's catalyst and deprotected nucleoside **150**, the long reaction times leading to deactivation of the catalyst render this approach impractical.

Scheme 34. Attempted selective reduction of the 5',6'-alkene of **150** using Crabtree's catalyst.

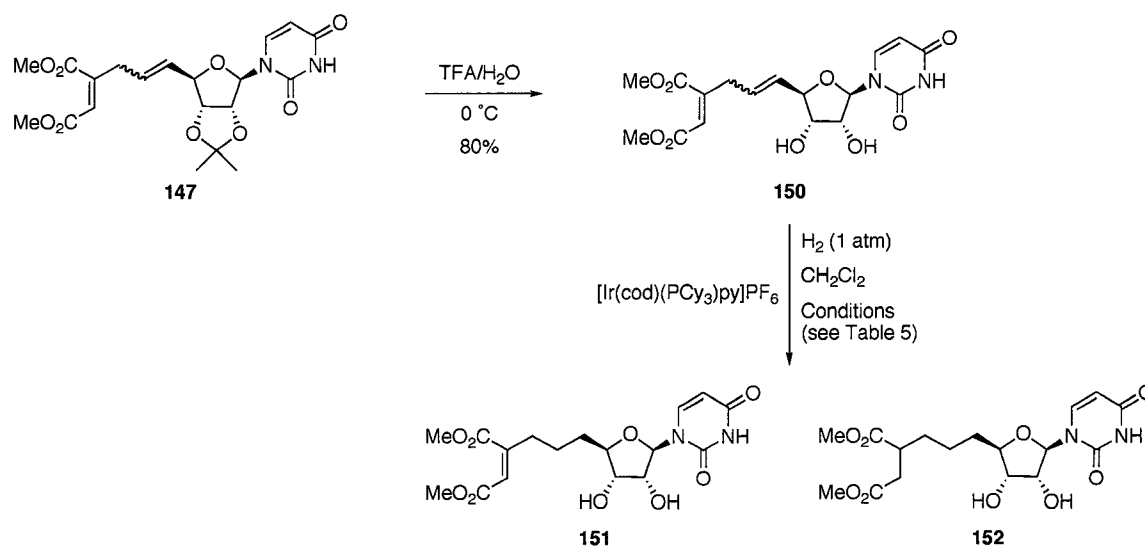


Table 4. Reactions attempted to selectively reduce the 5',6'-alkene of **150**.

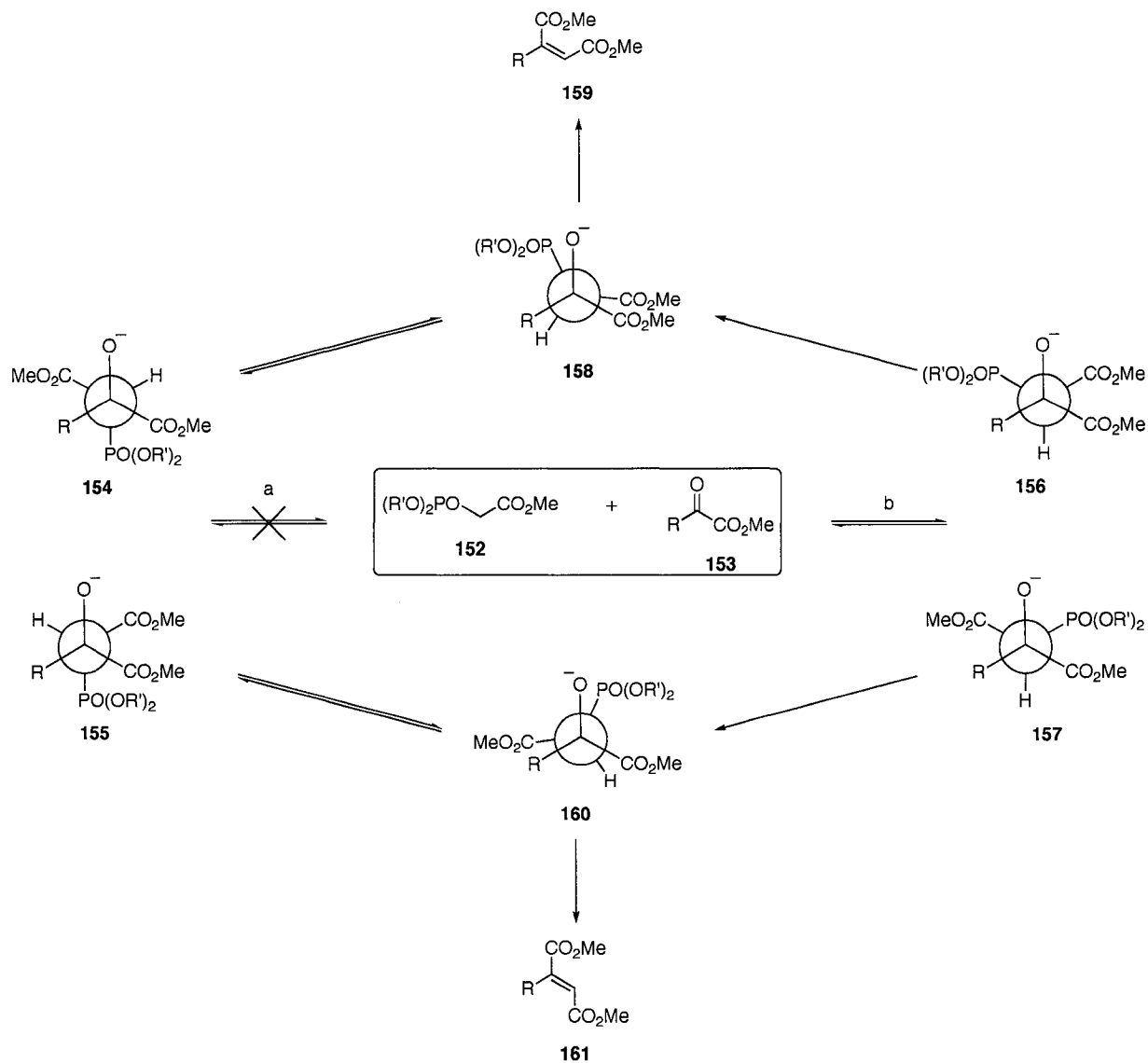
Entry	Conditions	151:152 ^a
1	2 mol % catalyst, 0 °C, 6.5 h	NR
2	7 mol % catalyst, 15 °C, 24 h	100% 151 (21% conversion)
3	5 mol % catalyst, rt, 17 h	3.3:1 (58% conversion)

^aNR = no reaction

Because selective reduction of the 5',6'-alkene over the maleate alkene was difficult to achieve, a new strategy was sought that would enable the double bond from CM to be reduced before the maleate double bond was formed. Fortunately, a report from the 1960s showed that phosphonates undergo a Horner-Emmons-Wadsworth reaction with α -keto esters to give predominantly maleates over the corresponding fumarates, in a ratio greater than 95:5 in most cases.^{138, 139} The reason for the unusual Z-

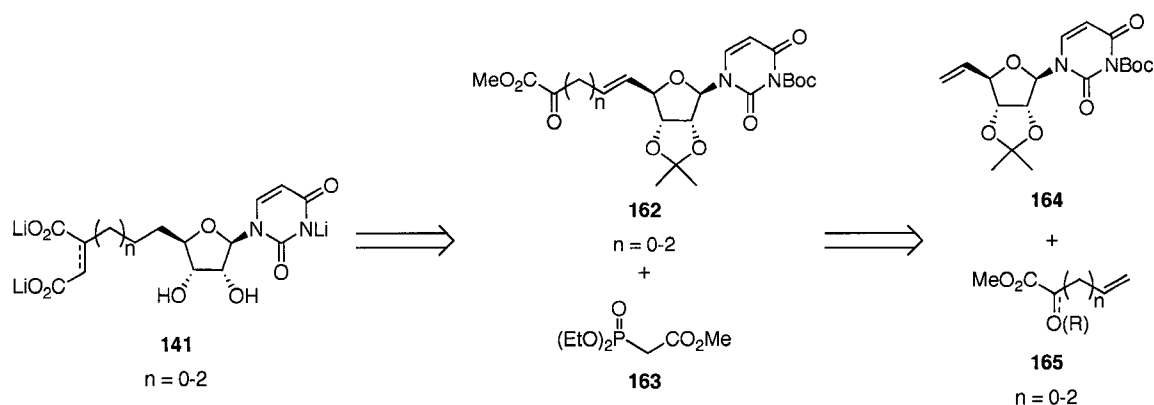
selectivity of this HEW reaction is explained in Scheme 35. The reaction between a phosphonate **152** and an α -keto ester **153** would be expected to proceed *via* path a, giving initial adducts **154** or **155**. These undergo rotation about the newly formed carbon-carbon bond to the conformers **158** or **160**, which upon elimination give maleate **159** or fumarate **161**, respectively. When R = H, the authors observe a **159:161** ratio of 65:35. For R= alkyl, the stability of adduct **154** would be expected to decrease *relative* to that of adduct **155**, thus leading to an erosion of selectivity. However, an increase in selectivity of > 95:5 in favour of maleate **159** is observed when R = Me, in contrast to that expected. Therefore, it appears that the generally accepted mode of addition leading to adducts **154** and **155** is not applicable in this case. Instead, the authors propose that adducts **156** and **157** are first formed (path b). When R= Me, **156** is expected to be slightly more stable than **157**. In the formation of simple α,β -unsaturated esters, all steps leading to the products are reversible, thus equilibration to the more stable fumarate **161** occurs. The opposite selectivity observed in the HEW with α -keto esters arises from the stability afforded to the incipient double bond in the transition state from the decomposition of intermediates **158** or **160**, due to its conjugation with the extra carbonyl group present in the molecule. This renders formation of the intermediates **158** and **160** irreversible, precluding equilibration to the fumarate. Thus, the selectivity arises only from the relative stabilities of adducts **156** and **157**.

Scheme 35. Explanation of the high Z-selectivity in the HEW reaction with α -keto esters.



The revised approach to access the uridine dicarboxylates is shown in Scheme 36.¹⁴⁰ The uridine maleate **141** is derived from a HEW reaction between an α -keto ester **162** and methyl diethylphosphonoacetate (**163**), which in turn arises from olefin CM between uridine derivative **164** and the simple alkene **165**. By selecting the appropriate starting material, the number of methylene groups contained in the spacer can be varied from two to four.

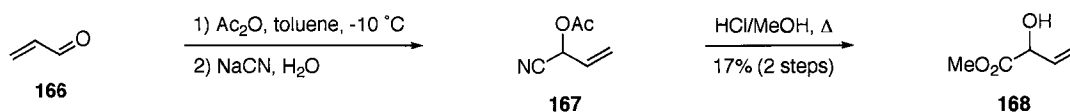
Scheme 36. Revised olefin CM approach for synthesis of uridine analogues **141**.



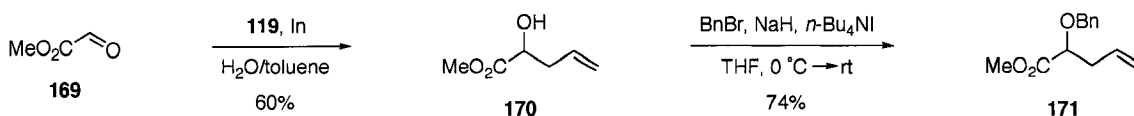
To this end, the alkene precursors for olefin CM were synthesized from readily available starting materials (Scheme 37). Methyl 2-hydroxybut-3-enoate¹⁴¹ (**168**), the olefin CM precursor to analogues containing a two-carbon spacer, is obtained from treatment of acrolein (**166**) with acetic anhydride and NaCN to first form 1-cyanoallyl acetate (**167**). Hydrolysis of the acetate and the nitrile with formation of the methyl ester is then achieved in refluxing HCl/MeOH to give the desired product **168** in low yield over two steps. The precursor to the three-carbon analogues, methyl 2-benzyloxy-pent-4-enoate (**171**), is obtained in two steps, first through an indium-mediated addition of **119** to methyl glyoxylate (**169**),¹⁴² then *via* protection¹⁴³ of the resulting alcohol **170** as its benzyl ether. Finally, methyl 2-oxohex-5-enoate (**174**), the olefin CM precursor for the analogues containing a four-carbon spacer, is synthesized in one step¹⁴² from the reaction of dimethyl oxalate (**172**) with 3-butenylmagnesium bromide (**173**).

Scheme 37. Synthesis of alkenes for olefin CM.

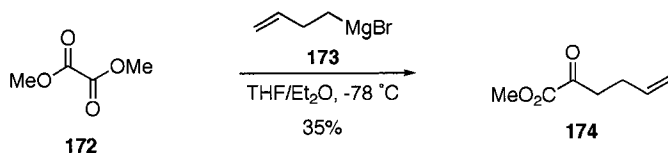
Precursor to analogues containing a two-carbon spacer:



Precursor to analogues containing a three-carbon spacer:



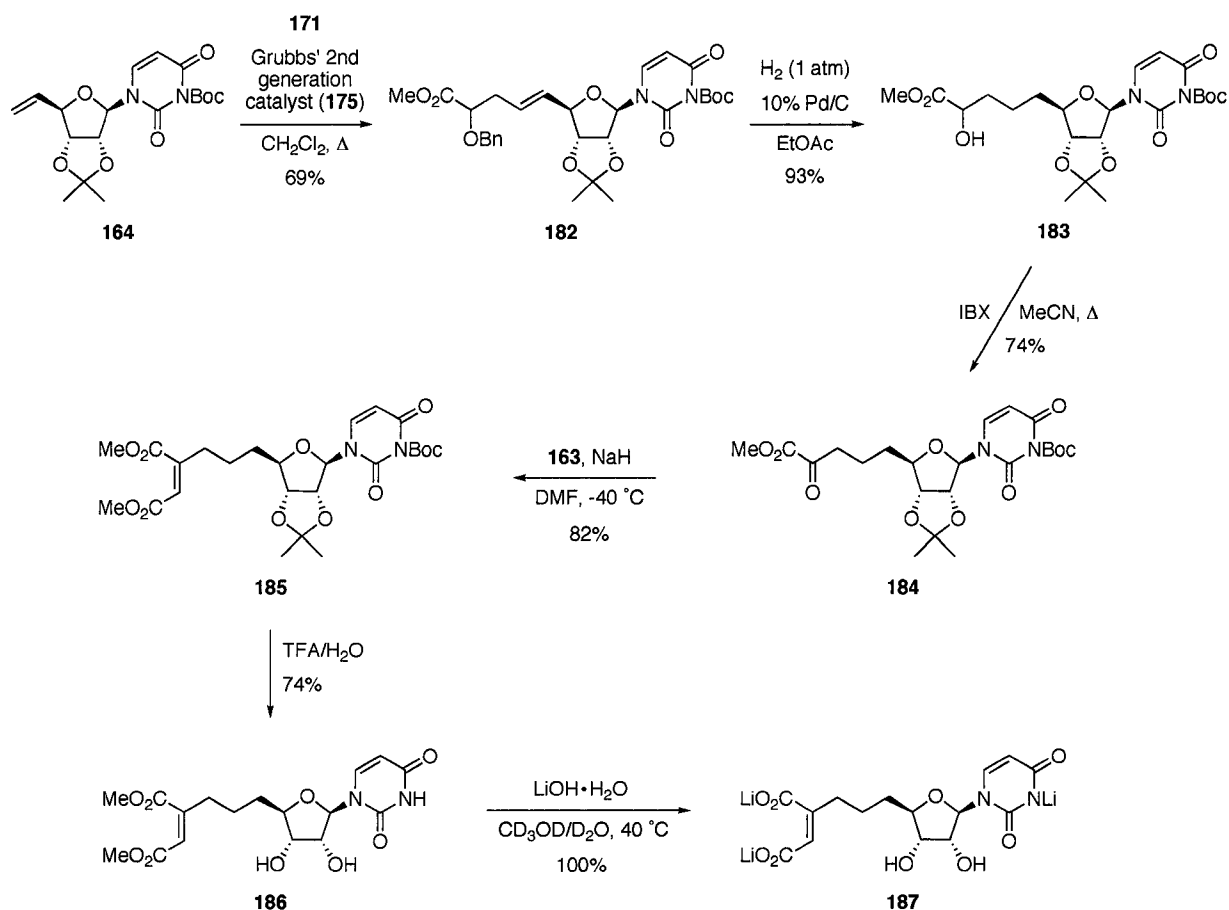
Precursor to analogues containing a four-carbon spacer:



The uridine maleate containing a two-carbon spacer is synthesized starting from uridine derivative **144** (Scheme 38). Reaction of this species with di-*tert*-butyl dicarbonate in pyridine affords protected derivative **164**. This undergoes olefin CM with alkene **168** in the presence of Grubbs' 2nd generation catalyst (**175**) to give **176**. Reduction of the double bond is achieved with hydrogen over 5% Pd/C to give alcohol **177**. Oxidation with IBX then generates α -keto ester **178**, which subsequently undergoes an HEW reaction upon treatment with methyl diethylphosphonoacetate (**163**) and NaH to give maleate derivative **179**. It has previously been reported that conducting this reaction at -5 °C gives > 95:5 ratio of maleate and fumarate products,¹⁴⁴ therefore it was decided to lower the temperature to -40 °C to further increase the selectivity. Consequently, the corresponding fumarate is not detected in the ¹H NMR spectrum of the crude product,

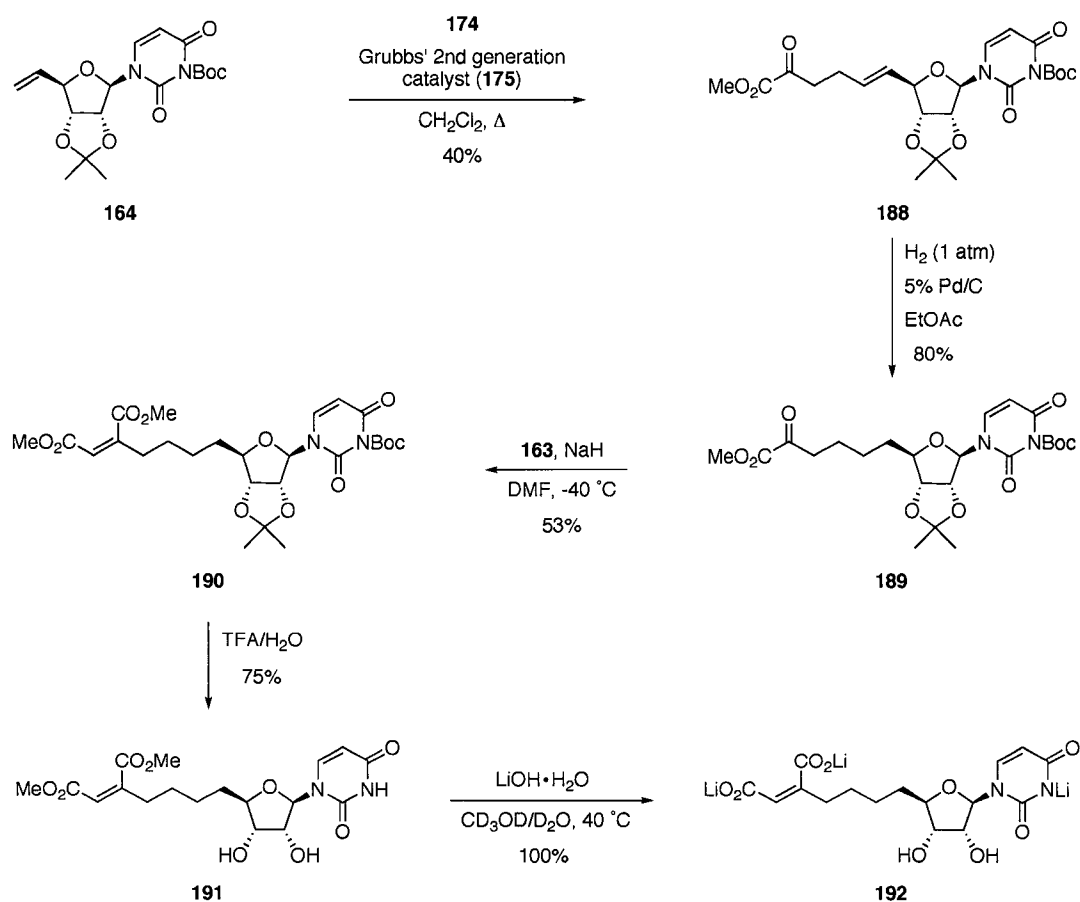
product. This may be due in part to nonproductive coordination of the alcohol to the ruthenium alkylidene centre. Simultaneous removal of the benzyl protecting group and reduction of the double bond of **182** is achieved by hydrogenation over Pd/C to give alcohol **183**. This is oxidized to α -keto ester **184** with IBX. The HEW is conducted under the same conditions as previously described to give maleate analogue **185**, with >99:1 *Z/E* selectivity as determined by ^1H NMR. Protecting group removal using aqueous TFA proceeds to give **186**, which undergoes hydrolysis with LiOH to afford lithium salt **187** quantitatively.

Scheme 39. Synthesis of uridine maleate analogue containing a three-carbon spacer **187**.



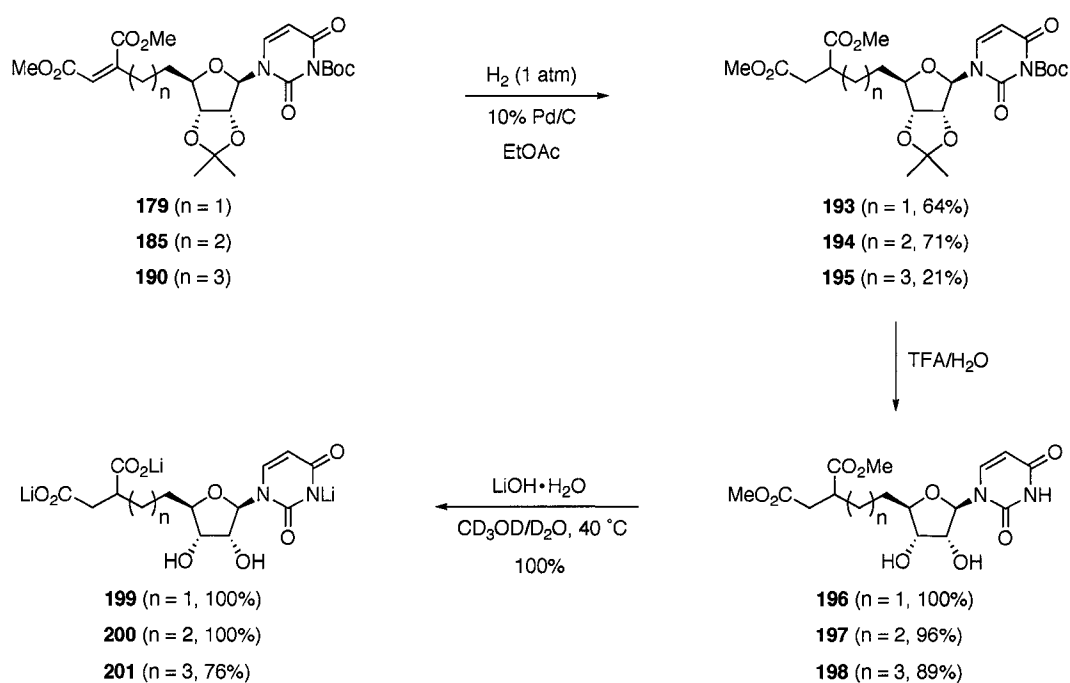
The maleate analogue containing a four-carbon spacer is accessed in a similar series of steps as for the previous target molecules (Scheme 40). Uridine derivative **164** undergoes olefin CM with alkene **174** to give the expected product **188** in relatively low yield. This is possibly due to facile coordination of the carbonyl group of the α -keto ester to the ruthenium centre upon formation of the ruthenium alkylidene intermediate. Hydrogenation of the double bond generates **189**, which undergoes a HEW reaction to afford maleate analogue **190**. Similar to the previous analogues, deprotection with aqueous TFA gives **191**, which is followed by basic hydrolysis to give lithium salt **192** quantitatively.

Scheme 40. Synthesis of uridine maleate analogue containing a four-carbon spacer **192**.



The corresponding succinate derivatives are obtained by hydrogenation of the maleates. Thus, hydrogenation over Pd/C of **179**, **185**, and **190** gives succinates **193**, **194**, and **195**, respectively (Scheme 41). Removal of the Boc and isopropylidene protecting groups is achieved with aqueous TFA to give **196**, **197**, and **198**, which are hydrolyzed with LiOH to their respective lithium salts **199**, **200**, and **201**.

Scheme 41. Synthesis of uridine succinate analogues **199-201**.



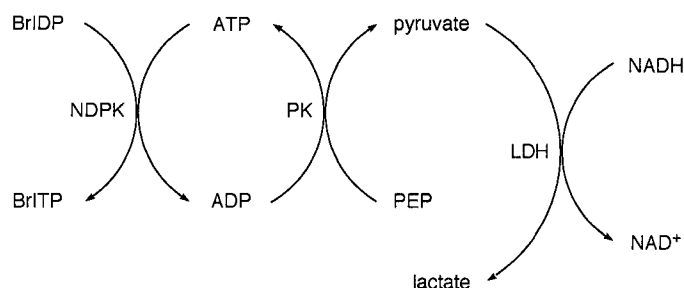
2. Biological Evaluation of Uridine Dicarboxylates

2.1 NDP Kinase Inhibition Assay

The six uridine dicarboxylates (**181**, **187**, **192**, and **199-201**) were assayed for their inhibitory activity against NDP kinase from *Dictyostelium discoideum*. The

inhibition studies were conducted with a coupled assay that utilizes pyruvate kinase and lactate dehydrogenase (Scheme 42).¹⁴⁵ ATP is used as the phosphate donor and 8-bromoinosine diphosphate (BrIDP) is the phosphate acceptor. BrIDP is used because it is a poor substrate for pyruvate kinase (PK).¹⁴⁵ NDP kinase (NDPK) catalyzes phosphate transfer from ATP to BrIDP. The ADP thus generated is the phosphate acceptor for PK, which catalyzes the formation of pyruvate from phosphoenolpyruvate (PEP) and regenerates ATP. The pyruvate in turn is reduced to lactate by lactate dehydrogenase (LDH), which uses NADH as a cofactor. The NDP kinase activity is thus measured as a decrease in A_{340} , corresponding to depletion of NADH, with time.

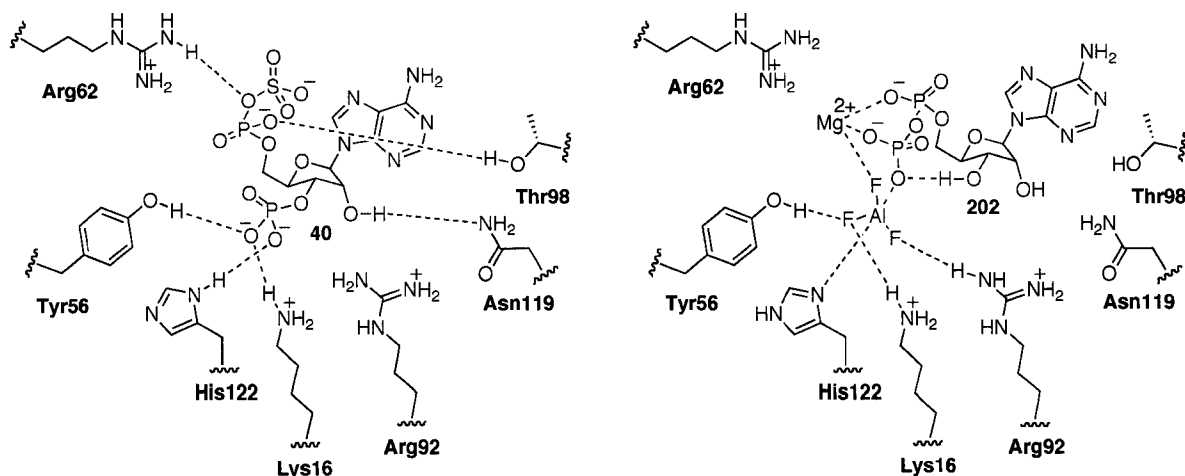
Scheme 42. Coupled assay¹⁴⁵ used for NDP kinase inhibition studies.



Unfortunately, none of the compounds are inhibitory of NDP kinase at a concentration of 1 mM. This may be a result of the constraints imposed by the methylene linkers, which may prevent the dicarboxylate oxygen atoms from occupying the positions in the enzyme active site normally assumed by the diphosphate oxygens of the parent compound.

Further insight into the absence of inhibition may be gained from comparison of the co-crystal structure of the NDP kinase inhibitor PAPS (**40**) in the active site of the enzyme with that of the transition state analogue ADP•AlF₃ (**202**) in the active site. The AlF₃ group occupies the expected position of the γ -phosphate of ATP during its transfer to His122, and thus **202** acts as a transition state analogue of ATP.¹⁴⁶ An overlay of both structures reveals that the 3'-phosphate of **40** is located only 1.7 Å from AlF₃ in the ternary complex (Figure 14).²⁸ Both AlF₃ and the 3'-phosphate of **40** make polar interactions with the N δ of His122, the N ξ group of Lys16, and the hydroxyl group of Tyr56. The AlF₃ group of **202** also makes hydrogen bonds with an N η group of Arg92 and the backbone amide NH of Gly123 (not shown). The 3'-phosphate of PAP (**41**) and the 3',5'-phosphate of cAMP (**39**) are also near the position of AlF₃ in the NDP kinase active site.²⁸ It thus appears that, at least in the context of nucleoside inhibitors discovered thus far, effective binding in the active site of NDP kinase requires a 3'-phosphate or equivalent moiety that assumes the expected position of the γ -phosphate of ATP during phosphate transfer to the enzyme. Interestingly, the 5'-phosphosulfate of **40** and the 5'-phosphate of **41** point out from the binding pocket and make few well-defined interactions.²⁸

Figure 14. Comparison of PAPS (40) with ADP·AlF₃ (202) in the active site of NDP kinase (adapted from references 59 and 60).



2.2 Antimicrobial Assays

The dicarboxylate salts as well as their diester precursors (180, 186, 191, and 196-198) were tested for their antimicrobial activity against several bacterial strains, namely *E. coli* DH5 α , *Pseudomonas aeruginosa* ATCC 14207, *Salmonella typhimurium* ATCC 23564, and *Staphylococcus aureus* ATCC 6538. Although the dicarboxylate salts may not penetrate the negatively-charged bacterial cell membranes, the corresponding esters might be expected to diffuse through such a barrier more readily and could then potentially be hydrolyzed by cellular esterases. None of the 12 compounds tested inhibited growth of any of these strains at a concentration of 20 mg/mL.

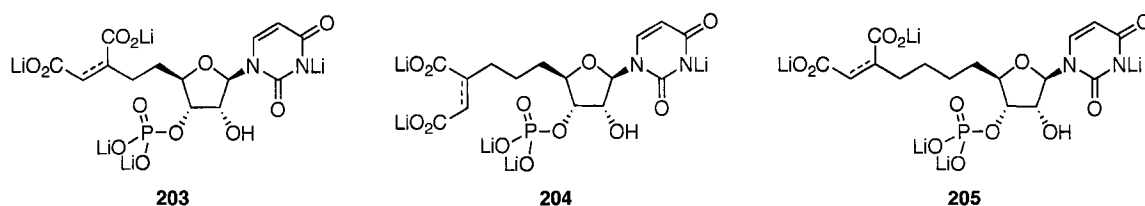
3. Conclusions and Future Work

A series of analogues of UDP containing either a maleate or a succinate unit were synthesized, using olefin CM to install the methylene spacers and a Z-selective HEW

reaction to construct the maleate unit. The compounds did not exhibit any activity towards NDP kinase nor did they or their corresponding methyl esters display antimicrobial activity.

Based on the previous discussion, it may be a worthwhile endeavour to modify the present analogues to their corresponding 3'-phosphates (Figure 15) for evaluation of their activity towards NDP kinase. By analogy to **40** and **41**, this may result in the dicarboxylate moiety pointing away from the active site upon binding of the analogue. However, the electrostatic interactions between the negatively charged carboxylates and the many positive charges surrounding the NDP kinase nucleotide binding site may lead to enhanced binding. In fact, these interactions are thought to be responsible for the higher activity of PAPS (**40**) than PAP (**41**) towards NDP kinase.²⁸

Figure 15. Proposed 3'-phosphate derivatives of UDP analogues.



Future studies may also involve the investigation of these UDP analogues as potential inhibitors of other enzymes that utilize substrates containing the nucleoside diphosphate unit. One example is the nucleoside monophosphate (NMP) kinase class of enzymes, which are responsible for converting nucleoside monophosphates to their corresponding diphosphates.¹⁴⁷ NMP kinases are known to be crucial for survival, whereas disruption of the NDP kinase gene in *E. coli*²⁰ and *S. cerevisiae*¹⁴⁸ does not affect cell growth to any significant extent. Furthermore, bacterial uridine

monophosphate kinases¹⁴⁹ have no closely related counterpart in eukaryotes, making them potential targets for the design of new antibiotics. Another interesting class of targets are the enzymes involved in bacterial peptidoglycan biosynthesis,⁵¹ as several activated precursors to peptidoglycan contain the UDP motif.

CHAPTER 2: Replacement of the Cysteine Residues of Pediocin PA-1 with Amino Acids Capable of Hydrophobic Interactions

INTRODUCTION

1. Bacteriocins as Alternatives to Conventional Antibiotics

Bacteriocins are ribosomally-synthesized antimicrobial peptides produced by many bacteria as a mode of defense against closely related bacterial species. Many bacteriocins are produced by Gram-positive bacteria such as lactic acid bacteria. They are active at nanomolar concentrations, and unlike traditional antibiotics, which mostly behave as enzyme inhibitors, they usually kill cells by membrane permeabilization through pore formation, causing leakage of cellular contents. Bacteriocins generally exhibit no toxicity towards humans or other eukaryotes. For these reasons, they are attractive candidates as alternatives to conventional antibiotics, which have experienced an alarming emergence of resistant bacterial strains over the past few decades.¹⁵⁰ Furthermore, because of the stability of many bacteriocins over a wide pH and temperature range, they have shown promise as food preservatives. For example, the lanthionine-containing bacteriocin nisin is currently approved in over 80 countries as an antimicrobial additive in dairy products. Other bacteriocins such as the pediocin-like type IIa bacteriocins are of interest due to their potent antilisterial activity, and are being studied as agents for the treatment of gastrointestinal infections.

1.1 Classification of Bacteriocins

Bacteriocins from lactic acid bacteria are usually grouped into three major classes as recently proposed by Cotter *et al.*¹⁵¹ Class I bacteriocins are termed lantibiotics. These are post-translationally modified peptides and contain the unusual amino acids lanthionine and methyllanthionine. Class II includes unmodified proteins and is divided into four subclasses: Class IIa which are known as “pediocin-like” bacteriocins and are small, heat stable peptides; class IIb which are two-peptide bacteriocins; class IIc which are cyclic peptides; and class IId which are non-pediocin single linear peptides. Finally, class III consists of large, heat labile, non-bacteriocin lytic proteins known as bacteriolysins. The class IIa bacteriocins have adopted the aforementioned name in reference to pediocin PA-1 (also known as pediocin AcH), one of the initial type IIa bacteriocins to have been characterized.^{152, 153} This class of peptides has received widespread attention as biopreservatives due to their nanomolar activity against pathogens such as *Listeria monocytogenes*.^{154, 155} They are usually described as being small (< 10 kDa), cationic, heat stable peptides containing between 37 and 48 amino acids. Leucocin A was the first class IIa bacteriocin whose sequence was reported.¹⁵⁶ Over 25 of such peptides are now known,^{154, 155} and in all cases they contain at least two cysteine residues forming a conserved disulfide bond, a highly conserved YGNGV “pediocin box” sequence at the N-terminus, and a variable hydrophobic C-terminal domain which may or may not contain a second disulfide bond (Table 5).

Table 5. Amino acid sequence alignment of several type IIa bacteriocins.

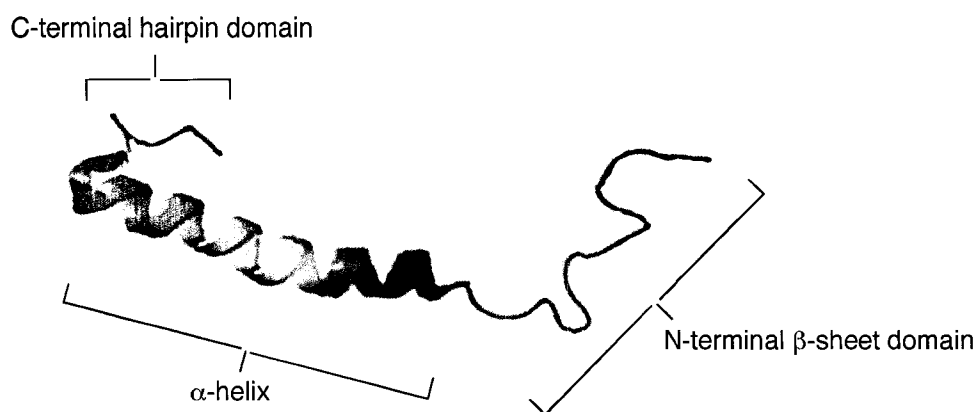
Bacteriocin	Amino Acid Sequence
Pediocin PA-1 ¹⁵⁷	KYYGNGVTCGKHSCSVDWGKATTTCIINNGAMAWATGGHQGNHKC
Leucocin A ¹⁵⁶	KYYGNGVHCTKSGCSVNWGEAFSAGVHRLANGGNGFW
Enterocin P ¹⁵⁸	ATRSYNGVYCNNSKCVNWGEAKENIAGIVISGWASGLAGMGH
Sakacin P ¹⁵⁹	KYYGNGVHCGKHSCTVDWGTAIGNIGNNAAANWATGGNAGWNK
Mesentericin Y105 ¹⁶⁰	KYYGNGVHCTKSGCSVNWGEAASAGIHRLANGGNGFW
Carnobacteriocin B2 ¹⁶¹	VNYGNGVSCSKTKCSVNWGQAFQERYTAGINSFVSGVASGAGSIGRRP
Curvacin A ¹⁶²	ARSYNGVYCNKKCVNVRGEATQSIIGGMISGWASGLAGM
Divercin V41 ¹⁶³	TKYYGNGVYCNKSKCVVDWGQASGCIGQTVVGGWLGGAI PGKC
Coagulin ¹⁶⁴	KYYGNGVTCGKHSCSVDWGKATTTCIINNGAMAWATGGHQGTHKC

2. Secondary Structure and Mechanism of Action of Class IIa Bacteriocins

Class IIa bacteriocins are unstructured in water, however they adopt a defined secondary structure in the presence of a membrane-mimicking environment.¹⁶⁵ The cationic and hydrophilic N-terminal domain of class IIa bacteriocins generally adopts a three-stranded β -sheet structure, stabilized by the conserved disulfide bond, and mediates binding to the negatively charged phospholipids of the bacterial cell membrane through electrostatic interactions.^{166, 167} In pediocin PA-1, the binding is specifically mediated by a “positive patch” consisting of Lys-11 and His-12 in the N-terminal domain. Mutation of these residues to Ile-11 and Leu-12 in an N-terminal fragment of pediocin PA-1 abolished all binding to lipid vesicles.¹⁶⁷ Following the N-terminal region is a central

amphiphilic α -helix,^{165, 168-171} which precedes a C-terminal tail that folds back onto the α -helix, thus forming a hairpin-like structure in the C-terminal domain.^{165, 168, 169} These features are exemplified in the ¹H NMR solution structure of carnobacteriocin B2 (Figure 16).¹⁶⁸

Figure 16. Schematic representation of a class IIa bacteriocin.



The hairpin domain is believed to penetrate into the hydrophobic portion of the target cell membrane, forming pores that lead to leakage of cellular contents¹⁷²⁻¹⁷⁵ and disruption of the proton motive force (PMF).¹⁷⁶⁻¹⁸¹ The PMF consists of two components: the pH gradient, which depends on protons, and the transmembrane potential, which is dependent on other cations.¹⁷⁹ The PMF plays crucial roles in ATP synthesis, active transport, and bacterial motion. A rapid depletion of ATP in target cells is observed, presumably due to the cell's consumption of ATP as it attempts to restore the proton motive force. The hinge region located between the N and C-terminal domains, usually consisting of one amino acid, apparently provides the structural flexibility required for the two domains to move relative to each other. This allows the C-terminal hairpin

domain to dip into the hydrophobic portion of the target cell membrane.¹⁶⁹ In most type IIa bacteriocins, the hinge is located at position 17 as a conserved aspartate or asparagine residue.

In some type IIa bacteriocins, the hairpin structure is stabilized by a second disulfide bond between a C-terminal cysteine residue and a cysteine residue located within the α -helix (Table 5). The stabilized hairpin model is supported by studies demonstrating that a sakacin P mutant containing this additional disulfide bond displayed similar potency but was more thermally stable than its natural counterpart.¹⁸² However, most peptides of this class lack these cysteine residues and instead contain a tryptophan residue near the C-terminal end of the peptide. This residue and a conserved central tryptophan residue (position 18 in most type IIa bacteriocins, Table 5), position themselves at the membrane-water interface, a common occurrence for tryptophan residues in membrane-penetrating peptides.¹⁸³ In type IIa bacteriocins, they aid in stabilizing the C-terminal hairpin and positioning it correctly in the membrane.¹⁷³

The C-terminal domain is also the specificity determinant of type IIa bacteriocins. Hybrid peptides constructed from the N and C- termini of two different bacteriocins displayed antimicrobial spectra similar to the bacteriocin from which the C-terminal half was derived.^{184, 185} Also, type IIa bacteriocins in which the C-terminal region was altered by site-directed *in vitro* mutagenesis generated mutant peptides that displayed different specificity to that of the wild-type bacteriocin.¹⁸² Most likely, the specificity-determining event involves interaction of the C-terminal domain with a membrane-bound protein. The synthetically prepared enantiomer of leucocin A (i.e. containing only D-amino acids) exhibited no antibacterial activity against several strains known to be susceptible to the

natural peptide,¹⁸⁶ strongly suggesting that interaction with a chiral receptor molecule is crucial for the activity of type IIa bacteriocins. Further evidence of the C-terminal domain docking to a receptor was obtained from results showing that a 15-mer peptide fragment derived from the C-terminus of pediocin PA-1 was able to inhibit pediocin PA-1 activity, suggesting that the fragment was competing with the full-length peptide for binding to the receptor protein.¹⁸⁷ It has been proposed that this receptor consists of components of the mannose phosphotransferase system (man-PTS), a multi-domain protein responsible for the transport and phosphorylation of sugars into both Gram-positive and Gram-negative bacteria.¹⁸⁸⁻¹⁹² The PTS permeases of the mannose family consist of three domains or subunits, IIAB, IIC, and IID.¹⁹³ The IIAB subunit is located on the cytosolic face of the membrane and is responsible for phosphorylation. The IIC and IID subunits are involved in transport. They form a membrane-located complex and are therefore attractive candidates as receptors for type IIa bacteriocins. Independent expression of each gene of the *mpt* operon of *Listeria monocytogenes* in the bacteriocin-resistant species *Lactococcus lactis* revealed that *mptC* alone was sufficient to render the strain sensitive to the type IIa bacteriocins pediocin PA-1, leucocin A, and enterocin A. Although this apparently suggested that the IIC subunit is the receptor molecule for this class of peptides,¹⁸⁹ it is important to note that *L. lactis* also contains a man-PTS complex. Heterologous expression of the IIC subunit of *L. monocytogenes* in this organism may result in a complex of this subunit with the endogenous IID subunit of *L. lactis*. These results therefore do not rule out whether or not the IID subunit is also required to confer bacteriocin sensitivity. More conclusive results were obtained from a recent study that used a *L. lactis* clone in which the man-PTS genes had been deleted.¹⁹⁴

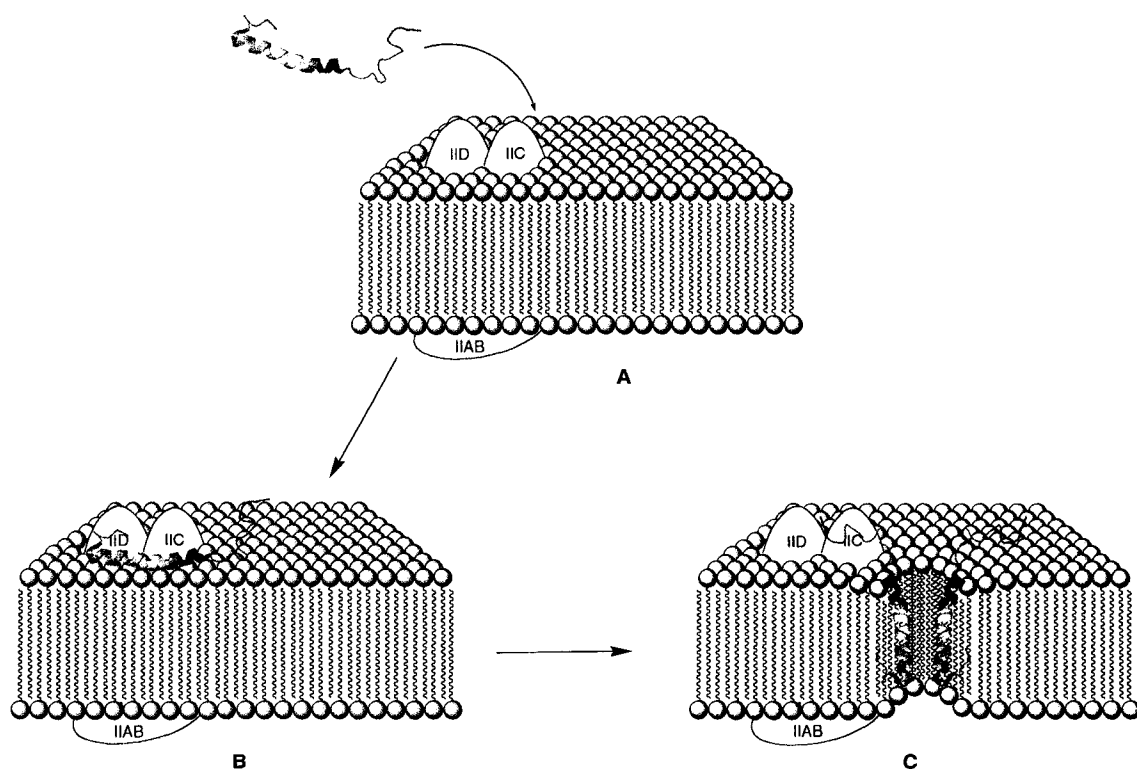
Heterologous expression of the gene pair encoding the IIC and IID subunits from the type IIa bacteriocin-sensitive strain *Lactobacillus sakei* was sufficient to cause the *L. lactis* deletion mutant to become sensitive to pediocin PA-1, enterocin P, sakacin A, and the non-pediocin-like bacteriocins lactococcin A and B. This strongly suggests that the IIC and IID subunits are the cellular receptors for class II bacteriocins.

The nature of the IIC and IID subunits of the man-PTS as the specificity-determining receptors for type IIa bacteriocins necessitates that they differ in amino acid composition and/or three-dimensional structure across bacterial strains to an extent that leads to strain-dependent variations in interactions between the C-terminal domain and the permease. However, at least in the case of the IIC subunit, it appears that the region required for sensitivity is not extensive. The IIC subunit from *L. lactis* shares 59% identity with that of *L. monocytogenes*¹⁸⁹ and 57% identity with the IIC subunit of *L. sakei*.¹⁹⁴

Thus, the mechanism of type IIa bacteriocins can be summarized as depicted in Figure 17. Initially, a non-specific, electrostatic interaction occurs between the cationic N-terminal domain of the bacteriocin and the anionic phospholipids of the cell membrane (**A**). The C-terminal domain of the peptide then undergoes a specific, chiral interaction with the IIC and IID subunits of the man-PTS (**B**). This may induce a conformational change in the bacteriocin, facilitated by the central hinge region, which allows its C-terminal domain to dip into the target cell membrane. In accordance with results demonstrating that the tryptophan residues position themselves at the membrane-water interface, the peptide orients its C-terminal domain diagonally into the membrane, while the N-terminal domain is expected to remain in contact with the membrane surface

(C).^{169, 173, 195, 196} In the case of type IIa bacteriocins, the structure of the pore, or whether the peptides act as a monomer or oligomers, is not yet known.

Figure 17. Proposed mechanism of action of class IIa bacteriocins.



2.1 Role of Disulfide Bonds in Class IIa Bacteriocins

Extensive studies conclude that the conserved disulfide bond between Cys-9 and Cys-14 is essential for biological activity of type IIa bacteriocins. Substitution of both cysteine residues with serine in mesentericin Y105 (Table 5) resulted in almost complete loss of antimicrobial activity.¹⁶⁰ Similarly, replacement of Cys-14 in pediocin PA-1 with 11 different amino acids, including leucine, valine, tyrosine, phenylalanine, serine,

threonine, or glycine, abolished detectable antibacterial activity,¹⁹⁷ as did substitution of the cysteine residues at positions 9 and 14 for serine in leucocin A.¹⁹⁸

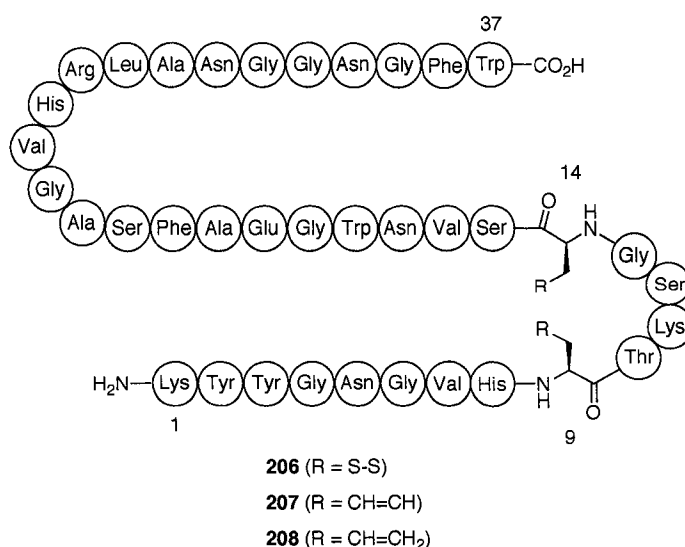
The Cys-24-Cys-44 disulfide bond found in pediocin PA-1 and some other type IIa bacteriocins plays a role in the potency, target cell specificity, and temperature dependency of antibacterial activity. Sakacin P mutants in which cysteines had been introduced at positions 24 and 44 showed an increased antimicrobial spectrum with respect to the wild type peptide, and were also more active at higher temperatures.¹⁸² A pediocin PA-1 mutant in which both of these cysteine residues were replaced with serine displayed decreased activity against several indicator strains, including a 10-1000-fold decrease at 37 °C.^{173, 182} In a separate study, it was found that the single mutants pediocin[C24S] and pediocin[C44S] were completely inactive against five indicator strains.¹⁷⁴ However, the assays were conducted with unpurified mutant bacteriocins from overproducing *E. coli* strains. Therefore, their stability and the correct formation of the disulfide bonds must be questioned.

Although elimination of the disulfide bonds in type IIa bacteriocins clearly decreases their potency, replacement of the bond with a disulfide-mimicking structure may afford peptide analogues with similar activity to the natural peptide but with increased stability. In this respect, replacement of the disulfide bonds in antimicrobial peptides with more stable carbocyclic rings has attracted significant interest. Dicarba analogues of the neuropeptide hormone oxytocin,^{199, 200} leucocin A (**207**, Figure 18),¹⁹⁸ the lantibiotic lactacin 3147 A2,²⁰¹ and fragments of nisin,^{202, 203} have recently been reported. The carbocyclic rings were constructed using ring-closing metathesis (RCM) of allyl glycine residues replacing cysteine residues in the peptide backbone. The oxytocin

and leucocin A analogues displayed IC_{50} values that were only one order of magnitude lower than the parent peptides, whereas the lacticin 3147 A2 analogue was found to be inactive. The results indicate that a carbocycle in place of a disulfide bridge may result in a peptide analogue that retains the correct geometry along the peptide backbone. Specifically, in the case of the 9,14-dicarba leucocin A analogue **207**, the results suggest that the disulfide bond holds the peptide in the required conformation for receptor recognition, but does not itself bind to the receptor surface.¹⁹⁸

Surprisingly, the 9,14-diallyl analogue **208** of leucocin A was nearly as active as the natural peptide.¹⁹⁸ This analogue had an IC_{50} of 50 nM against *Carnobacterium maltaromaticum*, compared to an IC_{50} of 35 nM for leucocin A (**206**). These results suggest that hydrophobic interactions between the allyl side chains of **208** are not only strong enough to hold the peptide in the required conformation, but also allow sufficient flexibility in order to achieve the requisite optimal geometry for full activity comparable to natural leucocin A.

Figure 18. Leucocin A (**206**) and non-cysteine-containing analogues.



3. Project Objectives: Synthesis and Biological Evaluation of Analogues of Pediocin PA-1 with Cysteine Residues Replaced by Amino Acids Capable of Hydrophobic Interactions

The fascinating results with respect to the activity of **208** prompted us to investigate whether or not the stabilization of peptide conformations by hydrophobic interactions between amino acid side chains is a general phenomenon for cysteine-containing peptides. This project focuses on the type IIa bacteriocin pediocin PA-1 (**209**, Figure 19). Unpublished results by Dr. Kamaljit Kaur show that the man-PTS is the target of leucocin A (**206**). It is hypothesized that because **206** and **209** have very similar N-terminal sequences and interact with the same putative receptors (the IIC and IID subunits of the man-PTS), then replacement of Cys-9 and Cys-14 with amino acids potentially capable of hydrophobic interactions may lead to analogues of **209** that display activity in the same order of magnitude as the natural peptide. Thus, the solid-phase peptide synthesis (SPPS) of four non-cysteine containing analogues of pediocin PA-1 can be proposed. These are shown in Figure 20, and include a 9,14-diallyl analogue (**210**), a 9,14-dibenzyl analogue (**211**), a 9,14-dipropyl analogue (**212**), and finally a 24,44-diallyl analogue (**213**). In all four analogues, the oxidatively unstable methionine residue at position 31 has been replaced by norleucine. Previous studies have demonstrated that this substitution is not deleterious to the activity of pediocin PA-1.¹⁷⁰

Figure 19. Structure of pediocin PA-1 (209).

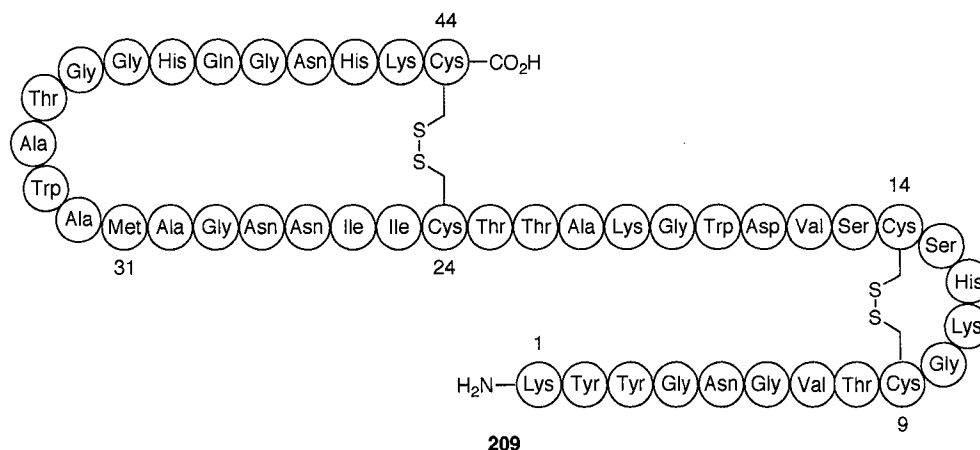
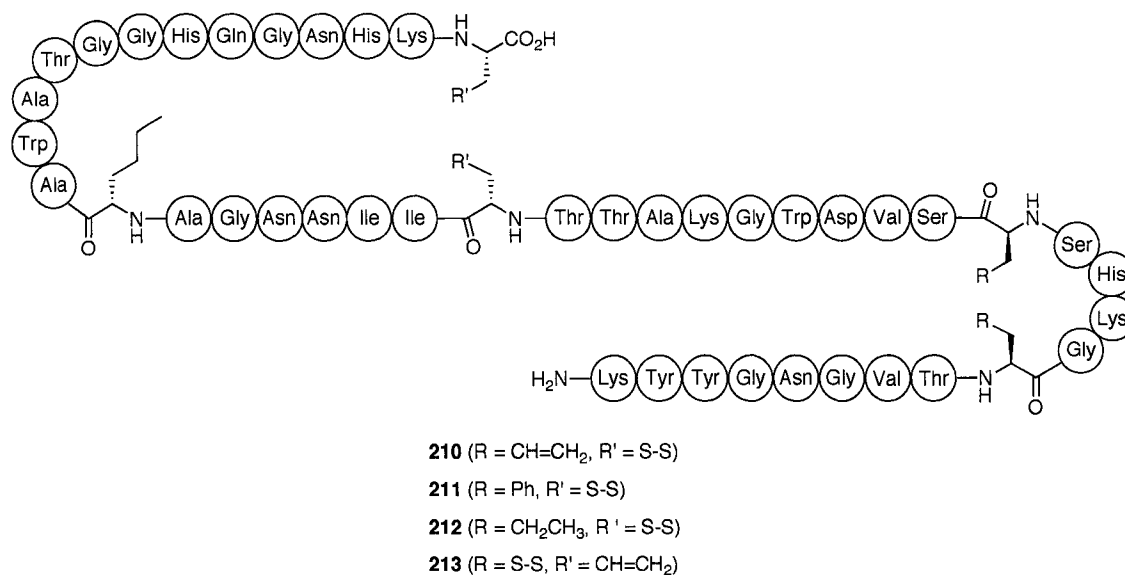


Figure 20. Proposed pediocin PA-1 analogues.



Biological evaluation of the analogues can be undertaken to allow a comparison of their activity to that of natural pediocin PA-1. This would provide insight as to what extent hydrophobic interactions can maintain the peptide in its native conformation. For **212**, the potential interactions between the norvaline side chains are expected to be weak,

whereas the possible interactions between the allylglycine side chains of **210** and **213** and the phenylalanine side chains of **211** are expected to be stronger due to the π -stacking element. Furthermore, **213** would allow conclusions to be drawn as to the potential of hydrophobic side chains to stabilize the α -helix of pediocin PA-1.

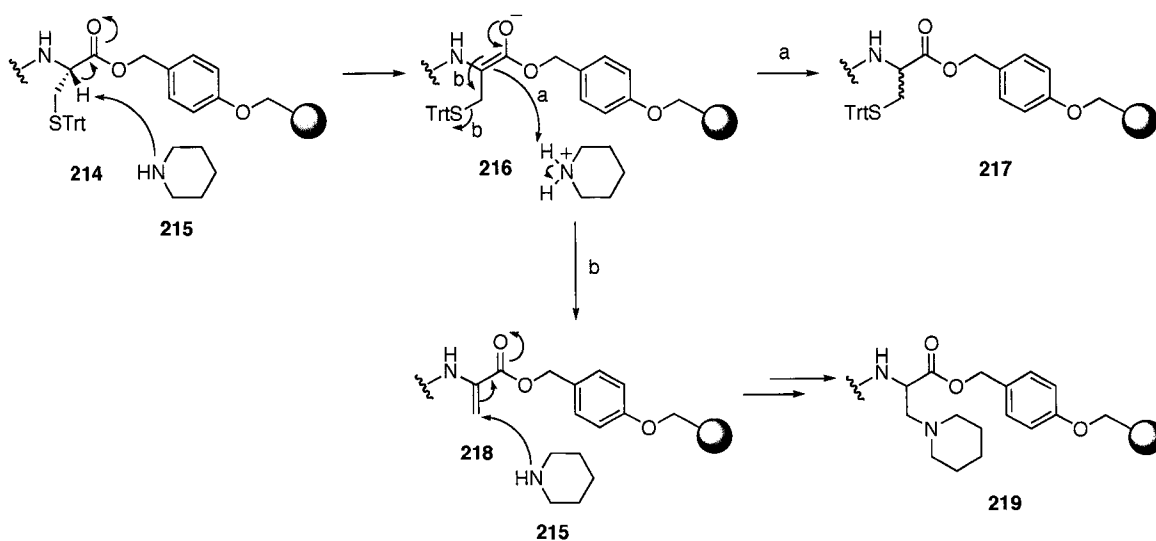
RESULTS AND DISCUSSION

1. General Strategy for Solid Phase Synthesis of Pediocin PA-1 Analogues

1.1 Choice of Resin

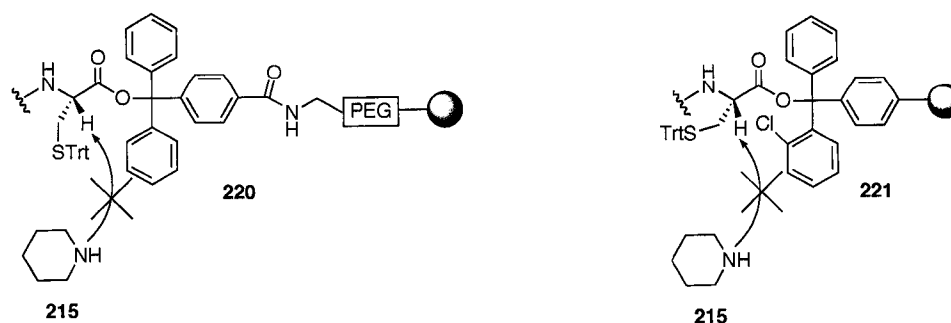
Because pediocin PA-1 is attached to the resin via its C-terminal cysteine residue, a hydroxymethyl functionalized resin such as Wang resin cannot be used as it leads to epimerization of the α -centre or piperidine adduct formation during the Fmoc deprotection steps. This arises due to the enhanced acidity of an α -proton on a C-terminal residue linked through a hydroxymethyl group, which exists as an ester (**214**, Scheme 43). Thus, deprotonation of the α -proton of this residue by piperidine (**215**) leads to an enolate intermediate (**216**), which can be protonated to give the product containing an epimerized centre (**217**), or it may undergo elimination of the S-trityl moiety to afford a dehydroalanine at this position (**218**). Conjugate addition of piperidine irreversibly yields the piperidine adduct **219**, which appears as a signal at $[M + 51]^+$ during MALDI-TOF MS analysis.

Scheme 43. Deprotonation of a C-terminal cysteine attached via a hydroxymethyl linker, leading to epimerization (a) or piperidine adduct formation (b).



To avoid this problem, a resin containing a sterically hindered linker must be used for the SPPS of peptides with a C-terminal cysteine residue.²⁰⁶ Two such resins are the NovaSyn™ TGT resin (**220**) and the 2-chlorotrityl resin (**221**) (Figure 21). Both contain a bulky triphenylmethyl group as a linker to the peptide, which prevents access to the C-terminal α -proton by piperidine (**215**).

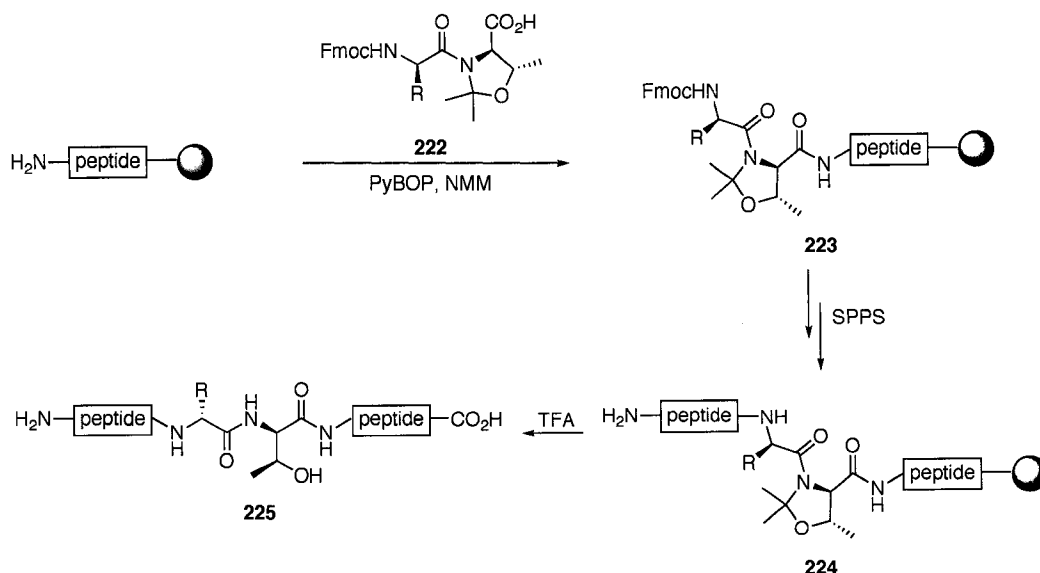
Figure 21. The bulky trityl groups of the NovaSyn™ TGT (**220**) and 2-chlorotrityl (**221**) resins prevent deprotonation at the α -centre of C-terminal cysteine.



1.2 Use of Pseudoproline Dipeptides

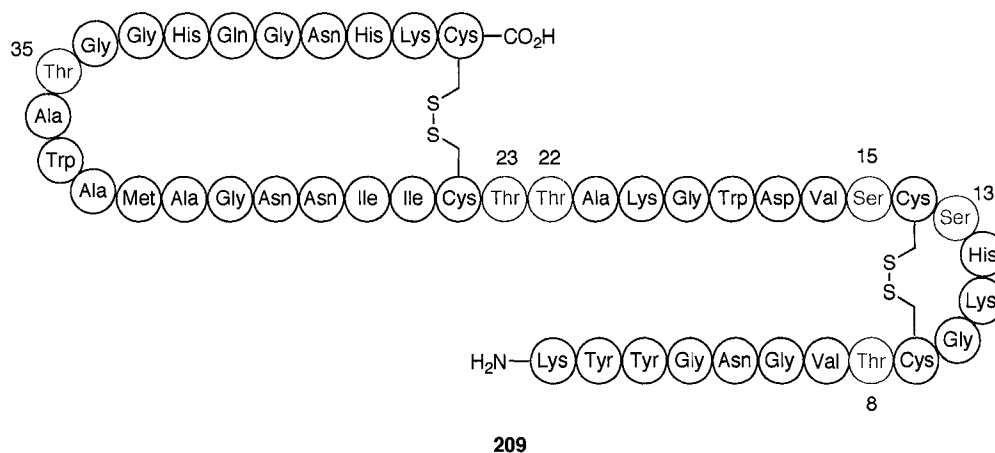
The synthesis of large peptides on solid phase can be problematic due to the decreased synthetic efficiency encountered as the peptide is elongated. This is a result of secondary structure formation or aggregation with other peptides, and is especially pronounced for peptides containing hydrophobic amino acids such as alanine, valine, and isoleucine, as well as those containing amino acids that can form intra-chain hydrogen bonds like glutamine, serine, and threonine. An effective way to minimize aggregation of the peptide chain is through the use of secondary amino acid surrogates known as pseudoproline dipeptides.^{204, 205} They consist of a dipeptide in which the serine or threonine residue has been protected by an acid-labile isopropylidene group, giving a proline-like oxazolidine (Scheme 44). Introduction of the pseudoproline residue as a dipeptide avoids acylation of the hindered oxazolidine nitrogen, and also has the advantage of extending the peptide chain by two residues in one step. The native sequence (**225**) is regenerated upon cleavage and deprotection with TFA.

Scheme 44. Incorporation of a pseudoproline dipeptide (**222**) during SPPS.



The incorporation of pseudoproline residues at regular intervals of 5-6 amino acids is very effective for the synthesis of long peptides. Pediocin PA-1 (**209**) contains threonine residues at positions 8, 22, 23, and 35, as well as serine residues at positions 13 and 15 (Figure 22). The threonine residues at positions 8, 22, and 35 are the most conveniently positioned for incorporation of pseudoproline dipeptides, as both Fmoc-Val-Thr($\Psi^{\text{Me,Me}}$ pro)-OH and Fmoc-Ala-Thr($\Psi^{\text{Me,Me}}$ pro)-OH are commercially available.²⁰⁶ Neither of the potential serine-derived dipeptides is commercially available.

Figure 22. Pediocin PA-1, with the positions of the threonine and serine residues highlighted.



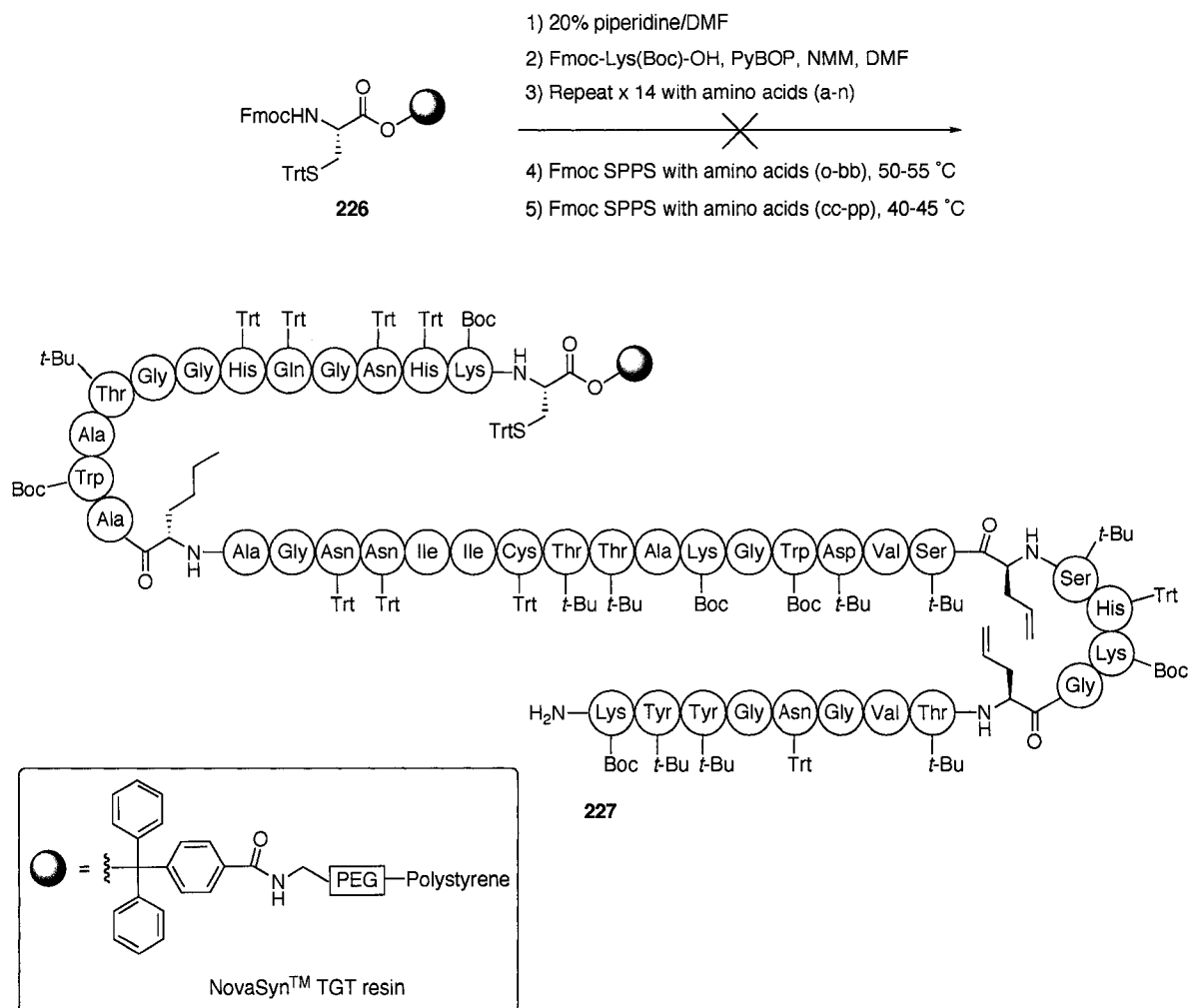
2. Solid Phase Peptide Synthesis (SPPS) of Pediocin PA-1 Analogues

2.1 Synthesis of 9,14-Diallyl 31-Butyl Pediocin PA-1 (**210**)

The synthesis of the 9,14-diallyl analogue of pediocin PA-1 was first attempted on NovaSyn™ TGT resin. In this early attempt, pseudoproline dipeptides were not used.

Starting with the NovaSyn™ TGT resin pre-loaded with Fmoc-Cys(Trt)-OH (**226**), extension of the peptide is accomplished using standard Fmoc chemistry (Scheme 45). The side chain protecting groups used are triphenylmethyl (Trt) for cysteine, histidine, asparagine, and glutamine, *tert*-butoxycarbonyl (Boc) for lysine and tryptophan, and *tert*-butyl (*t*-Bu) for threonine, serine, and tyrosine. Extension of the peptide to the first 16 residues proceeds smoothly, however, the coupling reactions become sluggish after this point. Heating the resin mixture to 50-55 °C during couplings results in complete reactions. These conditions can be employed up to residue 30, at which point leaching of the polyethylene glycol (PEG) chains from the resin begins to occur, as evident from the appearance of several peaks differing by 44 mass units during MALDI-TOF MS, corresponding to the -OCH₂CH₂- groups of PEG. As the PEG chain is linked to the polystyrene backbone via an acid-stable ethyl ether, treatment of the resin with TFA during deprotection is not expected to cause PEG leakage. The breakdown of PEG presumably arises through the formation of PEG peroxides from oxygen and light during prolonged storage,²⁰⁶ a process that is probably exacerbated by heating during the coupling reactions. In an attempt to minimize PEG leaching, the reaction temperature was decreased to 45-50 °C for the coupling of amino acids 31 to 44. Although MALDI-TOF MS analysis of the crude material indicated that a small amount of the desired peptide had formed, as evident by a weak signal at 4597 ([MH]⁺), the product could not be isolated after attempted purification by reverse phase HPLC. Thus, although the NovaSyn™ TGT resin may be appropriate for the synthesis of short peptides, it clearly does not offer the robustness required for the synthesis of a longer peptide. The synthesis of the 9,14-diallyl analogue was thus re-initiated with several improvements.

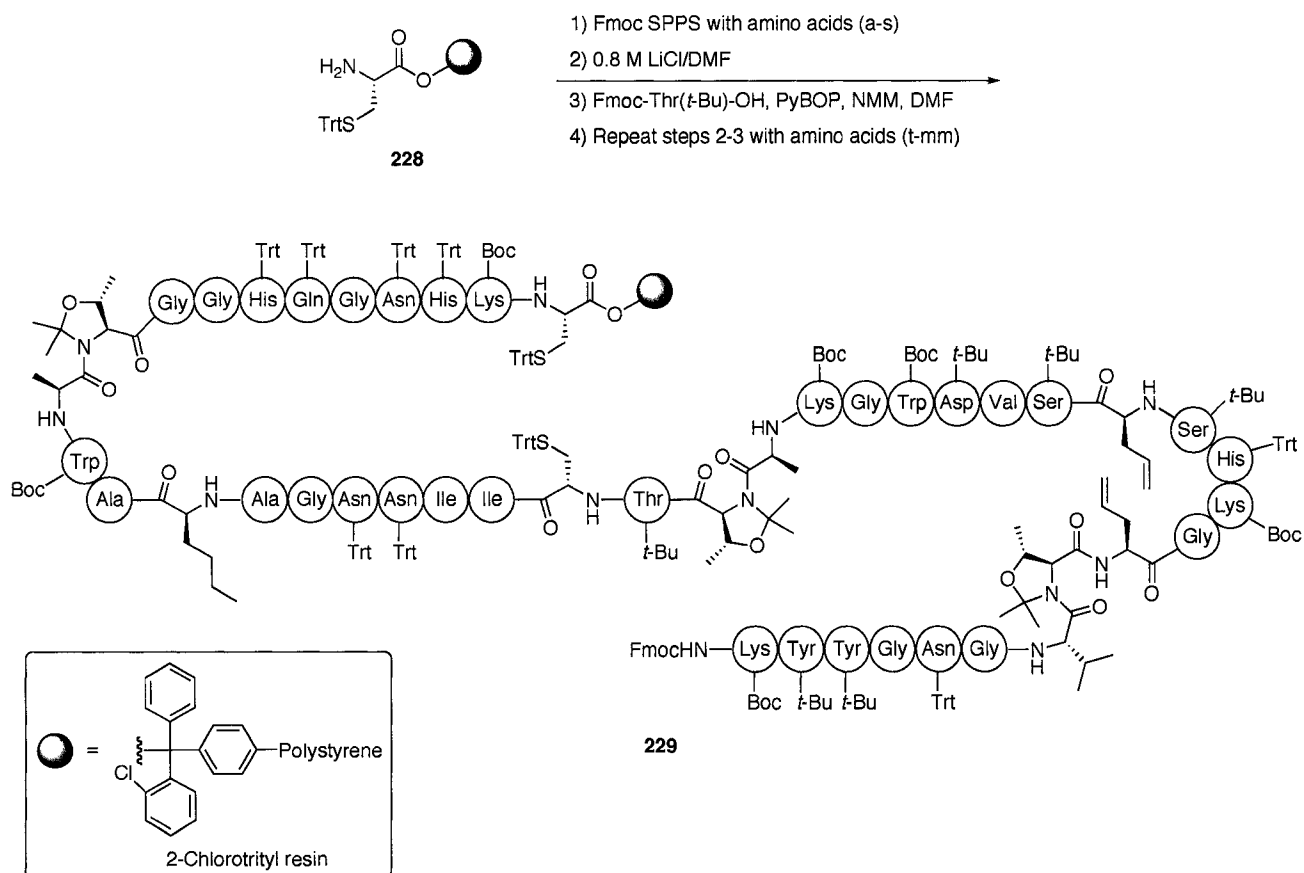
Scheme 45. Attempted synthesis of pediocin analogue using NovaSyn™ TGT resin.^{a,b,c}



^a Conditions: (a) Fmoc-His(Trt)-OH, (b) Fmoc-Asn(Trt)-OH, (c) Fmoc-Gly-OH, (d) Fmoc-Gln(Trt)-OH, (e) Fmoc-His(Trt)-OH, (f) Fmoc-Gly-OH, (g) Fmoc-Gly-OH, (h) Fmoc-Thr(*t*-Bu)-OH, (i) Fmoc-Ala-OH, (j) Fmoc-Trp(Boc)-OH, (k) Fmoc-Ala-OH, (l) Fmoc-Nle-OH, (m) Fmoc-Ala-OH, (n) Fmoc-Gly-OH, ^b Conditions: (o) Fmoc-Asn(Trt)-OH, (p) Fmoc-Asn(Trt)-OH, (q) Fmoc-Ile-OH, (r) Fmoc-Ile-OH, (s) Fmoc-Cys(Trt)-OH, (t) Fmoc-Thr(*t*-Bu)-OH, (u) Fmoc-Thr(*t*-Bu)-OH, (v) Fmoc-Ala-OH, (w) Fmoc-Lys(Boc)-OH, (x) Fmoc-Gly-OH, (y) Fmoc-Trp(Boc)-OH, (z) Fmoc-Asp(*t*-Bu)-OH, (aa) Fmoc-Val-OH, (bb) Fmoc-Ser(*t*-Bu)-OH, ^c Conditions: (cc) Fmoc-AllGly-OH, (dd) Fmoc-Ser(*t*-Bu)-OH, (ee) Fmoc-His(Trt)-OH, (ff) Fmoc-Lys(Boc)-OH, (gg) Fmoc-Gly-OH, (hh) Fmoc-AllGly-OH, (ii) Fmoc-Thr(*t*-Bu)-OH, (jj) Fmoc-Val-OH, (kk) Fmoc-Gly-OH, (ll) Fmoc-Asn(Trt)-OH, (mm) Fmoc-Gly-OH, (nn) Fmoc-Tyr(*t*-Bu)-OH, (oo) Fmoc-Tyr(*t*-Bu)-OH, (pp) Fmoc-Lys(Boc)-OH.

The 2-chlorotrityl resin offers the same protection to the C-terminal cysteine residue as does the NovaSyn™ TGT resin due to the bulky trityl group, however it does not contain PEG as part of its linker to the polystyrene matrix. This eliminates the problem of PEG leaching during a lengthy synthesis. Thus, starting with the 2-chlorotrityl resin pre-loaded with H-Cys(Trt)-OH (**228**), coupling of the first 21 amino acids using Fmoc-SPPS proceeds readily. The positions corresponding to 34 and 35 of the final peptide are coupled using the pseudoproline dipeptide Fmoc-Val-Thr($\Psi^{\text{Me,Me}}$ pro)-OH, and Fmoc-norleucine (Fmoc-Nle) is introduced in place of the oxidatively unstable methionine at position 31 (Scheme 46). Starting at the 22nd residue, it is necessary to treat the resin with 0.8 M LiCl in DMF before Fmoc removal. This chaotropic salt prevents aggregation of the peptide through lithium coordination to main-chain and side-chain carbonyl groups, and therefore allows the deprotection and coupling steps to proceed more efficiently. Use of LiCl also eliminates the need for harsher reaction conditions such as the use of stronger bases for deprotection (e.g. DBU) or heating during the coupling steps. The remaining residues (1-23) are coupled using standard Fmoc SPPS chemistry, with positions 21 and 22 introduced as Fmoc-Ala-Thr($\Psi^{\text{Me,Me}}$ pro)-OH and positions 7 and 8 coupled as Fmoc-Val-Thr($\Psi^{\text{Me,Me}}$ pro)-OH. Fmoc-AllGly-OH is incorporated at positions 9 and 14 in place of cysteine.

Scheme 46. Synthesis of resin-bound 9,14-diallyl 31-butyl pediocin PA-1 (**229**).^{a,b}

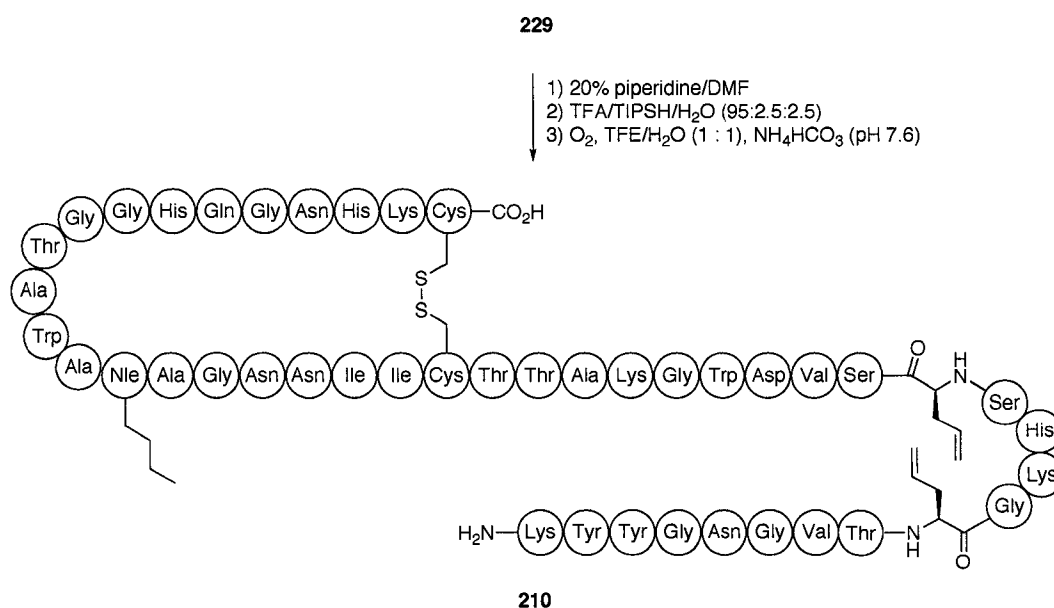


^a Conditions: (a) Fmoc-Lys(Boc)-OH, (b) Fmoc-His(Trt)-OH, (c) Fmoc-Asn(Trt)-OH, (d) Fmoc-Gly-OH, (e) Fmoc-Gln(Trt)-OH, (f) Fmoc-His(Trt)-OH, (g) Fmoc-Gly-OH, (h) Fmoc-Gly-OH, (i) Fmoc-Ala-Thr($\Psi^{\text{Me,Me}}$ pro)-OH, (j) Fmoc-Trp(Boc)-OH, (k) Fmoc-Ala-OH, (l) Fmoc-Nle-OH, (m) Fmoc-Ala-OH, (n) Fmoc-Gly-OH, (o) Fmoc-Asn(Trt)-OH, (p) Fmoc-Asn(Trt)-OH, (q) Fmoc-Ile-OH, (r) Fmoc-Ile-OH, (s) Fmoc-Cys(Trt)-OH,
^b Conditions: (t) Fmoc-Ala-Thr($\Psi^{\text{Me,Me}}$ pro)-OH, (u) Fmoc-Lys(Boc)-OH, (v) Fmoc-Gly-OH, (w) Fmoc-Trp(Boc)-OH, (x) Fmoc-Asp(*t*-Bu)-OH, (y) Fmoc-Val-OH, (z) Fmoc-Ser(*t*-Bu)-OH, (aa) Fmoc-AllGly-OH, (bb) Fmoc-Ser(*t*-Bu)-OH, (cc) Fmoc-His(Trt)-OH, (dd) Fmoc-Lys(Boc)-OH, (ee) Fmoc-Gly-OH, (ff) Fmoc-AllGly-OH, (gg) Fmoc-Val-Thr($\Psi^{\text{Me,Me}}$ pro)-OH, (hh) Fmoc-Gly-OH, (ii) Fmoc-Asn(Trt)-OH, (jj) Fmoc-Gly-OH, (kk) Fmoc-Tyr(*t*-Bu)-OH, (ll) Fmoc-Tyr(*t*-Bu)-OH, (mm) Fmoc-Lys(Boc)-OH.

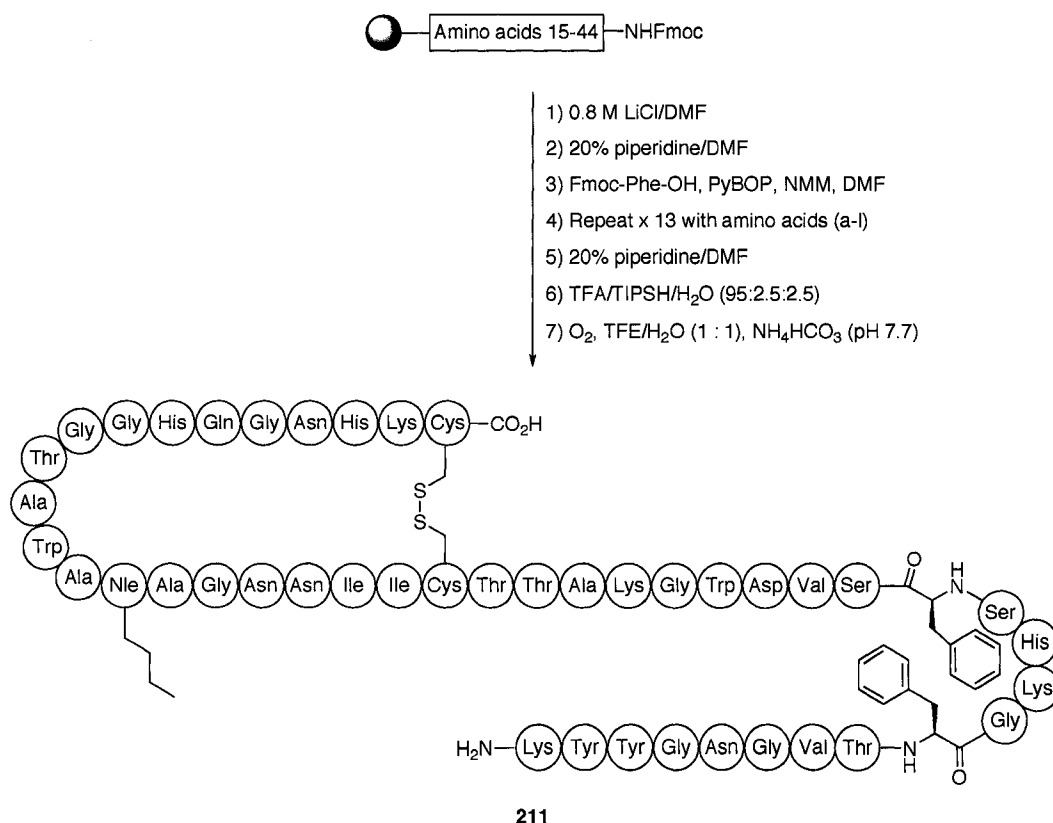
The final Fmoc removal is accomplished with 20% piperidine in DMF, and the peptide is then cleaved from the resin with global deprotection using a 95:2.5:2.5 (v/v/v) mixture of TFA/TIPSH/H₂O (Scheme 47). The 24,44-disulfide bond is formed by

bubbling oxygen through a solution of the crude peptide in a 1:1 mixture of TFE/H₂O buffered to pH 7.6 with NH₄HCO₃.¹⁷⁰ Trifluoroethanol provides a membrane-mimicking environment and thus induces α -helix formation in the central region of the peptide. Purification yields pediocin PA-1 analogue **210** that is > 90% pure by analytical HPLC. The mass of **210** as determined by MALDI-TOF MS is in agreement with that of the calculated mass (4596.7, [MH]⁺), and MS/MS analysis of residues 1-20 after trypsin digestion confirms the correct sequence (attempted sequencing of residues 21-44 was unsuccessful). The major impurity in the sample is the product arising from transamidation of Asp17 with piperidine, which appears as an [M + 67]⁺ peak during MALDI-TOF MS analysis (**230**, Figure 23). The position of the transamidation was confirmed by MS/MS analysis, and presumably arises through formation of an aspartimide and subsequent ring-opening with piperidine.²⁰⁶

Scheme 47. Final steps in the synthesis of **210**.



Scheme 48. Synthesis of 9,14-dibenzyl 31-butyl pediocin PA-1 (**211**).^a



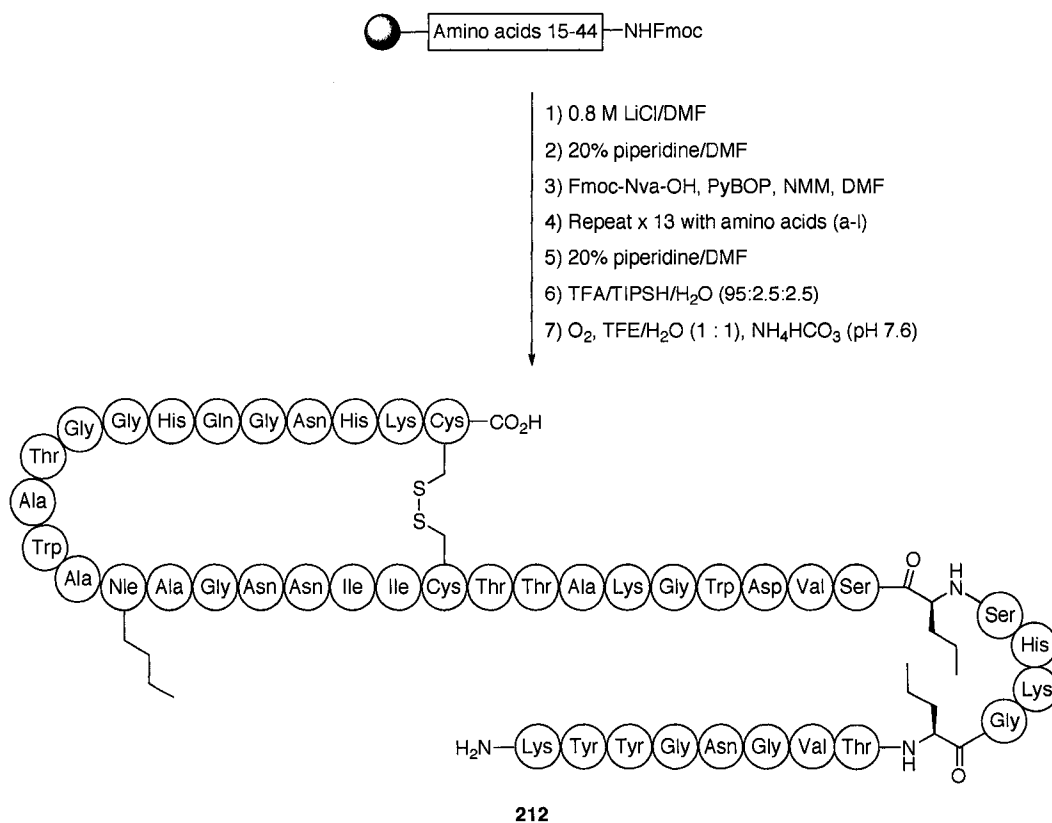
^a Conditions: (a) Fmoc-Ser(*t*-Bu)-OH, (b) Fmoc-His(Trt)-OH, (c) Fmoc-Lys(Boc)-OH, (d) Fmoc-Gly-OH, (e) Fmoc-Phe-OH, (f) Fmoc-Val-Thr($\Psi^{\text{Me,Me}}$ pro)-OH, (g) Fmoc-Gly-OH, (h) Fmoc-Asn(Trt)-OH, (i) Fmoc-Gly-OH, (j) Fmoc-Tyr(*t*-Bu)-OH, (k) Fmoc-Tyr(*t*-Bu)-OH, (l) Fmoc-Lys(Boc)-OH.

2.3 Synthesis of 9,14-Dipropyl 31-Butyl Pediocin PA-1 (**212**)

The synthesis of pediocin PA-1 analogue **212** is achieved using the same protocol as for **211**, except that Fmoc-norvaline is coupled at positions 9 and 14 instead of Fmoc-Phe-OH (Scheme 49). Cleavage from the resin with deprotection and 24,44-disulfide bond formation is achieved as previously described. As for **211**, purification of **212** by reverse phase HPLC required several runs, and resulted in only a small amount of material (0.5 mg) which appeared to be ~ 75% pure by analytical HPLC. Purification

was not pursued any further and the peptide was used in biological assays as a mixture of ~ 75% purity. The major contaminants were the same as those observed in **211**, which is not surprising considering both these peptides originated from the same batch of resin.

Scheme 49. Synthesis of 9,14-dipropyl 31-butyl pediocin PA-1 (**212**).^a



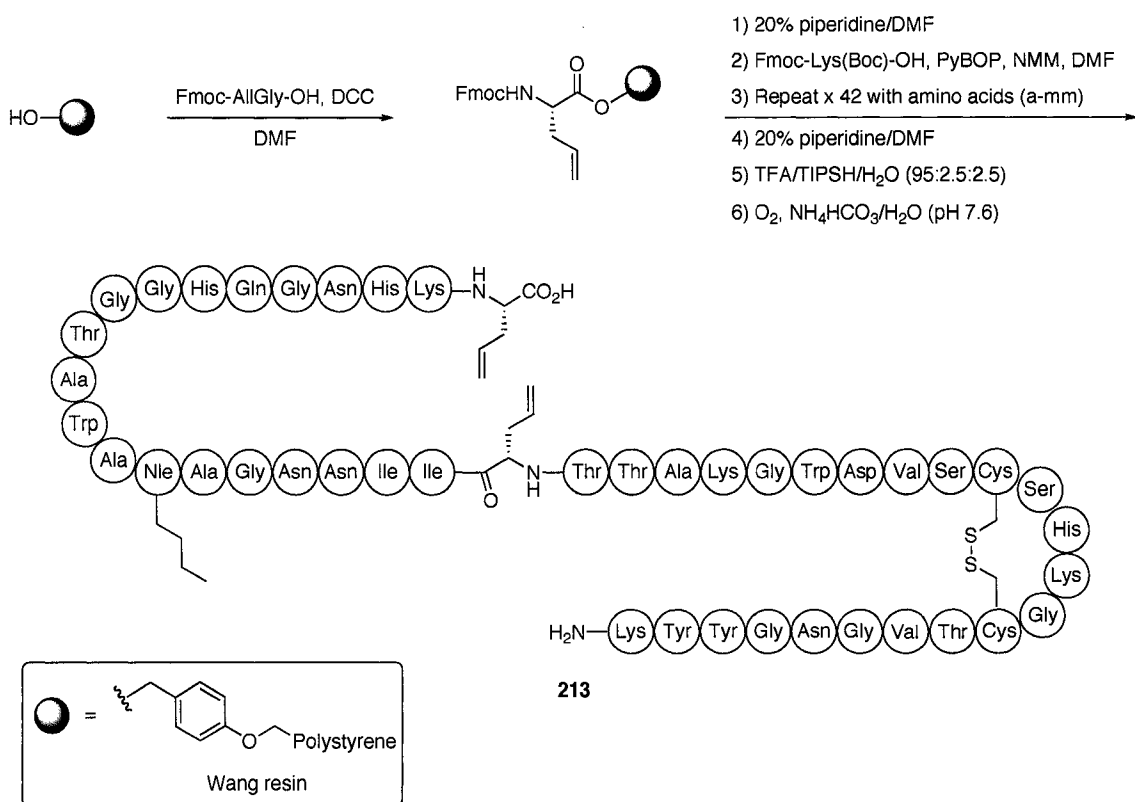
^a Conditions: (a) Fmoc-Ser(*t*-Bu)-OH, (b) Fmoc-His(Trt)-OH, (c) Fmoc-Lys(Boc)-OH, (d) Fmoc-Gly-OH, (e) Fmoc-Nva-OH, (f) Fmoc-Val-Thr($\Psi^{\text{Me,Me}}$ pro)-OH, (g) Fmoc-Gly-OH, (h) Fmoc-Asn(Trt)-OH, (i) Fmoc-Gly-OH, (j) Fmoc-Tyr(*t*-Bu)-OH, (k) Fmoc-Tyr(*t*-Bu)-OH, (l) Fmoc-Lys(Boc)-OH.

2.4 Synthesis of 24,44-Diallyl 31-Butyl Pediocin PA-1 (213)

Because pediocin PA-1 analogue **213** does not contain a C-terminal cysteine, its synthesis can be conducted using Wang resin. The first residue, allylglycine, is coupled

to the resin using DCC (Scheme 50). SPPS then proceeds using the same conditions as for the previously described analogues, except that allylglycine residues are incorporated at positions 24 and 44, and cysteine residues are coupled at positions 9 and 14 (the first 27 residues were coupled by 2006 summer student Zhendong Li). The extended linear peptide on resin is treated with piperidine to remove the final Fmoc group, and the peptide is cleaved from the resin with simultaneous deprotection using TFA. The N-terminal disulfide bond is formed by bubbling O₂ through a solution of the peptide in H₂O buffered to pH 7.6. Purification by reverse phase HPLC gives product **213**, which is > 90% pure by analytical HPLC. The mass is in accordance with the calculated mass (4596.7, [MH]⁺).

Scheme 50. Synthesis of 24,44-diallyl 31-butyl pediocin PA-1 (**213**).^a



^a Conditions: (a) Fmoc-His(Trt)-OH, (b) Fmoc-Asn(Trt)-OH, (c) Fmoc-Gly-OH, (d) Fmoc-Gln(Trt)-OH, (e) Fmoc-His(Trt)-OH, (f) Fmoc-Gly-OH, (g) Fmoc-Gly-OH, (h) Fmoc-Ala-Thr($\Psi^{\text{Me,Me}}$ pro)-OH, (i) Fmoc-Trp(Boc)-OH, (j) Fmoc-Ala-OH, (k) Fmoc-Nle-OH, (l) Fmoc-Ala-OH, (m) Fmoc-Gly-OH, (n) Fmoc-Asn(Trt)-OH, (o) Fmoc-Asn(Trt)-OH, (p) Fmoc-Ile-OH, (q) Fmoc-Ile-OH, (r) Fmoc-AllGly-OH, (s) Fmoc-Thr(*t*-Bu)-OH, (t) Fmoc-Ala-Thr($\Psi^{\text{Me,Me}}$ pro)-OH, (u) Fmoc-Lys(Boc)-OH, (v) Fmoc-Gly-OH, (w) Fmoc-Trp(Boc)-OH, (x) Fmoc-Asp(*t*-Bu)-OH, (y) Fmoc-Val-OH, (z) Fmoc-Ser(*t*-Bu)-OH, (aa) Fmoc-Cys(Trt)-OH, (bb) Fmoc-Ser(*t*-Bu)-OH, (cc) Fmoc-His(Trt)-OH, (dd) Fmoc-Lys(Boc)-OH, (ee) Fmoc-Gly-OH, (ff) Fmoc-Cys(Trt)-OH, (gg) Fmoc-Val-Thr($\Psi^{\text{Me,Me}}$ pro)-OH, (hh) Fmoc-Gly-OH, (ii) Fmoc-Asn(Trt)-OH, (jj) Fmoc-Gly-OH, (kk) Fmoc-Tyr(*t*-Bu)-OH, (ll) Fmoc-Tyr(*t*-Bu)-OH, (mm) Fmoc-Lys(Boc)-OH.

3. Biological Evaluation of Pediocin PA-1 Analogues

The four synthesized pediocin PA-1 analogues were tested for antimicrobial activity using the spot on lawn assay. The indicator organisms used were *Listeria*

monocytogenes ATCC 43256 and *Carnobacterium divergens* LV13. None of the four analogues display any activity against these strains at a concentration of 70 μM . It is conceivable that the potential interactions between the propyl groups of Nva-9 and Nva-14 in **212** are too weak to stabilize the β -hairpin in this region as the native disulfide bond does. For dibenzyl analogue **211**, the π -stacking between the phenyl rings of Phe-9 and Phe-14 may compete with other nearby aromatic residues, such as Tyr-2, Tyr-3, and Trp-18. Interaction of one of the phenylalanine residues with Trp-18 would be expected to be detrimental to the activity of the peptide, since Trp-18 is crucial for proper positioning of the peptide in the plasma membrane of the target cell.¹⁷³

It is surprising that **210** does not display any antimicrobial activity considering the potency of the corresponding diallyl leucocin A analogue **208**. Both leucocin A and pediocin PA-1 are believed to bind to the same cell surface receptor, namely the IIC and IID subunits of the man-PTS. To determine whether the diallyl pediocin PA-1 analogues **210** and **213** could still bind to the receptor, their antagonistic activity against leucocin A (**206**) was tested using a spot on lawn assay (done by a graduate student in our group, Darren Derksen). At a leucocin A concentration of 9 μM , neither **210** nor **213** acts as an antagonist at a concentration of 500 μM . This suggests that **210** and **213** do not bind to the cell surface receptors, or at best, bind very weakly such that they are readily displaced by **208**. Presumably, the absence of receptor binding by **213** is due to the modifications introduced in its C-terminal domain, the region responsible target cell specificity.^{184, 185} It is apparent that hydrophobic interactions between the allyl side chains of allylglycine residues are not sufficient to stabilize the α -helix in the conformation required for activity. Previously, it was shown that the mutant pediocin[C24S,C44S] retained some

activity against several indicator strains, exhibiting 10-100 times lower potency than pediocin PA-1.^{173, 182} However, the strains tested did not include *L. monocytogenes* or *C. divergens*. Therefore, it cannot be concluded whether or not the absence of activity found in this study is strain specific. It is less clear why **210** displays no receptor binding, as its C-terminal domain is unchanged from the wild type peptide except for the Met31Nle mutation, which should not affect activity.¹⁷⁰ An alternative explanation may be that pediocin PA-1 and leucocin A bind to different parts of the putative receptor. A C-terminal fragment of pediocin PA-1 that was not antimicrobially active but was able to inhibit pediocin PA-1 activity, presumably through competition for receptor binding, was unable to inhibit the closely related bacteriocins leucocin A, sakacin P, and curvacin A.¹⁸⁷

It is tempting to speculate that the absence of activity for **210** may arise from the inability of hydrophobic interactions between the allyl side chains at positions 9 and 14 to stabilize the intervening β -turn sequence -G10-K11-H12-S13-. Based on the probability of an amino acid to occur at a given position in a β -turn, this sequence shows weak identity¹⁷⁴ with six known types of consensus β -turns,²⁰⁷ including the commonly observed type I' (YNGK), type II' (YGNT), and type VIII (PPNP) (Table 6). Therefore, it may require the covalent bonds of the disulfide bridge to stabilize it. In contrast, the corresponding leucocin A sequence -T10-K11-S12-G13- shows 58% identity with a type II' β -turn (Table 6). It may consequently be able to maintain an active conformation requiring merely the assistance of non-covalent interactions, such as those apparently present in 9,14-diallyl leucocin A (**208**).

Table 6. Percent identity with selected β -turn consensus sequences of positions 10-13 in pediocin PA-1 and leucocin A.

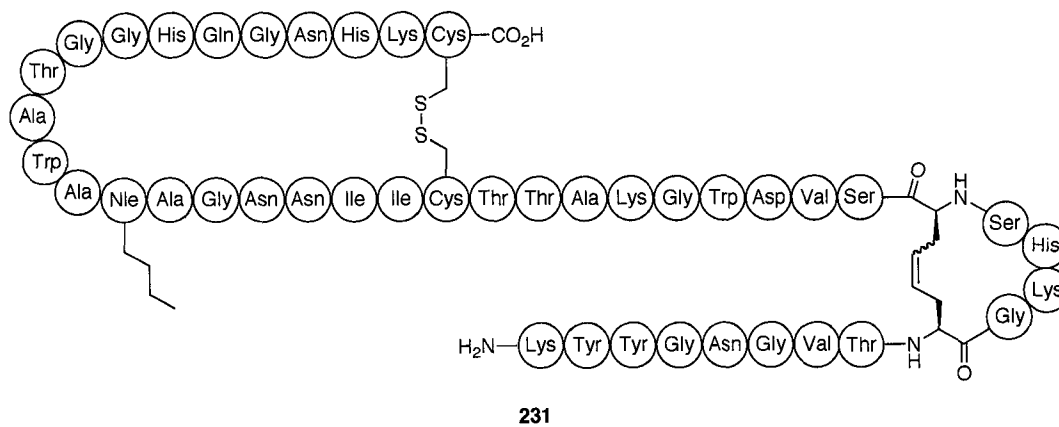
Sequence	% identity to selected β -turn consensus sequences		
	I' (YNGK)	II' (YNGT)	VIII (PPNP)
-G10-K11-H12-S13- (Ped PA-1)	12	25	48
-T10-K11-S12-G13- (Leu A)	13	58	39

4. Conclusions and Future Directions

The synthesis of four analogues of pediocin PA-1 wherein the cysteine residues were replaced with amino acids potentially capable of hydrophobic interactions was undertaken to test the ability of these structures to mimic the disulfide bridge, based on positive results shown for 9,14-diallyl leucocin A (**206**).¹⁹⁸ None of the analogues displayed any antimicrobial activity, thus it does not appear that the trend observed for leucocin A analogue **206** can be extended to the related type IIa bacteriocin pediocin PA-1.

Future studies may be directed towards the synthesis of the 9,14-dicarba analogue of pediocin PA-1 (**231**, Figure 24). Previously, it has been shown that dicarba analogues of leucocin A¹⁹⁸ and oxytocin,^{199, 200} formed *via* ring-closing metathesis of allylglycine residues, are only one order of magnitude less active than the parent peptides. It would be interesting to determine if this also holds true for pediocin PA-1.

Figure 24. Structure of proposed 9,14-dicarba 31-butyl pediocin PA-1 (**231**).



CHAPTER 3. Experimental Procedures

1. General Procedures

1.1 Reagents, Solvents, and Solutions

All reagents and solvents employed were purchased from the Aldrich Chemical Company Inc. (Madison, WI), Sigma Chemical Company (St. Louis, MO), or Fisher Scientific Ltd. (Ottawa, ON). Unless otherwise stated, all protected amino acids, derivatives, and SPPS solid supports were purchased from the Calbiochem-Novabiochem Corporation (San Diego, CA), Sigma-Aldrich Canada Ltd. (Oakville, ON), or Bachem California Inc. (Torrance, CA). All reagents and solvents were of American Chemical Society (ACS) grade and were used without further purification unless otherwise stated. All processes involving air or moisture sensitive reactants and/or requiring anhydrous conditions were performed under a positive pressure of argon using oven or flame-dried glassware. Solvents for anhydrous reactions were dried according to Perrin *et al.*²⁰⁸ and Vogel.²⁰⁹ Tetrahydrofuran and diethyl ether were freshly distilled over sodium and benzophenone under an atmosphere of dry argon prior to use. Acetonitrile, dichloromethane, pyridine, and triethylamine were distilled over calcium hydride. Ethyl acetate was distilled over potassium carbonate. Methanol and ethanol were distilled over potassium carbonate. Dimethylformamide was HPLC grade. The removal of solvent *in vacuo* refers to evaporation under reduced pressure below 40 °C using a Büchi rotary evaporator followed by evacuation (< 0.1 mm Hg) to a constant sample mass. Deionized water was obtained from a Milli-Q reagent water system (Millipore Co., Milford, MA).

Unless otherwise specified, solutions of NH_4Cl , NaHCO_3 , HCl , citric acid, LiOH , and $\text{Na}_2\text{S}_2\text{O}_3$ refer to aqueous solutions. Brine refers to a saturated aqueous solution of NaCl .

1.2 Purification Techniques

Unless stated otherwise, all reactions and fractions from column chromatography were monitored by thin layer chromatography (TLC) using glass-backed plates (1.5 x 5 cm) pre-coated (0.25 mm) with silica gel containing a UV fluorescent indicator (normal silica gel, Merck 60 F₂₅₄; reverse-phase, Merck RP-8 and RP-18 F_{254S}). Compounds were visualized by exposing the plates to UV light, iodine staining, or by dipping the plates in solutions of $\text{Ce}(\text{SO}_4)\cdot 4\text{H}_2\text{O}/(\text{NH}_4)\text{MoO}_4\cdot 4\text{H}_2\text{O}/\text{H}_2\text{SO}_4/\text{H}_2\text{O}$ (5 g:12.5 g:28 mL:472 mL) or phosphomolybdic acid/ethanol (5:95) followed by heating on a hot plate. Flash chromatography was performed according to the method of Still *et al.*²¹⁰ using grade 60 silica gel (Rose Scientific, 230-400 mesh). Semi-preparative reverse-phase HPLC was performed on a Varian ProStar chromatograph equipped with model 210 pump heads, a model 325 dual wavelength UV detector, and a Rheodyne 7725i injector fitted with a 500 μL sample loop. The column used was a Vydac C₈ steel walled column (10 μm , 10 x 250 mm). The mobile phases used for nucleotide analogue purification were as follows. System A: eluting with 10% MeCN/90% H₂O (0.1% TFA) for 5 min, then a gradient of 10-48% MeCN over 13 min, at a flow rate of 3 mL/min. System B: eluting with 5% MeCN/95% H₂O (0.1% TFA) for 5 min, then a gradient of 5-60% MeCN over 17 min, at a flow rate of 3 mL/min. System C: eluting with 20% MeCN/80% H₂O (0.1% TFA) for 5 min, then a gradient of 20-57% MeCN over 15.5 min, at a flow rate of 3 mL/min. The nucleotide analogues were monitored at 220 and 280 nm. All HPLC solvent systems

were filtered through a Millipore (Bedford, MA) filtration system under vacuum prior to use.

1.3 Instrumentation for Compound Characterization

Nuclear magnetic resonance (NMR) spectra were obtained on Varian Inova 300, 400, 500, and 600 MHz spectrometers. ^1H NMR chemical shifts are reported in parts per million (ppm) downfield relative to tetramethylsilane using the residual proton resonance of solvents as the reference: CDCl_3 , δ 7.24; CD_3OD , δ 3.30; D_2O , δ 4.79. ^{13}C NMR chemical shifts are reported relative to: CDCl_3 , δ 77.0; CD_3OD , δ 49.0; D_2O referenced to 1% acetone, δ 31.1. Signals are quoted to within 0.1 ppm except where close peaks necessitate an additional significant figure. Additional assignments were made using pulsed field gradient versions of shift correlation spectroscopy (gCOSY), heteronuclear multiple quantum coherence spectroscopy (gHMQC), and heteronuclear multiple bond correlation spectroscopy (gHMBC).

^1H NMR data are reported in the following order: multiplicity (app, apparent, s, singlet; d, doublet; t, triplet; q, quartet; quin, quintet; and m, multiplet), number of protons, coupling constant (J) in Hertz (Hz), and assignment. When appropriate, the multiplicity is preceded by br, indicating that the signal was broad. The coupling constants reported are within an error range of 0.2-0.4 Hz, and have been rounded to the nearest 0.1 Hz. All literature compounds had IR, ^1H NMR, and mass spectra consistent with the assigned structures.

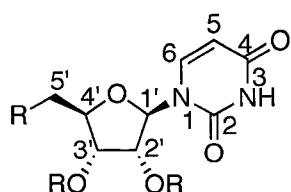
Infrared spectra (IR) were recorded on a Nicolet Magna-IR 750 with Nic-Plan microscope FT-IR spectrometer. Cast refers to the evaporation of a solution on a NaCl

plate. Mass spectra (MS) were recorded on a Kratos AEIMS-50 high resolution mass spectrometer (HRMS), using electron impact ionization (EI), or a Micromass ZabSpec Hybrid Sector-TOF positive or negative mode electrospray ionization (ES). Optical rotations were measured on a Perkin Elmer 241 polarimeter with a microcell (10 cm path length, 1 mL) at ambient temperature and are reported in units of $10^{-1} \text{ deg cm}^2 \text{ g}^{-1}$. All reported optical rotations were referenced against air and were measured at the sodium D line ($\lambda = 589.3 \text{ nm}$).

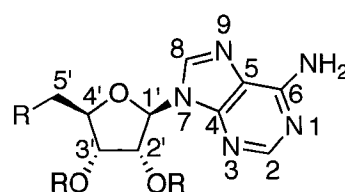
2. Nucleoside Dicarboxylates

2.1 Experimental Data for Compounds

^1H NMR assignments within the ribose and uracil groups of uridine derivatives and the ribose and adenine groups of adenosine derivatives are made using the following numbering schemes:



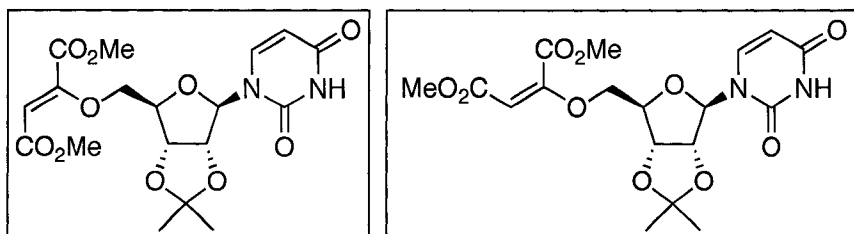
Uridine: ribose and uracil numbering



Adenosine: ribose and adenine numbering

Dimethyl 2-(((3a*R*,4*R*,6*R*,6a*R*)-6-(2,4-dioxo-3,4-dihydropyrimidin-1(2*H*)-yl)-2,2-dimethyltetrahydrofuro[3,4-*d*][1,3]dioxol-4-yl)methoxy)fumarate (48a)

Dimethyl 2-(((3a*R*,4*R*,6*R*,6a*R*)-6-(2,4-dioxo-3,4-dihydropyrimidin-1(2*H*)-yl)-2,2-dimethyltetrahydrofuro[3,4-*d*][1,3]dioxol-4-yl)methoxy)maleate (48b)

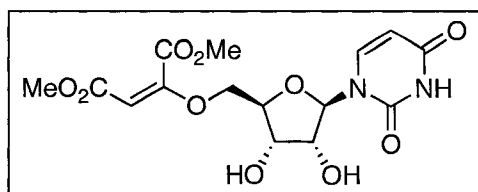


These compounds were prepared by a modification of the procedure of

Inanaga *et al.*⁹¹ A solution of dimethyl acetylenedicarboxylate (20.0 μ L, 0.163 mmol) in MeCN (800 μ L) was added dropwise over 15 min to a solution of 2',3'-*O*-isopropylideneuridine (40.7 mg, 0.142 mmol) and trimethylphosphine (1.00 M in THF, 28.0 μ L, 0.0280 mmol) in MeCN (2.0 mL) at 0 °C. The mixture was warmed to rt and stirred for 69 h, at which point it was cooled to 0 °C and extra dimethyl acetylenedicarboxylate (20.0 μ L, 0.163 mmol) in MeCN (800 μ L) was added. It was again warmed to rt and stirred for another 21 h, then concentrated *in vacuo*. Purification by flash chromatography (SiO₂, CHCl₃/MeOH, 99:1) afforded fumarate **48a** as a colourless glass (18.9 mg, 31%) and maleate **48b** as a colourless glass (17.4 mg, 29%). Data for **48a**: R_f 0.34 (CHCl₃/MeOH, 95:5); $[\alpha]_D^{20} = -30.88$ (c 0.31, CHCl₃); IR (CHCl₃, cast) ν 3492, 3092, 2990, 2955, 1725, 1677, 1279, 1084 cm⁻¹; ¹H NMR (CDCl₃, 500 MHz) δ 1.35 (s, 3H, CH₃), 1.57 (s, 3H, CH₃), 3.71-3.80 (m, 1H, CH_aH_b-5'), 3.74 (s, 3H, OCH₃), 3.84-3.91 (m, 1H, CH_aH_b-5'), 3.85 (s, 3H, OCH₃), 4.29 (dd, 1H, $J = 6.5, 4.0$ Hz, H-4'), 4.92 (dd, 1H, $J = 6.5, 4.0$ Hz, H-3'), 5.05 (dd, 1H, $J = 6.5, 2.3$ Hz, H-2'), 5.58 (d, 1H, $J = 2.3$ Hz, H-1'), 5.81 (d, 1H, $J = 8.0$ Hz, H-5), 7.17 (s, 1H, C=CH), 7.44 (d, 1H, $J =$

8.0 Hz, H-6); ^{13}C NMR (CDCl_3 , 125 MHz) δ 25.2, 27.2, 52.4, 53.4, 62.5, 80.2, 84.3, 87.5, 96.7, 101.9, 114.2, 128.6, 134.9, 141.8, 149.5, 161.4, 162.0, 163.0; HRMS (ES+) calcd for $\text{C}_{18}\text{H}_{22}\text{N}_2\text{O}_{10}\text{Na}$ 449.1167, found 449.1167 $[\text{MNa}]^+$. Data for **48b**: R_f 0.28 ($\text{CHCl}_3/\text{MeOH}$, 95:5); $[\alpha]_{\text{D}}^{20} = -19.71$ (c 0.07, CHCl_3); IR (CH_2Cl_2 , cast) ν 3488, 2989, 2954, 1724, 1676, 1273, 1214, 1084 cm^{-1} ; ^1H NMR (CDCl_3 , 500 MHz) δ 1.33 (s, 3H, CH_3), 1.55 (s, 3H, CH_3), 3.77 (dd, 1H, $J = 12.0, 3.1$ Hz, $\text{CH}_a\text{H}_b\text{-5}'$), 3.78 (s, 3H, OCH_3), 3.81 (s, 3H, OCH_3), 3.89 (dd, 1H, $J = 12.0, 3.1$ Hz, $\text{CH}_a\text{H}_b\text{-5}'$), 4.29 (app q, 1H, $J = 3.1$ Hz, H-4'), 4.89 (dd, 1H, $J = 6.4, 3.1$ Hz, H-3'), 4.96 (dd, 1H, $J = 6.4, 3.0$ Hz, H-2'), 5.60 (d, 1H, $J = 3.0$ Hz, H-1'), 5.80 (d, 1H, $J = 8.5$ Hz, H-5), 6.49 (s, 1H, C=CH), 7.43 (d, 1H, $J = 8.5$ Hz, H-6); ^{13}C NMR (CDCl_3 , 125 MHz) δ 25.2, 27.2, 52.5, 53.0, 62.6, 80.3, 84.1, 87.1, 96.2, 101.9, 114.3, 130.7, 131.0, 141.3, 149.9, 161.1, 161.9, 164.0; HRMS (ES+) calcd for $\text{C}_{18}\text{H}_{22}\text{N}_2\text{O}_{10}\text{Na}$ 449.1167, found 449.1168 $[\text{MNa}]^+$.

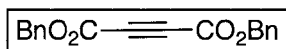
Dimethyl 2-(((2*R*,3*S*,4*R*,5*R*)-5-(2,4-dioxo-3,4-dihydropyrimidin-1(2*H*)-yl)-3,4-dihydroxytetrahydrofuran-2-yl)methoxy)maleate (50b)



48b (14.0 mg, 0.0330 mmol) was stirred in $\text{HCO}_2\text{H}/\text{H}_2\text{O}$ (4:1, 820 μL) at rt for 8 h, then the solvent was removed *in vacuo*. The resulting brown residue was purified by flash chromatography (SiO_2 , EtOAc/MeOH , 100:0 to 95:5) to give **50b** as a pale yellow glass (6.30 mg, 49%): R_f 0.19 (EtOAc/MeOH , 95:5); $[\alpha]_{\text{D}}^{20} = +10.92$ (c 0.73, MeOH); IR (μscope) ν 3650-3150, 3099, 2956, 1713, 1654, 1272, 1216, 1101 cm^{-1} ; ^1H NMR (CD_3OD , 500 MHz) δ 3.74 (dd, 1H, $J = 12.0, 2.8$ Hz, $\text{CH}_a\text{H}_b\text{-5}'$), 3.75 (s, 3H, OCH_3), 3.82 (s, 3H, OCH_3), 3.86 (dd, 1H, $J = 12.0, 2.8$ Hz,

CH_aH_b-5'), 4.01 (ddd, 1H, $J = 5.5, 2.8, 2.8$ Hz, H-4'), 4.14-4.19 (m, 2H, H-3', H-2'), 5.81 (d, 1H, $J = 8.3$ Hz, H-5), 5.87 (d, 1H, $J = 3.0$ Hz, H-1'), 6.73 (s, 1H, C=CH), 8.13 (d, 1H, $J = 8.3$ Hz, H-6); ¹³C NMR (CD₃OD, 125 MHz) δ 53.0, 53.4, 62.0, 71.0, 75.9, 86.4, 91.8, 102.0, 132.1, 133.1, 141.9, 151.7, 163.6, 166.2 (1 carbon signal not observed due to overlap); HRMS (ES+) calcd for C₁₅H₁₈N₂O₁₀Na 409.0854, found 409.0859 [MNa]⁺.

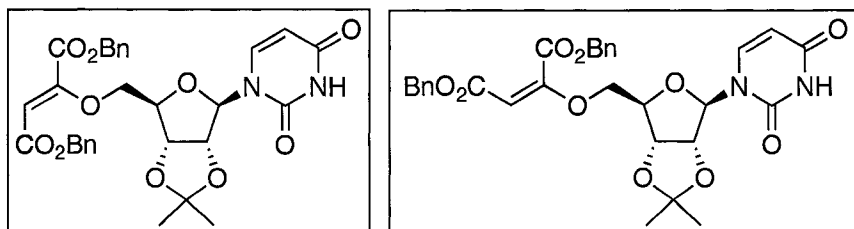
Dibenzyl acetylenedicarboxylate (**52**)



This known compound was prepared as described by Lowe *et al.*⁹⁵ Acetylenedicarboxylic acid (7.50 g, 65.8 mmol), *p*-TsOH (788 mg, 4.60 mmol) and quinol (192 mg, 0.926 mmol) were dissolved in benzyl alcohol (100 mL), and the mixture was distilled at 110 °C under high vacuum. The remaining brown oil in the distillation flask was purified by flash chromatography (SiO₂, petroleum ether/Et₂O, 95:5 to 85:15) to give diester **52** as a yellow oil (14.82 g, 77%): R_f 0.37 (petroleum ether/Et₂O, 85:15); IR (neat) ν 3066, 3035, 2962, 1724, 1587, 1498, 1456, 1259 cm⁻¹; ¹H NMR (CDCl₃, 300 MHz) δ 2.26 (s, 4H, benzylic CH₂), 7.35-7.39 (m, 10H, ArH); ¹³C NMR (CDCl₃, 125 MHz) δ 68.6, 74.9, 128.7, 128.8, 128.9, 134.1, 151.6; HRMS (ES+) calcd for C₁₈H₁₄O₄Na 317.0784, found 317.0787 [MNa]⁺.

Dibenzyl 2-(((3a*R*, 4*R*,6*R*,6a*R*)-6-(2,4-dioxo-3,4-dihydropyrimidin-1(2*H*)-yl)-2,2-dimethyltetrahydrofuro[3,4-*d*][1,3]dioxol-4-yl)methoxy)fumarate (53a)

Dibenzyl 2-(((3a*R*, 4*R*,6*R*,6a*R*)-6-(2,4-dioxo-3,4-dihydropyrimidin-1(2*H*)-yl)-2,2-dimethyltetrahydrofuro[3,4-*d*][1,3]dioxol-4-yl)methoxy)maleate (53b)

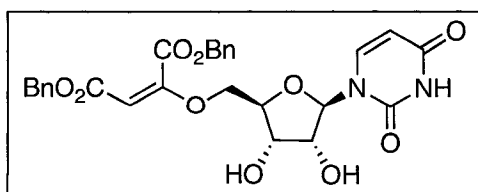


These compounds were synthesized using the same procedure as for

48a and **48b**.⁹¹ A solution of alkyne **52** (2.23 g, 7.58 mmol) in MeCN (27.5 mL) was added dropwise over 15 min to a solution of 2',3'-*O*-isopropylideneuridine (712 mg, 2.50 mmol) and trimethylphosphine (1.00 M in THF, 510 μ L, 0.51 mmol) in MeCN (30.0 mL) at 0 °C. The mixture was warmed to rt and stirred for 4.5 h, then concentrated *in vacuo*. Purification by flash chromatography (SiO₂, CHCl₃/MeOH, 99:1) gave fumarate **53a** as a pale orange foam (304 mg, 21%) and maleate **53b** as a yellow foam (155 mg, 11%). Data for **53a**: *R*_f 0.44 (CHCl₃/MeOH, 95:5); [α]_D²⁰ = -5.04 (*c* 0.25, MeOH); IR (μ scope) ν 3493, 3092, 3034, 2987, 2939, 1722, 1674, 1499, 1268, 1215, 1084; ¹H NMR (CDCl₃, 500 MHz) δ 1.35 (s, 3H, CH₃), 1.57 (s, 3H, CH₃), 3.75 (dd, 1H, *J* = 12.1, 4.2 Hz, CH_aH_b-5'), 3.87 (dd, 1H, *J* = 12.1, 2.5 Hz, CH_aH_b-5'), 4.27-4.29 (m, 1H, H-4'), 4.89-4.91 (m, 1H, H-3'), 4.98 (dd, 1H, *J* = 6.5, 2.3 Hz, H-2'), 5.11 (d, 1H, *J* = 12.3 Hz, benzylic CH_aH_b), 5.16 (d, 1H, *J* = 12.3 Hz, benzylic CH_aH_b), 5.25 (d, 1H, *J* = 12.3 Hz, benzylic CH_cH_d), 5.29 (d, 1H, *J* = 12.3 Hz, benzylic CH_cH_d), 5.50 (d, 1H, *J* = 2.3 Hz, H-1'), 5.74 (d, 1H, *J* = 8.0 Hz, H-5), 7.22 (d, 1H, *J* = 8.0 Hz, H-6), 7.24-7.38 (m, 11H, ArH, C=CH); ¹³C NMR (CDCl₃, 125 MHz) δ 25.3, 27.3, 62.6, 67.4, 68.3, 80.3, 84.2, 87.6, 97.0, 101.8,

114.2, 128.2, 128.50, 128.52, 128.62, 128.64, 129.0, 129.1, 134.7, 134.9, 141.7, 149.5, 161.2, 161.4, 162.4 (1 carbon signal not observed due to overlap); HRMS (ES+) calcd for $C_{30}H_{30}N_2O_{10}Na$ 601.1793, found 601.1791 $[MNa]^+$. Data for **53b**: R_f 0.32 (CHCl₃/MeOH, 95:5); $[\alpha]_D^{20} = -5.56$ (*c* 1.28, CHCl₃); IR (CHCl₃, cast) ν 3500, 3065, 3034, 2988, 2935, 1723, 1677, 1269, 1083 cm^{-1} ; ¹H NMR (CDCl₃, 500 MHz) δ 1.35 (s, 3H, CH₃), 1.57 (s, 3H, CH₃), 3.78 (dd, 1H, *J* = 12.0, 6.4 Hz, CH_aH_b-5'), 3.89 (dd, 1H, *J* = 12.0, 3.4 Hz, CH_aH_b-5'), 4.29 (dd, 1H, *J* = 6.4, 3.4 Hz, H-4'), 4.89 (dd, 1H, *J* = 6.4, 3.4 Hz, H-3'), 4.94 (dd, 1H, *J* = 6.4, 2.8 Hz, H-2'), 5.03 (s, 2H, benzylic CH₂), 5.13 (d, 1H, *J* = 12.3 Hz, benzylic CH_aH_b), 5.16 (d, 1H, *J* = 12.3 Hz, benzylic CH_aH_b), 5.58 (d, 1H, *J* = 2.8 Hz, H-1'), 5.81 (d, 1H, *J* = 8.3 Hz, H-5), 6.56 (s, 1H, C=CH), 7.26-7.36 (m, 19H, ArH), 7.41 (d, 1H, *J* = 8.3 Hz, H-6); ¹³C NMR (CDCl₃, 125 MHz) δ 25.3, 27.2, 62.6, 67.3, 68.0, 80.4, 84.3, 87.2, 96.1, 101.8, 114.3, 128.35, 128.38, 128.4, 128.50, 128.55, 130.6, 131.1, 134.7, 134.9, 141.2, 149.9, 161.2, 161.3, 163.4 (a carbon signal not observed due to overlap); HRMS (ES+) calcd for $C_{30}H_{30}N_2O_{10}Na$ 601.1793, found 601.1797 $[MNa]^+$.

Dibenzyl 2-(((2*R*, 3*S*,4*R*,5*R*)-5-(2,4-dioxo-3,4-dihydropyrimidin-1(2*H*)-yl)-3,4-dihydroxytetrahydrofuran-2-yl)methoxy)maleate (54b)

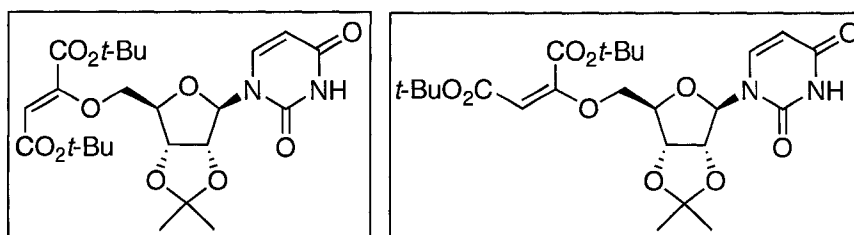


Nucleoside derivative **53b** (23.1 mg, 0.0399 mmol) was stirred in TFA/H₂O (7:1, 1.0 mL) at 0 °C for 45 min, then the solvent was removed *in vacuo*. Purification by flash chromatography (SiO₂, CHCl₃/MeOH, 95:5) gave **54b** as a colourless glass (14.3 mg, 67%): R_f 0.11 (CHCl₃/MeOH, 95:5); $[\alpha]_D^{20} = +11.27$ (*c* 0.11,

CHCl₃); IR (CHCl₃, cast) ν 3650-3100, 3092, 3064, 3033, 2931, 1720, 1669, 1498, 1454, 1271, 1213, 1082 cm⁻¹; ¹H NMR (CDCl₃, 500 MHz) δ 3.76 (dd, 1H, J = 11.0, 4.0 Hz, CH_aH_b-5'), 3.89 (d, 1H, J = 11.0 Hz, CH_aH_b-5'), 4.11 (br s, 1H, H-4'), 4.21-4.25 (m, 2H, H-3', H-2'), 5.01 (s, 2H, benzylic CH₂), 5.11 (d, 1H, J = 12.5 Hz, benzylic CH_aH_b), 5.14 (d, 1H, J = 12.5 Hz, benzylic CH_aH_b), 5.67 (d, 1H, J = 3.5 Hz, H-1'), 5.79 (d, 1H, J = 8.3 Hz, H-5), 6.58 (s, 1H, C=CH), 7.25-7.34 (m, 10H, ArH), 7.76 (d, 1H, J = 8.3 Hz, H-6); ¹³C NMR (CDCl₃, 125 MHz) δ 61.7, 67.5, 68.2, 70.4, 74.9, 85.5, 92.5, 101.7, 128.4, 128.6, 130.6, 131.3, 134.6, 134.8, 140.0, 150.6, 161.3, 161.6, 163.8 (4 carbon signals not observed due to overlap); HRMS (ES⁺) calcd for C₂₇H₂₆N₂O₁₀Na 561.1480, found 561.1479 [MNa]⁺.

Di-*tert*-butyl 2-(((3*aR*,4*R*,6*R*,6*aR*)-6-(2,4-dioxo-3,4-dihydropyrimidin-1(2*H*)-yl)-2,2-dimethyltetrahydrofuro[3,4-*d*][1,3]dioxol-4-yl)methoxy)fumarate (58a)

Di-*tert*-butyl 2-(((3*aR*,4*R*,6*R*,6*aR*)-6-(2,4-dioxo-3,4-dihydropyrimidin-1(2*H*)-yl)-2,2-dimethyltetrahydrofuro[3,4-*d*][1,3]dioxol-4-yl)methoxy)maleate (58b)

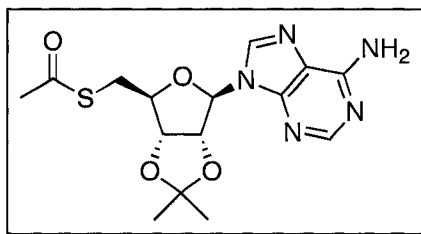


A solution of di-*tert*-butyl acetylenedicarboxylate (852 mg, 3.76

mmol) in MeCN (12.0 mL) was added dropwise to a solution of 2',3'-*O*-isopropylideneadenosine (348 mg, 1.22 mmol) and trimethylphosphine (1.00 M solution in THF, 24.5 μ L, 0.245 mmol) in MeCN (25.0 mL) at 0 °C, and the pale yellow mixture was stirred while slowly warming to rt. After 6 h at rt, starting material was still evident

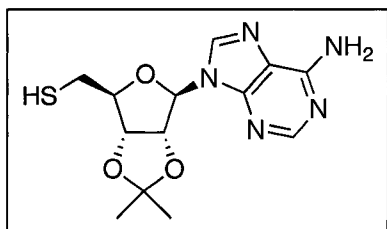
by TLC, so the mixture was heated at 50 °C with stirring for an additional 18 h. The solvent was removed *in vacuo*, and the crude product was purified by flash chromatography (hexanes/EtOAc, 2:1 to 2:3) to yield fumarate **58a** as a white foam (210 mg, 34%) and maleate **58b** as a white foam (228 mg, 37%). Data for **58a**: R_f 0.22 (EtOAc/hexanes, 3:2); $[\alpha]_D^{20} = -23.33$ (*c* 0.15, CHCl₃); IR (CHCl₃, cast) ν 3494, 2981, 2937, 1720, 1676, 1287, 1084 cm⁻¹; ¹H NMR (CDCl₃, 500 MHz) δ 1.34 (s, 3H, CH₃), 1.43 (s, 9H, C(CH₃)₃), 1.51 (s, 9H, C(CH₃)₃), 1.57 (s, 3H, CH₃), 3.77 (dd, 1H, $J = 12.2$, 3.4 Hz, CH_aH_b-5'), 3.88 (dd, 1H, $J = 12.2$, 2.8 Hz, CH_aH_b-5'), 4.25-4.28 (m, 1H, H-4'), 4.95 (dd, 1H, $J = 6.3$, 3.8 Hz, H-3'), 5.09 (dd, 1H, $J = 6.3$, 2.8 Hz, H-2'), 5.51 (s, 1H, H-1'), 5.81 (d, 1H, $J = 8.0$ Hz, H-5), 6.99 (s, 1H, C=CH), 7.35 (d, 1H, $J = 8.0$ Hz, H-6); ¹³C NMR (CDCl₃, 125 MHz) δ 25.2, 27.2, 27.80, 27.84, 62.5, 80.2, 82.4, 83.6, 84.3, 87.1, 87.6, 101.8, 114.1, 130.0, 134.3, 141.6, 149.5, 160.7, 161.4, 162.1; HRMS (ES+) calcd for C₂₄H₃₄N₂O₁₀Na 533.2106, found 533.2100 [MNa⁺]. Data for **58b**: R_f 0.18 (EtOAc/hexanes, 3:2); $[\alpha]_D^{20} = -28.72$ (*c* 0.11, CHCl₃); IR (CHCl₃, cast) ν 3501, 2981, 2937, 1720, 1678, 1278, 1084 cm⁻¹; ¹H NMR (CDCl₃, 500 MHz) δ 1.35 (s, 3H, CH₃), 1.49 (s, 9H, C(CH₃)₃), 1.53 (s, 9H, C(CH₃)₃), 1.57 (s, 3H, CH₃), 3.80 (dd, 1H, $J = 12.3$, 3.3 Hz, CH_aH_b-5'), 3.91 (dd, 1H, $J = 12.3$, 3.3 Hz, CH_aH_b-5'), 4.30 (ddd, 1H, $J = 6.0$, 3.3, 3.3 Hz, H-4'), 4.93 (dd, 1H, $J = 6.3$, 3.3 Hz, H-3'), 5.01 (dd, 1H, $J = 6.3$, 2.8 Hz, H-2'), 5.56 (d, 1H, $J = 2.8$ Hz, H-1'), 5.80 (d, 1H, $J = 8.5$ Hz, H-5), 6.33 (s, 1H, C=CH), 7.37 (d, 1H, $J = 8.5$ Hz, H-6); ¹³C NMR (CDCl₃, 125 MHz) δ 25.2, 27.2, 27.7, 28.1, 62.7, 80.3, 82.5, 83.3, 84.1, 87.1, 96.6, 101.9, 114.3, 130.9, 131.5, 141.2, 150.0, 160.6, 161.3, 162.6; HRMS (ES+) calcd for C₂₄H₃₄N₂O₁₀Na 533.2106, found 533.2105 [MNa⁺].

***S*-((3*aS*,4*S*,6*R*,6*aR*)-6-(6-amino-9*H*-purin-9-yl)-2,2-dimethyltetrahydrofuro[3,4-*d*][1,3]dioxol-4-yl)methyl ethanethioate (63)**



This known compound was prepared as reported by Pignot *et al.*⁹⁸ DEAD (1.10 mL, 6.99 mmol) was added dropwise over 5 min to a solution of triphenylphosphine (1.90 g, 7.24 mmol) in THF (14.0 mL) at 0 °C, and the resulting orange mixture was stirred at 0 °C for 30 min. 2',3'-*O*-Isopropylideneadenosine (1.01 g, 3.30 mmol) was then added, and the orange suspension was stirred at 0 °C for 10 min. Following this, a solution of thiolacetic acid (500 μ L, 7.00 mmol) in THF (1.7 mL) was added and the reaction mixture was stirred at 0°C for 1 h. The solvent was removed *in vacuo*, and the resulting orange residue was purified by flash chromatography (SiO₂, CHCl₃/MeOH, 9:1) to afford thioacetate **63** as a white foam (1.20 g, 100%): *R*_f 0.57 (CHCl₃/MeOH, 9:1); [α]_D²⁰ = -33.20 (*c* 0.22, MeOH); IR (μ scope) ν 3322, 3168, 2988, 2937, 1670, 1646, 1596, 1507, 1475, 1085 cm⁻¹; ¹H NMR (CDCl₃, 300 MHz) δ 1.39 (s, 3H, CH₃), 1.60 (s, 3H, CH₃), 2.35 (s, 3H, CH₃C=O), 3.17 (dd, 1H, *J* = 13.8, 6.9 Hz, CH_aH_b-5'), 3.30 (dd, 1H, *J* = 13.8, 6.9 Hz, CH_aH_b-5'), 4.35 (app td, 1H, *J* = 6.9, 3.3 Hz, H-4'), 4.98 (dd, 1H, *J* = 6.3, 3.3 Hz, H-3'), 5.52 (dd, 1H, *J* = 6.3, 2.0 Hz, H-2'), 5.65 (br s, 2H, NH₂), 6.07 (d, 1H, *J* = 2.0 Hz, H-1'), 7.90 (s, 1H, H-8), 8.37 (s, 1H, H-2); ¹³C NMR (CDCl₃, 100 MHz) δ 25.3, 27.0, 30.5, 31.2, 83.7, 84.2, 86.1, 90.9, 114.5, 120.3, 140.0, 149.2, 153.1, 155.6, 194.5; HRMS (ES⁺) calcd for C₁₅H₁₉N₅O₄NaS 388.1050, found 388.1055 [MNa]⁺.

((3*aS*,4*S*,6*R*,6*aR*)-6-(6-Amino-9*H*-purin-9-yl)-2,2-dimethyltetrahydrofuro[3,4-*d*][1,3]dioxol-4-yl)methyl methanethiol (64**)²¹¹**



The procedure used to obtain this known compound was adapted from the one described by Wallace *et al.*⁹⁹

Thioacetate **63** (174 mg, 0.476 mmol) was dissolved in MeOH (5.2 mL) and flushed with argon for 1 h, then a

solution of sodium thiomethoxide (46.0 mg, 0.656 mmol) in MeOH (1.0 mL) was added.

The pale yellow reaction mixture was stirred at rt for 1.5 h, then poured into 0.1 M HCl (16.5 mL). This was then extracted with CH₂Cl₂ (3 x 30 mL), and the combined organic

layers were washed with brine (30 mL) and dried (MgSO₄). The solvent was removed *in*

vacuo to give thiol **64** as a white solid (148 mg, 96%): *R*_f 0.50 (CHCl₃/MeOH, 9:1);

[α]_D²⁰ = -25.51 (*c* 0.29, CHCl₃); IR (CHCl₃, cast) ν 3323, 3174, 2963, 2926, 2854, 1647,

1599, 1505, 1476, 1214, 1091 cm⁻¹; ¹H NMR (CDCl₃, 300 MHz) δ 1.41 (s, 3H, CH₃),

1.63 (s, 3H, CH₃), 2.82 (dd, 1H, *J* = 13.8, 6.7 Hz, CH_aH_b-5'), 2.85 (dd, 1H, *J* = 13.8, 6.7

Hz, CH_aH_b-5'), 4.34 (ddd, 1H, *J* = 6.7, 6.7, 3.3 Hz, H-4'), 5.09 (dd, 1H, *J* = 6.6, 3.3 Hz,

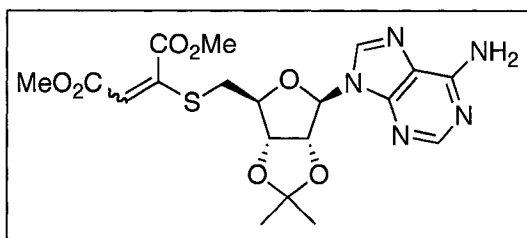
H-3'), 5.50 (dd, 1H, *J* = 6.6, 2.4 Hz, H-2'), 5.81 (br s, 2H, NH₂), 6.07 (d, 1H, *J* = 2.4 Hz,

H-1'), 7.93 (s, 1H, H-8), 8.36 (s, 1H, H-2); ¹³C NMR (CDCl₃, 100 MHz) δ 25.3, 26.9,

27.1, 83.1, 83.9, 87.8, 90.7, 114.7, 120.3, 140.1, 149.2, 152.7, 155.5; HRMS (ES⁺) calcd

for C₁₃H₁₈N₅O₃S 324.1125, found 324.1123 [MH]⁺.

Dimethyl 2-(((3a*S*,4*S*,6*R*,6a*R*)-6-(6-amino-9*H*-purin-9-yl)-2,2-dimethyltetrahydrofuro[3,4-*d*][1,3]dioxol-4-yl)methylthio)but-2-enedioate (65**)**

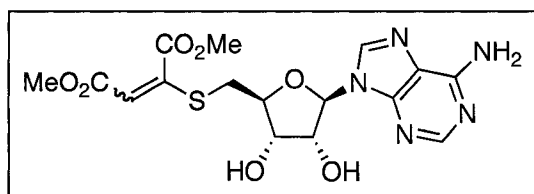


This compound was synthesized by an adaptation of the procedure reported by Journet *et al.*¹⁰⁰ NMM (85.0 μ L, 0.773 mmol) was added dropwise to a suspension

of thiol **64** (190 mg, 0.586 mmol) and dimethyl acetylenedicarboxylate (72.0 μ L, 0.586 mmol) in MeCN (15.0 mL) at 0 °C. The pale yellow mixture immediately became clear. It was then warmed to rt and stirred for 1 h. It was diluted with MeCN (6 mL), and a saturated solution of NH₄Cl (5 mL) was added. The layers were separated, and the aqueous layer was extracted with CH₂Cl₂ (2 x 4 mL). The combined organic layers were dried (MgSO₄) and concentrated *in vacuo*. The crude product was purified by flash chromatography (SiO₂, EtOAc, 100%) to yield **65** as a pale yellow foam, isolated as a ~3:2 mixture of *E/Z* isomers (192 mg, 70%): *R_f* 0.25 (CHCl₃/MeOH, 95:5); IR (CHCl₃, cast) ν 3324, 3169, 2989, 2952, 1732, 1645, 1597, 1475, 1434, 1202, 1090 cm⁻¹; ¹H NMR (CDCl₃, 500 MHz) δ 1.38 (s, ~1.2H, minor isomer, CH₃), 1.39 (s, ~1.8H, major isomer, CH₃), 1.60 (s, ~1.2H, minor isomer, CH₃), 1.61 (s, ~1.8H, major isomer, CH₃), 3.11 (dd, ~0.6H, major isomer, *J* = 13.5, 6.9 Hz, CH_aH_b-5'), 3.15 (dd, ~0.4H, minor isomer, *J* = 14.4, 5.9 Hz, CH_aH_b-5'), 3.28 (dd, ~0.6H, major isomer, *J* = 13.5, 6.9 Hz, CH_aH_b-5'), 3.43 (dd, ~0.4H, minor isomer, *J* = 14.4, 5.9 Hz, CH_aH_b-5'), 3.60 (s, ~1.2H, minor isomer, OCH₃), 3.70 (s, ~1.8H, major isomer, OCH₃), 3.78 (s, ~1.2H, minor isomer, OCH₃), 3.85 (s, ~1.8H, major isomer, OCH₃), 4.37 (ddd, ~0.4H, minor isomer, *J* = 5.9, 5.9, 4.0 Hz, H-4'), 4.42 (ddd, 0.6H, major isomer, *J* = 6.9, 6.9, 3.3 Hz, H-4'), 5.10

(dd, ~0.4H, minor isomer, $J = 6.3, 4.0$ Hz, H-3'), 5.11 (dd, ~0.6H, major isomer, $J = 6.4, 3.3$ Hz, H-3'), 5.44 (dd, ~0.4H, minor isomer, $J = 6.3, 2.7$ Hz, H-2'), 5.50 (dd, ~0.6H, major isomer, $J = 6.4, 2.0$ Hz, H-2'), 5.66 (br s, ~1.8H, major isomer, NH₂), 5.69 (br s, ~1.2H, minor isomer, NH₂), 5.86 (s, ~0.6H, major isomer, C=CH), 6.04 (d, ~0.4H, minor isomer, $J = 2.7$ Hz, H-1'), 6.06 (d, ~0.6H, major isomer, $J = 2.0$ Hz, H-1'), 6.36 (s, ~0.4H, minor isomer, C=CH), 7.87 (s, ~0.6H, major isomer, H-8), 7.90 (s, ~0.4H, minor isomer, H-8), 8.35 (s, ~0.4H, minor isomer, H-2), 8.36 (s, ~0.6H, major isomer, H-2); ¹³C NMR (CDCl₃, 125 MHz) δ 25.3, 25.4, 27.06, 27.13, 29.3, 34.0, 34.5, 51.9, 52.9, 53.1, 82.9, 83.80, 83.82, 84.1, 85.5, 85.8, 90.0, 91.0, 114.65, 114.71, 114.8, 120.0, 120.3, 121.2, 140.6, 147.1, 148.2, 148.9, 149.3, 153.1, 155.7, 155.8, 163.9, 164.2, 165.4, 165.5 (2 carbon signals not observed due to overlap); HRMS (ES⁺) calcd for C₁₉H₂₃N₅O₇SNa 488.1210, found 488.1209 [MNa]⁺.

Dimethyl 2-(((2*S*,3*S*,4*R*,5*R*)-5-(6-amino-9*H*-purin-9-yl)-3,4-dihydroxytetrahydrofuran-2-yl)methylthio)but-2-enedioate (66**)**

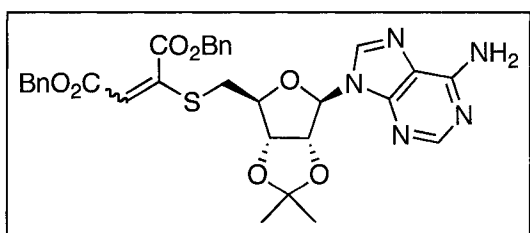


Nucleoside derivative **65** (73.3 mg, 0.157 mmol) was stirred in TFA/H₂O (4:1, 5.6 mL) at 0 °C for 10 min, then the solvent was

removed *in vacuo*. Purification by flash chromatography (SiO₂, CHCl₃/MeOH, 95:5) gave **66** as a colourless glass, isolated as a ~3:2 mixture of *E/Z* isomers (34.5 mg, 52%): R_f 0.07 (CHCl₃/MeOH, 95:5); IR (μ scope) ν 3650-3100, 3338, 2956, 1681, 1603, 1438, 1200, 1141 cm⁻¹; ¹H NMR (CD₃OD, 500 MHz) δ 3.14 (dd, ~0.4H, minor isomer, $J = 15.0, 4.5$ Hz, CH_aH_b-5'), 3.30 (dd, ~0.6H, major isomer, $J = 14.4, 6.5$ Hz, CH_aH_b-5'),

3.38 (dd, ~0.6H, major isomer, $J = 14.4, 4.8$ Hz, $\text{CH}_a\text{H}_b\text{-5}'$), 3.56 (s, ~1.2H, minor isomer, OCH_3), 3.61 (dd, ~0.4H, minor isomer, $J = 15.0, 4.5$ Hz, $\text{CH}_a\text{H}_b\text{-5}'$), 3.63 (s, ~1.8H, major isomer, OCH_3), 3.73 (s, ~1.2H, minor isomer, OCH_3), 3.78 (s, ~1.8H, major isomer, OCH_3), 4.16 (ddd, ~0.4H, minor isomer, $J = 5.9, 4.5, 4.5$ Hz, $\text{H-4}'$), 4.23 (ddd, ~0.6H, major isomer, $J = 6.5, 4.8, 4.8$ Hz, $\text{H-4}'$), 4.41 (app t, ~0.6H, major isomer, $J = 4.8$ Hz, $\text{H-3}'$), 4.56 (app t, ~0.4H, minor isomer, $J = 5.9$ Hz, $\text{H-3}'$), 4.74 (dd, ~0.4H, minor isomer, $J = 5.8, 4.0$ Hz, $\text{H-2}'$), 4.80 (br s, 2H, both isomers, NH_2), 4.85 (app t, ~0.6H, major isomer, $J = 5.0$ Hz, $\text{H-2}'$), 5.93 (s, 1H, major isomer $\text{C}=\text{CH}$ + minor isomer $\text{H-1}'$), 5.98 (d, ~0.6H, major isomer, $J = 5.0$ Hz, $\text{H-1}'$), 6.11 (s, ~0.4H, minor isomer, $\text{C}=\text{CH}$), 8.20-8.26 (m, 2H, both isomers, $\text{H-2}, \text{H-8}$); ^{13}C NMR (CDCl_3 , 125 MHz) δ 29.6, 34.5, 35.0, 52.3, 53.3, 53.6, 72.9, 74.2, 74.6, 74.7, 84.1, 84.2, 90.4, 90.7, 114.9, 120.9, 133.8, 138.6, 149.9, 150.8, 157.1, 157.2, 165.5, 165.6, 166.9, 167.5 (6 carbon signals not observed due to overlap); HRMS (ES+) calcd for $\text{C}_{16}\text{H}_{19}\text{N}_5\text{O}_7\text{SNa}$ 448.0897, found 448.0899 $[\text{MNa}]^+$.

Dibenzyl 2-(((3*aS*,4*S*,6*R*,6*aR*)-6-(6-amino-9*H*-purin-9-yl)-2,2-dimethyltetrahydrofuro[3,4-*d*][1,3]dioxol-4-yl)methylthio)but-2-enedioate (67)



The same procedure as for the preparation of **65** was employed. Thus, NMM (150 μL , 1.37 mmol) was added dropwise to a solution of thiol **66** (347 mg, 1.07 mmol) and alkyne

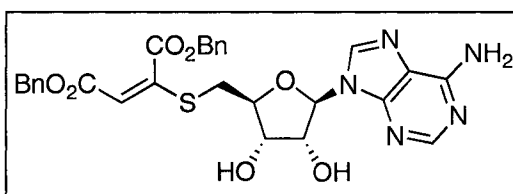
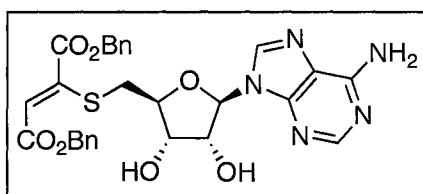
52 (317 mg, 1.08 mmol) in MeCN (28.0 mL) at 0 $^\circ\text{C}$. The resulting clear mixture was then warmed to rt and stirred for 1.5 h, followed by dilution with MeCN (10 mL) and

addition of a saturated solution of NH_4Cl (10 mL). The layers were separated, and the aqueous layer was extracted with CH_2Cl_2 (2 x 8 mL). The combined organic layers were dried (MgSO_4) and concentrated *in vacuo*. Purification by flash chromatography (SiO_2 , EtOAc/hexanes, 3:1) afforded **67** as a pale yellow foam, isolated as a ~1.3:1 mixture of *E/Z* isomers (498 mg, 75%): R_f 0.56 ($\text{CHCl}_3/\text{MeOH}$, 9:1); IR (μscope) ν 3325, 3174, 3034, 2986, 1712, 1643, 1595, 1498, 1475, 1455, 1159, 1080 cm^{-1} ; ^1H NMR (CDCl_3 , 500 MHz) δ 1.37 (s, 3H, both isomers, CH_3), 1.58 (s, 3H, both isomers, CH_3), 3.04 (dd, ~0.57H, major isomer, $J = 13.5, 6.8$ Hz, $\text{CH}_a\text{H}_b-5'$), 3.13 (dd, ~0.43H, minor isomer, $J = 14.0, 6.0$ Hz, $\text{CH}_a\text{H}_b-5'$), 3.19 (dd, ~0.57H, major isomer, $J = 13.5, 6.8$ Hz, $\text{CH}_a\text{H}_b-5'$), 3.40 (dd, ~0.43H, minor isomer, $J = 14.0, 5.5$ Hz, $\text{CH}_a\text{H}_b-5'$), 4.34-4.37 (m, 0.43H, minor isomer, H-4'), 4.39 (ddd, 0.57H, major isomer, $J = 6.8, 6.8, 3.5$ Hz, H-4'), 5.01-5.04 (m, 1H, both isomers, H-3'), 5.03 (d, ~0.43H, minor isomer, $J = 12.0$ Hz, benzylic CH_aH_b), 5.08 (d, ~0.43H, minor isomer, $J = 12.0$ Hz, benzylic CH_aH_b), 5.10 (s, ~1.14H, major isomer, benzylic CH_2), 5.16 (s, ~1.14H, major isomer, benzylic CH_2), 5.21 (s, ~0.86H, minor isomer, benzylic CH_2), 5.34 (d, ~0.43H, minor isomer, $J = 6.5$ Hz, H-2'), 5.46 (d, ~0.57H, major isomer, $J = 6.5$ Hz, H-2'), 5.76 (br s, ~1.14H, major isomer, NH_2), 5.87 (br s, ~0.86H, minor isomer, NH_2), 5.89 (s, ~0.57H, major isomer, $\text{C}=\text{CH}$), 6.01 (d, ~0.43H, minor isomer, $J = 2.5$ Hz, H-1'), 6.03 (d, ~0.57H, major isomer, $J = 2.0$ Hz, H-1'), 6.41 (s, ~0.43H, minor isomer, $\text{C}=\text{CH}$), 7.32-7.40 (m, 10H, both isomers, ArH), 7.86 (s, 1H, both isomers, H-8), 8.33 (s, ~0.43H, minor isomer, H-2), 8.34 (s, ~0.57H, major isomer, H-2); ^{13}C NMR (CDCl_3 , 100 MHz) δ 25.3, 25.4, 27.0, 27.1, 33.9, 34.5, 66.69, 66.75, 68.0, 68.2, 82.9, 83.8, 84.1, 85.3, 91.1, 114.6, 114.8, 114.9, 128.36, 128.44, 128.47, 128.51, 128.53, 128.55, 128.6, 128.7, 134.8, 135.4, 147.7, 148.3, 155.5, 163.1,

164.7, 164.8 (20 carbon signals not observed due to overlap); HRMS (ES+) calcd for C₃₁H₃₂N₅O₇S 618.2022, found 618.2022 [MH]⁺.

Dibenzyl 2-(((2*S*,3*S*,4*R*,5*R*)-5-(6-amino-9*H*-purin-9-yl)-3,4-dihydroxytetrahydrofuran-2-yl)methylthio)fumarate (68a)

Dibenzyl 2-(((2*S*,3*S*,4*R*,5*R*)-5-(6-amino-9*H*-purin-9-yl)-3,4-dihydroxytetrahydrofuran-2-yl)methylthio)maleate (68b)

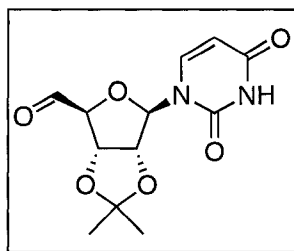


Nucleoside
derivative
67 (101 mg,
0.164

mmol) was stirred in TFA/H₂O (4:1, 5.9 mL) at 0 °C for 1.5 h, then the solvent was removed *in vacuo* and the crude product was purified by flash chromatography (SiO₂, CHCl₃/MeOH/TFA, 95:4:1) to yield fumarate **68a** as a white foam (52.4 mg, 46%) and maleate **68b** as a white foam (59.2 mg, 52%). Data for **68a**: R_f 0.32 (CHCl₃/MeOH/TFA, 95:4:1); [α]_D²⁰ = 4.18 (*c* 0.11, MeOH); IR (μscope) ν 3700-3100, 1670, 1508, 1455, 1191, 1137 cm⁻¹; ¹H NMR (CD₃OD, 400 MHz) δ 3.13 (dd, 1H, *J* = 14.8, 4.8 Hz, CH_aH_b-5'), 3.60 (dd, 1H, *J* = 14.8, 4.4 Hz, CH_aH_b-5'), 4.13-4.17 (m, 1H, H-4'), 4.43 (app t, 1H, *J* = 5.7 Hz, H-3'), 4.62 (dd, 1H, *J* = 5.7, 4.0 Hz, H-2'), 5.01 (d, 1H, *J* = 12.4 Hz, benzylic CH_aH_b), 5.11 (d, 1H, *J* = 12.4 Hz, benzylic CH_aH_b), 5.16 (d, 1H, *J* = 12.4 Hz, benzylic CH_cH_d), 5.24 (d, 1H, *J* = 12.4 Hz, benzylic CH_cH_d), 5.92 (d, 1H, *J* = 4.0 Hz, H-1'), 6.23 (s, 1H, C=CH), 7.25-7.40 (m, 10H, ArH), 8.18 (s, 1H, H-8), 8.20 (s, 1H, H-2); ¹³C NMR (CD₃OD, 125 MHz) δ 34.4, 67.6, 68.9, 72.9, 75.0, 84.4, 90.5, 120.3, 120.9, 129.29,

129.32, 129.4, 129.59, 129.62, 129.7, 136.4, 137.3, 141.8, 146.3, 150.0, 150.3, 152.7, 164.8, 166.2; HRMS (ES+) calcd for C₂₈H₂₈N₅O₇S 578.1704, found 578.1709 [MH]⁺. Data for **68b**: R_f 0.27 (CHCl₃/MeOH/TFA, 95:4:1); [α]_D²⁰ = 14.77 (c 0.13, MeOH); IR (CHCl₃, cast) ν 3359, 3192, 2957, 2924, 2853, 1705, 1660, 1633, 1238, 1088 cm⁻¹; ¹H NMR (CD₃OD, 500 MHz) δ 3.24 (dd, 1H, J = 14.2, 6.7 Hz, CH_aH_b-5'), 3.33 (dd, 1H, J = 14.2, 4.9 Hz, CH_aH_b-5'), 4.24 (ddd, 1H, J = 6.7, 4.9 Hz, H-4'), 4.36 (app t, 1H, J = 4.9 Hz, H-3'), 4.74 (app t, 1H, J = 4.9 Hz, H-2'), 5.04 (s, 1H, benzylic CH₂), 5.07 (s, 1H, benzylic CH₂), 5.98 (s, 1H, C=CH), 6.01 (d, 1H, J = 4.9 Hz, H-1'), 7.25-7.33 (m, 10H, ArH), 8.31 (s, 1H, H-8), 8.38 (s, 1H, H-2); ¹³C NMR (CD₃OD, 125 MHz) δ 34.9, 67.7, 69.1, 74.0, 75.0, 84.2, 90.9, 115.4, 120.8, 129.3, 129.50, 129.55, 129.58, 129.60, 136.4, 137.1, 142.1, 146.2, 149.9, 150.7, 152.6, 164.8, 166.6 (1 carbon signal not observed due to overlap); HRMS (ES+) calcd for C₂₈H₂₈N₅O₇S 578.1704, found 578.1705 [MH]⁺.

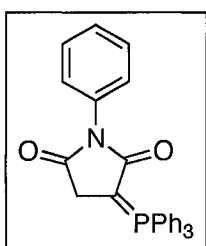
(3a*S*,4*S*,6*R*,6a*R*)-6-(2,4-Dioxo-3,4-dihydropyrimidin-1(2*H*)-yl)-2,2-dimethyl-tetrahydrofuro[3,4-*d*][1,3]dioxole-4-carbaldehyde (72**)²¹²**



This known compound was prepared using the procedure of More *et al.*²¹³ IBX (9.02 g, 32.2 mmol) was added to a solution of 2',3'-*O*-isopropylideneuridine (3.45 g, 12.1 mmol) in MeCN (88.0 mL), and the resulting white suspension was stirred at 80 °C for 1 h. It was then cooled to 0 °C and filtered through a sintered glass funnel. The filter cake was washed with MeCN, and the combined filtrates were concentrated *in vacuo* to give aldehyde **72** as a white foam (3.43 g, 100%): [α]_D²⁰ -41.00 (c 0.26, CHCl₃); IR (μscope) ν 3212, 3064, 2990, 2940, 2826, 1690, 1210, 1087 cm⁻¹; ¹H NMR (CDCl₃,

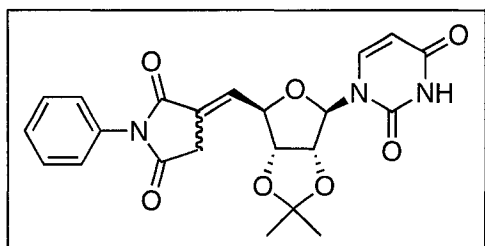
300 MHz) δ 1.34 (s, 3H, CH₃), 1.52 (s, 3H, CH₃), 4.54 (d, 1H, J = 1.8 Hz, H-4'), 5.08 (d, 1H, J = 6.3 Hz, H-3'), 5.20 (dd, 1H, J = 6.3, 1.5 Hz, H-2'), 5.46 (s, 1H, H-1'), 5.74 (dd, 1H, J = 8.2, 2.3 Hz, H-5), 7.22 (d, 1H, J = 8.2 Hz, H-6), 8.39 (br s, 1H, NH), 9.42 (s, 1H, CHO); ¹³C NMR (CDCl₃, 125 MHz) δ 24.7, 26.4, 83.7, 84.8, 94.0, 100.0, 102.8, 113.6, 144.2, 150.6, 163.5, 199.2; HRMS (ES⁺) calcd for C₁₂H₁₄N₂O₆Na 305.0744, found 305.0745 [MNa⁺].

***N*-Phenyltriphenylphosphoranylidenesuccinimide (73)**



This known compound was prepared as reported by Hedaya *et al.*¹⁰¹ *N*-Phenylmaleimide (911 mg, 5.26 mmol) was added to a solution of triphenylphosphine (1.51 g, 5.77 mmol) in AcOH (20.0 mL), and the clear colourless mixture was stirred at 100 °C for 1 h. It was then cooled to rt and concentrated *in vacuo* to give a red oil. This was recrystallized twice, first from CH₂Cl₂/Et₂O to give a pale red solid, then from acetone to give **73** as coarse off-white crystals (790 mg, 34%): mp = 172-174 °C (lit.¹⁰¹ 176.5-178.5 °C); R_f 0.42 (EtOAc, 100%); IR (μscope) ν 2917, 2832, 1985, 1631, 1479, cm⁻¹; ¹H NMR (CDCl₃, 300 MHz) δ 3.14 (d, 2H, J = 1.5 Hz, CH₂), 7.35-7.54 (m, 10H, ArH), 7.58-7.67 (m, 10H, ArH); ¹³C NMR (CDCl₃, 125 MHz) δ 36.0, 37.1, 125.1, 125.9, 126.7, 128.5, 129.2, 132.8, 133.4, 134.2, 169.9, 176.1; HRMS (ES⁺) calcd for C₂₈H₂₂NO₂NaP 458.1280, found 458.1280 [MNa⁺].

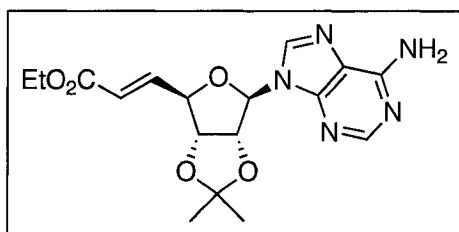
1-((3a*R*,4*R*,6*R*,6a*R*)-6-((*E*)-2,5-Dioxo-1-phenylpyrrolidin-3-ylidene)methyl)-2,2-dimethyltetrahydrofuro[3,4-*d*][1,3]dioxol-4-yl)pyrimidine-2,4(1*H*,3*H*)-dione (74)



An adaptation of the procedure of Hedaya *et al*¹⁰¹ was employed to prepare this compound. Ylide **73** (67.9 mg, 0.156 mmol) was added to a solution of aldehyde **72** (47.1 mg, 0.166 mmol) in

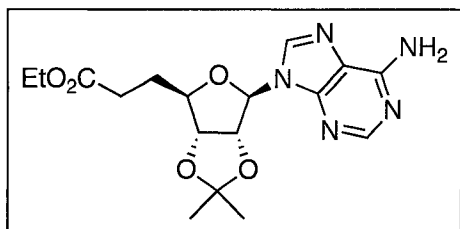
MeOH (8.0 mL). The mixture was stirred at rt for 4 h, then concentrated *in vacuo* to give a red residue. Purification by flash chromatography (SiO₂, CHCl₃/MeOH, 98:2) followed by HPLC (C₁₈, MeCN gradient in H₂O containing 0.1 % TFA) afforded **74** as a white solid (11.4 mg, 16%): *R_f* 0.32 (CHCl₃/MeOH, 98:2); [α]_D²⁰ +22.06 (*c* 1.2, CHCl₃); IR (CH₂Cl₂, cast) ν 3198, 3063, 2989, 1772, 1715, 1691, 1598, 1501, 1456, 1083 cm⁻¹; ¹H NMR (CDCl₃, 400 MHz) δ 1.33 (s, 3H, CH₃), 1.57 (s, 3H, CH₃), 3.43 (dd, 1H, *J* = 21.8, 2.4 Hz, maleimide CH_aH_b), 3.52 (dd, 1H, *J* = 21.8, 2.4 Hz, maleimide CH_aH_b), 4.75 (dd, 1H, *J* = 6.0, 4.7 Hz, H-4'), 4.95 (dd, 1H, *J* = 6.2, 4.7 Hz, H-3'), 5.10 (dd, 1H, *J* = 6.2, 1.1 Hz, H-2'), 5.52 (d, 1H, *J* = 1.1 Hz, H-1'), 5.72 (dd, 1H, *J* = 8.0, 2.0 Hz, H-5), 6.99 (dt, 1H, *J* = 6.0, 2.4 Hz, C=CH), 7.18 (d, 1H, *J* = 8.0 Hz, H-6), 7.28-7.32 (m, 2H, ArH), 7.37 (tt, 1H, *J* = 7.4, 1.2 Hz, ArH), 7.43-7.47 (m, 2H, ArH), 9.47 (br s, 1H, NH); ¹³C NMR (CDCl₃, 125 MHz) δ 25.3, 27.2, 32.6, 84.6, 84.8, 86.3, 96.3, 103.0, 115.0, 126.4, 127.1, 128.5, 129.1, 131.9, 135.2, 143.1, 150.2, 163.1, 168.4, 172.9; HRMS (ES+) calcd for C₂₂H₂₁N₃O₇Na 462.1272, found 462.1269 [MNa]⁺.

(E)-Ethyl 3-((3aR,4R,6R,6aR)-6-(6-amino-9H-purin-9-yl)-2,2-dimethyltetrahydrofuro[3,4-d][1,3]dioxol-4-yl)acrylate (80)²¹⁴



This known compound was prepared as reported by Lerner *et al.*¹⁰³ IBX (6.87 g, 24.5 mmol) and ((ethoxycarbonyl)methylene)triphenylphosphorane (8.55 g, 24.5 mmol) were added to a solution of 2',3'-*O*-isopropylideneadenosine (3.01 g, 9.81 mmol) in DMSO (24.5 mL), and the brown mixture was stirred at rt for 76 h. H₂O (100 mL) was added, and the mixture was extracted with EtOAc (2 x 100 mL). The combined organic layers were dried (Na₂SO₄) and concentrated *in vacuo*. Purification by flash chromatography (SiO₂, toluene/acetone, 9:1, then EtOAc/MeOH, 96:4) afforded α,β -unsaturated ester **80** as a brown foam (2.84 g, 77%): *R*_f 0.23 (EtOAc/MeOH, 96:4); [α]_D²⁰ = +12.40 (*c* 0.15, CHCl₃); IR (μ scope) ν 3324, 3170, 2985, 2938, 1715, 1645, 1598, 1505, 1476, 1210, 1081 cm⁻¹; ¹H NMR (CDCl₃, 500 MHz) δ 1.23 (t, 3H, *J* = 7.2 Hz, OCH₂CH₃), 1.41 (s, 3H, CH₃), 1.63 (s, 3H, CH₃), 4.12 (q, 2H, *J* = 7.2 Hz, OCH₂CH₃), 4.80-4.82 (m, 1H, H-4'), 5.14 (dd, 1H, *J* = 6.4, 3.8 Hz, H-3'), 5.57 (dd, 1H, *J* = 6.4, 2.0 Hz, H-2'), 5.70 (br s, 2H, NH₂), 5.82 (dd, 1H, *J* = 16.0, 1.8 Hz, CH₃O₂CCH=CH), 6.14 (d, 1H, *J* = 2.0 Hz, H-1'), 6.96 (dd, 1H, *J* = 16.0, 5.5 Hz, CH₃O₂CCH=CH), 7.87 (s, 1H, H-8), 8.34 (s, 1H, H-2); ¹³C NMR (CDCl₃, 100 MHz) δ 14.1, 25.3, 27.0, 60.5, 83.9, 84.3, 86.2, 90.5, 114.7, 120.3, 122.5, 132.0, 143.3, 149.4, 153.0, 155.4, 165.5; HRMS (ES⁺) calcd for C₁₇H₂₁N₅O₅Na 398.1435, found 398.1430 [MNa]⁺.

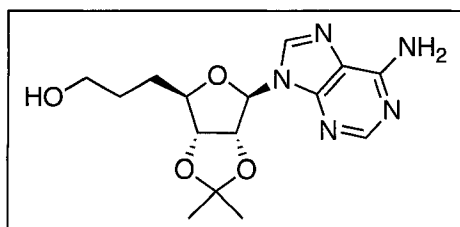
Ethyl 3-((3a*R*,4*R*,6*R*,6a*R*)-6-(6-amino-9*H*-purin-9-yl)-2,2-dimethyltetrahydrofuro[3,4-*d*][1,3]dioxol-4-yl)propanoate (81**)²¹⁴**



10% Pd/C (152 mg) was added to a solution of α,β -unsaturated ester **80** (1.26 g, 3.37 mmol) in EtOH (100.0 mL), and the mixture was shaken on a Parr hydrogenator under 60 psi H₂ for 22 h. The

mixture was filtered through Celite and the Celite was washed with hot EtOH. Concentration of the filtrate *in vacuo* was followed by purification by flash chromatography (SiO₂, CHCl₃/MeOH, 95:5) to give ester **81** as a yellow foam (1.10 g, 87%); R_f 0.09 (EtOAc, 100%); [α]_D²⁰ = -3.61 (*c* 0.36, MeOH); IR (μ scope) ν 3328, 3173, 2986, 2938, 1729, 1643, 1599, 1505, 1477, 1210, 1091 cm⁻¹; ¹H NMR (CDCl₃, 500 MHz) δ 1.18 (t, 3H, *J* = 7.3 Hz, OCH₂CH₃), 1.36 (s, 3H, CH₃), 1.58 (s, 3H, CH₃), 2.02 (app q, 2H, *J* = 7.4 Hz, CH₂-5'), 2.35 (app t, 2H, *J* = 7.4 Hz, CH₂ α), 4.06 (q, 2H, *J* = 7.3 Hz, OCH₂CH₃), 4.19 (ddd, 1H, *J* = 7.4, 7.4, 4.0 Hz, H-4'), 4.86 (dd, 1H, *J* = 6.5, 4.0 Hz, H-3'), 5.46 (dd, 1H, *J* = 6.5, 2.3 Hz, H-2'), 5.51 (br s, 2H, NH₂), 6.01 (d, 1H, *J* = 2.3 Hz, H-1'), 7.85 (s, 1H, H-8), 8.34 (s, 1H, H-2); ¹³C NMR (CDCl₃, 125 MHz) δ 14.1, 25.4, 27.2, 28.4, 30.3, 60.4, 83.99, 84.00, 85.8, 90.2, 114.6, 120.3, 139.7, 149.4, 153.1, 155.7, 172.7; HRMS (ES⁺) calcd for C₁₇H₂₃N₅O₅Na 400.1591, found 400.1598 [MNa]⁺.

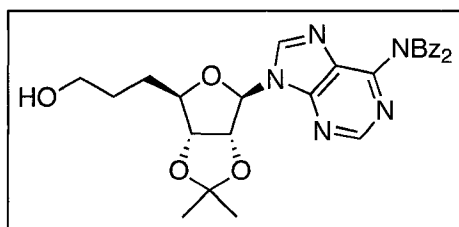
3-((3a*R*,4*R*,6*R*,6a*R*)-6-(6-Amino-9*H*-purin-9-yl)-2,2-dimethyltetrahydrofuro[3,4-*d*][1,3]dioxol-4-yl)propan-1-ol (82**)²¹⁴**



DIBAL-H (1.00 M in toluene, 710 μ L, 0.710 mmol) was added dropwise to a solution of ester

81 (33.1 mg, 0.0879 mmol) in CH₂Cl₂ (260 μL) at -78 °C, and the yellow mixture was stirred at -78 °C for 2 h. A scoop of Na₂SO₄ 10H₂O was added, and the resulting colourless mixture was warmed to rt and stirred for 18 h. EtOAc (4 mL) and H₂O (4 mL) were added, and the aqueous layer was extracted with EtOAc (3 x 4 mL). The combined organic layers were dried (Na₂SO₄), and concentrated *in vacuo* to give alcohol **82** as a yellow gum (15.0 mg, 51%): R_f 0.19 (EtOAc/MeOH, 9:1); [α]_D²⁰ -3.54 (*c* 0.16, MeOH); IR (CHCl₃, cast) ν 3600-3000, 3335, 3186, 3060, 3032, 2927, 2855, 1647, 1600, 1477, 1210, 1076 cm⁻¹; ¹H NMR (CD₃OD, 500 MHz) δ 1.36 (s, 3H, CH₃), 1.53-1.59 (m, 2H, CH₂), 1.70-1.75 (m, 2H, CH₂-5'), 3.46-3.54 (m, 2H, CH₂OH), 4.15 (ddd, 1H, *J* = 7.3, 7.3, 3.9 Hz, H-4'), 4.86 (dd, 1H, *J* = 6.5, 3.9 Hz, H-3'), 5.46 (dd, 1H, *J* = 6.5, 3.0 Hz, H-2'), 6.12 (d, 1H, *J* = 3.0 Hz, H-1'), 8.21 (s, 1H, H-8), 8.24 (s, 1H, H-2); ¹³C NMR (CD₃OD, 125 MHz) δ 25.6, 27.5, 29.7, 31.0, 62.5, 85.3, 85.5, 87.8, 90.9, 115.7, 120.5, 142.6; 148.8, 153.8, 157.3; HRMS (ES⁺) calcd for C₁₅H₂₂N₅O₄ 336.1666, found 336.1670 [MH]⁺.

***N*-Benzoyl-*N*-(9-((3*aR*,4*R*,6*R*,6*aR*)-6-(3-hydroxypropyl)-2,2-dimethyltetrahydrofuro[3,4-*d*][1,3]dioxol-4-yl)-9*H*-purin-6-yl)benzamide (**83**)**

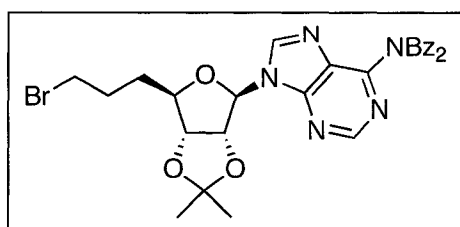


This compound was prepared using an adaptation of the procedure of Ti *et al.*²¹⁵ Chlorotrimethylsilane (105 μL, 0.828 mmol) was added to a suspension of alcohol **82** (57.3 mg,

0.171 mmol) in pyridine (870 μL), and the mixture was stirred at rt for 25 min. Benzoyl chloride (99.0 μL, 0.850 mmol) was added, and the cloudy pale orange mixture was

stirred at rt for 2 h. It was then cooled to 0 °C and H₂O (200 μL) followed by a saturated solution of NaHCO₃ (2.0 mL) were added. The mixture was again warmed to rt and stirred for 4 h, then extracted with EtOAc (2 x 2 mL). The combined organic layers were dried (MgSO₄) and concentrated *in vacuo*. Purification by flash chromatography (SiO₂, EtOAc/hexanes, 1:1 to 7:3) yielded **83** as a white foam (53.0 mg, 57%): *R_f* 0.20 (EtOAc/petroleum ether, 7:3); [α]_D²⁰ = -12.94 (*c* 0.19, CHCl₃); IR (CHCl₃, cast) ν 3600-3100, 3064, 2927, 2855, 1705, 1600, 1578, 1493, 1239, 1077 cm⁻¹; ¹H NMR (CDCl₃, 300 MHz) δ 1.26 (t, 3H, *J* = 7.2 Hz, OCH₂CH₃), 1.39 (s, 3H, CH₃), 1.59-1.68 (m, 2H, CH₂), 1.62 (s, 3H, CH₃), 1.73-1.81 (m, 2H, CH₂), 3.60 (t, 2H, *J* = 6.2 Hz, CH₂OH), 4.13 (q, 2H, *J* = 7.2 Hz, OCH₂CH₃), 4.26 (ddd, 1H, *J* = 7.1, 7.1, 3.9 Hz, H-4'), 4.82 (dd, 1H, *J* = 6.6, 3.9 Hz, H-3'), 5.50 (dd, 1H, *J* = 6.6, 2.6 Hz, H-2'), 6.11 (d, 1H, *J* = 2.6 Hz, H-1'), 7.36 (t, 4H, *J* = 7.5 Hz, ArH), 7.49 (tt, 2H, *J* = 7.5, 1.6 Hz, ArH), 7.86 (d, 4H, *J* = 7.5 Hz, ArH), 8.16 (s, 1H, H-8), 8.68 (s, 1H, H-2); ¹³C NMR (CDCl₃, 125 MHz) δ 25.4, 27.1, 28.7, 29.9, 62.1, 84.0, 84.1, 86.9, 90.7, 114.9, 117.2, 128.7, 129.5, 133.0, 134.0, 145.6, 152.0, 152.4, 166.1, 172.2; HRMS (ES⁺) calcd for C₂₉H₂₉N₅O₆Na 566.2010, found 566.2011 [MNa]⁺.

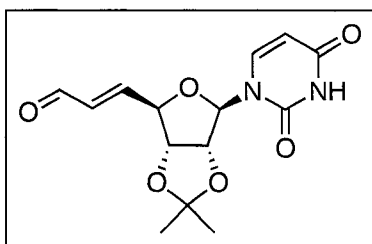
***N*-Benzoyl-*N*-(9-((3*aR*,4*R*,6*R*,6*aR*)-6-(3-bromopropyl)-2,2-dimethyltetrahydro-furo[3,4-*d*][1,3]dioxol-4-yl)-9*H*-purin-6-yl)benzamide (**84**)**



A solution of CB₄ (92.4 mg, 0.279 mmol) in MeCN (500 μL) was added to a solution of alcohol **83** (116 mg, 0.213 mmol) and triphenylphosphine (84.4 mg, 0.322 mmol) in

MeCN (2.0 mL) and the mixture was stirred at rt for 1 h, then concentrated *in vacuo*. The residue was purified by flash chromatography (SiO₂, EtOAc, 100%) to give bromide **84** as a white foam (30.9 mg, 24%): *R_f* 0.66 (CHCl₃/MeOH, 95:5); IR (μscope) ν 2924, 2854, 1702, 1634, 1599, 1578, 1491, 1239, 1076 cm⁻¹; ¹H NMR (CDCl₃, 400 MHz) δ 1.40 (s, 3H, CH₃), 1.62 (s, 3H, CH₃), 1.85-2.02 (m, 4H, 2 x CH₂), 3.38 (t, 2H, *J* = 6.4 Hz, CH₂Br), 4.22 (m, 1H, H-4'), 4.86 (dd, 1H, *J* = 6.6, 4.2 Hz, H-3'), 5.48 (dd, 1H, *J* = 6.6, 2.3 Hz, H-2'), 6.10 (d, 1H, *J* = 2.3 Hz, H-1'), 7.37 (t, 4H, *J* = 7.8 Hz, ArH), 7.49 (tt, 2H, *J* = 7.8, 1.2 Hz, ArH), 7.86 (dd, 4H, *J* = 7.8, 1.2 Hz, ArH), 8.14 (s, 1H, H-8), 8.69 (s, 1H, H-2); ¹³C NMR (CDCl₃, 100 MHz) δ 25.3, 27.1, 28.7, 31.7, 32.9, 83.87, 83.95, 86.2, 90.4, 114.9, 128.6, 129.4, 132.9, 133.9, 143.9, 152.0, 152.2, 172.1 (2 carbon signals not observed due to overlap); HRMS (ES⁺) calcd for C₂₉H₂₉N₅O₅Br 606.1347, found 606.1343 [MH]⁺.

(E)- 3-(((3aR,4R,6R,6aR)-6-(2,4-Dioxo-3,4-dihydropyrimidin-1(2H)-yl)-2,2-dimethyl-tetrahydrofuro[3,4-d][1,3]dioxol-4-yl)acrylaldehyde (87)²¹⁶

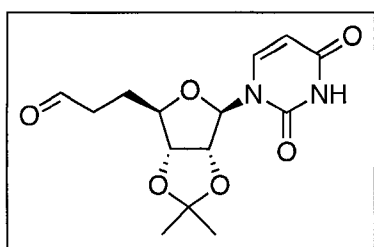


(Triphenylphosphoranylidene)acetaldehyde (3.60 g, 11.8 mmol) was added to a solution of aldehyde **72** (3.03 g, 10.7 mmol) in CH₂Cl₂ (107 mL), and the clear brown mixture was stirred at rt for 6 h. The solvent was

removed *in vacuo*, and the brown residue was purified by flash chromatography (SiO₂, EtOAc, 100%) to give α,β -unsaturated aldehyde **87** as a pale yellow foam (1.88 g, 57%): *R_f* 0.38 (EtOAc, 100%); [α]_D²⁰ = +34.62 (*c* 0.13, MeOH); IR (CH₂Cl₂, cast) ν 3200, 3062, 2750, 2820, 2990, 1691, 1073 cm⁻¹; ¹H NMR (CDCl₃, 300 MHz) δ 1.38 (s, 3H,

CH₃), 1.60 (s, 3H, CH₃), 4.79 (ddd, 1H, *J* = 5.7, 4.5, 1.4 Hz, H-4'), 4.94 (dd, 1H, *J* = 6.3, 4.5 Hz, H-3'), 5.16 (dd, 1H, *J* = 6.3, 1.4 Hz, H-2'), 5.56 (d, 1H, *J* = 1.4 Hz, H-1'), 5.76 (dd, 1H, *J* = 8.1, 2.3 Hz, H-5), 6.27 (ddd, 1H, *J* = 15.9, 7.8, 1.4 Hz, OHCCH=CH), 6.92 (dd, 1H, *J* = 15.9, 5.7 Hz, OHCCH=CH), 7.20 (d, 1H, *J* = 8.1 Hz, H-6), 8.46 (br s, 1H, NH), 9.60 (d, 1H, *J* = 7.8 Hz, CHO); ¹³C NMR (CDCl₃, 125 MHz) δ 25.2, 27.0, 84.5, 84.7, 87.7, 96.7, 102.9, 114.7, 132.2, 143.4, 150.1, 152.2, 163.4, 193.1; HRMS (ES+) calcd for C₁₄H₁₆N₂O₆Na 331.0901, found 331.0902 [MNa]⁺.

3-((3*aR*,4*R*,6*R*,6*aR*)-6-(2,4-Dioxo-3,4-dihydropyrimidin-1(2*H*)-yl)-2,2-dimethyl-tetrahydrofuro[3,4-*d*][1,3]dioxol-4-yl)propanal (88)

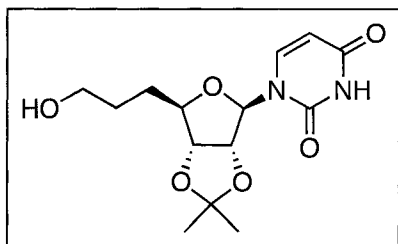


10% Pd/C (235 mg) was added to a solution of α,β -unsaturated aldehyde **87** (1.62 g, 5.25 mmol) in EtOAc (87.0 mL) and the reaction mixture was stirred under 1 atm H₂ for 11 h. The mixture was filtered through Celite

and concentrated *in vacuo* to afford aldehyde **88** as a white foam (1.59 g, 98%): *R_f* 0.38 (EtOAc, 100%); [α]_D²⁰ = +19.30 (*c* 0.18, CHCl₃); IR (CHCl₃, cast) ν 3200, 2959, 2925, 2854, 2700, 1694, 1087 cm⁻¹; ¹H NMR (CDCl₃, 300 MHz) δ 1.32 (s, 3H, CH₃), 1.53 (s, 3H, CH₃), 2.04 (app q, 2H, *J* = 7.1 Hz, CH₂-5'), 2.57 (app td, 2H, *J* = 7.1, 1.3 Hz, CH₂_α), 4.01 (ddd, 1H, *J* = 7.1, 7.1, 5.0 Hz, H-4'), 4.60 (dd, 1H, *J* = 6.6, 5.0 Hz, H-3'), 4.95 (dd, 1H, *J* = 6.6, 2.3 Hz, H-2'), 5.54 (d, 1H, *J* = 2.3 Hz, H-1'), 5.72 (dd, 1H, *J* = 8.0, 2.3 Hz, H-5), 7.17 (d, 1H, *J* = 8.0 Hz, H-6), 8.41 (br s, 1H, NH), 9.75 (t, 1H, *J* = 1.3 Hz, CHO); ¹³C NMR (CDCl₃, 100 MHz) δ 25.3, 25.4, 27.2, 39.8, 83.5, 84.3, 86.1, 94.1, 102.7, 114.8,

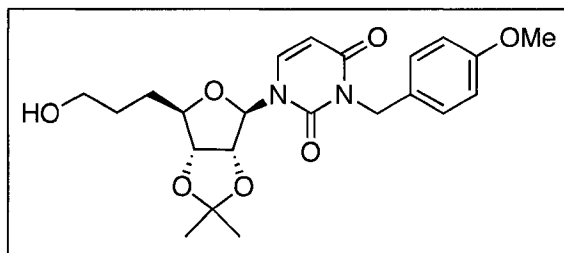
142.5, 149.8, 163.2, 201.1; HRMS calcd for $C_{14}H_{18}N_2O_6Na$ 333.1057, found 333.1058 [MNa]⁺.

3-((3a*R*,4*R*,6*R*,6a*R*)-6-(2,4-Dioxo-3,4-dihydropyrimidin-1(2*H*)-yl)-2,2-dimethyl-tetrahydrofuro[3,4-*d*][1,3]dioxol-4-yl)propanol (89**)**



NaBH₄ (494 mg, 13.1 mmol) was added to a solution of aldehyde **88** (1.35 g, 4.35 mmol) in EtOH (13.4 mL), and the mixture was stirred at rt for 30 min. The solvent was removed *in vacuo* and a saturated solution of NH₄Cl (30 mL) was added to the residue. The mixture was extracted with EtOAc (4 x 30 mL) and the combined organic layers were dried (MgSO₄). Concentration *in vacuo* was followed by purification by flash chromatography (SiO₂, EtOAc, 100%) to give alcohol **89** as a white foam (1.20 g, 88%): *R_f* 0.13 (EtOAc, 100%); [α]_D²⁰ = +10.32 (*c* 0.31, MeOH); IR (μscope) ν 3700-3300, 3206, 3062, 2987, 2939, 1677, 1065 cm⁻¹; ¹H NMR (CDCl₃, 500 MHz) δ 1.33 (s, 3H, CH₃), 1.55 (s, 3H, CH₃), 1.65-1.73 (m, 2H, CH₂-5'), 1.77-1.82 (m, 2H, CH₂), 3.67 (t, 2H, *J* = 6.3 Hz, CH₂OH), 4.05 (ddd, 1H, *J* = 6.8, 6.8, 5.0 Hz, H-4'), 4.57 (dd, 1H, *J* = 6.9, 4.8 Hz, H-3'), 4.91 (dd, 1H, *J* = 6.9, 2.5 Hz, H-2'), 5.61 (d, 1H, *J* = 2.5 Hz, H-1'), 5.71 (dd, 1H, *J* = 8.0, 2.5 Hz, H-5), 7.21 (d, 1H, *J* = 8.0 Hz, H-6), 8.36 (br s, 1H, NH); ¹³C NMR (CDCl₃, 125 MHz) δ 25.3, 27.2, 28.7, 29.8, 62.3, 83.7, 84.4, 86.9, 93.8, 102.6, 114.8, 142.0, 149.9, 163.0; HRMS (ES⁺) calcd for $C_{14}H_{20}N_2O_6Na$ 335.1219, found 335.1223 [MNa]⁺.

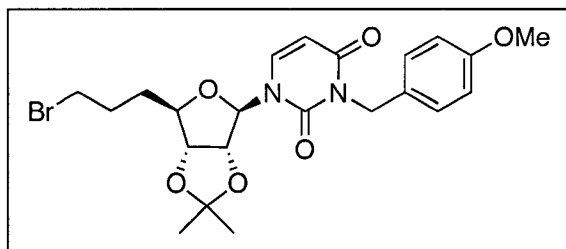
3-((3a*R*,4*R*,6*R*,6a*R*)-6-(3-(4-Methoxybenzyl)-2,4-Dioxo-3,4-dihydropyrimidin-1(2*H*)-yl)-2,2-dimethyltetrahydrofuro[3,4-*d*][1,3]dioxol-4-yl)propanol (90)



DBU (390 μ L, 2.61 mmol) and *p*-methoxybenzyl chloride (360 μ L, 2.66 mmol) were added to a solution of **89** (404 mg, 1.29 mmol) in MeCN (11.0

mL), and the mixture was stirred at reflux for 3 h. It was then cooled to rt and concentrated *in vacuo*. This was followed by purification by flash chromatography (SiO₂, Et₂O/MeOH, 98:2 to 90:10) to yield **90** as a white sticky foam (429 mg, 79%): *R_f* 0.26 (EtOAc, 100%); $[\alpha]_D^{20} = +15.99$ (*c* 0.24, CHCl₃); IR (CHCl₃, cast) ν 3600-3100, 2928, 2855, 1711, 1688, 1613, 1513, 1455, 1248, 1071 cm⁻¹; ¹H NMR (CDCl₃, 400 MHz) δ 1.32 (s, 3H, CH₃), 1.54 (s, 3H, CH₃), 1.63-1.69 (m, 2H, CH₂), 1.74-1.80 (m, 2H, CH₂-5'), 3.61-3.66 (m, 2H, CH₂OH), 3.75 (s, 3H, ArOCH₃), 4.04 (ddd, 1H, *J* = 6.6, 4.7 Hz, H-4'), 4.56 (dd, 1H, *J* = 6.6, 4.7 Hz, H-3'), 4.86 (dd, 1H, *J* = 6.6, 2.4 Hz, H-2'), 4.99 (d, 1H, *J* = 13.6 Hz, benzylic CH_aH_b), 5.04 (d, 1H, *J* = 13.6 Hz, benzylic CH_aH_b), 5.64 (d, 1H, *J* = 2.4 Hz, H-1'), 5.75 (d, 1H, *J* = 8.2 Hz, H-5), 6.80 (d, 2H, *J* = 8.8 Hz, ArH), 7.16 (d, 1H, *J* = 8.2 Hz, H-6), 7.42 (d, 2H, *J* = 8.8 Hz, ArH); ¹³C NMR (CDCl₃, 100 MHz) δ 25.4, 27.2, 28.8, 29.8, 43.5, 55.2, 62.3, 83.7, 84.7, 86.6, 93.9, 102.2, 113.7, 114.7, 128.8, 130.7, 139.2, 150.5, 159.1, 162.4; HRMS (ES⁺) calcd for C₂₂H₂₈N₂O₇Na 455.1789, found 455.1793 [MNa]⁺.

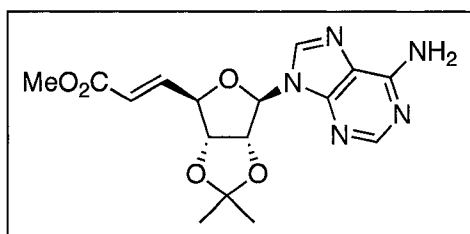
1-((3aR,4R,6R,6aR)-6-(3-Bromopropyl)-2,2-dimethyltetrahydrofuro[3,4-d][1,3]dioxol-4-yl)-3-(4-methoxybenzyl)pyrimidine-2,4(1H,3H)-dione (91)



Alcohol **90** (344 mg, 0.796 mmol) and triphenylphosphine (316 mg, 1.20 mmol) were dissolved in MeCN (7.5 mL) and a solution of CBr₄ (346 mg, 1.04 mmol) in

MeCN (2.0 mL) was added. The light orange mixture was stirred at rt for 3 h, then concentrated *in vacuo*. The resulting dark red residue was purified by flash chromatography (SiO₂, EtOAc/hexanes, 3:2) to give bromide **91** as a white foam (336 mg, 85%): R_f 0.62 (EtOAc, 100%); [α]_D²⁰ = +15.79 (*c* 0.19, CHCl₃); IR (CHCl₃, cast) ν 2933, 1712, 1670, 1612, 1513, 1453, 1248, 1083 cm⁻¹; ¹H NMR (CDCl₃, 300 MHz) δ 1.34 (s, 3H, CH₃), 1.56 (s, 3H, CH₃), 1.81-1.90 (m, 2H, CH₂-5'), 1.91-2.04 (m, 2H, CH₂), 3.41 (t, 2H, *J* = 6.4, CH₂Br), 3.78 (s, 3H, ArOCH₃), 4.03 (ddd, 1H, *J* = 6.9, 5.1 Hz, H-4'), 4.61 (dd, 1H, *J* = 6.7, 4.7 Hz, H-3'), 4.92 (dd, 1H, *J* = 6.7, 2.2 Hz, H-2'), 5.03 (s, 2H, benzylic CH₂), 5.61 (d, 1H, *J* = 2.2 Hz, H-1'), 5.77 (d, 1H, *J* = 8.0 Hz, H-5), 6.83 (d, 2H, *J* = 8.7 Hz, ArH), 7.15 (d, 1H, *J* = 8.0 Hz, H-6), 7.44 (d, 2H, *J* = 8.7 Hz, ArH); ¹³C NMR (CDCl₃, 100 MHz) δ 25.3, 27.2, 28.9, 31.8, 33.2, 43.5, 55.2, 83.7, 84.6, 86.3, 94.4, 102.3, 113.7, 114.7, 128.8, 130.7, 139.5, 150.5, 159.1, 162.4; HRMS (ES⁺) calcd for C₂₂H₂₇N₂O₆NaBr 517.0950, found 517.0950 [MNa]⁺.

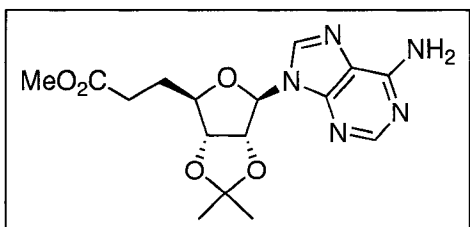
(E)-Methyl 3-((3a*R*,4*R*,6*R*,6a*R*)-6-(6-amino-9*H*-purin-9-yl)-2,2-dimethyltetrahydrofuro[3,4-*d*][1,3]dioxol-4-yl)acrylate (94**)²¹⁷**



This known compound was prepared using the same procedure as for **80**. Thus, reaction of 2',3'-*O*-isopropylideneadenosine (3.12 g, 10.2 mmol) with IBX (7.12 g, 25.4 mmol) and

((methoxycarbonyl)methylene)triphenylphosphorane (8.50 g, 25.4 mmol) in DMSO (25.5 mL) for 95 h was followed by flash chromatography (SiO₂, toluene/acetone, 9:1 to 4:1, then EtOAc/MeOH, 100:0 to 95:5) to give **94** as a pale orange foam (3.52 g, 96%): *R_f* 0.27 (EtOAc/MeOH, 95:5); [α]_D²⁰ = -13.33 (*c* 0.33, MeOH); IR (μscope) ν 3327, 3172, 2990, 2951, 1722, 1650, 1599, 1210, 1084 cm⁻¹; ¹H NMR (CDCl₃, 500 MHz) δ 1.41 (s, 3H, CH₃), 1.63 (s, 3H, CH₃), 3.67 (s, 3H, OCH₃), 4.81 (ddd, 1H, *J* = 5.5, 3.5, 1.7 Hz, H-4'), 5.14 (dd, 1H, *J* = 6.5, 3.5 Hz, H-3'), 5.56 (dd, 1H, *J* = 6.5, 2.0 Hz, H-2'), 5.83 (dd, 1H, *J* = 15.9, 1.7 Hz, CH₃O₂CCH=CH), 6.14 (d, 1H, *J* = 2.0 Hz, H-1'), 6.97 (dd, 1H, *J* = 15.9, 5.5 Hz, CH₃O₂CCH=CH), 7.87 (s, 1H, H-8), 8.33 (s, 1H, H-2); ¹³C NMR (CDCl₃, 125 MHz) δ 25.4, 27.1, 51.7, 84.0, 84.3, 86.3, 90.6, 114.7, 120.3, 122.1, 132.1, 143.7, 149.5, 153.2, 155.5, 166.0; HRMS (ES⁺) calcd for C₁₆H₁₉N₅O₅Na 384.1278, found 384.1280 [MNa]⁺.

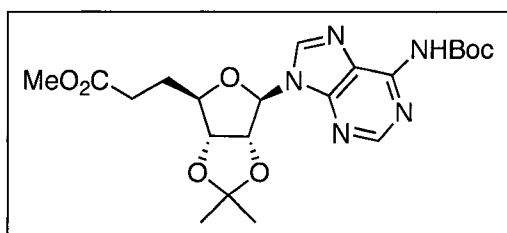
Methyl 3-((3a*R*,4*R*,6*R*,6a*R*)-6-(6-amino-9*H*-purin-9-yl)-2,2-dimethyltetrahydrofuro[3,4-*d*][1,3]dioxol-4-yl)propanoate (95**)²¹⁷**



10% Pd/C (205 mg) was added to a solution of α,β-unsaturated ester **94** (1.99 g, 5.50 mmol) in

EtOH (90.0 mL), and the mixture was shaken on a Parr hydrogenator at 60 psi for 18 h then filtered through Celite. The Celite was washed with hot EtOH, and the filtrate was concentrated *in vacuo* to give **95** as a yellow foam (1.89 g, 95%): R_f 0.40 (EtOAc/MeOH, 95:5); $[\alpha]_D^{20} = -7.04$ (c 0.27, MeOH); IR (μ scope) ν 3326, 3172, 2989, 2951, 1731, 1641, 1598, 1504, 1476, 1204, 1075 cm^{-1} ; ^1H NMR (CDCl_3 , 300 MHz) δ 1.34 (s, 3H, CH_3), 1.56 (s, 3H, CH_3), 2.01 (app q, 2H, $J = 7.3$ Hz, $\text{CH}_2\text{-5}'$), 2.35 (app t, 2H, $J = 7.3$ Hz, $\text{CH}_2\alpha$), 3.57 (s, 3H, OCH_3), 4.15-4.21 (m, 1H, H-4'), 4.85 (dd, 1H, $J = 6.3, 3.9$ Hz, H-3'), 5.45 (dd, 1H, $J = 6.3, 2.0$ Hz, H-2'), 6.02 (d, 1H, $J = 2.0$ Hz, H-1'), 6.65 (br s, 2H, NH_2), 7.89 (s, 1H, H-8), 8.29 (s, 1H, H-2); ^{13}C NMR (CDCl_3 , 100 MHz) δ 25.4, 27.1, 28.4, 30.1, 51.6, 83.96, 83.99, 85.8, 90.2, 114.6, 120.1, 139.9, 149.2, 152.7, 155.8, 173.2; HRMS (ES+) calcd for $\text{C}_{16}\text{H}_{22}\text{N}_5\text{O}_5$ 364.1616, found 364.1617 $[\text{MH}]^+$.

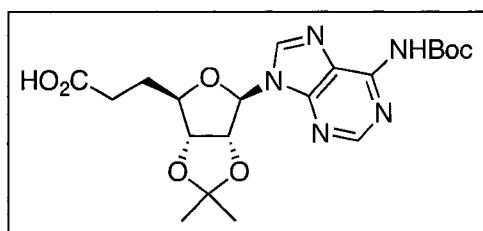
Methyl 3-((3a*R*,4*R*,6*R*,6a*R*)-6-(6-(*tert*-butoxycarbonylamino)-9*H*-purin-9-yl)-2,2-dimethyltetrahydrofuro[3,4-*d*][1,3]dioxol-4-yl)propanoate (96)



This compound was prepared by the procedure of Ubukata *et al.*²¹⁸ Di-*tert*-butyl dicarbonate (1.10 g, 5.04 mmol) in DMF (2.0 mL) was added to a suspension of **95** (1.67 g, 4.60 mmol) and NaH (60% in mineral oil, 1.02 g, 25.5 mmol) in DMF (41.0 mL) at -40 °C. The mixture was stirred at -40 °C for 20 min, then a saturated solution of NH_4Cl (16 mL) was added, and the orange mixture was allowed to warm to rt. EtOAc (80 mL) was added, and the layers were separated. The aqueous layer was extracted with EtOAc (3 x 30 mL), and the combined organic layers were washed with brine then dried (Na_2SO_4).

Concentration *in vacuo* was followed by flash chromatography (SiO₂, EtOAc/hexanes, 4:1) to yield **96** as an off-white foam (894 mg, 42%): *R_f* 0.34 (EtOAc/hexanes, 4:1); $[\alpha]_D^{20} = -6.13$ (*c* 0.31, MeOH); IR (μscope) ν 3182, 2980, 1737, 1607, 1585, 1524, 1462, 1214, 1142, 1074 cm⁻¹; ¹H NMR (CDCl₃, 300 MHz) δ 1.39 (s, 3H, CH₃), 1.57 (s, 9H, C(CH₃)₃), 1.61 (s, 3H, CH₃), 2.04 (app q, 2H, *J* = 7.3 Hz, CH₂-5'), 2.37 (app t, 2H, *J* = 7.3 Hz, CH_{2 α}), 3.61 (s, 3H, OCH₃), 4.24 (ddd, 1H, *J* = 7.3, 7.3, 3.9 Hz, H-4'), 4.89 (dd, 1H, *J* = 6.5, 3.9 Hz, H-3'), 5.50 (dd, 1H, *J* = 6.5, 2.5 Hz, H-2'), 6.06 (d, 1H, *J* = 2.5 Hz, H-1'), 7.99-8.01 (m, 2H, H-8 + NH), 8.76 (s, 1H, H-2); ¹³C NMR (CDCl₃, 125 MHz) δ 25.4, 27.2, 28.1, 28.4, 30.0, 51.6, 82.3, 83.96, 83.99, 86.0, 90.5, 114.8, 122.4, 141.9, 149.6, 150.0, 150.3, 153.1, 173.0; HRMS (ES⁺) calcd for C₂₁H₃₀N₅O₇ 464.2140, found 464.2138 [MH]⁺.

3-((3*aR*,4*R*,6*R*,6*aR*)-6-(6-(*tert*-Butoxycarbonylamino)-9*H*-purin-9-yl)-2,2-dimethyl-tetrahydrofuro[3,4-*d*][1,3]dioxol-4-yl)propanoic acid (97**)**

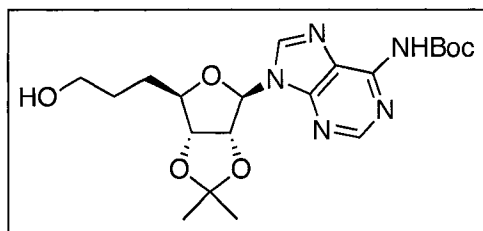


LiOH·H₂O (229 mg, 5.45 mmol) was added to a solution of ester **96** (834 mg, 1.80 mmol) in THF/H₂O (5:3, 61.0 mL) at 0 °C, and the pale yellow mixture was stirred at 0 °C for 7.5 h.

While still at 0 °C, it was acidified to pH 4.0 with 1 M citric acid and extracted with EtOAc (3 x 20 mL). The combined organic layers were dried (MgSO₄) and concentrated *in vacuo* to afford carboxylic acid **97** as an off-white foam (809 mg, 100%): *R_f* 0.04 (EtOAc/hexanes, 4:1); $[\alpha]_D^{20} = -7.65$ (*c* 0.34, MeOH); IR (μscope) ν 3600-2300, 3188, 2981, 2937, 1747, 1611, 1588, 1525, 1467, 1233, 1147, 1080 cm⁻¹; ¹H NMR (CD₃OD,

500 MHz) δ 1.37 (s, 3H, CH₃), 1.58 (s, 12H, C(CH₃)₃ + CH₃), 1.97 (app q, 2H, J = 7.5 Hz, CH₂-5'), 2.32 (app t, 2H, J = 7.5 Hz, CH_{2 α}), 4.21 (ddd, 1H, J = 7.5, 7.5, 3.7 Hz, H-4'), 4.94 (dd, 1H, J = 6.5, 3.7 Hz, H-3'), 5.51 (dd, 1H, J = 6.5, 2.5 Hz, H-2'), 6.20 (d, 1H, J = 2.5 Hz, H-1'), 8.42 (s, 1H, H-8), 8.58 (s, 1H, H-2); ¹³C NMR (CD₃OD, 125 MHz) δ 24.1, 26.0, 27.0, 28.2, 29.4, 81.3, 83.8, 83.9, 85.8, 89.8, 114.3, 122.0, 142.1, 150.0, 150.6, 150.9, 151.8, 175.0; HRMS (ES⁺) calcd for C₂₀H₂₈N₅O₇ 450.1983, found 450.1984 [MH]⁺.

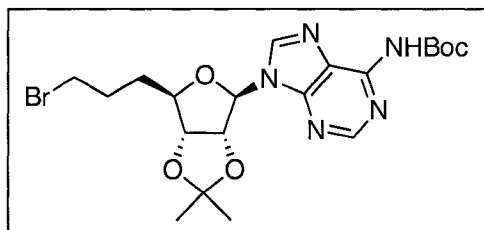
***tert*-Butyl 9-((3*aR*,4*R*,6*R*,6*aR*)-6-(3-hydroxypropyl)-2,2-dimethyltetrahydrofuro[3,4-*d*][1,3]dioxol-4-yl)-9*H*-purin-6-ylcarbamate (**98**)**



Et₃N (1.00 mL, 7.17 mmol) was added to a solution of carboxylic acid **97** (829 mg, 1.84 mmol) in THF (3.0 mL), and the mixture was cooled to -7 °C. Ethyl chloroformate (190 μ L, 1.99 mmol) in THF (5.0 mL) was then added and the dark orange mixture was stirred at -7 °C for 2 h. The resulting suspension was filtered to remove Et₃NHCl, then it was cooled to 0 °C and NaBH₄ (141 mg, 3.72 mmol) in H₂O (2.0 mL) was added. The mixture was allowed to warm to rt and was stirred for 4 h, then it was acidified to pH 3 with 3 M HCl. Extraction with EtOAc (3 x 40 mL) was followed by washing of the combined organic layers with 0.5M NaOH (2 x 50 mL), H₂O (50 mL), and finally brine (50 mL). After drying of the organic layer (Na₂SO₄) and concentration *in vacuo*, the crude product was purified by flash chromatography (SiO₂, EtOAc/hexanes, 4:1, then EtOAc/MeOH, 9:1) to give alcohol **98** as a colourless glass (305 mg, 38%) as well as 212

mg of unreacted mixed anhydride (22%): R_f 0.06 (EtOAc/hexanes, 4:1); $[\alpha]_D^{20} = -16.00$ (c 0.22, MeOH); IR (μ scope) ν 3600-3200, 3259, 2981, 2937, 1749, 1611, 1586, 1525, 1466, 1233, 1147, 1076 cm^{-1} ; ^1H NMR (CDCl_3 , 300 MHz) δ 1.39 (s, 3H, CH_3), 1.57 (s, 9H, $\text{C}(\text{CH}_3)_3$), 1.62 (s, 3H, CH_3), 1.63-1.69 (m, 2H, CH_2 -5'), 1.75-1.82 (m, 2H, CH_2), 3.61 (t, 2H, $J = 6.2$ Hz, CH_2OH), 4.25 (ddd, 1H, $J = 6.9, 6.9, 3.8$ Hz, H-4'), 4.86 (dd, 1H, $J = 6.5, 3.8$ Hz, H-3'), 5.51 (dd, 1H, $J = 6.5, 2.5$ Hz, H-2'), 6.07 (d, 1H, $J = 2.5$ Hz, H-1'), 8.02 (s, 1H, H-8), 8.76 (s, 1H, H-2); ^{13}C NMR (CDCl_3 , 125 MHz) δ 25.4, 27.2, 28.1, 28.7, 29.9, 62.2, 82.3, 84.0, 84.2, 87.0, 90.6, 114.8, 122.3, 139.5, 149.6, 150.0, 150.3, 153.1; HRMS (ES+) calcd for $\text{C}_{20}\text{H}_{30}\text{N}_5\text{O}_6$ 436.2191, found 436.2195 $[\text{MH}]^+$.

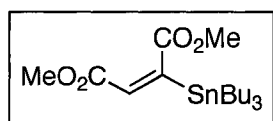
***tert*-Butyl 9-((3*aR*,4*R*,6*R*,6*aR*)-6-(3-bromopropyl)-2,2-dimethyltetrahydrofuro[3,4-*d*][1,3]dioxol-4-yl)-9*H*-purin-6-ylcarbamate (**99**)**



Alcohol **98** (278 mg, 0.638 mmol) and triphenylphosphine (262 mg, 1.00 mmol) were dissolved in MeCN (6.2 mL) and a solution of CBr_4 (304 mg, 0.915 mmol) in MeCN (2.0 mL) was added. The mixture was stirred at rt for 6 h, then concentrated *in vacuo*. The residue was purified by flash chromatography (SiO_2 , EtOAc/hexanes, 1:1) to give bromide **99** as a white foam (97.9 mg, 31%): R_f 0.40 (EtOAc/hexanes, 4:1); IR (μ scope) ν 3181, 2980, 2936, 1750, 1610, 1586, 1524, 1465, 1230, 1146, 1078 cm^{-1} ; ^1H NMR (CDCl_3 , 300 MHz) δ 1.40 (s, 3H, CH_3), 1.58 (s, 9H, $\text{C}(\text{CH}_3)_3$), 1.62 (s, 3H, CH_3), 1.80-2.00 (m, 4H, CH_2 -5', CH_2), 3.33-3.40 (m, 2H, CH_2Br), 4.22 (ddd, 1H, $J = 7.2, 7.2, 3.8$ Hz, H-4'), 4.90 (dd, 1H, $J = 6.5, 3.8$ Hz, H-3'), 5.54 (dd, 1H, $J = 6.5, 2.2$ Hz, H-2'), 6.07 (d, 1H, $J = 2.2$

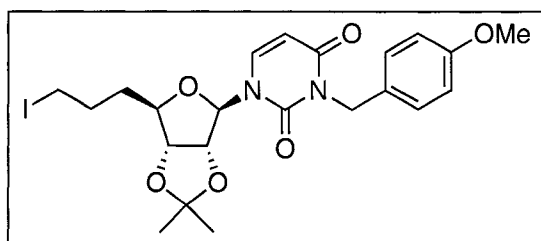
Hz, H-1'), 7.90 (br s, 1H, NH), 8.01 (s, 1H, H-8), 8.77 (s, 1H, H-2); ^{13}C NMR (CDCl_3 , 100 MHz) δ 25.4, 27.1, 28.1, 28.8, 31.8, 33.0, 82.3, 83.9, 84.1, 86.4, 90.5, 114.7, 122.3, 139.9, 149.7, 150.1, 150.3, 153.1; HRMS (ES+) calcd for $\text{C}_{20}\text{H}_{29}\text{N}_5\text{O}_5\text{Br}$ 498.1347, found 498.1343 $[\text{MH}]^+$.

Dimethyl 2-(tributylstannyl)maleate (**100**)²¹⁹



This known compound was prepared as reported by Rossi *et al.*¹⁰⁷ $\text{Pd}(\text{PPh}_3)_4$ (139 mg, 0.121 mmol) was added to a solution of dimethyl acetylenedicarboxylate (300 μL , 2.44 mmol) in THF (3.7 mL). The reaction vessel was wrapped in aluminum foil and a solution of tri-*n*-butyltin hydride (600 μL , 2.06 mmol) in THF (3.3 mL) was added dropwise over 1.5 h. The mixture was stirred at rt for 4 h, then concentrated *in vacuo*. The resulting residue was diluted with hexanes (25 mL) and stirred for 1 h, at which point the precipitated Pd catalyst was removed by filtration. The solvent was removed *in vacuo* to give a yellow oil. This was purified by flash chromatography (SiO_2 , hexanes/EtOAc, 9:1) to afford vinyl stannane **100** as a pale yellow oil (738 mg, 83%): R_f 0.22 (hexanes/EtOAc, 9:1); IR (CH_2Cl_2 , cast) ν 2955, 2926, 2872, 2853, 1718, 1605, 1224 cm^{-1} ; ^1H NMR (CDCl_3 , 300 MHz) δ 0.87 (t, 9H, $J = 7.3$ Hz, 3 x $\text{CH}_2\text{CH}_2\text{CH}_2\text{CH}_3$), 1.04 (t, 6H, $J = 8.1$ Hz, 3 x $\text{CH}_2\text{CH}_2\text{CH}_2\text{CH}_3$), 1.29 (sextet, 6H, $J = 7.3$ Hz, 3 x $\text{CH}_2\text{CH}_2\text{CH}_2\text{CH}_3$), 1.44-1.53 (m, 6H, 3 x $\text{CH}_2\text{CH}_2\text{CH}_2\text{CH}_3$), 3.70 (s, 3H, OCH_3), 3.77 (s, 3H, OCH_3), 5.99 (s, 0.83H, $\text{C}=\text{CH}$, flanked by d, $\sim 0.08\text{H}$, $^3J^{117}_{\text{Sn-H}} = 46.8$ Hz, and d, $\sim 0.09\text{H}$, $^3J^{119}_{\text{Sn-H}} = 48.0$ Hz, $\text{C}=\text{CH}$); ^{13}C NMR (CDCl_3 , 100 MHz) δ 10.7, 13.6, 27.2, 28.5, 51.6, 51.8, 128.8, 159.1, 163.3, 172.9; HRMS (ES+) calcd for $\text{C}_{18}\text{H}_{34}\text{O}_4\text{NaSn}$ 457.1371, found 457.1375 $[\text{MNa}]^+$.

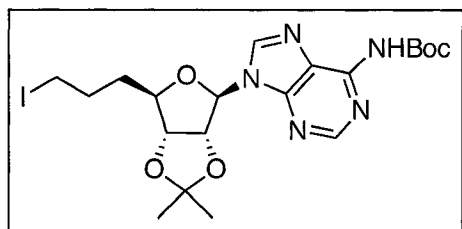
1-((3a*R*,4*R*,6*R*,6a*R*)-6-(3-Iodopropyl)-2,2-dimethyltetrahydrofuro[3,4-*d*][1,3]dioxol-4-yl)-3-(4-methoxybenzyl)pyrimidine-2,4(1*H*,3*H*)-dione (108)



NaI (457 mg, 3.05 mmol) was added to a solution of bromide **91** (201 mg, 0.405 mmol) in acetone (2.5 mL), and the reagents were stirred at reflux for 26 h.

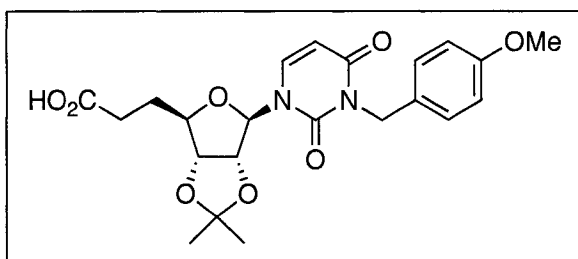
Upon cooling to rt, the solvent was removed *in vacuo* and the green residue was partitioned between EtOAc (3 mL) and H₂O (3 mL). The layers were separated and the aqueous layer was extracted with EtOAc (3 x 3 mL). The combined organic layers were washed with 1M Na₂S₂O₃ (3 mL), H₂O (3 mL), then dried (Na₂SO₄). After concentration *in vacuo*, the residue was purified by flash chromatography (SiO₂, EtOAc/hexanes, 1:1) to afford iodide **108** as a pale yellow foam (119 mg, 54%): *R_f* 0.68 (EtOAc, 100%); $[\alpha]_D^{20} = +15.56$ (*c* 0.18, MeOH); IR (μ scope) ν 3093, 2987, 2936, 2836, 1709, 1660, 1612, 1585, 1512, 1450, 1244, 1067 cm⁻¹; ¹H NMR (CDCl₃, 500 MHz) δ 1.34 (s, 3H, CH₃), 1.56 (s, 3H, CH₃), 1.82 (t, 2H, *J* = 7.5 Hz, CH₂), 1.85-1.96 (m, 2H, CH₂), 3.15-3.21 (m, 2H, CH₂I), 3.78 (s, 3H, ArOCH₃), 4.01-4.04 (m, 1H, H-4'), 4.61 (app t, 1H, *J* = 6.0 Hz, H-3'), 4.92 (d, 1H, *J* = 6.0 Hz, H-2'), 5.03 (s, 2H, benzylic CH₂), 5.61 (s, 1H, H-1'), 5.78 (d, 1H, *J* = 8.0 Hz, H-5), 6.83 (d, 2H, *J* = 8.3 Hz, ArH), 7.16 (d, 1H, *J* = 8.0 Hz, H-6), 7.44 (d, 2H, *J* = 8.3 Hz, ArH); ¹³C NMR (CDCl₃, 100 MHz) δ 6.1, 25.4, 27.2, 29.6, 34.1, 43.5, 55.2, 83.8, 84.6, 86.2, 94.4, 102.3, 113.7, 114.7, 128.8, 130.7, 139.6, 150.5, 159.2, 162.4; HRMS (ES⁺) calcd for C₂₂H₂₇N₂O₆NaI 565.0806, found 565.0803 [MNa]⁺.

***tert*-Butyl 9-((3*aR*,4*R*,6*R*,6*aR*)-6-(3-iodopropyl)-2,2-dimethyltetrahydrofuro[3,4-*d*][1,3]-dioxol-4-yl)-9*H*-purin-6-ylcarbamate (110)**



NaI (187 mg, 1.25 mmol) was added to a solution of bromide **99** (78.2 mg, 0.157 mmol) in acetone (2.0 mL), and the mixture was stirred at reflux for 28.5 h. The solvent was removed *in vacuo* and the yellow residue was partitioned between EtOAc (1.5 mL) and H₂O (1.5 mL). The layers were separated and the aqueous layer was extracted with EtOAc (2 x 1.5 mL). The combined organic layers were dried (Na₂SO₄) and concentrated *in vacuo*. Purification by flash chromatography (SiO₂, EtOAc/hexanes, 1:1) gave iodide **110** as a white foam (63.6 mg, 74%): R_f 0.11 (EtOAc/hexanes, 1:1); [α]_D²⁰ = -4.58 (*c* 0.12, MeOH); IR (μscope) ν 3180, 2979, 2935, 1750, 1609, 1585, 1525, 1464, 1227, 1145, 1077 cm⁻¹; ¹H NMR (CDCl₃, 500 MHz) δ 1.40 (s, 3H, CH₃), 1.57 (s, 9H, C(CH₃)₃), 1.62 (s, 3H, CH₃), 1.81 (app q, 2H, *J* = 6.9 Hz, CH₂-5'), 1.86-1.91 (m, 2H, CH₂), 3.10-3.16 (m, 2H, CH₂I), 4.22 (ddd, 1H, *J* = 6.9, 6.9, 3.7 Hz, H-4'), 4.90 (dd, 1H, *J* = 6.5, 3.7 Hz, H-3'), 5.54 (dd, 1H, *J* = 6.5, 2.5 Hz, H-2'), 6.06 (d, 1H, *J* = 2.5 Hz, H-1'), 7.91 (br s, 1H, NH), 8.01 (s, 1H, H-8), 8.77 (s, 1H, H-2); ¹³C NMR (CDCl₃, 100 MHz) δ 5.9, 25.4, 27.2, 28.1, 29.5, 34.0, 82.3, 83.9, 84.1, 86.3, 90.5, 114.7, 122.4, 141.8, 149.7, 150.1, 150.3, 153.1; HRMS (ES⁺) calcd for C₂₀H₂₈N₅O₅INa 568.1027, found 568.1025 [MNa]⁺.

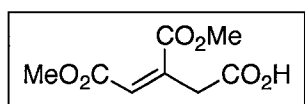
3-((3a*R*,4*R*,6*R*,6a*R*)-6-(3-(4-Methoxybenzyl)-2,4-dioxo-3,4-dihydropyrimidin-1(2*H*)-yl)-2,2-dimethyltetrahydrofuro[3,4-*d*][1,3]dioxol-4-yl)propanoic acid (117)



LiOH·H₂O (106 mg, 2.53 mmol) was added to a solution of ester **124** (459 mg, 1.00 mmol) in H₂O/THF (1:1, 30.0 mL) cooled to 0 °C. The mixture was stirred

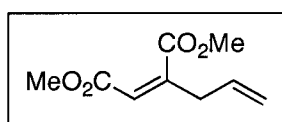
at 0 °C for 2 h. It was then acidified to pH 4 with 1 M citric acid and extracted with EtOAc (3 x 20 mL). The combined organic layers were dried (Na₂SO₄) and concentrated *in vacuo* to give carboxylic acid **117** as a white foam (445 mg, 100%): *R_f* 0.03 (EtOAc/hexanes, 1:1); [α]_D²⁰ = +7.88 (*c* 0.34, MeOH); IR (μscope) ν 3700-2400, 2989, 2938, 2838, 1704, 1658, 1650, 1612, 1513, 1454, 1297, 1081 cm⁻¹; ¹H NMR (CDCl₃, 500 MHz) δ 1.34 (s, 3H, CH₃), 1.56 (s, 3H, CH₃), 2.06 (app q, 2H, *J* = 7.5 Hz, CH₂-5'), 2.47 (app t, 2H, *J* = 7.5 Hz, CH_{2α}), 3.78 (s, 3H, ArOCH₃), 4.05-4.08 (m, 1H, H-4'), 4.64 (dd, 1H, *J* = 6.5, 5.0 Hz, H-3'), 4.94 (dd, 1H, *J* = 6.5, 2.5 Hz, H-2'), 5.01 (d, 1H, *J* = 13.5 Hz, benzylic CH_aH_b), 5.05 (d, 1H, *J* = 13.5 Hz, benzylic CH_aH_b), 5.60 (d, 1H, *J* = 2.5 Hz, H-1'), 5.78 (d, 1H, *J* = 8.0 Hz, H-5), 6.83 (d, 2H, *J* = 8.8 Hz, ArH), 7.15 (d, 1H, *J* = 8.0 Hz, H-6), 7.44 (d, 2H, *J* = 8.8 Hz, ArH); ¹³C NMR (CDCl₃, 125 MHz) δ 25.4, 27.2, 28.1, 30.1, 43.6, 55.2, 83.5, 84.6, 86.0, 94.4, 102.1, 113.7, 114.7, 128.7, 130.7, 140.0, 150.5, 159.1, 162.9, 177.8; HRMS (ES⁺) calcd for C₂₂H₂₆N₂O₈Na 469.1581, found 469.1580 [MNa]⁺.

(Z)-5-Methoxy-3-(methoxycarbonyl)-5-oxpent-3-enoic acid (**118**)



This compound was prepared by a modification of the procedure reported by Kar *et al.*¹²⁵ Alkene **120** (790 mg, 4.29 mmol) was dissolved in acetone (50.0 mL) and the dye Sudan Red 7B¹²⁴ (~ 5 mg) was added. The solution was cooled to -78 °C, and ozone was bubbled through until dissipation of the red colour of the indicator (~7 min). Excess ozone was purged from the system by flushing with argon for 30 min, then the solvent was removed *in vacuo*. The resulting oil was dissolved in Et₂O (35.0 mL) and cooled to 0 °C. A 5% solution of Na₂Cr₂O₇ · 2H₂O in 4 M H₂SO₄ (23.0 mL) was added dropwise, and the resulting black mixture was stirred at 0 °C for 3 h. It was then extracted with EtOAc (3 x 35 mL) and dried (Na₂SO₄). Purification by flash chromatography (SiO₂, hexanes/EtOAc, 3:2) yielded carboxylic acid **118** as a yellow oil (487 mg, 56%): R_f 0.03 (EtOAc/pentane, 7:3); IR (CH₂Cl₂, cast) ν 3450-2400, 3009, 2957, 1731, 1655, 1277, 1176 cm⁻¹; ¹H NMR (CDCl₃, 300 MHz) δ 3.41 (s, 2H, CH₂), 3.76 (s, 3H, OCH₃), 3.80 (s, 3H, OCH₃), 6.18 (s, 1H, C=CH); ¹³C NMR (CDCl₃, 125 MHz) δ 38.6, 52.2, 52.7, 127.9, 136.4, 165.4, 166.5, 174.4; HRMS (ES⁺) calcd for C₈H₁₀O₆Na 225.0370, found 225.0372 [MNa]⁺.

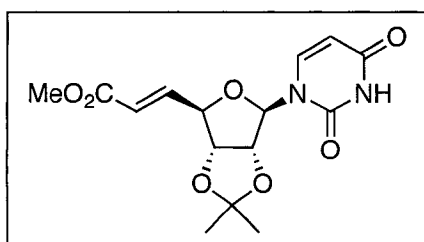
Dimethyl 2-allylmaleate (**120**)²²⁰



This known compound was prepared using an adaptation of the procedure of Baldwin *et al.*²²¹ A crystal of iodine was added to a suspension of magnesium turnings (1.01 g, 41.4 mmol) in Et₂O (6.0 mL). Upon dissipation of the purple colour, allyl bromide (1.50 mL, 17.2 mmol) in Et₂O (10.0 mL) was added dropwise, and the reaction mixture was heated at reflux for 2 h. Upon cooling

to rt, the Grignard mixture was transferred *via* canula to a dropping funnel connected to a round bottom flask containing a suspension of freshly prepared²²² CuBr·SMe₂ (4.24 g, 20.6 mmol) in THF (112.0 mL) at -40 °C. The Grignard solution was added dropwise, and the resulting orange reaction mixture was stirred at -40 °C for 1 h. It was then cooled to -78 °C and dimethyl acetylenedicarboxylate (1.80 mL, 14.6 mmol) in THF (25.0 mL) was added dropwise over 30 min. The resulting dark red mixture was stirred at -78 °C for 1 h, then a saturated solution of NH₄Cl (34 mL, adjusted to pH 8 with NH₄OH) was added. The mixture was allowed to warm to rt, then it was partitioned between Et₂O (50 mL) and H₂O (50 mL). The aqueous layer was extracted with Et₂O (3 x 75 mL) and the combined organic layers were washed with saturated NH₄Cl (100 mL) then brine (100 mL). After drying (Na₂SO₄) and concentration *in vacuo*, the resulting crude oil was purified by flash chromatography (SiO₂, pentane/Et₂O, 9:1) to afford **120** as a yellow liquid (2.40 g, 89%): R_f 0.07 (pentane/Et₂O, 9:1); IR (neat) ν 3082, 2954, 2845, 1732, 1652, 1170, 1092 cm⁻¹; ¹H NMR (CDCl₃, 500 MHz) δ 3.10 (dd, 2H, *J* = 6.8, 1.0 Hz, allylic CH₂), 3.74 (s, 3H, OCH₃), 3.83 (s, 3H, OCH₃), 5.16-5.21 (m, 2 H, CH=CH₂), 5.78 (dddd, 1H, *J* = 17.0, 10.5, 6.8, 6.8 Hz, CH=CH₂), 5.87 (t, 1H, *J* = 1.8 Hz, =CH); ¹³C NMR (CDCl₃, 125 MHz) δ 38.0, 51.9, 52.3, 119.3, 120.5, 131.9, 148.0, 165.4, 168.7; HRMS (ES⁺) calcd for C₉H₁₂O₄Na 207.0628, found 207.0628 [MNa]⁺.

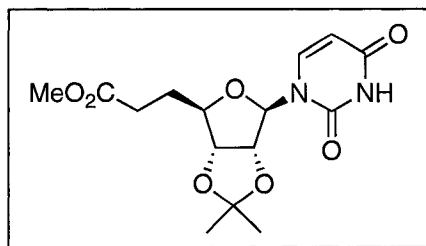
(E)-Methyl 3-((3a*R*,4*R*,6*R*,6a*R*)-6-(2,4-dioxo-3,4-dihydropyrimidin-1(2*H*)-yl)-2,2-dimethyltetrahydrofuro[3,4-*d*][1,3]dioxol-4-yl)acrylate (121)²²³



This known compound was prepared using the same method as for the preparation of **80**. IBX (4.90 g,

17.5 mmol) and ((methoxycarbonyl)methylene)-triphenylphosphorane (5.85 g, 17.5 mmol) were added to a solution of 2',3'-*O*-isopropylideneuridine (1.98 g, 6.98 mmol) in DMSO (17.5 mL), and the mixture was stirred at rt for 98.5 h. H₂O (50 mL) and EtOAc (50 mL) were added, and the mixture was filtered to remove insoluble material. The layers were separated, and the aqueous layer was extracted with EtOAc (3 x 100 mL). The combined organic layers were dried (Na₂SO₄) and concentrated *in vacuo*. Purification by flash chromatography (SiO₂, EtOAc/hexanes, 3:2 to 7:3) afforded **121** as a pale orange foam (2.15 g, 91%): *R_f* 0.44 (EtOAc, 100%); [α]_D²⁰ = +36.66 (*c* 0.33, CHCl₃); IR (μscope) ν 3206, 3063, 2992, 2953, 2822, 1689, 1645, 1268, 1068 cm⁻¹; ¹H NMR (CDCl₃, 400 MHz) δ 1.36 (s, 3H, CH₃), 1.59 (s, 3H, CH₃), 3.75 (s, 3H, OCH₃), 4.67 (ddd, 1H, *J* = 6.0, 4.8, 1.6 Hz, H-4'), 4.85 (dd, 1H, *J* = 6.4, 4.8 Hz, H-3'), 5.08 (dd, 1H, *J* = 6.4, 2.0 Hz, H-2'), 5.63 (d, 1H, *J* = 2.0 Hz, H-1'), 5.75 (dd, 1H, *J* = 8.0, 2.4 Hz, H-5), 6.05 (dd, 1H, *J* = 15.9, 1.6 Hz, CH₃O₂CCH=CH), 7.02 (dd, 1H, *J* = 15.9, 6.0 Hz, CH₃O₂CCH=CH), 7.19 (d, 1H, *J* = 8.0 Hz, H-6), 8.46 (br s, 1H, NH); ¹³C NMR (CDCl₃, 125 MHz) δ 25.3, 27.1, 51.8, 84.0, 84.5, 86.9, 95.2, 102.9, 114.8, 122.2, 142.6, 143.7, 149.8, 163.0, 166.2; HRMS (ES⁺) calcd for C₁₅H₁₈N₂O₇Na 361.1012, found 361.1010 [MNa]⁺.

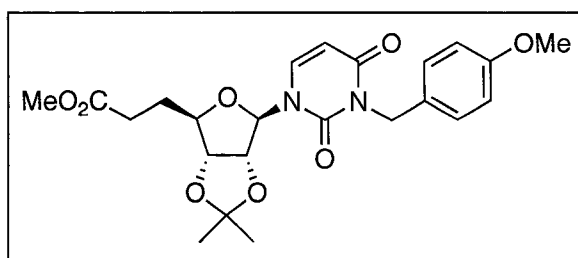
Methyl 3-((3*aR*, 4*R*, 6*R*, 6*aR*)-6-(2,4-dioxo-3,4-dihydropyrimidin-1(2*H*)-yl)-2,2-dimethyltetrahydrofuro[3,4-*d*][1,3]dioxol-4-yl)propanoate (122)



10% Pd/C (158 mg) was added to a solution of α,β-unsaturated ester **121** (1.50 g, 4.42 mmol) in EtOH (73.0 mL), and the mixture was stirred under 1 atm

H₂ for 14 h. It was then filtered through Celite and concentrated *in vacuo* to afford **122** as a white foam (1.41 g, 94%): R_f 0.18 (EtOAc/hexanes, 2:1); [α]_D²⁰ = +27.47 (*c* 0.23, CHCl₃); IR (μscope) ν 3209, 3063, 2990, 2953, 1692, 1270, 1090 cm⁻¹; ¹H NMR (CDCl₃, 500 MHz) δ 1.35 (s, 3H, CH₃), 1.56 (s, 3H, CH₃), 2.06 (app q, 2H, *J* = 7.6 Hz, CH₂-5'), 2.40-2.50 (m, 2H, CH_{2α}), 3.67 (s, 3H, OCH₃), 4.06 (ddd, 1H, *J* = 7.6, 7.6, 5.3 Hz, H-4'), 4.62 (dd, 1H, *J* = 6.3, 5.3 Hz, H-3'), 4.96 (dd, 1H, *J* = 6.3, 2.0 Hz, H-2'), 5.61 (d, 1H, *J* = 2.0 Hz, H-1'), 5.74 (dd, 1H, *J* = 8.0, 2.0 Hz, H-5), 7.21 (d, 1H, *J* = 8.0 Hz, H-6), 8.45 (br s, 1H, NH); ¹³C NMR (CDCl₃, 125 MHz) δ 25.3, 27.1, 28.3, 30.1, 51.6, 83.5, 84.3, 86.0, 93.6, 102.5, 114.6, 142.6, 150.1, 164.0, 173.3; HRMS (ES+) calcd for C₁₅H₂₀N₂O₇Na 363.1168, found 363.1166 [MNa]⁺.

Methyl 3-((3a*R*,4*R*,6*R*,6a*R*)-6-(3-(4-methoxybenzyl)-2,4-dioxo-3,4-dihydropyrimidin-1(2*H*)-yl)-2,2-dimethyltetrahydrofuro[3,4-*d*][1,3]dioxol-4-yl)propanoate (123**)**

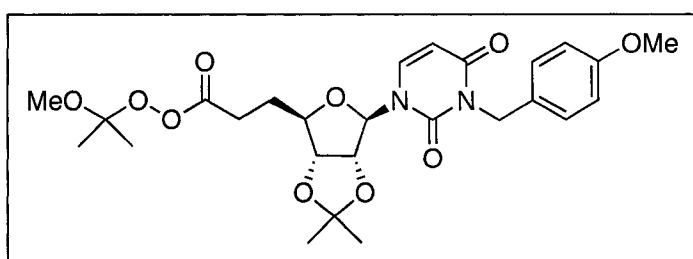


p-Methoxybenzyl chloride (810 μL, 5.97 mmol) and DBU (890 μL, 5.95 mmol) were added to a solution of nucleoside derivative **122** (1.01 g, 2.97 mmol) in

MeCN (25.2 mL), and the reaction mixture was stirred at reflux for 14 h. Upon cooling to rt, the solvent was removed *in vacuo*, and the residue was partitioned between EtOAc (40 mL) and H₂O (40 mL). The layers were separated, and the aqueous layer was acidified with 1 M citric acid, then extracted with EtOAc (3 x 40 mL). The combined organic layers were washed with brine, dried (MgSO₄), and concentrated *in vacuo*. The resulting orange oil was purified by flash chromatography (SiO₂, EtOAc/hexanes, 1:1) to

give **123** as a pale yellow gum (1.14 g, 83%): R_f 0.21 (EtOAc/hexanes, 1:1); $[\alpha]_D^{20} = +24.76$ (c 0.21, MeOH); IR (CHCl₃, cast) ν 2988, 2952, 2837, 1736, 1712, 1669, 1612, 1513, 1453, 1248, 1085 cm⁻¹; ¹H NMR (CDCl₃, 500 MHz) δ 1.34 (s, 3H, CH₃), 1.56 (s, 3H, CH₃), 2.05 (app q, 2H, $J = 7.7$ Hz, CH₂-5'), 2.38-2.48 (m, 2H, CH₂ $_{\alpha}$), 3.67 (s, 3H, CO₂CH₃), 3.78 (s, 3H, ArOCH₃), 4.03-4.06 (m, 1H, H-4'), 4.61 (dd, 1H, $J = 6.8, 4.8$ Hz, H-3'), 4.91 (dd, 1H, $J = 6.8, 2.2$ Hz, H-2'), 5.00 (d, 1H, $J = 13.5$ Hz, benzylic CH_aH_b), 5.07 (d, 1H, $J = 13.5$ Hz, benzylic CH_aH_b), 5.63 (d, 1H, $J = 2.2$ Hz, H-1'), 5.77 (d, 1H, $J = 8.3$ Hz, H-5), 6.83 (d, 2H, $J = 8.8$ Hz, ArH), 7.16 (d, 1H, $J = 8.3$ Hz, H-6), 7.45 (d, 2H, $J = 8.8$ Hz, ArH); ¹³C NMR (CDCl₃, 125 MHz) δ 25.4, 27.2, 28.4, 30.2, 43.6, 51.7, 55.2, 83.6, 84.6, 85.9, 94.2, 102.3, 113.7, 114.8, 128.8, 130.8, 139.5, 150.5, 159.1, 162.4, 173.2; HRMS (ES+) calcd for C₂₃H₂₈N₂O₈Na 483.1738, found 483.1737 [MNa]⁺.

2-Methoxypropan-2-yl peroxy-3-((3*aR*,4*R*,6*R*,6*aR*)-6-(3-(4-methoxybenzyl)-2,4-dioxo-3,4-dihydropyrimidin-1(2*H*)-yl)-2,2-dimethyltetrahydrofuro[3,4-*d*][1,3]dioxol-4-yl)propanoate (125)

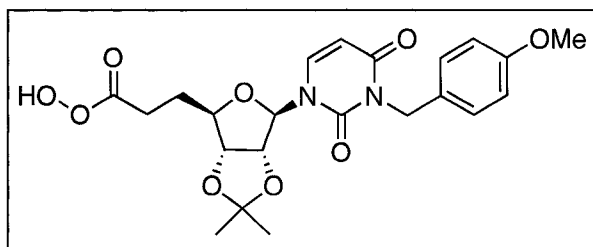


DCC (108 mg, 0.524 mmol), 2-methoxyprop-2-yl hydroperoxide^{126, 127} (60 mg/mL in CH₂Cl₂, 714 μ L, 0.404 mmol)

and DMAP (4.40 mg, 0.0360 mmol), were added to a solution of carboxylic acid **117** (150 mg, 0.336 mmol) in CH₂Cl₂ (2.0 mL) at 0 °C. The pale yellow suspension was stirred for 2.5 h while allowing it to slowly warm to rt. The mixture was then filtered through Celite to remove the dicyclohexylurea byproduct, and the filtrate was

concentrated *in vacuo*. Purification was done by flash chromatography (SiO₂, hexanes/EtOAc, 3:2) to give perester **125** as a colourless glass (130 mg, 72%): *R_f* 0.23 (EtOAc/hexanes, 1:1); $[\alpha]_D^{20} = +23.17$ (*c* 0.51, CHCl₃); IR (CHCl₃, cast) ν 2992, 2939, 2836, 1775, 1712, 1669, 1612, 1513, 1453, 1297, 1068 cm⁻¹; ¹H NMR (CDCl₃, 300 MHz) δ 1.33 (s, 3H, CH₃), 1.45 (s, 6H, methoxypropyl 2 x CH₃), 1.54 (s, 3H, CH₃), 2.03-2.13 (m, 2H, CH₂-5'), 2.41-2.47 (m, 2H, CH_{2 α}), 3.32 (s, 3H, methoxypropyl OCH₃), 3.77 (s, 3H, ArOCH₃), 4.00-4.06 (m, 1H, H-4'), 4.63 (dd, 1H, *J* = 6.6, 5.1 Hz, H-3'), 4.92 (dd, 1H, *J* = 6.6, 2.1 Hz, H-2'), 4.99 (d, 1H, *J* = 13.5 Hz, benzylic CH_aH_b), 5.06 (d, 1H, *J* = 13.5 Hz, benzylic CH_aH_b), 5.59 (d, 1H, *J* = 2.1 Hz, H-1'), 5.77 (d, 1H, *J* = 8.0 Hz, H-5), 6.83 (d, 2H, *J* = 8.7 Hz, ArH), 7.14 (d, 1H, *J* = 8.0 Hz, H-6), 7.43 (d, 2H, *J* = 8.7 Hz, ArH); ¹³C NMR (CDCl₃, 125 MHz) δ 22.5, 25.4, 27.2, 27.3, 28.3, 43.6, 49.8, 55.2, 83.5, 84.6, 85.7, 94.4, 102.4, 107.0, 113.7, 114.9, 128.8, 130.8, 139.7, 150.5, 159.2, 162.4, 169.8; HRMS (ES⁺) calcd for C₂₆H₃₄N₂O₁₀Na 557.2106, found 557.2107 [MNa]⁺.

3-((3*aR*,4*R*,6*R*,6*aR*)-6-(3-(4-Methoxybenzyl)-2,4-dioxo-3,4-dihydropyrimidin-1(2*H*)-yl)-2,2-dimethyltetrahydrofuro[3,4-*d*][1,3]dioxol-4-yl)peroxypropanoic acid (126)

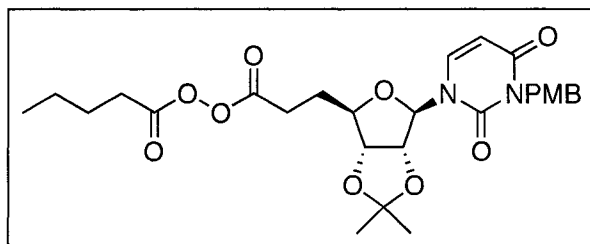


Perester **125** (88.4 mg, 0.165 mmol) was stirred in AcOH/H₂O (1:1, 1.1 mL) at rt for 3 h, then EtOAc (7.0 mL) was added, followed by a saturated solution

of NaHCO₃. The layers were separated, and the organic layer was washed with H₂O (2 x 1 mL) then dried (MgSO₄). The solvent was removed *in vacuo* to give peracid **126** as a white foam (69.3 mg, 91%): $[\alpha]_D^{20} = +23.69$ (*c* 0.13, CHCl₃); IR (CHCl₃, cast) ν 3450-

3150, 2932, 1767, 1712, 1667, 1611, 1513, 1455, 1248, 1178 cm^{-1} ; ^1H NMR (CDCl_3 , 500 MHz) δ 1.34 (s, 3H, CH_3), 1.54 (s, 3H, CH_3), 2.04-2.15 (m, 2H, CH_2 -5'), 2.45-2.50 (m, 2H, CH_2 $_{\alpha}$), 3.78 (s, 3H, ArOCH_3), 4.02-4.06 (m, 1H, H-4'), 4.69 (dd, 1H, $J = 6.5, 5.0$ Hz, H-3'), 4.98-5.05 (m, 3H, H-2' + benzylic CH_2), 5.49 (d, 1H, $J = 1.5$ Hz, H-1'), 5.77 (d, 1H, $J = 8.0$ Hz, H-5), 6.83 (d, 2H, $J = 8.7$ Hz, ArH), 7.10 (d, 1H, $J = 8.0$ Hz, H-6), 7.43 (d, 2H, $J = 8.7$ Hz, ArH), 11.29 (br s, 1H, CO_3H); ^{13}C NMR (CDCl_3 , 125 MHz) δ 25.4, 26.9, 27.2, 27.9, 43.5, 55.3, 83.6, 84.5, 86.2, 95.7, 102.4, 113.7, 114.7, 128.7, 130.7, 140.4, 150.5, 159.1, 162.5, 173.7; HRMS (ES+) calcd for $\text{C}_{22}\text{H}_{26}\text{N}_2\text{O}_9\text{Na}$ 485.1531, found 485.1533 $[\text{MNa}]^+$.

3-((3aR,4R,6R,6aR)-6-(3-(4-Methoxybenzyl)-2,4-dioxo-3,4-dihydropyrimidin-1(2H)-yl)-2,2-dimethyltetrahydrofuro[3,4-d][1,3]dioxol-4-yl)propanoic pentanoic peroxy-anhydride (129)

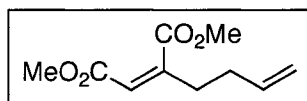


DCC (10.8 mg, 0.0523 mmol) was added to a solution of peracid **126** (13.0 mg, 0.0281 mmol) and valeric acid (6.00 μL , 0.0552 mmol) in CH_2Cl_2 (400

μL) at -20 $^\circ\text{C}$, and the solution was stored at -20 $^\circ\text{C}$ for 15 h. It was then filtered through Celite, and the filtrate was concentrated *in vacuo*. Purification by chromatography (SiO_2 , hexanes/EtOAc, 3:2) yielded diacyl peroxide **129** as a white gum (7.90 mg, 51%); R_f 0.07 (hexanes/EtOAc, 3:2); $[\alpha]_D^{20} +16.39$ (c 0.61, CHCl_3); IR (CHCl_3 , cast) ν 2933, 2855, 1809, 1781, 1713, 1671, 1612, 1513, 1454, 1249, 1067 cm^{-1} ; ^1H NMR (CDCl_3 , 50 MHz) δ 0.94 (t, 3H, $J = 7.4$ Hz, CH_2 $_{\alpha}\text{CH}_2\text{CH}_2\text{CH}_3$), 1.34 (s, 3H, CH_3), 1.41 (sext, 2H, $J = 7.4$

Hz, CH_{2α}CH₂CH₂CH₃), 1.55 (s, 3H, CH₃), 1.69 (pent, 2H, *J* = 7.4 Hz, CH_{2α}CH₂CH₂CH₃), 2.15 (app q, 2H, *J* = 7.5 Hz, CH_{2-5'}), 2.41 (t, 2H, *J* = 7.4 Hz, CH_{2α}CH₂CH₂CH₃), 2.50-2.58 (m, 2H, CH_{2α}), 3.78 (s, 3H, ArOCH₃), 4.06-4.10 (m, 1H, H-4'), 4.67 (dd, 1H, *J* = 6.5, 5.0 Hz, H-3'), 4.97 (dd, 1H, *J* = 6.5, 2.0 Hz, H-2'), 5.00 (d, 1H, *J* = 13.8 Hz, benzylic CH_aH_b), 5.06 (d, 1H, *J* = 13.8 Hz, benzylic CH_aH_b), 5.56 (d, 1H, *J* = 2.0 Hz, H-1'), 5.77 (d, 1H, *J* = 8.0 Hz, H-5), 6.83 (d, 2H, *J* = 8.8 Hz, ArH), 7.13 (d, 1H, *J* = 8.0 Hz, H-6), 7.44 (d, 2H, *J* = 8.8 Hz, ArH); ¹³C NMR (CDCl₃, 125 MHz) δ 13.5, 22.1, 25.4, 26.4, 26.8, 27.2, 28.1, 29.7, 43.6, 55.2, 83.5, 84.6, 85.8, 95.1, 102.3, 113.7, 114.8, 128.8, 130.7, 140.1, 150.5, 159.1, 162.4, 168.6, 169.1; HRMS (ES⁺) calcd for C₂₇H₃₄N₂O₁₀Na 569.2106, found 569.2108 [MNa]⁺.

Dimethyl 2-(but-3-enyl)maleate (131)

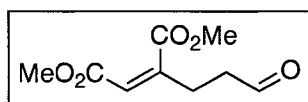


The same method as for the preparation of **120** was employed.

Thus, reaction of 3-butenyl bromide (1.50 mL, 14.8 mmol) with magnesium turnings (659 mg, 27.1 mmol) in Et₂O (12.0 mL) was followed by dropwise addition of the resulting Grignard solution to a freshly prepared suspension of CuBr·SMe₂ (3.67 g, 17.9 mmol) in THF (100.0 mL) at -40 °C. After stirring at -40 °C for 1 h, it was cooled to -78 °C and dimethyl acetylenedicarboxylate (2.00 mL, 16.3 mmol) in THF (25.0 mL) was added dropwise. The reaction mixture was stirred at -78 °C for 1h, then a saturated NH₄Cl solution (30 mL, adjusted to pH 8 with NH₄OH) was added. After allowing the mixture to warm to rt, it was partitioned between H₂O (40 mL) and Et₂O (40 mL) and the aqueous layer was extracted with Et₂O (3 x 60 mL). The combined organic layers were washed with saturated NH₄Cl (85 mL) followed by brine (85 mL),

then dried (Na₂SO₄). The solvent was removed *in vacuo*, and the crude product was purified by flash chromatography (SiO₂, pentane/Et₂O, 9:1 to 3:2) to give **131** as a pale yellow oil (1.83 g, 62%): R_f 0.44 (petroleum ether/Et₂O, 9:1); IR (CHCl₃, cast) ν 2953, 2846, 1728, 1680, 1651, 1268, 1169 cm⁻¹; ¹H NMR (CDCl₃, 500 MHz) δ 2.25-2.29 (m, 2H, CH₂CH₂CH=CH₂), 2.46 (td, 2H, *J* = 7.5, 1.5 Hz, CH₂CH₂CH=CH₂), 3.73 (s, 3H, OCH₃), 3.83 (s, 3H, OCH₃), 5.04 (app dq, 1H, *J* = 10.5, 1.6 Hz, CH=CH_{cis}H_{trans}), 5.07 (app dq, 1H, *J* = 17.3, 1.6 Hz, CH=CH_{cis}H_{trans}), 5.79 (dddd, 1H, *J* = 17.5, 10.5, 7.0, 7.0 Hz, CH=CH₂), 5.83 (t, 1H, *J* = 1.5 Hz, C=CH); ¹³C NMR (CDCl₃, 125 MHz) δ 31.0, 33.6, 51.8, 52.3, 116.1, 119.7, 136.2, 149.6, 165.3, 169.1; HRMS (ES⁺) calcd for C₁₀H₁₄O₄Na 221.0784, found 221.0784 [MNa]⁺.

Dimethyl-2(3-oxopropyl)maleate (**132**)

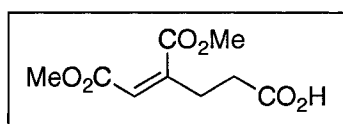


Alkene **131** (419 mg, 2.11 mmol) was dissolved in CH₂Cl₂ (20.0 mL) and the dye Sudan Red 7B¹²⁴ (~ 5 mg) was added.

The solution was cooled to -78 °C, and ozone was bubbled through it until the red colour of the indicator dissipated (~2 min). Excess ozone was purged from the system by flushing with argon for 10 min, then a solution of triphenylphosphine (554 mg, 2.11 mmol) in CH₂Cl₂ (5.0 mL) was added. The pale yellow mixture was warmed to rt and stirred for 1 h. The solvent was then removed *in vacuo*, and the crude orange oil was purified by flash chromatography (SiO₂, EtOAc/hexanes, 1:1) to give aldehyde **132** as a yellow liquid (387 mg, 92%): R_f 0.22 (EtOAc/hexanes, 1:1); IR (CHCl₃, cast) ν 2954, 2850, 2740, 1724, 1651, 1271, 1122 cm⁻¹; ¹H NMR (CDCl₃, 500 MHz) δ 2.66-2.74 (m, 4H, 2 x CH₂), 3.73 (s, 3H, OCH₃), 3.83 (s, 3H, OCH₃), 5.89 (t, 1H, *J* = 1.0 Hz, C=CH),

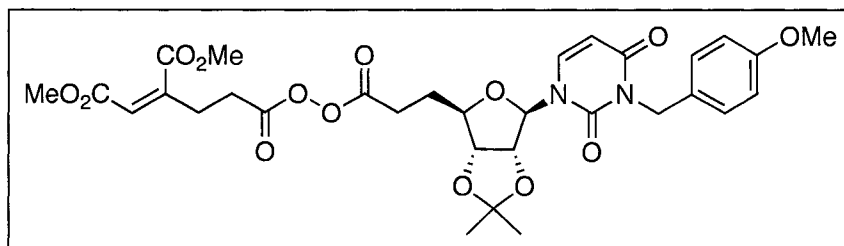
9.78 (s, 1H, CHO); ^{13}C NMR, 125 MHz) δ 26.5, 41.0, 51.9, 52.5, 121.0, 147.6, 165.1, 168.6, 204.1; HRMS (ES+) calcd for $\text{C}_9\text{H}_{12}\text{O}_5\text{Na}$ 223.0577, found 223.0578 $[\text{MNa}]^+$.

(Z)-6-Methoxy-4-(methoxycarbonyl)-6-oxohex-4-enoic acid (133)



2-Methyl-2-butene (590 μL , 5.57 mmol), $\text{NaH}_2\text{PO}_4 \cdot \text{H}_2\text{O}$ (191 mg, 1.38 mmol), and NaClO_2 (362 mg, 4.01 mmol) were added to a solution of aldehyde **132** in *t*-BuOH/ H_2O (3:1, 14.0 mL), and the resulting yellow solution was stirred at rt for 1 h. It was then diluted with brine (82 mL) and extracted with EtOAc (3 x 125 mL). The combined organic layers were dried (MgSO_4) and concentrated *in vacuo*. Purification by flash chromatography (SiO_2 , EtOAc/hexanes, 1:1) yielded carboxylic acid **133** as a pale yellow oil (267 mg, 96%); R_f 0.11 (EtOAc/hexanes, 1:1); IR (CHCl_3 , cast) ν 3650-2500, 2955, 1727, 1652, 1272, 1116 cm^{-1} ; ^1H NMR (CDCl_3 , 400 MHz) δ 2.58-2.62 (m, 2H, $\text{CH}_2\text{CH}_2\text{CH}=\text{CH}_2$), 2.67-2.71 (m, 2H, $\text{CH}_2\text{CH}_2\text{CH}=\text{CH}_2$), 3.73 (s, 3H, OCH_3), 3.83 (s, 3H, OCH_3), 5.91 (t, 1H, $J = 1.4$ Hz, $\text{C}=\text{CH}$); ^{13}C NMR, 125 MHz) δ 28.8, 31.4, 51.9, 52.5, 121.0, 147.3, 165.2, 168.5, 176.9; HRMS (ES+) calcd for $\text{C}_9\text{H}_{12}\text{O}_6\text{Na}$ 239.0526, found 239.0528 $[\text{MNa}]^+$.

(Z)-6-Methoxy-4-(methoxycarbonyl)-6-oxohex-4-enoic 3-((3aR,4R,6R,6aR)-6-(3-(4-methoxybenzyl)-2,4-dioxo-3,4-dihydropyrimidin-1(2H)-yl)-2,2-dimethyltetrahydrofuro[3,4-d][1,3]dioxol-4-yl)propanoic peroxyanhydride (134)

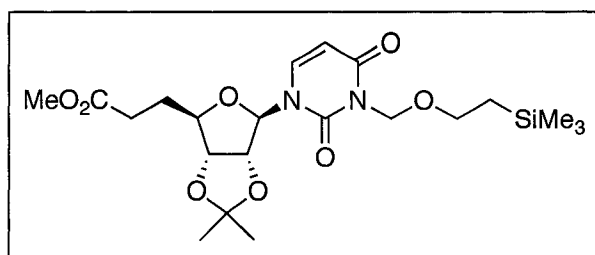


DCC (63.5 mg, 0.306 mmol) was added to a solution of peracid **126**

(67.3 mg, 0.146 mmol) and carboxylic acid **133** (50.4 mg, 0.233 mmol) in CH₂Cl₂ (2.1 mL) at -20 °C, and the reaction flask was stored at -20 °C for 22 h. It was then filtered through Celite and the Celite was washed with CH₂Cl₂. Concentration *in vacuo* was followed by flash chromatography (SiO₂, hexanes/EtOAc, 2:1 to 3:2) to afford **134** as a pale pink glass (35.1 mg, 36%): R_f 0.04 (hexanes/EtOAc, 2:1); [α]_D²⁰ = +22.26 (*c* 0.15, CHCl₃); IR (CHCl₃, cast) ν 2953, 1781, 1715, 1668, 1512, 1513, 1453, 1206, 1175, 1081 cm⁻¹; ¹H NMR (CDCl₃, 500 MHz) δ 1.34 (s, 3H, CH₃), 1.55 (s, 3H, CH₃), 2.13-2.18 (m, 2H, CH₂-5'), 2.53 (app t, 2H, *J* = 7.5 Hz, CH₂), 2.63-2.67 (m, 2H, CH₂), 2.71-2.75 (m, 2H, CH₂), 3.74 (s, 3H, OCH₃), 3.78 (s, 3H, OCH₃), 3.84 (s, 3H, ArOCH₃), 4.05-4.09 (ddd, 1H, *J* = 7.5, 7.5, 5.2 Hz, H-4'), 4.68 (dd, 1H, *J* = 6.9, 5.2 Hz, H-3'), 4.99 (dd, 1H, *J* = 6.9, 2.2 Hz, H-2'), 5.00 (d, 1H, *J* = 13.8 Hz, benzylic CH_aH_b), 5.05 (d, 1H, *J* = 13.8 Hz, benzylic CH_aH_b), 5.54 (d, 1H, *J* = 2.2 Hz, H-1'), 5.77 (d, 1H, *J* = 8.0 Hz, H-5), 5.96 (t, 1H, *J* = 1.3 Hz, C=CH), 6.83 (d, 2H, *J* = 8.5 Hz, ArH), 7.12 (d, 1H, *J* = 8.0 Hz, H-6), 7.43 (d, 2H, *J* = 8.5 Hz, ArH); ¹³C NMR (CDCl₃, 125 MHz) δ 25.4, 26.4, 27.2, 27.8, 28.1, 28.8, 43.6, 52.0, 52.6, 55.2, 83.5, 84.5, 85.8, 95.3, 102.3, 113.7, 114.8, 122.2, 128.8,

130.7, 140.2, 145.7, 150.5, 159.1, 162.5, 165.1, 167.4, 168.0, 168.4; HRMS (ES+) calcd for C₃₁H₃₆N₂O₁₄Na 683.2059, found 683.2056 [MNa]⁺.

Methyl 3-((3a*R*,4*R*,6*R*,6a*R*)-6-(2,4-dioxo-3-((2-(trimethylsilyl)ethoxy)methyl)-3,4-dihydro-pyrimidin-1(2*H*)-yl)-2,2-dimethyltetrahydrofuro[3,4-*d*][1,3]dioxol-4-yl)propanoate (136)

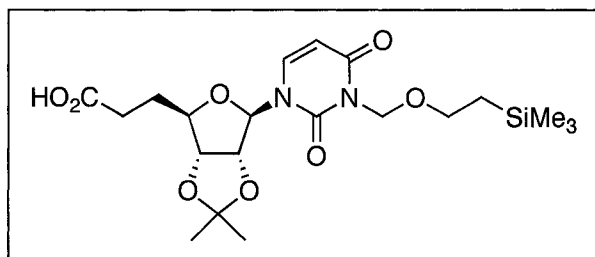


2-(Trimethylsilyl)ethoxymethyl chloride (300 μ L, 1.70 mmol) and DIPEA (960 μ L, 5.50 mmol) were added to a solution of nucleoside

derivative **122** (376 mg, 1.10 mmol) in CH₂Cl₂ (8.5 mL) at 0 °C, and the pale yellow mixture was warmed to rt and stirred for 1 h. The solvent was removed *in vacuo* and purification was done by flash chromatography (SiO₂, hexanes/EtOAc, 2:1, then CHCl₃/MeOH, 99:1) to give **136** as a colourless gum (297 mg, 57%), as well as recovered starting material (40.9 mg, 11%): R_f 0.09 (hexanes/EtOAc, 2:1); [α]_D²⁰ = +30.99 (*c* 0.14, CHCl₃); IR (CHCl₃, cast) ν 2952, 1721, 1673, 1090 cm⁻¹; ¹H NMR (CDCl₃, 400 MHz) δ 0.00 (s, 9H, Si(CH₃)₃), 0.95-0.99 (m, 2H, CH₂Si), 1.34 (s, 3H, CH₃), 1.56 (s, 3H, CH₃), 2.06 (app q, 2H, *J* = 7.1 Hz, CH₂-5'), 2.44 (app t, 2H, *J* = 7.4 Hz, CH₂ $_{\alpha}$), 3.67 (s, 3H, OCH₃), 3.69 (m, 2H, CH₂O), 4.05 (ddd, 1H, *J* = 7.1, 7.1, 4.9 Hz, H-4'), 4.64 (dd, 1H, *J* = 6.6, 4.9 Hz, H-3'), 4.97 (dd, 1H, *J* = 6.6, 2.3 Hz, H-2'), 5.36 (d, 1H, *J* = 9.6 Hz, NCH_aH_bO), 5.40 (d, 1H, *J* = 9.6 Hz, NCH_aH_bO), 5.58 (d, 1H, *J* = 2.3 Hz, H-1'), 5.77 (d, 1H, *J* = 8.0 Hz, H-5), 7.19 (d, 1H, *J* = 8.0 Hz, H-6); ¹³C NMR (CDCl₃, 125 MHz) δ -1.4, 18.1, 25.4, 27.2, 28.4, 30.2, 51.7, 67.6, 69.9, 83.6, 84.5, 86.1, 94.6,

102.2, 114.7, 140.6, 150.6, 162.5, 173.2; HRMS (ES+) calcd for C₂₁H₃₄N₂O₈SiNa 493.1977, found 493.1975 [MNa]⁺.

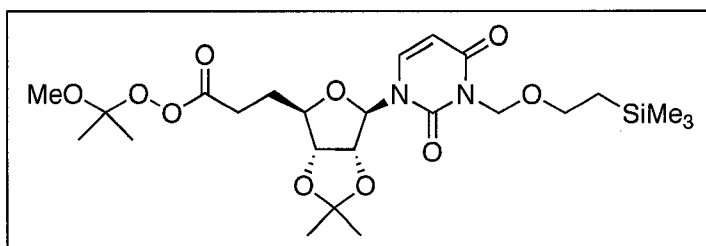
3-((3a*R*,4*R*,6*R*,6a*R*)-6-(2,4-Dioxo-3-((2-(trimethylsilyl)ethoxy)methyl)-3,4-dihydropyrimidin-1(2*H*)-yl)-2,2-dimethyltetrahydrofuro[3,4-*d*][1,3]dioxol-4-yl)propanoic acid (137)



LiOH·H₂O (60.8 mg, 1.45 mmol) was added to a solution of ester **136** (263 mg, 0.560 mmol) in THF/H₂O (1:1, 17.0 mL) at 0 °C, and the mixture was

stirred at 0 °C for 2 h. It was then acidified to pH 4 with 1M citric acid and extracted with EtOAc (3 x 15 mL). The combined organic layers were dried (Na₂SO₄) and concentrated *in vacuo* to afford carboxylic acid **137** as a white foam (255 mg, 100%): R_f 0.06 (EtOAc/hexanes, 1:1); [α]_D²⁰ = +18.60 (*c* 0.10, MeOH); IR (CHCl₃, cast) ν 3600-2400, 1721, 1678, 1250, 1212, 1093 cm⁻¹; ¹H NMR (CD₃OD, 500 MHz) δ -0.02 (s, 9H, Si(CH₃)₃), 0.91 (t, 2H, *J* = 8.2 Hz, CH₂Si), 1.33 (s, 3H, CH₃), 1.52 (s, 3H, CH₃), 1.97-2.03 (m, 2H, CH₂-5'), 2.39 (app t, 2H, *J* = 7.5 Hz, CH_{2,α}), 3.68 (t, 2H, *J* = 8.2 Hz, CH₂O), 4.03 (ddd, 1H, *J* = 6.5, 6.5, 5.0 Hz, H-4'), 4.66 (dd, 1H, *J* = 6.5, 5.0 Hz, H-3'), 4.99 (dd, 1H, *J* = 6.5, 2.0 Hz, H-2'), 5.34 (s, 2H, NCH₂O), 5.74 (d, 1H, *J* = 2.0 Hz, H-1'), 5.77 (d, 1H, *J* = 8.0 Hz, H-5), 7.62 (d, 1H, *J* = 8.0 Hz, H-6); ¹³C NMR (CD₃OD, 125 MHz) δ -1.1, 19.0, 25.8, 27.7, 29.6, 31.1, 68.6, 71.1, 84.9, 85.7, 87.3, 95.0, 102.5, 115.7, 143.6, 152.2, 164.8, 176.6; HRMS (ES+) calcd for C₂₀H₃₂N₂O₈SiNa 479.1820, found 479.1818 [MNa]⁺.

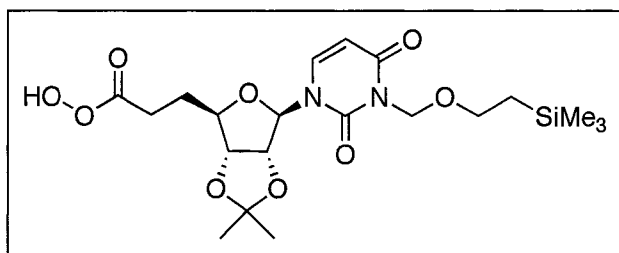
2-Methoxypropan-2-yl peroxy-3-((3a*R*,4*R*,6*R*,6a*R*)-6-(2,4-dioxo-3-((2-(trimethylsilyl)ethoxy)methyl)-3,4-dihydropyrimidin-1(2*H*)-yl)-2,2-dimethyltetrahydrofuro[3,4-*d*][1,3]dioxol-4-yl)propanoate (138**)**



DCC (189 mg, 0.916 mmol),
 DMAP (7.30 mg, 0.0600
 mmol) and 2-methoxyprop-2-yl
 hydroperoxide^{126, 127} (60

mg/mL in CH₂Cl₂, 1.20 mL, 0.678 mmol), were added to a solution of carboxylic acid **137** (255 mg, 0.559 mmol) in CH₂Cl₂ (3.3 mL) at 0 °C. The resulting orange mixture was stored at -20 °C for 16 h, then filtered through Celite. The solvent was removed *in vacuo* and the crude orange oil was purified by flash chromatography (SiO₂, hexanes/EtOAc, 2:1) to give perester **138** as a pale yellow gum (174 mg, 57%): *R_f* 0.28 (EtOAc/hexanes, 1:1); [α]_D²⁰ = +34.99 (*c* 0.18, CH₂Cl₂); IR (CH₂Cl₂, cast) ν 3095, 2991, 2951, 2896, 1778, 1721, 1675, 1639, 1215, 1092 cm⁻¹; ¹H NMR (CDCl₃, 500 MHz) δ 0.00 (s, 9H, Si(CH₃)₃), 0.95-0.98 (m, 2H, CH₂Si), 1.33 (s, 3H, CH₃), 1.45 (s, 6H, methoxypropyl 2 x CH₃), 1.54 (s, 3H, CH₃), 2.10 (app q, 2H, *J* = 7.5 Hz, CH₂-5'), 2.43-2.47 (m, 2H, CH₂_α), 3.33 (s, 3H, methoxypropyl OCH₃), 3.66-3.70 (m, 2H, CH₂O), 4.01-4.04 (m, 1H, H-4'), 4.66 (dd, 1H, *J* = 6.5, 5.0 Hz, H-3'), 4.99 (dd, 1H, *J* = 6.5, 2.0 Hz, H-2'), 5.34 (d, 1H, *J* = 9.8 Hz, NCH_aH_bO), 5.39 (d, 1H, *J* = 9.8 Hz, NCH_aH_bO), 5.54 (d, 1H, *J* = 2.0 Hz, H-1'), 5.77 (d, 1H, *J* = 8.0 Hz, H-5), 7.18 (d, 1H, *J* = 8.0 Hz, H-6); ¹³C NMR (CDCl₃, 125 MHz) δ -1.4, 18.1, 22.5, 25.4, 27.2, 27.4, 28.2, 49.8, 67.6, 69.9, 83.5, 84.5, 85.9, 94.9, 102.3, 107.0, 114.8, 140.9, 150.6, 162.5, 169.8; HRMS (ES⁺) calcd for C₂₄H₄₀N₂O₁₀SiNa 567.2345, found 567.2349 [MNa]⁺.

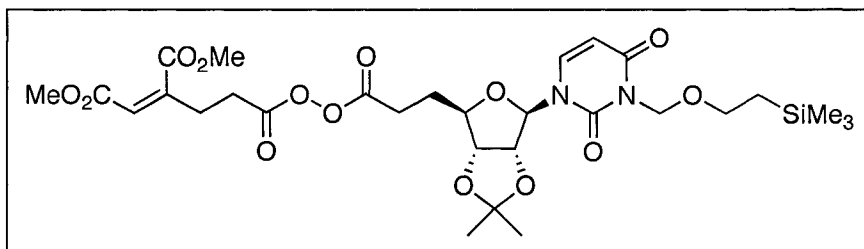
3-((3a*R*,4*R*,6*R*,6a*R*)-6-(2,4-Dioxo-3-((2-(trimethylsilyl)ethoxy)methyl)-3,4-dihydropyrimidin-1(2*H*)-yl)-2,2-dimethyltetrahydrofuro[3,4-*d*][1,3]dioxol-4-yl)peroxypropanoic acid (139)



Perester **138** (148 mg, 0.271 mmol) was stirred in AcOH/H₂O (1:1, 2.0 mL) at rt for 3 h, then EtOAc (12 mL) was added followed by a saturated

solution of NaHCO₃. The layers were separated, and the organic layer was washed with H₂O (2 x 2 mL) then dried (MgSO₄). The solvent was removed *in vacuo* to yield peracid **139** as a viscous gum (117 mg, 91%): $[\alpha]_D^{20} = +19.68$ (*c* 0.19, CH₂Cl₂); IR (CH₂Cl₂, cast) ν 2980, 2952, 2890, 1725, 1719, 1671, 1089 cm⁻¹; ¹H NMR (CDCl₃, 500 MHz) δ 0.01 (s, 9H, Si(CH₃)₃), 0.96-1.00 (m, 2H, CH₂Si), 1.34 (s, 3H, CH₃), 1.55 (s, 3H, CH₃), 2.11-2.21 (m, 2H, CH₂-5'), 2.53 (app t, 2H, *J* = 7.3 Hz, CH_{2 α}), 3.68-3.71 (m, 2H, CH₂O), 4.06 (ddd, 1H, *J* = 8.5, 8.5, 5.0 Hz, H-4'), 4.73 (dd, 1H, *J* = 6.5, 5.0 Hz, H-3'), 5.09 (dd, 1H, *J* = 6.5, 2.0 Hz, H-2'), 5.36 (d, 1H, *J* = 9.5 Hz, NCH_aH_bO), 5.40 (d, 1H, *J* = 9.5 Hz, NCH_aH_bO), 5.46 (d, 1H, *J* = 2.0 Hz, H-1'), 5.78 (d, 1H, *J* = 8.0 Hz, H-5), 7.15 (d, 1H, *J* = 8.0 Hz, H-6); ¹³C NMR (CDCl₃, 125 MHz) δ -1.5, 18.1, 25.3, 27.0, 27.1, 27.8, 67.7, 69.9, 83.5, 84.5, 86.3, 95.7, 102.2, 114.6, 141.6, 150.6, 162.8, 173.4; HRMS (ES⁺) calcd for C₂₀H₃₂N₂O₉SiNa 495.1769, found 495.1773 [MNa]⁺.

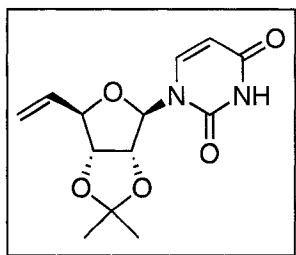
(Z)-6-Methoxy-4-(methoxycarbonyl)-6-oxohex-4-enoic 3-((3aR,4R,6R,6aR)-6-(2,4-dioxo-3-((2-(trimethylsilyl)ethoxy)methyl)-3,4-dihydropyrimidin-1(2H)-yl)-2,2-dimethyltetrahydrofuro[3,4-d][1,3]dioxol-4-yl)propanoic peroxyanhydride (140)



DCC (89.9 mg,
0.436 mmol) was
added to a
solution of

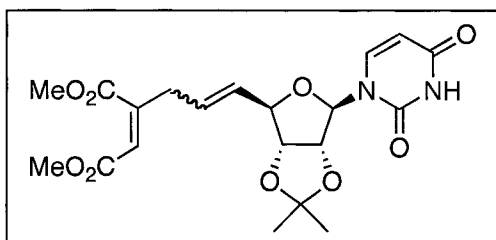
carboxylic acid **133** (76.1 mg, 0.352 mmol) and peracid **139** (100 mg, 0.212 mmol) in CH_2Cl_2 (3.0 mL) at -20°C , and the reaction mixture was stored at -20°C for 15 h. The mixture was then filtered through Celite and concentrated *in vacuo*. Purification by flash chromatography (SiO_2 , hexanes/EtOAc, 2:1 to 1:1) gave **140** as a pale yellow gum (86.8 mg, 61%): R_f 0.06 (hexanes/EtOAc, 2:1); $[\alpha]_D^{20} = +20.83$ (c 0.24, CH_2Cl_2); IR (CHCl_3 , cast) ν 3090, 2980, 2953, 1811, 1782, 1724, 1672, 1206, 1083 cm^{-1} ; ^1H NMR (CDCl_3 , 500 MHz) δ 0.00 (s, 9H, $\text{Si}(\text{CH}_3)_3$), 0.95-0.99 (m, 2H, CH_2Si), 1.34 (s, 3H, CH_3), 1.55 (s, 3H, CH_3), 2.13-2.18 (m, 2H, $\text{CH}_2\text{-5}'$), 2.55 (app t, 2H, $J = 7.3$ Hz, CH_2), 2.64-2.70 (m, 2H, CH_2), 2.74 (t, 2H, $J = 7.5$ Hz, CH_2), 3.66-3.70 (m, 2H, CH_2O), 3.74 (s, 3H, OCH_3), 3.84 (s, 3H, OCH_3), 4.08 (ddd, 1H, $J = 8.3, 5.0, 5.0$ Hz, H-4'), 4.71 (dd, 1H, $J = 6.5, 5.0$ Hz, H-3'), 5.06 (dd, 1H, $J = 6.5, 1.8$ Hz, H-2'), 5.34 (d, 1H, $J = 9.5$ Hz, $\text{NCH}_a\text{H}_b\text{O}$), 5.39 (d, 1H, $J = 9.5$ Hz, $\text{NCH}_a\text{H}_b\text{O}$), 5.50 (d, 1H, $J = 1.8$ Hz, H-1'), 5.77 (d, 1H, $J = 8.0$ Hz, H-5), 5.94 (br s, 1H, $\text{C}=\text{CH}$), 7.16 (d, 1H, $J = 8.0$ Hz, H-6); ^{13}C NMR (CDCl_3 , 125 MHz) δ -1.5, 18.1, 25.3, 26.4, 27.1, 27.9, 28.9, 31.2, 52.0, 52.6, 67.6, 69.9, 83.5, 84.5, 86.1, 95.6, 102.1, 114.6, 122.1, 141.4, 145.7, 150.6, 162.6, 165.1, 167.4, 168.0, 168.4; HRMS (ES⁺) calcd for $\text{C}_{29}\text{H}_{42}\text{N}_2\text{O}_{14}\text{SiNa}$ 693.2298, found 693.2296 $[\text{MNa}]^+$.

1-((3aR,4R,6R,6aR)-2,2-Dimethyl-6-vinyltetrahydrofuro[3,4-d][1,3]dioxol-4-yl)-pyrimidine-2,4(1H,3H)-dione (144)²²⁴



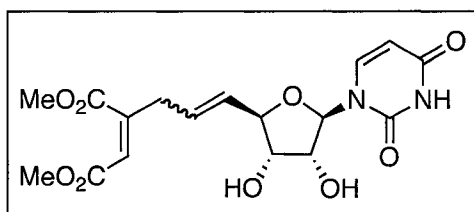
This known compound was prepared using an adaptation of the procedure of Trafelet *et al.*²²⁵ NaHMDS (1.00 M in THF, 51.0 mL, 51.0 mmol) was added dropwise to a suspension of methyltriphenylphosphonium bromide (16.1 g, 44.9 mmol) in THF (112.0 mL). The resulting yellow suspension was stirred at rt for 30 min, then at reflux for 1.5 h. It was then cooled to -78 °C, and aldehyde **72** (3.42 g, 12.1 mmol) in THF (10.0 mL) was added dropwise. The mixture was stirred overnight, while warming to rt, then diluted with EtOAc (100 mL) and poured into a saturated NH₄Cl solution (100 mL). After filtration to remove the insoluble salts, the layers were separated, and the aqueous layer was extracted with EtOAc (3 x 100 mL). The combined organic layers were dried (MgSO₄) and concentrated *in vacuo*. Purification by flash chromatography (2 columns, SiO₂, petroleum ether/EtOAc, 2:1 to 1:1) gave **144** as a pale yellow foam (2.11 g, 64%): *R_f* 0.20 (petroleum ether/EtOAc, 1:1); [α]_D²⁰ = +22.5 ° (*c* 0.19, CHCl₃); IR (CHCl₃, cast) ν 3198, 2990, 2937, 1694, 1646, 1085 cm⁻¹; ¹H NMR (CDCl₃, 500 MHz) δ 1.36 (s, 3H, CH₃), 1.59 (s, 3H, CH₃), 4.54 (m, 1H, H-4'), 4.75 (dd, 1H, *J* = 6.5, 4.0 Hz, H-3'), 5.01 (dd, 1H, *J* = 6.5, 2.0 Hz, H-2'), 5.28 (ddd, 1H, *J* = 10.5, 1.3, 1.3 Hz, CH=CH_{cis}H_{trans}), 5.38 (ddd, 1H, *J* = 17.0, 1.3, 1.3 Hz, CH=CH_{cis}CH_{trans}), 5.67 (d, 1H, *J* = 2.0 Hz, H-1'), 5.73 (dd, 1H, *J* = 8.0, 2.3 Hz, H-5), 5.98 (ddd, 1H, *J* = 17.0, 10.5, 7.0 Hz, CH=CH₂), 7.24 (d, 1H, *J* = 8.0 Hz, H-6), 8.50 (br s, 1H, NH); ¹³C NMR (CDCl₃, 125 MHz) δ 25.3, 27.1, 84.2, 84.7, 88.7, 94.4, 102.6, 114.6, 118.5, 134.9, 142.3, 150.0, 163.5; HRMS (ES⁺) calcd for C₁₃H₁₆N₂O₅Na 303.0951, found 303.0954 [MNa]⁺.

Dimethyl 2-(3-((3a*R*,4*R*,6*R*,6a*R*)-6-(2,4-dioxo-3,4-dihydropyrimidin-1(2*H*)-yl)-2,2-dimethyltetrahydrofuro[3,4-*d*][1,3]dioxol-4-yl)allyl)maleate (147)



Hoveyda-Grubbs' 2nd generation catalyst (50.9 mg, 0.0810 mmol) was added to a solution of olefins **144** (218 mg, 0.778 mmol) and **120** (299 mg, 1.62 mmol) in CH₂Cl₂ (5.0 mL) and the mixture was stirred at reflux for 6 h. Extra **120** (100 mg, 0.543 mol) dissolved in CH₂Cl₂ (1.0 mL) and catalyst (27.4 mg, 0.0437 mmol) were then added, and stirring was continued at reflux for another 19 h. Upon cooling the mixture to rt, DMSO (500 μL, 7.04 mmol, 57 equiv. relative to catalyst) was added and stirring was continued at rt for 24 h. The CH₂Cl₂ was removed *in vacuo*, and the crude product was purified by flash chromatography (SiO₂, hexanes/EtOAc, 3:2) to yield **147** as a brown foam, isolated as an inseparable mixture of *E* and *Z* isomers (225 mg, 66%): *R_f* 0.06 (EtOAc/hexanes, 1:1); IR (CHCl₃, cast) ν 2990, 2953, 1716, 1693, 1270, 1084 cm⁻¹; ¹H NMR (CDCl₃, 600 MHz) δ 1.36 (s, 3H, CH₃), 1.58 (s, 3H, CH₃), 3.10-3.12 (m, 2H, allylic CH₂), 3.75 (s, 3H, OCH₃), 3.82 (s, 3H, OCH₃), 4.55 (app t, 1H, *J* = 4.4 Hz, H-4'), 4.75 (dd, 1H, *J* = 6.0, 4.4 Hz, H-3'), 5.05 (dd, 1H, *J* = 6.0, 1.5 Hz, H-2'), 5.60 (d, 1H, *J* = 1.5 Hz, H-1'), 5.74 (dd, 1H, *J* = 8.0, 2.1 Hz, H-5), 5.76-5.78 (m, 2H, CH=CH), 5.89 (t, 1H, *J* = 1.5 Hz, C=CH), 7.22 (d, 1H, *J* = 8.0 Hz, H-6), 8.12 (br s, 1H, NH); ¹³C NMR (CDCl₃, 125 MHz) δ 25.3, 27.1, 36.3, 52.0, 52.4, 84.3, 84.7, 88.2, 94.9, 102.6, 114.5, 121.1, 128.2, 131.6, 142.6, 147.0, 149.9, 163.4, 165.4, 168.4; HRMS (ES⁺) calcd for C₂₀H₂₄N₂O₉Na 459.1374, found 459.1374 [MNa]⁺.

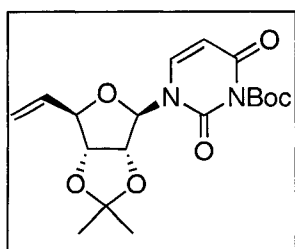
Dimethyl 2-(3-((2*R*, 3*S*, 4*R*, 5*R*)-5-(2,4-dioxo-3,4-dihydropyrimidin-1(2*H*)-yl)-3,4-dihydroxytetrahydrofuran-2-yl)allyl)maleate (150)



Maleate derivative **147** (45.4 mg, 0.104 mmol) was stirred in TFA/H₂O (7:3, 3.8 mL) at 0 °C for 1.5 h, then the solvent was removed *in vacuo*. Purification by flash chromatography (SiO₂,

EtOAc/pentane, 9:1) afforded **150** as a colourless gum, isolated as an inseparable mixture of *E* and *Z* isomers (32.9 mg, 80%): *R_f* 0.22 (CHCl₃/MeOH, 9:1); IR (μscope) ν 3600-3100, 3026, 2954, 1715, 1270, 1108 cm⁻¹; ¹H NMR (CD₃OD, 500 MHz) δ 3.14-3.16 (m, 2H, allylic CH₂), 3.70 (s, 3H, OCH₃), 3.77 (s, 3H, OCH₃), 3.93 (app t, 1H, *J* = 5.4 Hz, H-4'), 4.17 (dd, 1H, *J* = 5.4, 4.0 Hz, H-3'), 4.34-4.36 (m, 1H, H-2'), 5.72 (d, 1H, *J* = 8.0 Hz, H-5), 5.80-5.83 (m, 3H, CH=CH, H-1'), 5.98 (t, 1H, *J* = 1.5 Hz, C=CH), 7.59 (d, 1H, *J* = 8.0 Hz, H-6); ¹³C NMR (CD₃OD, 125 MHz) δ 37.5, 52.4, 52.9, 75.11, 75.14, 84.8, 92.0, 102.9, 122.0, 129.4, 132.9, 142.5, 149.2, 152.2, 166.1, 167.0, 170.2; HRMS (ES⁺) calcd for C₁₇H₂₀N₂O₉Na 419.1061, found 419.1062 [MNa]⁺.

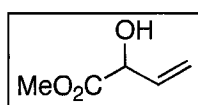
***tert*-Butyl 3-((3*aR*, 4*R*, 6*R*, 6*aR*)-2,2-dimethyl-6-vinyltetrahydrofuro[3,4-*d*][1,3]dioxol-4-yl)-2,6-dioxo-2,3-dihydropyrimidine-1(6*H*)-carboxylate (164)**



Di-*tert*-butyl dicarbonate (5.24 g, 24.0 mmol), and DMAP (42.3 mg, 0.350 mmol) were added to a solution of nucleoside **144** (1.26 g, 4.50 mmol) in pyridine (26.0 mL) and the orange mixture was stirred at rt for 2 h. The solvent was removed *in vacuo*, and the crude product was purified by flash chromatography (SiO₂ petroleum

ether/EtOAc, 4:1 to 2:1) to yield olefin **164** as a pale yellow foam (1.64 g, 96%): R_f 0.38 (petroleum ether/EtOAc, 2:1); $[\alpha]_D^{20} = +34.18$ (c 0.35, CHCl_3); IR (CHCl_3 , cast) ν 3200, 2989, 1692, 1631, 1084 cm^{-1} ; ^1H NMR (CDCl_3 , 600 MHz) δ 1.36 (s, 3H, CH_3), 1.58 (s, 3H, CH_3), 1.61 (s, 9H, $\text{C}(\text{CH}_3)_3$), 4.60 (dd, 1H, $J = 7.2, 4.2$ Hz, H-4'), 4.73 (dd, 1H, $J = 6.0, 4.2$ Hz, H-3'), 5.02 (dd, 1H, $J = 6.0, 1.8$ Hz, H-2'), 5.29 (dt, 1H, $J = 10.2, 1.2$ Hz, $\text{CH}=\underline{\text{C}}_{\text{cis}}\text{H}_{\text{trans}}$), 5.38 (dt, 1H, $J = 17.4, 1.2$ Hz, $\text{CH}=\underline{\text{C}}_{\text{cis}}\text{H}_{\text{trans}}$), 5.65 (d, 1H, $J = 1.8$ Hz, H-1'), 5.75 (d, 1H, $J = 8.1$ Hz, H-5), 5.96 (ddd, 1H, $J = 17.4, 10.2, 7.2$ Hz, $\underline{\text{C}}\text{H}=\text{CH}_2$), 7.23 (d, 1H, $J = 8.1$ Hz, H-6); ^{13}C NMR (CDCl_3 , 125 MHz) δ 25.3, 27.1, 27.5, 83.9, 84.8, 87.0, 88.7, 94.5, 102.1, 114.6, 118.9, 134.7, 141.0, 147.4, 148.2, 160.3; HRMS (ES+) calcd for $\text{C}_{18}\text{H}_{24}\text{N}_2\text{O}_7\text{Na}$ 403.1476, found 403.1475 $[\text{MNa}]^+$.

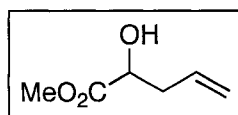
Methyl 2-hydroxy-but-3-enoate (168)



This known compound was prepared by the procedure of Stach *et al.*¹⁴¹ Acetic anhydride (14.5 mL, 153.4 mmol) was added dropwise to a solution of acrolein (10.0 mL, 149.7 mmol) in toluene (39.0 mL) at -10°C , followed by dropwise addition of sodium cyanide (11.0 g, 223.9 mmol) in H_2O (55.0 mL). The yellow biphasic mixture was stirred at -10° for 2.5 h, then the layers were separated. The aqueous layer was extracted with toluene (3 x 25 mL), and the combined organic layers were washed successively with 1 M acetic acid (50 mL), a saturated solution of NaHCO_3 (50 mL), and finally H_2O (50 mL). After drying the organic layer (MgSO_4), the solvent was removed *in vacuo* to give the crude acrolein cyanohydrin acetate intermediate. This was dissolved in MeOH (27.0 mL) and heated to reflux. A saturated HCl/MeOH solution (30.0 mL) and conc. HCl (7.0 mL) were added dropwise to the reaction mixture. After

stirring for 4.5 h at reflux, the suspension was cooled to 0 °C and filtered. The filtrate was concentrated *in vacuo* then Et₂O (70 mL) added. The organic layer was washed with a saturated solution of NaHCO₃ (25 mL) then H₂O (25 mL), and dried (Na₂SO₄). After solvent removal *in vacuo*, the crude oil was purified by distillation under high vacuum (50 °C) to afford title compound **168** as a clear colourless liquid (2.96 g, 17%): R_f 0.59 (EtOAc/pentane, 1:1); IR (neat) ν 3466, 3007, 2957, 1742, 1644, 1215, 1084 cm⁻¹; ¹H NMR (CDCl₃, 500 MHz) δ 2.92 (br s, 1H, OH), 3.82 (s, 3H, OCH₃), 4.68 (br s, 1H, CHOH), 5.29 (ddd, 1H, *J* = 10.5, 2.0, 1.5 Hz, CH=CH_{cis}CH_{trans}), 5.51 (ddd, 1H, *J* = 16.1, 2.0, 1.0 Hz, CH=CH_{cis}CH_{trans}), 5.94 (ddd, 1H, *J* = 16.1, 10.5, 5.3 Hz, CH=CH₂); ¹³C NMR (CDCl₃, 125 MHz) δ 52.8, 71.5, 117.2, 134.2, 173.6; HRMS (EI) calcd for C₅H₈O₃ 116.0474, found 116.0472 [M]⁺ 2.2%.

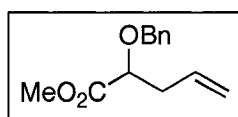
Methyl 2-hydroxy-pent-4-enoate (**170**)²²⁶



This known alcohol was prepared by the procedure of Macritchie *et al.*¹⁴² Freshly prepared²²⁷ methyl glyoxylate (5.10 g, 57.9 mmol) and allyl bromide (7.50 mL, 86.7 mmol) were added to a suspension of indium powder (7.31 g, 63.6 mmol) in H₂O/toluene (9:1, 580 mL). The mixture was stirred at rt for 24 h, then EtOAc (200 mL) was added and the mixture was stirred for an additional 30 min. The aqueous layer was extracted with EtOAc (3 x 200 mL), and the combined organic extracts were dried (Na₂SO₄). The solvent was removed *in vacuo* and the crude product was purified by column chromatography (SiO₂, pentane/EtOAc, 4:1) to give alcohol **170** as a pale yellow liquid (4.51 g, 60%): R_f 0.27 (pentane/EtOAc, 4:1); IR (neat) ν 3600-3100, 3080, 2982, 2955, 2920, 1742, 1642, 1218, 1086 cm⁻¹; ¹H NMR (CDCl₃, 400

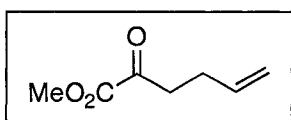
MHz) 2.41-2.48 (m, 1 H, CH_aH_b), 2.55-2.62 (m, 1H, CH_aH_b), 2.74 (d, 1H, $J = 5.3$ Hz, OH), 3.80 (s, 3H CH_3), 4.29 (ddd, 1 H, $J = 10.4, 10.4, 5.3$ Hz, CH), 5.13-5.19 (m, 2H, $\text{CH}=\text{CH}_2$), 5.81 (dddd, 1H, $J = 17.2, 14.4, 10.4, 7.2$ Hz, $\text{CH}=\text{CH}_2$); ^{13}C NMR (CDCl_3 , 125 MHz) δ 38.7, 52.5, 70.0, 118.8, 132.4, 174.8; HRMS (ES+) calcd for $\text{C}_6\text{H}_{10}\text{O}_3\text{Na}$ 153.0522, found 153.0521 $[\text{MNa}]^+$.

Methyl 2-benzyloxypent-4-enoate (171)



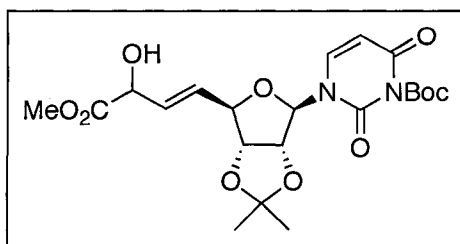
This compound was prepared by an adaptation of the procedure of Czernecki *et al.*¹⁴³ NaH (60% suspension in mineral oil, 1.11 g, 27.8 mmol), *n*-Bu₄NI (994 mg, 2.69 mmol), and benzyl bromide (3.50 mL, 29.5 mmol) were added to a solution of alcohol **170** (3.51 g, 27.0 mmol) in THF (45.0 mL) at 0 °C. The mixture was warmed to rt and stirred for 5 h. A saturated NH₄Cl solution (30 mL) was added, then the aqueous layer was extracted with Et₂O (3 x 30 mL). The combined organic layers were dried (MgSO₄), and concentrated *in vacuo*. Purification by flash chromatography (SiO₂, petroleum ether/Et₂O, 95:5), followed by concentration *in vacuo* at 0 °C afforded **171** as a colourless liquid (4.39 g, 74%): R_f 0.27 (petroleum ether/Et₂O, 95:5); IR (neat) ν 3066, 3032, 2952, 1752, 1642, 1497, 1455, 1203, 1028 cm^{-1} ; ^1H NMR (CDCl_3 , 400 MHz) δ 2.53-2.56 (m, 2H, allylic CH_2), 3.75 (s, 3H, OCH_3), 4.03 (t, 1H, $J = 6.2$, CH_α), 4.46 (d, 1H, $J = 11.8$, benzylic CH_aH_b), 4.72 (d, 1H, $J = 11.8$, benzylic CH_aH_b), 5.08-5.15 (m, 2H, $\text{CH}=\text{CH}_2$), 5.83 (dddd, 1H, $J = 17.2, 14.0, 10.2, 6.9$, $\text{CH}=\text{CH}_2$), 7.28-7.37 (m, 5H, ArH); ^{13}C NMR (CDCl_3 , 125 MHz), δ 37.3, 51.8, 72.3, 77.8, 117.9, 127.8, 127.9, 128.4, 133.0, 137.4, 172.6; HRMS (ES+) calcd for $\text{C}_{13}\text{H}_{16}\text{O}_3\text{Na}$ 243.0992, found 243.0992 $[\text{MNa}]^+$.

Methyl 2-oxohex-5-enoate (**174**)²²⁸



This known compound was synthesized using the procedure of Macritchie *et al.*¹⁴² 3-Butenylmagnesium bromide (0.500 M in THF, 20.5 mL, 10.3 mmol) was added dropwise to a solution of dimethyl oxalate (1.01 g, 8.55 mmol) in Et₂O/THF (2:1, 18.0 mL) at -78 °C. The solution was stirred at -78 °C for 4 h, then a saturated solution of NH₄Cl (12 mL) was added. After warming the mixture to rt, the aqueous layer was extracted with EtOAc (3 x 12 mL) and the combined organic layers were dried (Na₂SO₄). Concentration *in vacuo* was followed by vacuum distillation (< 1mm Hg, 75 °C) to give **174** as a pale yellow liquid (468 mg, 40%): R_f 0.34 (petroleum ether/Et₂O, 3:2); IR (μscope) ν 3080, 2957, 1740, 1774, 1677, 1251, 1116 cm⁻¹; ¹H NMR (CDCl₃, 500 MHz) δ 2.39 (app qt, 2H, *J* = 7.0, 1.5 Hz, allylic CH₂), 2.95 (t, 2H, *J* = 7.0 Hz, CH_{2α}), 3.87 (s, 3H, OCH₃), 5.02 (app dq, 1H, *J* = 10.4, 1.5 Hz, CH=CH_{cis}H_{trans}), 5.07 (app dq, 1H, *J* = 17.1, 1.5 Hz, CH=CH_{cis}H_{trans}), 5.81 (ddd, 1H, *J* = 17.1, 10.4, 7.0 Hz, CH=CH₂); ¹³C NMR (CDCl₃, 125 MHz), δ 26.9, 38.5, 52.9, 115.9, 136.0, 161.4, 193.4.

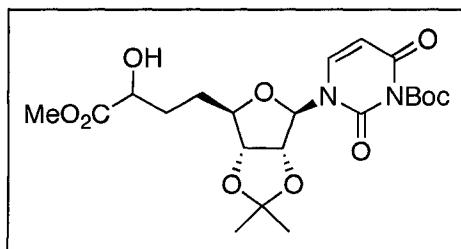
tert-Butyl 3-((3*aR*,4*R*,6*R*,6*aR*)-6-((*E*)-3-hydroxy-4-methoxy-4-oxobut-1-enyl)-2,2-dimethyltetrahydrofuro[3,4-*d*][1,3]dioxol-4-yl)-2,6-dioxo-2,3-dihydropyrimidine-1(6*H*)-carboxylate (**176**)



Grubbs' 2nd generation catalyst (183 mg, 0.220 mmol) was added to a solution of olefins **164** (569 mg, 1.50 mmol) and **168** (529 mg, 4.56 mmol) in CH₂Cl₂ (7.50 mL). The dark mixture was stirred at

reflux for 24 h, then extra catalyst (81.1 mg, 0.0960 mmol) was added and the reaction was allowed to continue at reflux for another 6 h. After cooling to rt, DMSO (2.80 mL, 127 equiv. relative to catalyst) was added and stirring was continued at rt for 12 h. The CH₂Cl₂ was removed *in vacuo*, and the crude product was purified by flash chromatography (SiO₂, pentane/EtOAc, 3:1 to 1:1) to give **176** as a clear orange gum, isolated as a mixture of diastereomers (596 mg, 85%): *R_f* 0.18 (pentane/EtOAc, 1:1); IR (CHCl₃, cast) ν 3463, 2987, 2956, 1785, 1744, 1722, 1680, 1633, 1148, 1086 cm⁻¹; ¹H NMR (CDCl₃, 500 MHz) δ 1.35 (s, 3H, CH₃), 1.57 (s, 3H, CH₃), 1.61 (s, 9H, C(CH₃)₃), 2.94 (br s, 1H, OH), 3.82 (s, 3H, OCH₃), 4.59-4.61 (m, 1H, H-4'), 4.70-4.76 (m, 2H, H-3', CHOH), 5.03 (dd, 1H *J* = 6.0, 1.8 Hz, H-2'), 5.64 (d, 1H, *J* = 1.8 Hz, H-1'), 5.75 (d, 1H, *J* = 8.0 Hz, H-5), 5.90-5.95 (m, 1H, CH=CHCHOH), 6.05-6.11 (m, 1H, CH=CHCHOH), 7.21 (d, 1H, *J* = 8.0 Hz, H-6); ¹³C NMR (CDCl₃, 125 MHz) δ 25.2, 25.3, 27.02, 27.05, 27.4, 52.85, 52.90, 70.4, 70.5, 83.88, 83.91, 84.66, 84.58, 87.1, 87.27, 87.33, 94.2, 94.4, 102.0, 114.56, 114.58, 128.5, 128.6, 130.5, 130.6, 141.4, 147.42, 147.45, 148.2, 160.36, 160.38, 172.97, 173.02 (5 carbon signals not observed due to overlap); HRMS (ES⁺) calcd for C₂₁H₂₈N₂O₁₀Na 491.1636, found 491.1635 [MNa]⁺.

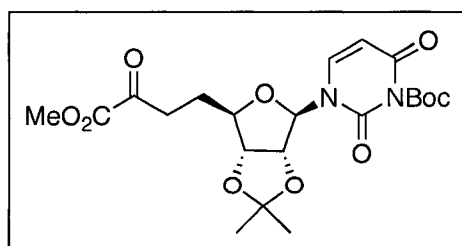
***tert*-Butyl 3-((3*aR*,4*R*,6*R*,6*aR*)-6-(3-hydroxy-4-methoxy-4-oxobutyl)-2,2-dimethyl-tetrahydrofuro[3,4-*d*][1,3]dioxol-4-yl)-2,6-dioxo-2,3-dihydropyrimidine-1(6*H*)-carboxylate (177)**



5% Pd/C (359 mg) was added to a solution of **176** (357 mg, 0.760 mmol) in EtOAc (6.0 mL) and the mixture was stirred under 1 atm H₂ for 24 h. The

mixture was filtered through Celite and washed with hot EtOAc. Concentration *in vacuo* followed by flash chromatography (SiO₂, pentane/EtOAc, 1:1) gave alcohol **177** as a pale yellow gum, isolated as a mixture of diastereomers (291 mg, 81%): R_f 0.10 (pentane/EtOAc, 1:1); IR (CHCl₃, cast) ν 3477, 3097, 2986, 2955, 1785, 1723, 1681, 1633, 1255, 1094 cm⁻¹; ¹H NMR (CDCl₃, 600 MHz) δ 1.34 (s, 3H, CH₃), 1.56 (s, 3H, CH₃), 1.61 (s, 9H, C(CH₃)₃), 1.94-2.05 (m, 2H, CH₂-5'), 2.76-2.98 (m, 2H, CH₂), 3.80 (s, 3H, OCH₃), 4.05-4.07 (m, 1H, H-4') 4.24 (br s, 1H, CHOH), 4.58 (dd, 1H, *J* = 6.6, 4.8 Hz, H-3'), 4.94 (dd, 1H, *J* = 4.8, 2.3 Hz, H-2'), 5.64 (d, 1H, *J* = 2.3 Hz, H-1'), 5.76 (d, 1H, *J* = 8.1 Hz, H-5), 7.22 (d, 1H, *J* = 8.1 Hz, H-6); ¹³C NMR (CDCl₃, 125 MHz) δ 25.3, 27.1, 27.4, 28.5, 28.7, 29.7, 29.9, 52.4, 52.5, 69.8, 69.9, 83.4, 83.5, 84.3, 86.3, 86.5, 86.9, 93.3, 93.4, 102.0, 102.1, 114.7, 114.8, 141.1, 147.5, 148.0, 148.1, 160.4, 175.1 (9 carbon signals not observed due to overlap); HRMS (ES⁺) calcd for C₂₁H₃₀N₂O₁₀Na 493.1793, found 493.1793 [MNa]⁺.

***tert*-Butyl 3-((3*aR*,4*R*,6*R*,6*aR*)-6-(4-methoxy-3,4-dioxobutyl)-2,2-dimethyltetrahydrofuro[3,4-*d*][1,3]dioxol-4-yl)-2,6-dioxo-2,3-dihydropyrimidine-1(6*H*)-carboxylate (178)**

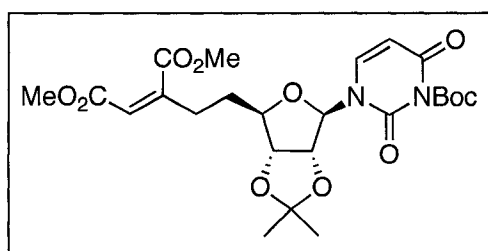


IBX (397 mg, 1.42 mmol) was added to a solution of alcohol **177** (267 mg, 0.570 mmol) in MeCN (4.1 mL), and the white suspension was stirred at reflux for 2 h, then cooled to 0 °C and filtered

through a sintered glass funnel. After concentration *in vacuo*, the product was purified by flash chromatography (SiO₂, petroleum ether/EtOAc, 2:1) to afford α -keto ester **178** as a

white foam (142 mg, 53%): R_f 0.10 (petroleum ether/EtOAc, 2:1); $[\alpha]_D^{20} = +26.41$ (c 0.12, CHCl_3); IR (CHCl_3 , cast) ν 3096, 2986, 2939, 1785, 1725, 1682, 1633, 1149, 1086 cm^{-1} ; ^1H NMR (CDCl_3 , 600 MHz) δ 1.33 (s, 3H, CH_3), 1.53 (s, 3H, CH_3), 1.60 (s, 9H, $\text{C}(\text{CH}_3)_3$), 2.08 (app q, 2H, $J = 7.2$ Hz, $\text{CH}_2\text{-5}'$), 2.94 (dt, 1H, $J = 18.7, 7.2$ Hz, $\text{CH}_{\text{a}\alpha}\text{H}_{\text{b}\alpha}$), 3.01 (dt, 1H, $J = 18.7, 7.2$ Hz, $\text{CH}_{\text{a}\alpha}\text{H}_{\text{b}\alpha}$), 3.85 (s, 3H, OCH_3), 4.03 (dd, 1H, $J = 7.2, 5.3$ Hz, H-4'), 4.61 (dd, 1H, $J = 6.6, 5.3$ Hz, H-3'), 4.97 (dd, 1H, $J = 6.6, 2.1$ Hz, H-2'), 5.56 (d, 1H, $J = 2.1$ Hz, H-1'), 5.75 (d, 1H, $J = 7.8$ Hz, H-5), 7.17 (d, 1H, $J = 7.8$ Hz, H-6); ^{13}C NMR (CDCl_3 , 125 MHz) δ 25.4, 26.5, 27.2, 27.4, 35.6, 53.0, 83.4, 84.3, 85.8, 87.1, 94.1, 102.3, 115.0, 141.3, 147.4, 148.0, 160.2, 161.1, 193.0; HRMS (ES+) calcd for $\text{C}_{21}\text{H}_{28}\text{N}_2\text{O}_{10}\text{Na}$ 491.1636, found 491.1636 [MNa^+].

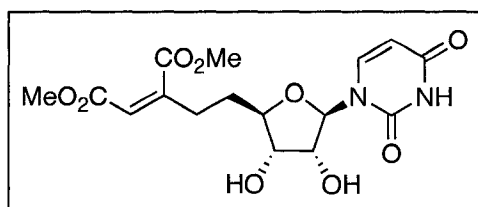
Dimethyl 2-(2-((3*aR*,4*R*,6*R*,6*aR*)-6-(3-(*tert*-butoxycarbonyl)-2,4-dioxo-3,4-dihydropyrimidin-1(2*H*)-yl)-2,2-dimethyltetrahydrofuro[3,4-*d*][1,3]dioxol-4-yl)ethyl)maleate (179)



This compound was prepared by a modification of the procedure of Massoudi *et al.*¹⁴⁴ Methyl diethylphosphonoacetate (29.0 μL , 0.160 mmol) in DMF (300 μL) was added dropwise to a suspension of NaH (60% in mineral oil, 14.0 mg, 0.350 mmol) in DMF (300 μL) at 0 $^\circ\text{C}$, and the mixture was stirred for 30 min at 0 $^\circ\text{C}$. It was then cooled to -40 $^\circ\text{C}$ and α -keto ester **178** (94.9 mg, 0.203 mmol) in DMF (600 μL) was added dropwise. The orange mixture was stirred at -40 $^\circ\text{C}$ for 5 h, then H_2O (1 mL) was added. After warming to rt, the aqueous layer was extracted with EtOAc (3 x 1 mL). The combined organic layers

were dried (MgSO₄) and concentrated *in vacuo*. Purification was done by flash chromatography (SiO₂, petroleum ether/EtOAc, 2:1) to give maleate **179** as a colourless glass (41.5 mg, 49%): R_f 0.13 (petroleum ether/EtOAc, 3:2); [α]_D²⁰ = +18.00 (*c* 0.09, CHCl₃); IR (CHCl₃, cast) ν 2925, 2854, 1786, 1724, 1682, 1254, 1075 cm⁻¹; ¹H NMR (CDCl₃, 500 MHz) δ 1.34 (s, 3H, CH₃), 1.55 (s, 3H, CH₃), 1.61 (s, 9H, C(CH₃)₃), 1.91 (app q, 2H, *J* = 7.7 Hz, CH₂-5'), 2.41-2.55 (m, 2H, allylic CH₂), 3.73 (s, 3H, OCH₃), 3.83 (s, 3H, OCH₃), 3.98-4.04 (m, 1H, H-4'), 4.61 (dd, 1H, *J* = 6.5, 5.0 Hz, H-3'), 4.98 (dd, 1H, *J* = 6.5, 2.5 Hz, H-2'), 5.55 (d, 1H, *J* = 2.5 Hz, H-1'), 5.76 (d, 1H, *J* = 8.0 Hz, H-5), 5.88 (s, 1H, C=CH), 7.17 (d, 1H, *J* = 8.0 Hz, H-6); ¹³C NMR (CDCl₃, 125 MHz) δ 25.4, 27.2, 27.5, 30.4, 30.6, 51.9, 52.4, 83.5, 84.3, 85.9, 87.1, 94.4, 102.3, 114.9, 120.5, 141.3, 147.4, 148.0, 148.6, 160.2, 165.3, 168.8; HRMS (ES⁺) calcd for C₂₄H₃₂N₂O₁₁Na 547.1898, found 547.1897 [MNa]⁺.

Dimethyl 2-(2-((2*R*,3*S*,4*R*,5*R*)-5-(2,4-dioxo-3,4-dihydropyrimidin-1(2*H*)-yl)-3,4-dihydroxytetrahydrofuran-2-yl)ethyl)maleate (180)

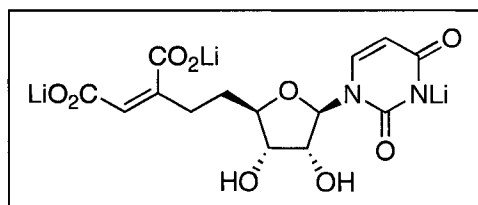


Maleate **179** (14.3 mg, 0.0270 mmol) was dissolved in TFA/H₂O (7:3, 1.0 mL) at 0 °C, and the mixture was stirred for 4.5 h while warming to rt. The solvent was removed *in vacuo*. The

crude product was first purified by flash chromatography (SiO₂, EtOAc/MeOH, 96:4) then by reverse phase HPLC using solvent system A (*t_R* 15.1 min). The combined fractions containing the desired product were lyophilized to give **180** as a white powder (7.80 mg, 75%): R_f 0.11 (EtOAc/MeOH, 96:4); [α]_D²⁰ = +24.20 (*c* 0.10, CHCl₃); IR

(CHCl₃, cast) ν 3650-3100, 2955, 2925, 2854, 1713, 1204, 1128 cm⁻¹; ¹H NMR (CD₃OD, 500 MHz) δ 1.80-1.88 (m, 1H, CH_aH_b-5'), 1.90-1.97 (m, 1H, CH_aH_b-5'), 2.45-2.51 (m, 1H, allylic CH_cH_d), 2.54-2.60 (m, 1H, allylic CH_cH_d), 3.70 (s, 3H, OCH₃), 3.78 (s, 3H, OCH₃), 3.85-3.91 (m, 2H, H-3', H-4'), 4.18 (dd, 1H, *J* = 5.3, 4.1 Hz, H-2'), 5.71 (d, 1H, *J* = 8.0 Hz, H-5), 5.75 (d, 1H, *J* = 4.1 Hz, H-1'), 5.99 (t, 1H, *J* = 1.5 Hz, C=CH), 7.56 (d, 1H, *J* = 8.0 Hz, H-6); ¹³C NMR (CDCl₃, 500 MHz) δ 31.5, 32.0, 52.3, 52.9, 74.7, 74.9, 83.7, 92.2, 103.0, 121.6, 142.9, 150.6, 152.2, 166.1, 167.0, 170.6; HRMS (ES⁺) calcd for C₁₆H₂₀N₂O₉Na 407.1061, found 407.1060 [MNa]⁺.

Lithium 1-((2*R*,3*R*,4*S*,5*R*)-5-((*Z*)-3,4-dicarboxylatobut-3-enyl)-3,4-dihydroxy-tetrahydrofuran-2-yl)-2,4-dioxo-2,4-dihydro-1*H*-pyrimidin-3-ide (181)

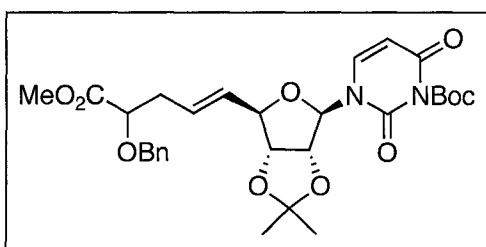


Dimethyl maleate derivative **180** (4.90 mg, 0.0130 mmol) was dissolved in CD₃OD/D₂O (4:3, 700 μ L) and placed in an NMR tube. A solution of LiOH·H₂O in D₂O (1.00 M, 52.0 μ L,

0.0520 mmol) was then added, and the mixture was heated at 40 °C. Reaction progress was monitored by ¹H NMR through disappearance of the methyl ester signals. After 24 h, the solvent was removed *in vacuo* and the residue was dissolved in H₂O. It was washed twice with CH₂Cl₂, then lyophilized to afford lithium salt **181** as an orange solid (4.90 mg, 100%): $[\alpha]_D^{20} = +3.82$ (*c* 0.11, H₂O); IR (μ scope) ν 3650-2700, 1684, 1135 cm⁻¹; ¹H NMR (D₂O, 500 MHz) δ 1.81-1.97 (m, 2H, CH₂-5'), 2.30-2.37 (m, 1H, allylic CH_aH_b), 2.41-2.47 (m, 1H, allylic CH_aH_b), 4.02-4.07 (m, 2H, H-3', H-4'), 4.28 (app t, 1H, *J* = 5.0 Hz, H-2'), 5.55 (s, 1H, C=CH), 5.82 (d, 1H, *J* = 7.7 Hz, H-5), 5.92 (d, 1H, *J* = 5.0

Hz, H-1'), 7.53 (d, 1H, $J = 7.7$ Hz, H-6); ^{13}C NMR (D_2O , 125 MHz) δ 31.4, 31.9, 73.8, 74.6, 83.7, 90.3, 103.8, 121.5, 141.1, 150.8, 160.5, 169.0, 175.2, 177.9; HRMS (ES-) calcd for $\text{C}_{14}\text{H}_{15}\text{N}_2\text{O}_9$ 355.0772, found 355.0775 $[\text{MH}]^-$.

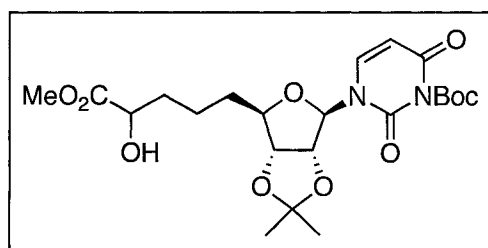
***tert*-Butyl 3-((3*aR*,4*R*,6*R*,6*aR*)-6-((*E*)-4-(benzyloxy)-5-methoxy-5-oxopent-1-enyl)-2,2-dimethyltetrahydrofuro[3,4-*d*][1,3]dioxol-4-yl)-2,6-dioxo-2,3-dihydropyrimidine-1(6*H*)-carboxylate (**182**)**



Grubbs' 2nd generation catalyst (160 mg, 0.188 mmol) was added to a solution of olefins **164** (702 mg, 1.85 mmol) and **171** (1.02 g, 4.63 mmol) in CH_2Cl_2 (9.0 mL), and the dark brown mixture was stirred at reflux for 24.5 h. After cooling to rt, DMSO (730 mL, 54 equiv. relative to catalyst) was added, and the mixture was stirred at rt for an extra 12 h. The CH_2Cl_2 was removed *in vacuo*, and the crude product was purified by flash chromatography (SiO_2 , petroleum ether/EtOAc, 3:1 to 2:1) to give **182** as an off-white foam, isolated as a 1:1 mixture of diastereomers (730 mg, 69%): R_f 0.14 (petroleum ether/EtOAc, 2:1); IR (CHCl_3 , cast) ν 3091, 2986, 2937, 1785, 1749, 1722, 1682, 1631, 1497, 1148, 1085 cm^{-1} ; ^1H NMR (CDCl_3 , 500 MHz) δ 1.35 (s, 3H, CH_3), 1.57 (s, 3H, CH_3), 1.60 (s, 9H, $\text{C}(\text{CH}_3)_3$), 2.52-2.55 (m, 2H, allylic CH_2), 3.74 (s, 3H, OCH_3), 4.00-4.02 (m, 1H, CHOBn), 4.43 (d, 1H, $J = 11.7$ Hz, benzylic CH_aH_b), 4.51-4.55 (m, 1H, H-4'), 4.62-4.66 (m, 1H, H-3'), 4.71 (d, 0.5H, $J = 11.7$ Hz, benzylic CH_aH_b), 4.72 (d, 0.5H, $J = 11.7$ Hz, benzylic CH_aH_b), 4.95 (app t, 0.5H, $J = 6.5$ Hz, H-2'), 4.96 (app t, 0.5H, $J = 6.5$ Hz, H-2'), 5.60-5.66 (m, 2H, $\text{CH}=\text{CH}$), 5.68 (d, 0.5H, $J = 8.1$ Hz, H-5), 5.70 (d, 0.5H,

$J = 8.1$ Hz, H-5), 5.79-5.87 (m, 1H, H-1'), 7.21 (d, 0.5H, $J = 8.1$ Hz, H-6), 7.22 (d, 0.5H, $J = 8.1$ Hz, H-6), 7.28-7.36 (m, 5H, ArH); ^{13}C NMR (CDCl_3 , 125 MHz) δ 25.4, 27.1, 27.5, 35.7, 35.8, 51.9, 72.4, 77.3, 83.9, 84.0, 84.87, 84.92, 87.0, 88.0, 88.1, 94.30, 94.33, 102.0, 102.1, 114.49, 114.52, 127.96, 127.99, 128.0, 128.4, 129.8, 130.0, 130.38, 130.44, 137.2, 137.3, 140.8, 140.9, 147.5, 148.2, 160.3, 172.3 (13 carbon signals not observed due to overlap); HRMS (ES+) calcd for $\text{C}_{29}\text{H}_{36}\text{N}_2\text{O}_{10}\text{Na}$ 595.2262, found 595.2263 [MNa] $^+$.

***tert*-Butyl 3-((3*aR*,4*R*,6*R*,6*aR*)-6-(4-hydroxy)-5-methoxy-5-oxopentyl)-2,2-dimethyl-tetrahydrofuro[3,4-*d*][1,3]dioxol-4-yl)-2,6-dioxo-2,3-dihydropyrimidine-1(6*H*)-carboxylate (**183**)**

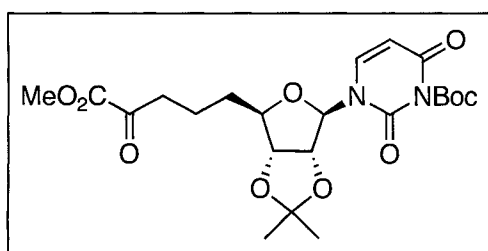


10% Pd/C (73.3 mg) was added to a solution of **182** (723 mg, 1.26 mmol) in EtOAc (13.0 mL), and the mixture was stirred under 1 atm H_2 for 7 h. The Pd/C was removed by filtration through

Celite and washed with hot EtOAc. The solvent was removed *in vacuo*, and the resulting viscous gum was purified by flash chromatography (SiO_2 , petroleum ether/EtOAc, 1:1) to yield alcohol **183** as a white foam, isolated as a 1:1 mixture of diastereomers (567 mg, 93%); R_f 0.14 (petroleum ether/EtOAc, 1:1); IR (CHCl_3 , cast) ν 3600-3300, 3094, 2985, 2939, 1785, 1722, 1681, 1632, 1149, 1084 cm^{-1} ; ^1H NMR (CDCl_3 , 500 MHz) δ 1.34 (s, 3H, CH_3), 1.48-1.89 (m, 6H, 3 x CH_2), 1.55 (s, 3H, CH_3), 1.60 (s, 9H, $\text{C}(\text{CH}_3)_3$), 3.79 (s, 3H, OCH_3), 4.01-4.06 (m, 1H, H-4'), 4.18-4.21 (m, 1H, CHOH), 4.55 (m, 1H, H-3'), 4.92 (dd, 1H, $J = 6.5, 2.3$ Hz, H-2'), 5.63 (br s, 1H, H-1'), 5.751 (d, 0.5H, $J = 8.1$ Hz, H-5), 5.755 (d, 0.5H, $J = 8.1$ Hz, H-5), 7.21 (d, 0.5H, $J = 8.1$ Hz, H-6), 7.22 (d, 0.5 H, $J = 8.1$

Hz, H-6); ^{13}C NMR (CDCl_3 , 125 MHz) δ 21.0, 21.1, 25.4, 27.2, 27.5, 32.8, 32.9, 33.90, 33.93, 52.6, 70.08, 70.12, 83.6, 84.4, 84.5, 86.66, 86.69, 87.0, 93.6, 93.7, 102.2, 114.78, 114.82, 140.70, 140.74, 147.5, 148.1, 160.3, 175.5 (11 carbon signals not observed due to overlap); HRMS (ES $^+$) calcd for $\text{C}_{22}\text{H}_{32}\text{N}_2\text{O}_{10}\text{Na}$ 507.1949, found 507.1949 [MNa] $^+$.

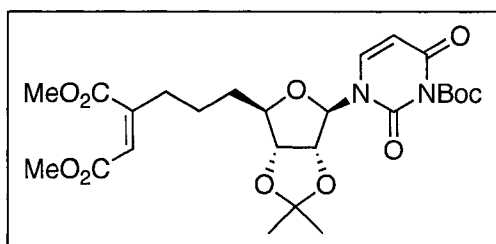
***tert*-Butyl 3-((3*aR*,4*R*,6*R*,6*aR*)-6-(5-methoxy-4,5-dioxopentyl)-2,2-dimethyl-tetrahydrofuro[3,4-*d*][1,3]dioxol-4-yl)-2,6-dioxo-2,3-dihydropyrimidine-1(6*H*)-carboxylate (**184**)**



IBX (1.02 g, 3.63 mmol) was added to a solution of alcohol **183** (560 mg, 1.16 mmol) in MeCN (8.0 mL) and the white suspension was stirred at reflux for 1.5 h. It was then cooled to 0 °C and filtered through a sintered glass funnel. The solvent was removed *in vacuo*, and the crude product was purified by flash chromatography (SiO_2 , petroleum ether/EtOAc, 2:1 to 1:1) to give α -keto ester **184** as a white foam (413 mg, 74%): R_f 0.19 (petroleum ether/EtOAc, 1:1); $[\alpha]_D^{20} = +10.44$ (c 0.09, CHCl_3); IR (CHCl_3 , cast) ν 3096, 2985, 2938, 1784, 1724, 1683, 1633, 1257, 1083 cm^{-1} ; ^1H NMR (CDCl_3 , 500 MHz) δ 1.34 (s, 3H, CH_3), 1.55 (s, 3H, CH_3), 1.61 (s, 9H, $\text{C}(\text{CH}_3)_3$), 1.73-1.81 (m, 4H, 2 x CH_2), 2.91 (t, 2H, $J = 6.8$ Hz, $\text{CH}_2\alpha$), 3.86 (s, 3H, OCH_3), 4.00-4.04 (m, 1H, H-4'), 4.56 (dd, 1H, $J = 6.6, 5.0$ Hz, H-3'), 4.93 (dd, 1H, $J = 6.6, 2.2$ Hz, H-2'), 5.62 (d, 1H, $J = 2.2$ Hz, H-1'), 5.77 (d, 1H, $J = 8.3$ Hz, H-5), 7.21 (d, 1H, $J = 8.3$ Hz, H-6); ^{13}C NMR (CDCl_3 , 125 MHz) δ 19.2, 25.4, 27.2, 27.5, 32.3, 38.7, 53.0, 83.5, 84.4, 86.5, 87.1, 93.7, 102.3, 114.9, 140.8, 147.4, 148.0,

160.3, 161.4, 193.5; HRMS (ES⁺) calcd for C₂₂H₃₀N₂O₁₀Na 505.1793, found 505.1793 [MNa]⁺.

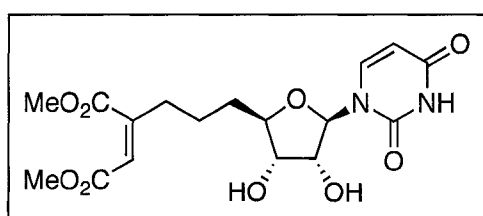
Dimethyl 2-(3-((3a*R*,4*R*,6*R*,6a*R*)-6-(3-(*tert*-butoxycarbonyl)-2,4-dioxo-3,4-dihydropyrimidin-1(2*H*)-yl)-2,2-dimethyltetrahydrofuro[3,4-*d*][1,3]dioxol-4-yl)propyl)-maleate (185)



This compound was prepared using the same procedure as for **179**. Methyl diethylphosphonoacetate (115 μ L, 0.634 mmol) in DMF (1.1 mL) was added dropwise to a suspension of NaH (60% in mineral oil, 41.0 mg, 1.03 mmol) in DMF (1.1 mL) at 0 °C, and the mixture was stirred at this temperature for 45 min. It was then cooled to -40 °C and α -keto ester **184** (380 mg, 0.787 mmol) in DMF (1.8 mL) was added dropwise. The mixture was stirred for 3.5 h with warming to -10 °C, then H₂O (2 mL) was added. After warming to rt, the aqueous layer was extracted with EtOAc (3 x 3 mL), and the combined organic layers were dried (MgSO₄). After concentration *in vacuo*, purification by flash chromatography (SiO₂, petroleum ether/EtOAc, 3:2) was done to give maleate **185** as a colourless gum (279 mg, 82%): R_f 0.20 (petroleum ether/EtOAc, 3:2); $[\alpha]_D^{20} = +7.75$ (c 0.08, CHCl₃); IR (CHCl₃, cast) ν 3092, 2985, 2951, 2927, 2853, 1784, 1723, 1682, 1633, 1257, 1085 cm⁻¹; ¹H NMR (CDCl₃, 500 MHz) δ 1.34 (s, 3H, CH₃), 1.55 (s, 3H, CH₃), 1.61 (s, 9H, C(CH₃)₃), 1.62-1.77 (m, 4H, 2 x CH₂), 2.41 (t, 2H, $J = 7.5$ Hz, allylic CH₂), 3.72 (s, 3H, OCH₃), 3.83 (s, 3H, OCH₃), 3.98-4.02 (m, 1H, H-4'), 4.55 (dd, 1H, $J = 6.6$, 5.0 Hz, H-3'), 4.92 (dd, 1H, $J = 6.6$, 2.2 Hz, H-2'), 5.62 (d, 1H, $J = 2.2$ Hz, H-1'), 5.76 (d,

1H, $J = 8.0$ Hz, H-5), 5.83 (s, 1H, C=CH), 7.21 (d, 1H, $J = 8.0$ Hz, H-6); ^{13}C NMR (CDCl_3 , 125 MHz) δ 23.1, 25.4, 27.2, 27.5, 32.3, 33.9, 51.9, 52.4, 83.5, 84.4, 86.4, 87.0, 93.6, 102.3, 114.9, 119.9, 140.8, 147.4, 148.1, 149.7, 160.3, 165.2, 169.0; HRMS (ES+) calcd for $\text{C}_{25}\text{H}_{34}\text{N}_2\text{O}_{11}\text{Na}$ 561.2055, found 561.2054 $[\text{MNa}]^+$.

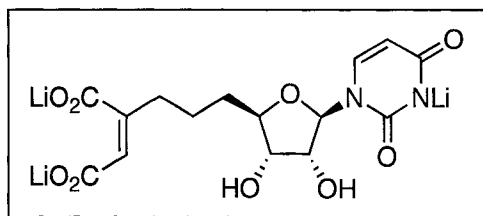
Dimethyl 2-(3-((2R,3S,4R,5R)-5-(2,4-dioxo-3,4-dihydropyrimidin-1(2H)-yl)-3,4-dihydroxytetrahydrofuran-2-yl)propyl)maleate (186)



Dimethyl maleate derivative **185** (126 mg, 0.234 mmol) was dissolved in TFA/ H_2O (7:3, 20.0 mL) and the mixture was stirred at rt for 3 h. Concentration *in vacuo* was followed by

purification, first by flash chromatography (SiO_2 , EtOAc/MeOH, 95:5) then by reverse phase HPLC using solvent system B (t_R 17.7 min). The combined fractions containing the desired product were lyophilized to yield **186** as a white powder (6.90 mg, 74%): R_f 0.16 (EtOAc/MeOH, 95:5); $[\alpha]_D^{20} = +37.79$ (c 0.10, CHCl_3); IR (CHCl_3 , cast) ν 3600-3150, 2956, 2924, 2853, 1712, 1202, 1103 cm^{-1} ; ^1H NMR (CD_3OD , 500 MHz) δ 1.58-1.80 (m, 4H, 2 x CH_2), 2.41-2.46 (m, 2H, allylic CH_2), 3.69 (s, 3H, OCH_3), 3.77 (s, 3H, OCH_3), 3.84-3.87 (m, 2H, H-3', H-4'), 4.13-4.15 (m, 1H, H-2'), 5.71 (d, 1H, $J = 8.0$ Hz, H-5), 5.77 (d, 1H, $J = 4.0$ Hz, H-1'), 5.93 (s, 1H, C=CH), 7.56 (d, 1H, $J = 8.0$ Hz, H-6); ^{13}C NMR (CDCl_3 , 125 MHz) δ 24.6, 33.4, 34.9, 52.3, 52.8, 74.8, 75.1, 84.5, 91.9, 102.9, 121.0, 142.6, 151.6, 152.2, 166.1, 166.9, 170.8; HRMS (ES+) calcd for $\text{C}_{17}\text{H}_{22}\text{N}_2\text{O}_9\text{Na}$ 421.1218, found 421.1222 $[\text{MNa}]^+$.

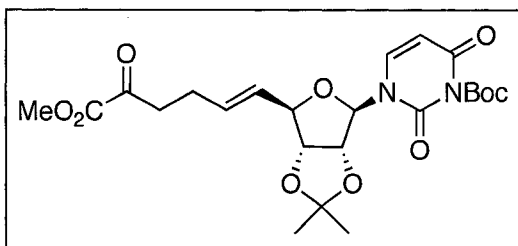
Lithium 1-((2*R*, 3*R*,4*S*,5*R*)-5-((*Z*)-4,5-dicarboxylatopent-4-enyl)-3,4-dihydroxy-tetrahydrofuran-2-yl)-2,4-dioxo-2,4-dihydro-1*H*-pyrimidin-3-ide (187)



Dimethyl maleate derivative **186** (4.20 mg, 0.0105 mmol) was dissolved in CD₃OD/D₂O (4:3, 700 μ L) in an NMR tube and a solution of LiOH·H₂O in D₂O (1.00 M, 42.3 μ L, 0.0476

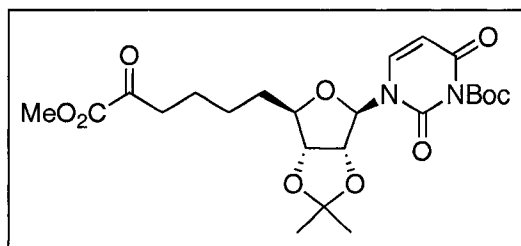
mmol) was added. The mixture was heated at 40 °C, with the reaction progress monitored by ¹H NMR. After 24 h, extra LiOH·H₂O in D₂O (8.00 μ L, 0.00530 mmol) was added, and the reaction continued at 35 °C for 24 h. The solvent was removed *in vacuo* and the residue dissolved in H₂O. Lyophilization gave lithium salt **187** as a white solid (4.20 mg, 100%): [α]_D²⁰ = +16.15 (*c* 0.13, H₂O); IR (μ scope) ν 3700-3000, 2942, 1688, 1568, 1072; ¹H NMR (D₂O, 600 MHz) δ 1.54-1.68 (m, 2H, CH₂-5'), 1.70-1.84 (m, 2H, CH₂), 2.29-2.31 (m, 2H, allylic CH₂), 4.03 (br s, 2H, H-3', H-4'), 4.26-4.28 (m, 1H, H-2'), 5.50 (s, 1H, C=CH), 5.81 (d, 1H, *J* = 7.8 Hz, H-5), 5.90 (d, 1H, *J* = 4.8 Hz, H-1'), 7.54 (d, 1H, *J* = 7.8 Hz, H-6); ¹³C NMR (D₂O, 125 MHz) δ 24.0, 33.0, 35.1, 73.8, 74.5, 84.3, 90.2, 103.8, 1221.2, 141.1, 151.8, 160.0, 167.0, 175.3, 177.2; HRMS (ES-) calcd for C₁₅H₁₇N₂O₉ 369.0929, found 369.0928 [MH]⁻.

***tert*-Butyl 3-((3*aR*,4*R*,6*R*,6*aR*)-6-((*E*)-6-methoxy-5,6-dioxohex-1-enyl)-2,2-dimethyl-tetrahydrofuro[3,4-*d*][1,3]dioxol-4-yl)-2,6-dioxo-2,3-dihydropyrimidine-1(6*H*)-carboxylate (188)**



Grubbs' 2nd generation catalyst (125 mg, 0.150 mmol) was added to a solution of olefins **164** (383 mg, 1.01 mmol) and **174** (405 mg, 2.59 mmol) in CH₂Cl₂ (5.0 mL), and the dark brown mixture was stirred at reflux for 16 h. Extra catalyst (43 mg, 0.051 mmol) was added, and stirring at reflux was continued for another 8h. The reaction mixture was then cooled to rt, and DMSO (770 μL, 54 equiv. relative to catalyst) was added. After stirring at rt for 12 h, the CH₂Cl₂ was removed *in vacuo* and the crude product was purified by flash chromatography (SiO₂, pentane/EtOAc, 3:1 to 2:1) to give **188** as a white foam (206 mg, 40%): R_f 0.08 (pentane/EtOAc, 2:1); [α]_D²⁰ = +32.99 (*c* 0.16, CHCl₃); IR (CHCl₃, cast) ν 3097, 2987, 2937, 1785, 1724, 1682, 1632, 1255, 1081 cm⁻¹; ¹H NMR (CDCl₃, 600 MHz) δ 1.35 (s, 3H, CH₃), 1.57 (s, 3H, CH₃), 1.61 (s, 9H, C(CH₃)₃), 2.42 (app qd, 2H, *J* = 6.9, 1.4 Hz, allylic CH₂), 2.97 (t, 2H, *J* = 6.9 Hz, CH_{2α}), 3.88 (s, 3H, OCH₃), 4.51 (dd, 1H, *J* = 7.9, 4.2 Hz, H-4'), 4.69 (dd, 1H, *J* = 6.5, 4.2 Hz, H-3'), 5.02 (dd, 1H, *J* = 6.5, 2.2 Hz, H-2'), 5.60 (d, 1H, *J* = 2.2 Hz, H-1'), 5.65 (ddt, 1H, *J* = 15.5, 7.9, 1.4 Hz, CH₂CH=CHCH), 5.76 (d, 1H, *J* = 8.4 Hz, H-5), 5.83 (dtd, 1H, *J* = 15.5, 6.9, 0.9 Hz, CH₂CH=CHCH), 7.23 (d, 1H, *J* = 8.4 Hz, H-6); ¹³C NMR (CDCl₃, 125 MHz) δ 25.3, 25.4, 27.1, 27.4, 38.3, 53.0, 83.9, 84.8, 86.9, 88.3, 94.5, 102.0, 114.5, 128.1, 133.5, 141.2, 147.4, 148.1, 160.3, 161.1, 193.0; HRMS (ES⁺) calcd for C₂₃H₃₀N₂O₁₀Na 517.1793, found 517.1794 [MNa]⁺.

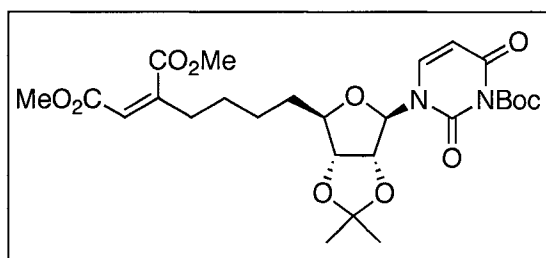
***tert*-Butyl 3-((3*aR*,4*R*,6*R*,6*aR*)-6-(6-methoxy-5,6-dioxohexyl)-2,2-dimethyl-tetrahydrofuro[3,4-*d*][1,3]dioxol-4-yl)-2,6-dioxo-2,3-dihydropyrimidine-1(6*H*)-carboxylate (189)**



5% Pd/C (25.1 mg) was added to a solution of alkene **188** (199 mg, 0.390 mmol) in EtOAc (3.1 mL). The mixture was stirred under 1 atm H₂ for 7 h, then filtered through

Celite and washed with hot EtOAc. After concentration *in vacuo*, the crude product was purified by flash chromatography (SiO₂, pentane/EtOAc, 3:1) to afford α -keto ester **189** as a white foam (155 mg, 80%): *R_f* 0.05 (petroleum ether/EtOAc, 3:1); [α]_D²⁰ = +18.82 (*c* 0.17, CHCl₃); IR (CHCl₃, cast) ν 3097, 2986, 2939, 1785, 1725, 1683, 1633, 1149, 1082 cm⁻¹; ¹H NMR (CDCl₃, 600 MHz) δ 1.34 (s, 3H, CH₃), 1.40-1.52 (m, 2H, CH₂), 1.56 (s, 3H, CH₃), 1.61 (s, 9H, C(CH₃)₃), 1.65-1.74 (m, 4H, 2 x CH₂), 2.87 (t, 2H, *J* = 7.2 Hz, CH_{2_α}), 3.87 (s, 3H, OCH₃), 4.01 (m, 1H, H-4'), 4.55 (dd, 1H, *J* = 6.8, 4.8 Hz, H-3'), 4.93 (dd, 1H, *J* = 6.8, 2.2 Hz, H-2'), 5.62 (d, 1H, *J* = 2.2 Hz, H-1'), 5.77 (d, 1H, *J* = 8.4 Hz, H-5), 7.21 (d, 1H, *J* = 8.4 Hz, H-6); ¹³C NMR (CDCl₃, 125 MHz) δ 22.6, 24.9, 25.4, 27.2, 27.4, 32.9, 39.0, 52.9, 83.5, 84.4, 86.5, 87.0, 93.4, 102.1, 114.8, 140.8, 147.5, 148.1, 160.3, 161.4, 193.9; *m/z* (ES⁺) calcd for C₂₃H₃₂N₂O₁₀Na 519.1949, found 519.1948 [MNa]⁺.

Dimethyl 2-(4-((3a*R*,4*R*,6*R*,6a*R*)-6-(3-(*tert*-butoxycarbonyl)-2,4-dioxo-3,4-dihydropyrimidin-1(2*H*)-yl)-2,2-dimethyltetrahydrofuro[3,4-*d*][1,3]dioxol-4-yl)butyl)maleate (190)

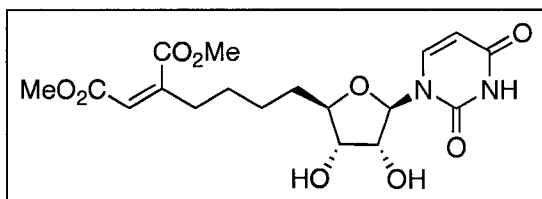


Methyl diethylphosphonoacetate (21.5 μ L, 0.120 mmol) in DMF (250 μ L) was added dropwise to a suspension of NaH (60% in mineral oil, 9.70 mg, 0.240 mmol) in DMF

(450 μ L) at 0 $^{\circ}$ C, and the mixture was stirred at 0 $^{\circ}$ C for 30 min. It was then cooled to -40 $^{\circ}$ C and α -keto ester **189** (76.0 mg, 0.153 mmol) in DMF (500 μ L) was added dropwise. The mixture was stirred for 5 h, allowing it to slowly warm to rt. H₂O (2 mL) was added, and the aqueous layer was extracted with EtOAc (3 x 2 mL). The combined organic layers were dried (MgSO₄) and concentrated *in vacuo*. Purification by flash chromatography (SiO₂, petroleum ether/EtOAc, 2:1) afforded dimethyl maleate derivative **190** as a colourless glass (35.3 mg, 53%): *R_f* 0.10 (petroleum ether/EtOAc, 2:1); [α]_D²⁰ = +20.00 (*c* 0.11, CHCl₃); IR (CHCl₃, cast) ν 3099, 2987, 2950, 2867, 1785, 1724, 1683, 1633, 1258, 1086 cm⁻¹; ¹H NMR (CDCl₃, 600 MHz) δ 1.33 (s, 3H, CH₃), 1.38-1.53 (m, 3H, CH₂ + CH_aH_b), 1.55 (s, 3H, CH₃), 1.60 (s, 9H, C(CH₃)₃), 1.65-1.72 (m, 3H, CH₂ + CH_aH_b), 2.37 (td, 2H, *J* = 7.5, 1.5 Hz, allylic CH₂), 3.72 (s, 3H, OCH₃), 3.82 (s, 3H, OCH₃), 3.98-4.01 (m, 1H, H-4'), 4.54 (dd, 1H, *J* = 6.6, 4.8 Hz, H-3'), 4.92 (dd, 1H, *J* = 6.6, 2.4 Hz, H-2'), 5.61 (d, 1H, *J* = 2.4 Hz, H-1'), 5.75 (d, 1H, *J* = 8.4 Hz, H-5), 5.81 (t, 1H, *J* = 1.5 Hz, C=CH), 7.21 (d, 1H, *J* = 8.4 Hz, H-6); ¹³C NMR (CDCl₃, 125 MHz) δ 24.9, 25.4, 26.7, 27.2, 27.5, 32.9, 34.1, 51.8, 52.3, 83.6, 84.4, 86.6, 87.0, 93.6,

102.2, 114.8, 119.5, 140.8, 147.5, 148.1, 150.2, 160.3, 165.3, 169.2; HRMS (ES+) calcd for $C_{26}H_{36}N_2O_{11}Na$ 575.2211, found 575.2211 [MNa]⁺.

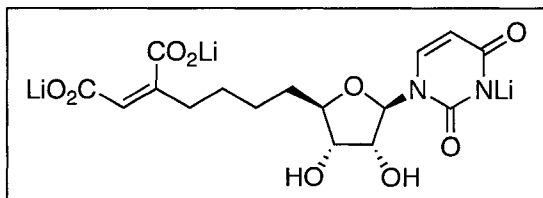
Dimethyl 2-(4-((2R,3S,4R,5R)-5-(2,4-dioxo-3,4-dihydropyrimidin-1(2H)-yl)-3,4-dihydroxytetrahydrofuran-2-yl)butyl)maleate (191)



Dimethyl maleate derivative **190** (3.90 mg, 0.00710 mmol) was dissolved in TFA/H₂O (7:3, 640 μ L) and the mixture was stirred at rt for 2.5 h. After concentration *in vacuo*,

purification was accomplished by reverse phase HPLC using solvent system C (t_R 17.5 min). The combined fractions containing the desired product were lyophilized to give **191** as a white powder (1.90 mg, 75%): R_f 0.18 (EtOAc/MeOH, 95:5); $[\alpha]_D^{20} = +34.99$ (c 0.10, CHCl₃); IR (CHCl₃, cast) ν 3700-3000, 2951, 2858, 1694, 1205, 1133 cm^{-1} ; ¹H NMR (CD₃OD, 600 MHz) δ 1.43-1.50 (m, 1H, CH_aH_b), 1.51-1.58 (m, 3H, CH₂ + CH_aH_b), 1.64-1.70 (m, 1H, CH_cH_d), 1.72-1.78 (m, 1H, CH_cH_d), 2.39 (td, 2H, $J = 7.3, 1.5$ Hz, allylic CH₂), 3.69 (s, 3H, OCH₃), 3.77 (s, 3H, OCH₃), 3.84-3.87 (m, 2H, H-3', H-4'), 4.14 (dd, 1H, $J = 5.4, 4.2$ Hz, H-2'), 5.71 (d, 1H, $J = 8.1$ Hz, H-5), 5.77 (d, 1H, $J = 4.2$ Hz, H-1'), 5.92 (t, 1H, $J = 1.5$ Hz, C=CH), 7.56 (d, 1H, $J = 8.1$ Hz, H-6); ¹³C NMR (CD₃OD, 125 MHz) δ 26.1, 28.0, 34.0, 35.0, 52.3, 52.8, 74.8, 75.1, 84.8, 91.6, 103.0, 120.7, 142.6, 151.9, 152.3, 166.1, 167.0, 170.9; HRMS (ES+) calcd for $C_{18}H_{24}N_2O_9Na$ 435.1374, found 435.1372 [MNa]⁺.

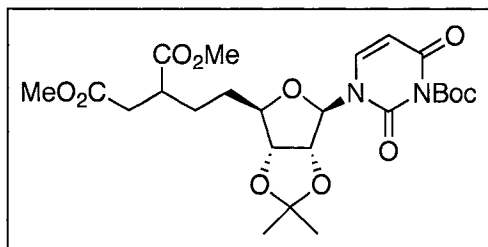
Lithium 1-((2R,3R,4S,5R)-5-((Z)-5,6-dicarboxylatohex-5-enyl)-3,4-dihydroxy-tetrahydrofuran-2-yl)-2,4-dioxo-2,4-dihydro-1H-pyrimidin-3-ide (192)



Dimethyl maleate derivative **191** (1.58 mg, 0.00380 mmol) was dissolved in CD₃OD/D₂O (7:3, 700 μL) in an NMR tube, and a solution of LiOH·H₂O in D₂O

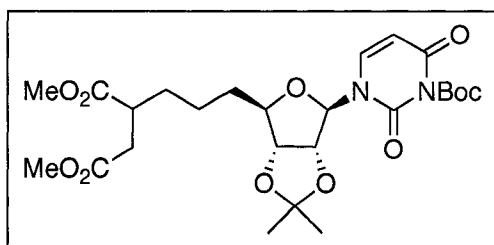
(1.00 M, 15.4 μL, 0.0154 mmol) was added. The mixture was heated at 40 °C, with the reaction progress monitored by ¹H NMR. After 20.5 h, LiOH·H₂O in D₂O (12.0 μL, 0.0120 mmol) was added, and the mixture heated at 40 °C for 24 h. The solvent was removed *in vacuo*, and the residue was dissolved in H₂O. It was lyophilized to afford lithium salt **192** as a white solid (2.00 mg, 100%): $[\alpha]_D^{20} = -4.14$ (*c* 0.14, H₂O); IR (μscope) ν 3650-3000, 2940, 1688, 1565, 1137; ¹H NMR (D₂O, 500 MHz) δ 1.42-1.55 (m, 4H, 2 x CH₂), 1.71-1.79 (m, 2H, CH₂), 2.24-2.27 (m, 2H, allylic CH₂), 4.01-4.04 (m, 2H, H-3', H-4'), 4.28 (app t, 1H, *J* = 5.0 Hz, H-2'), 5.49 (s, 1H, C=CH), 5.82 (d, 1H, *J* = 7.8 Hz, H-5), 5.91 (d, 1H, *J* = 5.0 Hz, H-1'), 7.54 (d, 1H, *J* = 7.8 Hz, H-6); ¹³C NMR (D₂O, 125 MHz) δ 25.4, 27.8, 33.2, 35.2, 73.8, 74.5, 84.5, 90.1, 103.8, 120.7, 141.1, 152.5, 161.1, 165.7, 175.4, 176.3; HRMS (ES-) calcd for C₁₆H₁₉N₂O₉ 383.1085, found 383.1084 [MH].

Dimethyl 2-(2-((3a*R*,4*R*,6*R*,6a*R*)-6-(3-(*tert*-butoxycarbonyl)-2,4-dioxo-3,4-dihydropyrimidin-1(2*H*)-yl)-2,2-dimethyltetrahydrofuro[3,4-*d*][1,3]dioxol-4-yl)ethyl)succinate (193)



Dimethyl maleate derivative **179** (30.0 mg, 0.0570 mmol) was dissolved in EtOAc (500 μ L) and 10% Pd/C (6 mg) was added. The mixture was stirred under 1 atm H₂ for 20 h, then filtered through Celite and the Celite washed with hot EtOAc. Concentration *in vacuo* was followed by flash chromatography (SiO₂, petroleum ether/EtOAc, 3:2) to give dimethyl succinate derivative **193** as a colourless gum, isolated as a mixture of diastereomers (19.2 mg, 64%): *R_f* 0.15 (petroleum ether/EtOAc, 3:2); IR (CHCl₃, cast) ν 2924, 2852, 1786, 1724, 1683, 1633, 1150, 1095 cm⁻¹; ¹H NMR (CDCl₃, 500 MHz) δ 1.33 (s, 3H, CH₃), 1.55 (s, 3H, CH₃), 1.61 (s, 9H, C(CH₃)₃), 1.62-1.84 (m, 4H, 2 x CH₂), 2.45 (ddd, 1H, *J* = 16.5, 5.5, 2.5 Hz, MeO₂CCH_aH_b), 2.73 (ddd, 1H, *J* = 16.5, 9.0, 1.0 Hz, CH₃O₂CCH_aH_b), 2.84-2.94 (m, 1H, CH₃O₂CCH), 3.67 (s, 3H, OCH₃), 3.70 (s, 3H, OCH₃), 3.96-4.04 (m, 1H, H-4'), 4.56 (dd, 1H, *J* = 6.5, 4.5 Hz, H-3'), 4.94 (dd, 1H, *J* = 6.5, 2.0 Hz, H-2'), 5.59 (d, 1H, *J* = 2.0 Hz, H-1'), 5.76 (d, 1H, *J* = 8.3 Hz, H-5), 7.20 (d, 1H, *J* = 8.3 Hz, H-6); ¹³C NMR (CDCl₃, 125 MHz) δ 25.4, 27.2, 27.5, 27.8, 27.9, 30.6, 30.8, 35.7, 35.9, 40.7, 40.9, 51.8, 52.0, 83.5, 83.6, 84.4, 86.6, 86.7, 87.1, 94.0, 94.1, 102.2, 114.8, 114.9, 140.9, 141.0, 147.4, 148.0, 160.3, 172.1, 172.2, 174.78, 174.82 (11 carbon signals not observed due to overlap); HRMS (ES⁺) calcd for C₂₄H₃₄N₂O₁₁Na 549.2055, found 549.2056 [MNa]⁺.

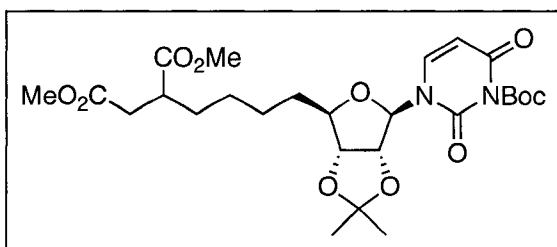
Dimethyl 2-(3-((3aR,4R,6R,6aR)-6-(3-(tert-butoxycarbonyl)-2,4-dioxo-3,4-dihydropyrimidin-1(2H)-yl)-2,2-dimethyltetrahydrofuro[3,4-d][1,3]dioxol-4-yl)propyl)succinate (194)



This compound was prepared using the same procedure as for **193**. Thus, a mixture of **185** (29.5 mg, 0.0550 mmol) and 10% Pd/C (7 mg) in EtOAc (500 μ L) was stirred under 1 atm H₂

for 20 h. Filtration through Celite and washing of the Celite with hot EtOAc was followed by concentration *in vacuo*. Purification was done by flash chromatography (SiO₂, petroleum ether/EtOAc, 2:1) to give dimethyl succinate derivative **194** as a colourless glass, isolated as a mixture of diastereomers (21.1 mg, 71%): R_f 0.17 (3:2 petroleum ether/EtOAc, 3:2); IR (CHCl₃, cast) ν 2986, 2938, 1785, 1724, 1683, 1635, 1150, 1085 cm⁻¹; ¹H NMR (CDCl₃, 500MHz) δ 1.34 (s, 3H, CH₃), 1.36-1.52 (m, 3H, CH₂ + CH_aH_b), 1.55 (s, 3H, CH₃), 1.61 (s, 9H, C(CH₃)₃), 1.64-1.73 (m, 3H, CH₂ + CH_aH_b), 2.45 (dd, 1H, *J* = 16.7, 5.5 Hz, CH₃O₂CCH_aH_b), 2.73 (dd, 1H, *J* = 16.7, 9.0 Hz, CH₃O₂CCH_aH_b), 2.83-2.89 (m, 1H, CH₃O₂CCH), 3.68 (s, 3H, OCH₃), 3.70 (s, 3H, OCH₃), 3.98-4.01 (m, 1H, H-4'), 4.53 (dd, 1H, *J* = 6.5, 5.0 Hz, H-3'), 4.91 (dd, 1H, *J* = 6.5, 2.3 Hz, H-2'), 5.62 (d, 1H, *J* = 2.3 Hz, H-1'), 5.76 (d, 1H, *J* = 8.3 Hz, H-5), 7.20 (d, 1H, *J* = 8.3 Hz, H-6); ¹³C NMR (CDCl₃, 125 MHz) δ 23.12, 23.14, 25.4, 27.2, 27.5, 31.6, 33.0, 35.8, 41.0, 51.8, 51.9, 83.5, 84.4, 86.5, 87.0, 93.5, 102.2, 114.9, 140.66, 140.70, 147.5, 148.1, 160.3, 172.2, 175.1 (21 carbon signals not observed due to overlap); HRMS (ES⁺) calcd for C₂₅H₃₆N₂O₁₁Na 563.2211, found 563.2209 [MNa]⁺.

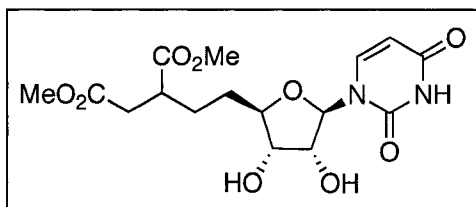
Dimethyl 2-(4-((3a*R*,4*R*,6*R*,6a*R*)-6-(3-(*tert*-butoxycarbonyl)-2,4-dioxo-3,4-dihydro-pyrimidin-1(2*H*)-yl)-2,2-dimethyltetrahydrofuro[3,4-*d*][1,3]dioxol-4-yl)butyl)-succinate (195)



This compound was prepared using the same procedure as for **193**. Dimethyl maleate derivative **190** (10.3 mg, 0.0190 mmol) and 10% Pd/C (4.10 mg) were

stirred under 1 atm H₂ in EtOAc (800 μL) for 12 h, then the mixture was filtered through Celite. The Celite was washed with hot EtOAc, and the filtrate was concentrated *in vacuo*. Purification by flash chromatography (SiO₂, petroleum ether/EtOAc, 2:1) yielded dimethyl succinate derivative **195** as a colourless glass, isolated as a mixture of diastereomers (2.20 mg, 21%): *R_f* 0.14 (petroleum ether/EtOAc, 2:1); IR (CHCl₃, cast) ν 2987, 2938, 1785, 1724, 1683, 1632, 1150, 1085 cm⁻¹; ¹H NMR (CDCl₃, 500 MHz) δ 1.34 (s, 3H, CH₃), 1.35-1.54 (m, 4H, 2 x CH₂), 1.55 (s, 3H, CH₃), 1.61 (s, 9H, C(CH₃)₃), 1.63-1.72 (m, 4H, 2 x CH₂), 2.43 (dd, 1H, *J* = 16.6, 5.3 Hz, CH₃O₂CCH_aH_b), 2.72 (dd, 1H, *J* = 16.6, 9.0 Hz, CH₃O₂CCH_aH_b), 2.82-2.88 (m, 1H, CH₃O₂CCH_c), 3.68 (s, 3H, OCH₃), 3.70 (s, 3H, OCH₃), 3.98-4.02 (m, 1H, H-4'), 4.53 (app t, 1H, *J* = 6.3 Hz, H-3'), 4.91 (dd, 1H, *J* = 6.3, 2.2 Hz, H-2'), 5.63 (d, 1H, *J* = 2.2 Hz, H-1'), 5.76 (d, 1H, *J* = 8.0 Hz, H-5), 7.20 (d, 1H, *J* = 8.0 Hz, H-6); ¹³C NMR (CDCl₃, 125 MHz) δ 25.3, 25.4, 26.7, 27.2, 27.5, 31.7, 33.0, 35.82, 35.83, 41.01, 41.03, 51.77, 51.84, 83.5, 84.5, 86.6, 86.7, 87.0, 93.38, 93.42, 102.2, 114.83, 114.85, 140.6, 147.5, 148.1, 160.3, 172.3, 175.2 (19 carbon signals not observed due to overlap); HRMS (ES⁺) calcd for C₂₆H₃₈N₂O₁₁Na 577.2368, found 577.2368 [MNa]⁺.

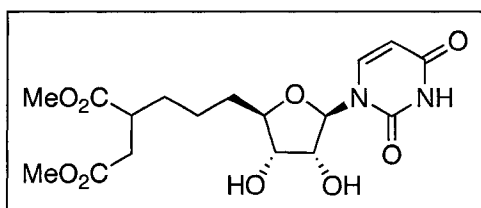
Dimethyl 2-(2-((2R,3S,4R,5R)-5-(2,4-dioxo-3,4-dihydropyrimidin-1(2H)-yl)-3,4-dihydroxytetrahydrofuran-2-yl)ethyl)succinate (196)



Succinate **193** (18.3 mg, 0.0350 mmol) was dissolved in TFA/H₂O (7:3, 3.2 mL) and the mixture was stirred at rt for 2.5 h then concentrated *in vacuo*. The crude product was

purified by flash chromatography (SiO₂, EtOAc/MeOH, 95:5) to give **196** as a colourless glass, isolated as a mixture of diastereomers (13.4 mg, 100%): R_f 0.20 (CHCl₃/MeOH, 9:1); IR (CHCl₃, cast) ν 3600-3100, 3026, 2954, 1693, 1268, 1168 cm⁻¹; ¹H NMR (CD₃OD, 500 MHz) δ 1.63-1.78 (m, 4H, 2 x CH₂), 2.54 (dd, 1H, *J* = 16.8, 5.3 Hz, CH₃O₂CCH_aH_b), 2.69 (dd, 1H, *J* = 16.8, 9.3 Hz, CH₃O₂CCH_aH_b), 2.85-2.91 (m, 1H, CH₃O₂CCH_cH), 3.64 (s, 3H, OCH₃), 3.68 (s, 3H, OCH₃), 3.80-3.86 (m, 2H, H-3', H-4'), 4.14-4.17 (m, 1H, H-2'), 5.71 (d, 1H, *J* = 8.0 Hz, H-5), 5.75 (d, 1H, *J* = 4.5 Hz, H-1'), 7.56 (d, 1H, *J* = 8.0 Hz, H-6); ¹³C NMR (CD₃OD, 125 MHz) δ 29.2, 29.3, 31.75, 31.78, 36.6, 36.7, 42.2, 42.3, 52.2, 52.4, 74.7, 74.8, 74.9, 75.0, 84.50, 84.54, 92.0, 102.9, 103.0, 142.8, 152.2, 166.1, 174.0, 176.8 (8 carbon signals not observed due to overlap); HRMS (ES⁺) calcd for C₁₆H₂₂N₂O₉Na 409.1218, found 409.1216 [MNa]⁺.

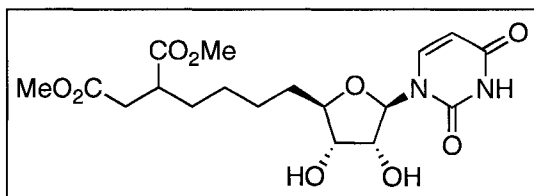
Dimethyl 2-(3-((2R,3S,4R,5R)-5-(2,4-dioxo-3,4-dihydropyrimidin-1(2H)-yl)-3,4-dihydroxytetrahydrofuran-2-yl)propyl)succinate (197)



Succinate **194** (16.0 mg, 0.0296 mmol) was stirred in TFA/H₂O (3:2, 1.6 mL) at 0 °C for 2 h, then the mixture was concentrated *in vacuo*.

Purification by flash chromatography (SiO₂, EtOAc/MeOH, 98:2) afforded **197** as a colourless glass, isolated as a mixture of diastereomers (11.0 mg, 96%): R_f 0.07 (CHCl₃/MeOH, 95:5); IR (CHCl₃, cast) ν 3600-3000, 3061, 2952, 2863, 1693, 1053; ¹H NMR (CD₃OD, 500 MHz) δ 1.39-1.78 (m, 6H, 3 x CH₂), 2.50 (dd, 1H, *J* = 16.5, 5.0 Hz, CH₃O₂CCH_aH_b), 2.67 (dd, 1H, *J* = 16.5, 9.2 Hz, CH₃O₂CCH_aH_b), 2.81-2.87 (m, 1H, CH₃O₂CCH_aH_b), 3.64 (s, 3H, OCH₃), 3.66 (s, 3H, OCH₃), 3.83-3.86 (m, 2H, H-3', H-4'), 4.14 (app t, 1H, *J* = 4.0 Hz, H-2'), 5.71 (d, 0.5H, *J* = 8.0 Hz, H-5), 5.72 (d, 0.5H, *J* = 8.0 Hz, H-5), 5.76 (d, 1H, *J* = 4.0 Hz, H-1'), 7.55 (d, 0.5H, *J* = 8.0 Hz, H-6), 7.56 (d, 0.5H, *J* = 8.0 Hz, H-6); ¹³C NMR (CD₃OD, 125 MHz) δ 24.38, 24.41, 32.8, 34.0, 34.1, 36.66, 36.68, 42.4, 52.2, 52.3, 74.7, 75.0, 75.1, 84.56, 84.61, 91.7, 103.0, 142.6, 152.3, 166.2, 174.1, 176.98, 177.01 (11 carbon signals not observed due to overlap); HRMS (ES+) calcd for C₁₆H₂₂N₂O₉Na 409.1218, found 409.1216 [MNa]⁺.

Dimethyl 2-(4-((2*R*,3*S*,4*R*,5*R*)-5-(2,4-dioxo-3,4-dihydropyrimidin-1(2*H*)-yl)-3,4-dihydroxytetrahydrofuran-2-yl)butyl)succinate (198)

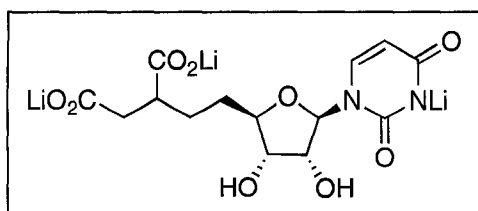


Succinate **195** (18.2 mg, 0.0328 mmol) was stirred in TFA/H₂O (3:2, 1.6 mL) at 0 °C for 2 h, the solvent was removed *in vacuo*.

Purification by flash chromatography (SiO₂, EtOAc/MeOH, 98:2) yielded **198** as a colourless glass, isolated as a mixture of diastereomers (12.0 mg, 89%): R_f 0.18 (EtOAc/MeOH, 95:5); IR (CHCl₃, cast) ν 3550-3100, 3025, 2948, 2860, 1717, 1202, 1049 cm⁻¹; ¹H NMR (CD₃OD, 300 MHz) δ 1.28-1.71 (m, 8 H, 4 x CH₂), 2.49 (dd, 1H, *J* = 16.6, 5.3 Hz, CH₃O₂CCH_aH_b), 2.66 (dd, 1H, *J* = 16.6, 9.3 Hz, CH₃O₂CCH_aH_b), 2.77-

2.86 (m, 1H, CH₃O₂CCH), 3.64 (s, 3H, OCH₃), 3.66 (s, 3H, OCH₃), 3.82-3.86 (m, 2H, H-3', H-4'), 4.12-4.15 (m, 1H, H-2'), 5.72 (d, 1H, *J* = 8.1 Hz, H-5), 5.77 (d, 1H, *J* = 4.2 Hz, H-1'), 7.56 (dd, 1H, *J* = 8.1, 0.9 Hz, H-6); ¹³C NMR (CD₃OD, 125 MHz) δ 26.7, 27.79, 27.80, 32.8, 34.1, 36.66, 36.68, 42.39, 42.41, 52.2, 52.3, 74.8, 75.066, 75.074, 84.8, 91.6, 103.0, 142.6, 152.3, 166.1, 174.1, 177.1 (14 carbon signals not observed due to overlap); HRMS (ES+) calcd for C₁₈H₂₆N₂O₉Na 437.1531, found 437.1530 [MNa]⁺.

Lithium 1-((2*R*,3*R*,4*S*,5*R*)-5-(3,4-dicarboxylatobutyl)-3,4-dihydroxytetrahydrofuran-2-yl)-2,4-dioxo-2,4-dihydro-1*H*-pyrimidin-3-ide (199)

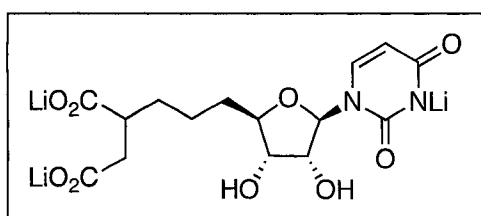


Dimethyl succinate derivative **196** (7.00 mg, 0.0180 mmol) was dissolved in CD₃OD/D₂O (4.5:3, 750 μL) in an NMR tube, and a solution of LiOH·H₂O in D₂O (1.00 M, 73.0 μL, 0.0730

mmol) was added. The reaction was conducted at rt with monitoring by ¹H NMR. After 5 h, the mixture was concentrated *in vacuo* and the residue was dissolved in H₂O. It was washed with CH₂Cl₂, then lyophilized to give lithium salt **199** as a white solid, isolated as a ~1:1 mixture of diastereomers (6.80 mg, 100%): IR (μscope) ν 3700-2800, 1675, 1570, 1130 cm⁻¹; ¹H NMR (D₂O, 400 MHz) δ 1.50-1.74 (m, 4H, 2 x CH₂), 2.19 (dd, 1H, *J* = 14.6, 9.8 Hz, LiO₂CCH_aH_b), 2.47 (dd, 1H, *J* = 14.6, 5.6 Hz, LiO₂CCH_aH_b), 2.55-2.62 (m, 1H, LiO₂CCH), 3.97-4.04 (m, 2H, H-3', H-4'), 4.27 (app t, 1H, *J* = 4.6 Hz, H-2'), 5.84 (d, 0.5H, *J* = 7.6 Hz, H-5), 5.86 (d, 0.5H, *J* = 8.0 Hz, H-5), 5.88 (d, 0.5H, *J* = 3.2 Hz, H-1'), 5.89 (d, 0.5H, *J* = 2.8 Hz, H-1'), 7.57 (d, 0.5H, *J* = 7.6 Hz, H-6), 7.58 (d, 0.5H, *J* = 8.0 Hz, H-6); ¹³C NMR (D₂O, 125 MHz) δ 28.9, 29.0, 31.80, 31.84, 41.85, 41.90, 46.9, 73.7,

73.8, 74.5, 74.6, 84.6, 84.7, 89.9, 103.76, 103.80, 141.2, 159.2, 165.1, 176.1, 182.3, 184.86, 184.89 (5 carbon signals not observed due to overlap); HRMS (ES-) calcd for $C_{14}H_{17}N_2O_9$, 357.0940, found 357.0939 $[MH_2]^-$.

Lithium 1-((2*R*,3*R*,4*S*,5*R*)-5-(4,5-dicarboxylatopentyl)-3,4-dihydroxytetrahydrofuran-2-yl)-2,4-dioxo-2,4-dihydro-1*H*-pyrimidin-3-ide (200)

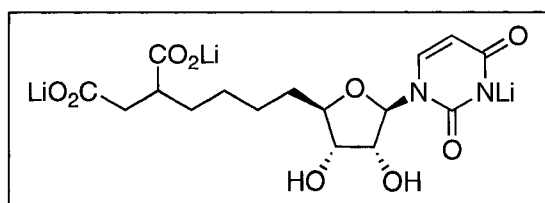


Dimethyl succinate derivative **197** (7.00 mg, 0.0170 mmol) was dissolved in CD_3OD/D_2O (1:1, 600 μL) in an NMR tube, and a solution of $LiOH \cdot H_2O$ in D_2O (1.00 M, 74.0 μL , 0.0740

mmol) was added. The reaction was conducted at rt for 5.5 h, then at 40 °C for 2 h, while monitoring by 1H NMR. Insoluble material was filtered, and the mixture lyophilized to give lithium salt **200** as a white solid, isolated as a ~ 1.3:1 mixture of diastereomers (6.80 mg, 100%): IR (μ scope) ν 3600-3150, 2941, 1695, 1576, 1426, 1205, 1088 cm^{-1} ; 1H NMR (D_2O , 600 MHz) δ 1.32-1.80 (m, 6H, both isomers, 3 x CH_2), 2.18 (dd, ~0.56H, major isomer, $J = 14.4, 10.2$ Hz, $LiO_2CCH_aH_b$), 2.37 (dd, ~0.44 H, minor isomer, $J = 15.9, 5.7$ Hz, $LiO_2CCCH_aH_b$), 2.47 (m, 1H, both isomers, $LiO_2CCH_aH_b$), 2.58 (m, ~0.56H, major isomer, LiO_2CCH), 2.79-2.85 (m, ~0.44H, minor isomer, LiO_2CCH), 3.99-4.05 (m, 2H, both isomers, H-3', H-4'), 4.29 (app q, 1H, both isomers, $J = 4.8$ Hz, H-2'), 5.85 (br s, 1H, both isomers, H-5), 5.88 (d, ~0.44H, minor isomer, $J = 4.2$ Hz, H-1'), 5.89 (d, ~0.56H, major isomer, $J = 4.8$ Hz, H-1'), 7.55 (dd, ~0.44H, minor isomer, $J = 7.8, 4.8$ Hz, H-6), 7.58 (d, ~0.56H, major isomer, $J = 7.8, 2.4$ Hz, H-6); ^{13}C NMR (D_2O , 125 MHz) δ 23.5, 24.0, 33.2 33.6, 40.5, 42.1, 43.3, 43.4, 46.9, 73.68, 73.73, 73.8, 74.45,

74.48, 84.2, 84.3, 84.7, 84.8, 89.99, 90.05, 90.5, 103.6, 141.68, 141.74, 149.2, 162.5, 182.5, 185.4 (2 carbon signals not observed due to overlap); HRMS (ES-) calcd for $C_{15}H_{19}N_2O_9$ 371.1096, found 371.1097 $[MH_2]^-$.

Lithium 1-((2*R*,3*R*,4*S*,5*R*)-5-(5,6-dicarboxylatohexyl)-3,4-dihydroxytetrahydrofuran-2-yl)-2,4-dioxo-2,4-dihydro-1*H*-pyrimidin-3-ide (201)



Dimethyl succinate derivative **198** (6.10 mg, 0.0150 mmol) was dissolved in CD_3OD/D_2O (1:1, 600 μL) in an NMR

tube, and a solution of $LiOH \cdot H_2O$ in D_2O (1.00 M, 58.5 μL , 0.0585 mmol) was added.

The mixture was heated at 50 °C and the reaction monitored by 1H NMR. After 5 h, it was lyophilized to afford lithium salt **201** as a white solid, isolated as a ~3.5:1 mixture of

diastereomers (4.50 mg, 76%): IR (μ scope) ν 3700-3000, 2935, 1681, 1579, 1087 cm^{-1} ;

1H NMR (D_2O , 600 MHz) δ 1.30-1.52 (m, 6H, both isomers, 3 x CH_2), 1.67-1.77 (m, 2H, both isomers, CH_2), 2.17 (dd, ~0.78H, major isomer, $J = 14.4, 9.6$ Hz, $LiO_2CCH_aH_b$),

2.37 (dd, ~0.22H, minor isomer, $J = 15.6, 6.0$ Hz, $LiO_2CCH_aH_b$), 2.44 (dd, ~0.78H, major

isomer, $J = 14.4, 5.4$ Hz, $LiO_2CCH_aH_b$), 2.47 (dd, ~0.22H, minor isomer, $J = 15.6, 9.0$

Hz, $LiO_2CCH_aH_b$), 2.56 (m, ~0.78H, major isomer, LiO_2CCH), 2.77-2.82 (m, ~0.22H,

minor isomer, LiO_2CCH), 4.00-4.04 (m, 2H, both isomers, H-3', H-4'), 4.28-4.30 (m, 1H,

both isomers, H-2'), 5.84 (d, 1H, both isomers, $J = 7.8$ Hz, H-5), 5.88 (d, ~0.22H, minor

isomer, $J = 4.8$ Hz, H-1'), 5.89 (d, ~0.78H, major isomer, $J = 5.4$ Hz, H-1'), 7.55 (d,

0.22H, minor isomer, $J = 7.8$ Hz, H-6), 7.56 (d, 0.78H, major isomer, $J = 7.8$ Hz, H-6);

^{13}C NMR (D_2O , 125 MHz) δ 25.5, 25.8, 27.7, 32.2, 32.6, 33.2, 33.4, 40.5, 42.1, 47.1,

73.8, 74.5, 84.4, 84.4, 84.7, 84.8, 90.1, 103.7, 141.5, 157.7, 163.0, 181.4, 182.6, 185.7 (8 carbon signals not observed due to overlap); HRMS (ES-) calcd for C₁₆H₂₁N₂O₉ 385.1253, found 385.1243 [MH₂]⁺.

2.2 NDP Kinase Assay

The coupled assay using pyruvate kinase and lactate dehydrogenase described by Kezdi *et al.*¹⁴⁵ was used and adapted to microtiter plates. The final assay volume was 100 mL, with the final concentrations as follows: 50 mM Tris-HCl (pH 7.6), 75 mM KCl, 5 mM MgCl₂, 1 mM phosphoenolpyruvate, 1 mM NADH, 0.2 mM ATP, 0.6 mM 8-bromoinosine diphosphate, 1 mg/mL bovine serum albumin, 50 U/mL pyruvate kinase, 50 U/mL lactate dehydrogenase, and 1mM nucleotide analogue. The reaction was initiated by adding NDP kinase (0.08 nM) with a multi-channel pipette to wells in the absence or presence of nucleotide analogue, and the activity was monitored at 30 °C by the decrease in absorbance at 340 nm.

2.3 Antimicrobial Assays

The spot-on-lawn overlay method²²⁹ was used. Luria broth was used to grow *E. coli* DH5a, *Pseudomonas aeruginosa* ATCC 14207, *Salmonella typhimurium* ATCC 23564, and tryptic soy broth was used to grow *Staphylococcus aureus* ATCC 6538. A culture tube containing the liquid media (8.0 mL) was inoculated from a frozen stock solution of the bacterial strain, and all strains were incubated overnight at 37 °C. The dimethyl diesters were dissolved in EtOH/H₂O (2:1) and the lithium dicarboxylate salts were dissolved in H₂O. A 10 µL portion of a 20 mg/mL solution of the nucleotide

analogue was spotted on a solid agar plate and allowed to dry. A 100 μ L portion of the test organism from the overnight culture tube was added to a tube containing melted soft agar (40 °C), and after gentle vortexing, this was poured onto the agar plate. After allowing the agar to solidify, the plates were incubated overnight at 37 °C. Activity was detected by the appearance of a clear zone of growth inhibition.

3. Pediocin PA-1 Analogues

3.1 General Method for Solid Phase Peptide Syntheses (SPPS)

All peptides were manually synthesized using a 50 mL SPPS vessel equipped with a 3-way stop-cock and 'C' fritted ground glass joint. All peptides were prepared using L-configured amino acids with N-terminal 9*H*-fluorenylmethoxycarbonyl (Fmoc) protection on Wang²³⁰ or 2-chlorotrityl²³¹ resins. All amino acids were coupled using either benzotriazol-1-yl-oxy-tris-pyrrolidino-phosphonium hexafluorophosphate (PyBOP) or dicyclohexylcarbodiimide (DCC) as the activating agent, 1.1 equivalents of amino acid (relative to PyBOP), or 2.1 equivalents of amino acid (relative to DCC) and 2-3 h coupling times. For the coupling of successive amino acids to the resin using PyBOP, *N*-methylmorpholine (NMM) was added to the N-Fmoc protected amino acid (2.00 equiv. relative to resin) followed by PyBOP (1.96 equiv. relative to resin). The mixture was stirred for 10 min and added to the resin (previously swollen in DMF) and agitated with bubbling argon for 2-3 h. For the coupling of amino acids to the resin with DCC, the N-Fmoc amino acid (4.00 equiv. relative to resin) in CH₂Cl₂ was added to a solution of DCC (2.00 equiv. relative to resin) in CH₂Cl₂ at 0 °C. This mixture was

stirred for 20 min at 0 °C and concentrated *in vacuo*. The residue was taken up in DMF and added to the resin, which was then agitated with bubbling argon for 2-3 h. After coupling of the 20th amino acid, Fmoc removal was preceded each time by treatment of the resin-bound peptide with a solution of 0.8 M LiCl in DMF to disrupt aggregation due to hydrogen bonding. As well, all amino acid coupling reactions after residue 15 were performed in duplicate (double coupling).

The Kaiser test²³² for free amines was used to determine the completion of the reaction as follows. To a small sample of resin-bound peptide in a test tube was added 3 drops each of ninhydrin (5 g in 100 mL EtOH), 90% aqueous phenol (80 g in 20 mL EtOH), and KCN (2 mL of aqueous KCN in 98 mL pyridine). This mixture was then heated with a heat gun for several seconds. The presence of blue coloured beads (positive test) is an indication of the presence of free amine and thus incomplete coupling. The coupling procedure was repeated until no blue colour was observed in the resin beads. Once no colour was present in the beads (negative test), the resin-bound peptide was treated with 20% acetic anhydride (Ac₂O) in DMF to acetylate any remaining free amine. N-Terminal Fmoc removal from the resin-bound peptide was accomplished with a 20% solution of piperidine in DMF (3 x 5 min). The Kaiser test was used to determine the presence of free amine as described above, only in this instance coloured beads were desired (positive test).

3.2 Purification Techniques

Preparative reverse-phase HPLC was performed on a Gilson high performance liquid chromatograph equipped with a 322 pump, a single wavelength Gilson 151/152

UV/VIS, and a manual injector fitted with a 1 mL sample loop. UniPoint™ System Software was used to record and analyze the chromatograms. The column used for preparative HPLC was a Waters PrepLC 25 mm radial compression module with μ Bondapak™ C₁₈ (10 μ m, 125 Å, 25 x 100 mm) preparative packing. Analytical reverse-phase HPLC was performed either on the same Gilson system or on a Varian Prostar chromatograph equipped with model 210 pump heads, a model 325 dual wavelength UV detector, and a Rheodyne 7725i injector fitted with a 100 μ L sample loop. The column used was a Vydac C₁₈ Protein and Peptide steel walled column (5 μ m, 300 Å, 10 x 250 mm). The solvent systems used for peptide purification were as follows. System A: eluting with 20% MeCN/80% H₂O (0.1% TFA) for 5 min, then a gradient of 20-43% MeCN over 35 min. System B: eluting with 20% MeCN/80% H₂O (0.1% TFA) for 5 min, then a gradient of 20-40% MeCN over 30 min. System C: eluting with 20% MeCN/80% H₂O (0.1% TFA) for 5 min, then a gradient of 20-37% MeCN over 30 min. The peptides were monitored at 220 nm on the Gilson system, and at both 220 and 280 nm on the Varian system. All HPLC solvent systems were filtered through a Millipore filtration system under vacuum prior to use.

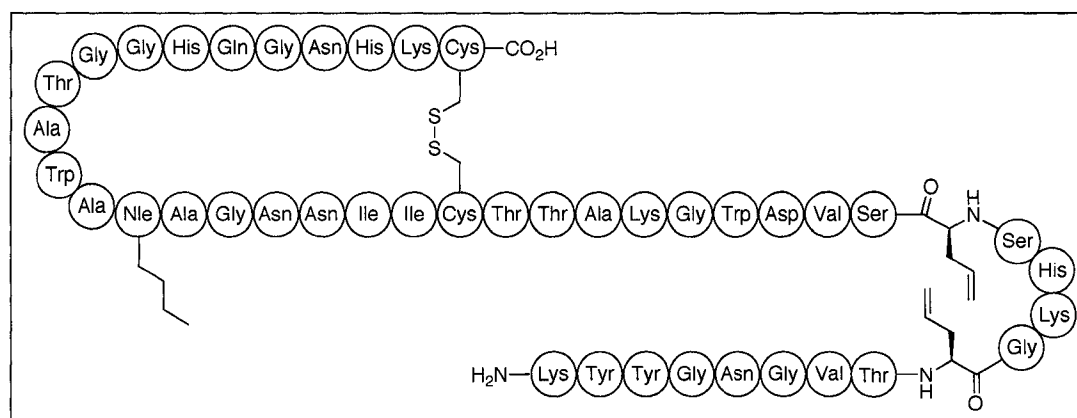
3.3 Instrumentation for Characterization

Samples for MALDI analysis were prepared using 3,5-dimethoxy-4-hydroxycinnamic acid (sinnapinic acid) as matrix. A solution of the sample peptide in 0.1% TFA (1 μ L) was mixed with an equal volume of a stock solution of sinnapinic acid (10 mg/mL) in 60% MeCN (0.1% TFA). A thin layer of sinnapinic acid was deposited on the surface of a stainless steel target plate by delivery of a small droplet (0.7 μ L) of a

solution containing sinnapinic acid (4 mg/mL) in acetone/MeOH (1:1). After evaporation of the solvent, a droplet of the solution containing the sample peptide-matrix mixture (0.4 μ L) was deposited on top of the fresh matrix layer. The solvent was evaporated at 1 atm prior to analysis. Mass spectra were recorded on a single stage reflectron, Applied BioSystems (Foster City, CA) Voyager Elite MALDI-TOF mass spectrometer. LC-MS/MS was performed on a Waters (Micromass) Q-TOF-Premier coupled with a Nano-Acquity UPLC system using a flow rate of 0.35 μ L/min.

3.4 Experimental Data for Compounds

9,14-Diallyl 31-butyl pediocin PA-1 (**210**)



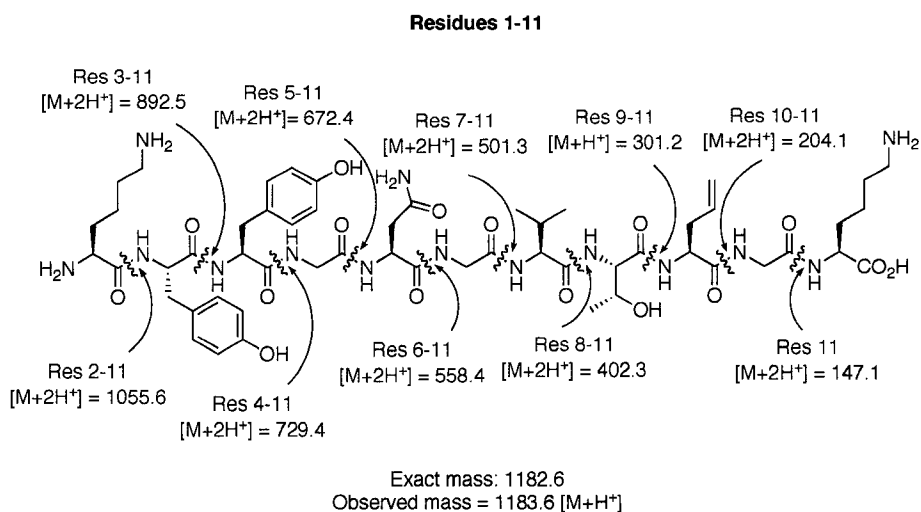
The linear precursor to **210** was synthesized on H-Cys(Trt)-2-chlorotrityl resin (1.93 g, 1.45 mmol) with 0.75 mmol/g loading. The second amino acid, Fmoc-Lys(Boc)-OH (450 mg, 0.960 mmol) was dissolved in DMF (10.0 mL), then PyBOP (490 mg, 0.940 mmol) and NMM (211 μ L, 1.92 mmol) were added. After 10 min, the mixture was added to the H-Cys(Trt)-2-chlorotrityl resin previously swollen in DMF, and the entire reaction mixture was agitated with bubbling argon for 2 h. It was then filtered and

washed with DMF (3 x 15 mL). The resin was treated with Ac₂O (20% in DMF, 20 mL) for 20 min to acetylate the remaining free amino groups and reduce the effective loading to 0.5 mmol/g. All other amino acids were coupled with PyBOP and NMM in the following order: Fmoc-His(Trt)-OH, Fmoc-Asn(Trt)-OH, Fmoc-Gly-OH, Fmoc-Gln(Trt)-OH, Fmoc-His(Trt)-OH, Fmoc-Gly-OH, Fmoc-Gly-OH, Fmoc-Ala-Thr($\Psi^{\text{Me,Me}}$ pro)-OH, Fmoc-Trp(Boc)-OH, Fmoc-Ala-OH, Fmoc-Nle-OH, Fmoc-Ala-OH, Fmoc-Gly-OH, Fmoc-Asn(Trt)-OH, Fmoc-Asn(Trt)-OH, Fmoc-Ile-OH, Fmoc-Ile-OH, Fmoc-Cys(Trt)-OH, Fmoc-Thr(*t*-Bu)-OH, Fmoc-Ala-Thr($\Psi^{\text{Me,Me}}$ pro)-OH, Fmoc-Lys(Boc)-OH, Fmoc-Gly-OH, Fmoc-Trp(Boc)-OH, Fmoc-Asp(*t*-Bu)-OH, Fmoc-Val-OH, Fmoc-Ser(*t*-Bu)-OH, Fmoc-AllGly-OH, Fmoc-Ser(*t*-Bu)-OH, Fmoc-His(Trt)-OH, Fmoc-Lys(Boc)-OH, Fmoc-Gly-OH, Fmoc-AllGly-OH, Fmoc-Val-Thr($\Psi^{\text{Me,Me}}$ pro)-OH, Fmoc-Gly-OH, Fmoc-Asn(Trt)-OH, Fmoc-Gly-OH, Fmoc-Tyr(*t*-Bu)-OH, Fmoc-Tyr(*t*-Bu)-OH, Fmoc-Lys(Boc)-OH. The N-terminal Fmoc group was removed by treatment of the resin-bound peptide with a 20% solution of piperidine in DMF (5 mL, 3 x 5 min), then the resin was washed several times with DMF, CH₂Cl₂, and MeOH. It was dried under a stream of argon for 1 h, then *in vacuo* for 16 h. Cleavage of the peptide from the resin and removal of the side chain protecting groups was accomplished by treatment with a freshly prepared solution of TFA/TIPSH/H₂O (95:2.5:2.5, v/v/v) for 4 h at rt with mechanical stirring. Filtration was followed by concentration of the filtrate *in vacuo* and precipitation with Et₂O. The crude peptide was dried *in vacuo* for 16 h. The 24,44-disulfide bond was formed by dissolving 32 mg of the crude peptide in TFE/H₂O (1:1, 100 mL) buffered to pH 7.6 with NH₄HCO₃ and bubbling O₂ through it for 16 h. After concentration *in vacuo*, the crude cyclized product was purified by reverse phase HPLC

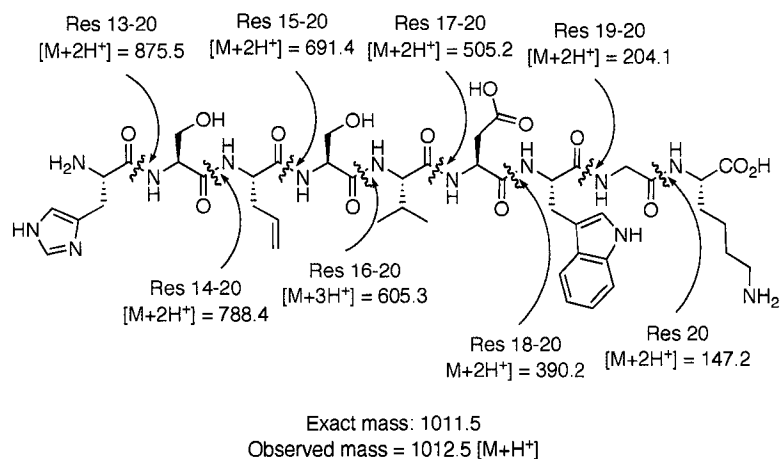
on a preparative C_{18} column using solvent system A at a flow rate of 10 mL/min. The desired peptide **210** was isolated as a broad peak (t_R 22.0 min). The fractions containing the peptide were concentrated *in vacuo* and re-injected on an analytical C_{18} column. Solvent system A was used again, except the flow rate was 1 mL/min. Pediocin PA-1 analogue **210** was isolated as a single peak (0.300 mg, 0.9% based on purification of 32.0 mg of dried crude product): MALDI-TOF MS calcd for $C_{201}H_{301}N_{61}O_{60}S_2$ 4596.0, found 4596.7 $[MH]^+$.

MS/MS analysis of residues 1-20 of **210**.

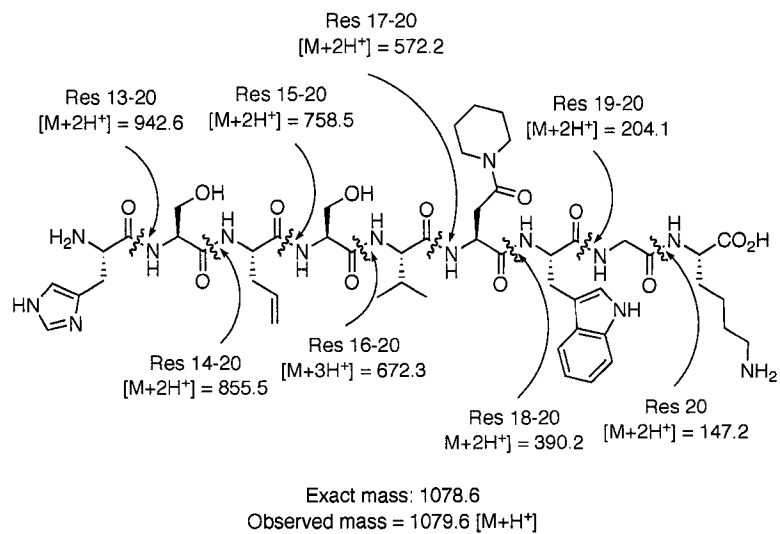
Pediocin PA-1 analogue **210** was treated with trypsin, which cleaves at the C-terminus of arginine and lysine. Fragments were obtained corresponding to residues 1-11, 2-11, 12-20, and 21-43. Residues 1-20 were successfully sequenced by MS/MS (see below). Attempted sequencing of residues 21-43 was unsuccessful.



Residues 12-20

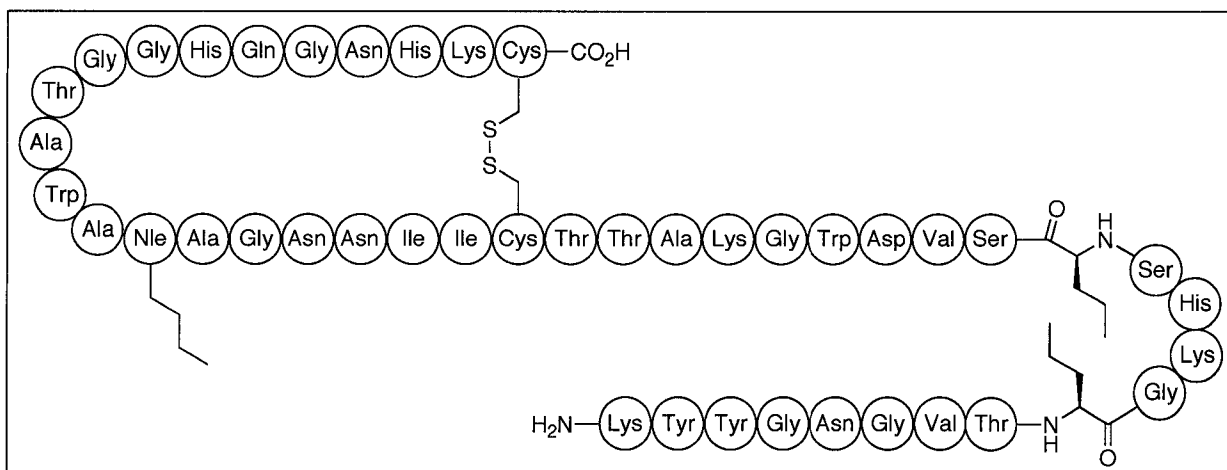


MS/MS analysis of residues 12-20 of transamidation product 230.



Solvent system A was used again, except the flow rate was 1 mL/min. Pediocin PA-1 analogue **211** was isolated as a broad peak (0.400 mg, ~75% pure as determined by analytical HPLC); MALDI-TOF MS calcd for C₂₀₉H₃₀₅N₆₁O₆₀S₂ 4696.2, found 4697.0 [MH]⁺.

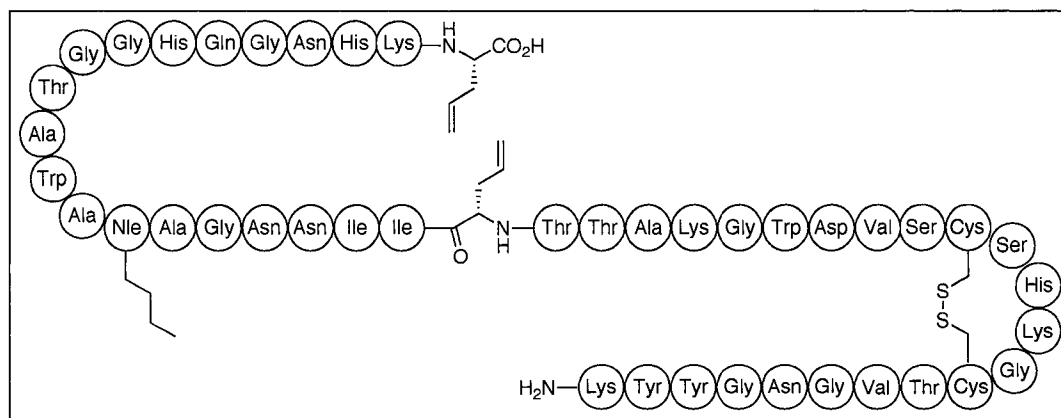
9,14-Dipropyl 31-butyl pediocin PA-1 (**212**)



This peptide was synthesized by SPPS using the same procedure as for the synthesis of **210**, except that Fmoc-Nva-OH was coupled instead of Fmoc-AllGly-OH at residues 9 and 14. The N-terminal Fmoc group was removed by treatment of the resin-bound peptide with a 20% solution of piperidine in DMF (5 mL, 3 x 5 min), then the resin was washed several times with DMF, CH₂Cl₂, and MeOH. It was dried under a stream of argon for 1 h, then *in vacuo* for 16 h. Cleavage of the peptide from the resin and removal of the side chain protecting groups was accomplished by treatment with a freshly prepared solution of TFA/TIPSH/H₂O (95:2.5:2.5, v/v/v) for 4 h at rt with mechanical stirring. Filtration was followed by concentration of the filtrate *in vacuo* and precipitation with Et₂O. The crude peptide was dried *in vacuo* for 16 h. The 24,44-

disulfide bond was formed by dissolving 25 mg of the crude peptide in TFE/H₂O (1:1, 70 mL) buffered to pH 7.6 with NH₄HCO₃ and bubbling O₂ through it for 15 h. After concentration *in vacuo*, the crude cyclized product was purified by reverse phase HPLC on a preparative C₁₈ column using solvent system A at a flow rate of 10 mL/min. The desired peptide **212** was isolated as a broad peak (*t_R* 25.5 min). The fractions containing the peptide were concentrated *in vacuo* and re-injected on an analytical C₁₈ column. Solvent system B was used, with a flow rate of 1 mL/min. Pediocin PA-1 analogue **212** was isolated as a broad peak (0.500 mg, ~75% pure as determined by analytical HPLC): MALDI-TOF MS calcd for C₂₀₁H₃₀₅N₆₁O₆₀S₂ 4600.1, found 4600.9 [MH]⁺.

24,44-Diallyl 31-butyl pediocin PA-1 (**213**)



The linear precursor to **213** was synthesized on Wang resin (750 mg, 0.80 mmol) with 1.1 mmol/g loading. The first amino acid, Fmoc-AllGly-OH (2.02 g, 6.00 mmol) was dissolved in CH₂Cl₂ (10.0 mL), then DCC (380 mg, 3.00 mmol) was added. The mixture was stirred at 0 °C for 20 min, then concentrated *in vacuo*. The residue was dissolved in DMF (10.0 mL), and the mixture was added to the Wang resin previously swollen in DMF. The reaction mixture was agitated with bubbling argon for 1 h. It was then

filtered and washed with DMF (3 x 15 mL). The resin was treated with Ac₂O (20% in DMF, 20 mL) for 20 min. All other amino acids were coupled with PyBOP and NMM in the following order: Fmoc-Lys(Boc)-OH, Fmoc-His(Trt)-OH, Fmoc-Asn(Trt)-OH, Fmoc-Gly-OH, Fmoc-Gln(Trt)-OH, Fmoc-His(Trt)-OH, Fmoc-Gly-OH, Fmoc-Gly-OH, Fmoc-Ala-Thr($\Psi^{\text{Me,Me}}$ pro)-OH, Fmoc-Trp(Boc)-OH, Fmoc-Ala-OH, Fmoc-Nle-OH, Fmoc-Ala-OH, Fmoc-Gly-OH, Fmoc-Asn(Trt)-OH, Fmoc-Asn(Trt)-OH, Fmoc-Ile-OH, Fmoc-Ile-OH, Fmoc-AllGly-OH, Fmoc-Thr(*t*-Bu)-OH, Fmoc-Ala-Thr($\Psi^{\text{Me,Me}}$ pro)-OH, Fmoc-Lys(Boc)-OH, Fmoc-Gly-OH, Fmoc-Trp(Boc)-OH, Fmoc-Asp(*t*-Bu)-OH, Fmoc-Val-OH, Fmoc-Ser(*t*-Bu)-OH, Fmoc-Cys(Trt)-OH, Fmoc-Ser(*t*-Bu)-OH, Fmoc-His(Trt)-OH, Fmoc-Lys(Boc)-OH, Fmoc-Gly-OH, Fmoc-Cys(Trt)-OH, Fmoc-Val-Thr($\Psi^{\text{Me,Me}}$ pro)-OH, Fmoc-Gly-OH, Fmoc-Asn(Trt)-OH, Fmoc-Gly-OH, Fmoc-Tyr(*t*-Bu)-OH, Fmoc-Tyr(*t*-Bu)-OH, Fmoc-Lys(Boc)-OH. The N-terminal Fmoc group was removed by treatment of the resin-bound peptide with a 20% solution of piperidine in DMF (5 mL, 3 x 5 min), then the resin was washed several times with DMF, CH₂Cl₂, and MeOH. It was dried under a stream of argon for 1 h, then *in vacuo* for 16 h. Cleavage of the peptide from the resin and removal of the side chain protecting groups was accomplished by treatment with a freshly prepared solution of TFA/TIPSH/H₂O (95:2.5:2.5, v/v/v) for 4 h at rt with mechanical stirring. Filtration was followed by concentration of the filtrate *in vacuo* and precipitation with Et₂O. The crude peptide was dried *in vacuo* for 16 h. The 9,14-disulfide bond was formed by dissolving 30 mg of the crude peptide in H₂O (100 mL) buffered to pH 7.6 with NH₄HCO₃ and bubbling O₂ through it for 16 h. After concentration *in vacuo*, the crude cyclized product was purified by reverse phase HPLC on a preparative C₁₈ column using solvent system A at a flow

rate of 10 mL/min. The desired peptide **213** was isolated as a broad peak (t_R 24.5 min). The fractions containing the peptide were concentrated *in vacuo* and re-injected on an analytical C₁₈ column. Solvent system C was used, with a flow rate of 1 mL/min. Pediocin PA-1 analogue **213** was isolated as a single peak (0.300 mg, 1.0% based on purification of 30.0 mg of dried crude product): MALDI-TOF MS calcd for C₂₀₁H₃₀₁N₆₁O₆₀S₂ 4596.0, found 4596.7 [MH]⁺.

3.5 Antimicrobial Assays

The spot-on-lawn overlay method was used. The known indicator organisms used were *Listeria monocytogenes* ATCC 43256 and *Carnobacterium divergens* LV13. A culture tube containing all-purpose tween (5.0 mL) was inoculated from a frozen stock solution of the bacterial strain. The tube containing *L. monocytogenes* ATCC 43256 was incubated overnight at 37 °C, and the tube containing *C. divergens* LV13 was incubated overnight at rt. A solution of pediocin PA-1 analogue in H₂O (10 µL) was spotted onto an APT agar plate using serial dilution series from 70 µM and allowed to dry. A 100 µL portion of the test organism from the overnight culture tube was added to a tube containing melted soft agar (40 °C), and after gentle vortexing, this was poured onto the agar plate. After allowing the agar to solidify, the plates were incubated overnight. Activity was detected by the appearance of a clear zone of growth inhibition.

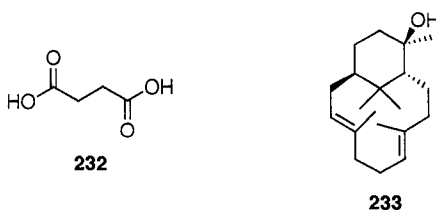
APPENDIX

Sciadopitys verticillata as a Potential Botanical Source of Baltic Amber: Summary of Extraction, Methanolysis, and GC-MS Studies

Objectives and Rationale for Experiments

This short study was conducted in collaboration with Dr. Karlis Muehlenbachs and Dr. Alexander Wolfe of the Department of Earth and Atmospheric Sciences at the University of Alberta. The objective of this study was to determine if the Japanese umbrella tree, *Sciadopitys verticillata*, is a potential candidate as a botanical source of Baltic amber. This was done through the search for two chemical markers, succinic acid (**232**) and verticillol (**233**). Baltic amber contains a high percentage of succinic acid, therefore its presence in high amounts in *Sciadopitys verticillata* would lend credence to its being the source of Baltic amber. Conversely, *Sciadopitys verticillata* is the only plant known to contain verticillol, therefore its detection in Baltic amber would strongly suggest this plant as the amber source.

Figure 1. Succinic acid (**232**) and verticillol (**233**).



Simple extraction of samples using Et₂O and/or MeOH was performed to separate the soluble portion of the material from the insoluble portion. In the case of Baltic amber, which is known to contain succinic acid,²³³ extraction was followed by treatment with diazomethane to yield dimethyl succinate. This facilitates GC-MS analysis because dimethyl succinate is more volatile than the parent diacid. All the extracted samples were analyzed by GC-MS to determine if verticillol was also present.

Methanolysis reactions of plant resin and needle extracts under basic and acidic conditions were performed to release any succinic acid that could be present as diterpenoid esters in the plant material. This is known to be the case for the ponderosa pine, *Pinus ponderosa*²³⁴, and as such this plant was used as a positive control. The basic methanolysis reactions were followed by diazomethane treatment to yield dimethyl succinate. The acidic methanolysis reaction gives dimethyl succinate directly.

1. Extraction and GC-MS analysis of Baltic amber

GC-MS analysis of the Et₂O extract of Baltic amber revealed that dimethyl succinate (obtained after methylation of endogenous succinic acid with diazomethane) was present in this material. This is in agreement with previous findings.²³³ Verticillol was not detected in the Baltic amber sample. It is worth noting that the alcohol functionality of verticillol should not be methylated by diazomethane as this process usually requires an additional catalyst such as boron trifluoride etherate. Given the extreme conditions under which Baltic amber is reported to form (oxidation, reduction, high temperatures and pressures), it must be acknowledged that even if *Sciadopitys verticillata* were the botanical source for Baltic amber, it would not be surprising if

verticillol in the original plant material were converted to a completely unrelated compound in the amber.

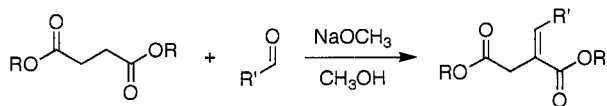
2. Extraction and GC-MS analysis of plant resins and needles

GC-MS analysis of the Et₂O extracts of the resins of *Sciadopitys verticillata* and *Pinus ponderosa* did not reveal any verticillol. However, after extraction of *Sciadopitys verticillata* needles with MeOH then Et₂O, GC-MS analysis did reveal verticillol to be present. Verticillol has previously been isolated from the seeds of *Sciadopitys verticillata*.²³⁵ Verticillol was not detected in the needle extract of *Pinus ponderosa*. Dimethyl succinate was not detected in any of the resin or needle extracts.

3. Basic methanolysis and GC-MS analysis of *Sciadopitys verticillata* and *Pinus ponderosa* resin extracts

Treatment of the resin extracts with methanolic NaOMe/MeOH by methylation with diazomethane did not yield any detectable dimethyl succinate upon GC-MS analysis. This result was somewhat surprising with respect to *Pinus ponderosa* as succinic acid had previously been isolated as a labdane diterpene ester from the needles of this plant.²³⁴ It is possible that the succinate being formed under basic conditions is reacting with any aldehydes present, a process known as the Stobbe condensation (Scheme 1). Based on this hypothesis, basic methanolysis of the samples was abandoned in favour of acidic methanolysis.

Scheme 1. Stobbe condensation between a succinate and an aldehyde



4. Acidic methanolysis and GC-MS analysis of *Sciadopitys verticillata* and *Pinus ponderosa* resin extracts

Treatment of the resin extracts from *Sciadopitys verticillata* and *Pinus ponderosa* with HCl/MeOH did not yield any detectable dimethyl succinate upon GC-MS analysis. However, the *Pinus ponderosa* sample was found to contain verticillol. It should be noted that a previous extensive study of *Pinus ponderosa* needles did not reveal any verticillol.²³⁴

5. Acidic methanolysis and GC-MS analysis of *Sciadopitys verticillata* and *Pinus ponderosa* needle extracts.

GC-MS analysis of the needle extract from *Sciadopitys verticillata* after acidic methanolysis indicated that verticillol was present in the sample, but dimethyl succinate was not detected. The *Pinus ponderosa* needle extract upon acidic methanolysis yielded dimethyl succinate as detected by GC-MS. This result is consistent with the previous isolation of labdane diterpene esters of succinic acid from *Pinus ponderosa* needles,²³⁴ and also verifies that the procedure employed is effective in releasing succinic acid from these endogenous esters.

Conclusions

From the results of the present study, it is not possible to establish *Sciadopitys verticillata* as the botanical source of Baltic amber. Neither was succinic acid detected in the resin and needle extracts of this species, nor was verticillol, known to be present in the plant, detected in Baltic amber. Table 1 provides a summary of the experiments performed and the results obtained.

Table 1. Summary of GC-MS results after extraction and methanolysis experiments.

Source	Procedure	GC-MS results
Baltic amber	A	Dimethyl succinate
<i>Sciadopitys verticillata</i> resin	B	-
<i>Sciadopitys verticillata</i> resin	B then D	-
<i>Sciadopitys verticillata</i> resin	B then E	-
<i>Pinus ponderosa</i> resin	B	-
<i>Pinus ponderosa</i> resin	B then D	-
<i>Pinus ponderosa</i> resin	B then E	Verticillol
<i>Sciadopitys verticillata</i> needles	C	Verticillol
<i>Sciadopitys verticillata</i> needles	C then E	Verticillol
<i>Pinus ponderosa</i> needles	C	-
<i>Pinus ponderosa</i> needles	C then E	Dimethyl succinate

Experimental Procedures

General

Removal of solvents *in vacuo* was carried out on a rotary evaporator with the water bath at room temperature. The samples were not placed under high vacuum to avoid evaporation of volatile components. Diazomethane was generated from diazald using the method described in the Aldrich Technical Bulletin, report AL-180. GC-MS analysis was performed on a 30 metre long ZB-5 column.

A. Extraction and methylation of Baltic amber

A published procedure²³³ was used. A sample of Baltic amber (193 mg) was crushed with a mortar and pestle and was extracted with Et₂O (4.0 mL) at 4 °C for 5 days. The mixture was then filtered through Celite, and the solvent removed *in vacuo* to give a clear yellow gum (27 mg). Of this, 16 mg was treated with diazomethane to give a yellow gum (14 mg) after solvent evaporation.

B. General procedure for extraction of plant resins

A sample of resin from either *Sciadopitys verticillata* or *Pinus ponderosa* was extracted with Et₂O at 4 °C for 24 h. The mixture was then filtered through Celite, and the solvent was removed *in vacuo* to give a pale orange gum.

C. General procedure for extraction of plant needles

Needles from either *Sciadopitys verticillata* or *Pinus ponderosa* were cut into 1-inch long pieces and frozen with liquid nitrogen in a mortar. The liquid nitrogen was allowed to evaporate, and the process was repeated. After the second evaporation, the frozen needles were ground to a fine powder with a pestle. The powder was stirred in MeOH (50.0 mL) for 1 h, then the MeOH was decanted. The powder was then stirred in Et₂O (50.0 mL) for 1 h. The MeOH and Et₂O extracts were combined and concentrated *in vacuo* to give a solid.

D. General procedure for basic methanolysis

To a flame-dried round bottom flask containing dry MeOH under argon was added sodium metal in small pieces to achieve a final concentration of approximately 4 M NaOMe. After the sodium was fully dissolved, a sample of resin or needle extract from *Sciadopitys verticillata* or *Pinus ponderosa* was added to the flask, and the mixture was stirred at rt for 24 h. It was then acidified to pH < 4.0 with 6 M HCl, and brine was added to promote separation of the layers. Et₂O was added, and any insoluble material present was filtered off. The layers were separated, and the aqueous layer was extracted three times with Et₂O. The combined organic layers were dried (Na₂SO₄) and concentrated *in vacuo*. The sample was then treated with diazomethane.

E. General procedure for acidic methanolysis

In a flame-dried round bottom flask under argon, a sample of resin or needle extract from *Sciadopitys verticillata* or *Pinus ponderosa* was stirred in a saturated

solution of HCl in MeOH at rt for 24 h. The mixture was then neutralized with a saturated solution of NaHCO₃, and the aqueous layer was extracted three times with Et₂O. The combined organic layers were dried (Na₂SO₄) and concentrated *in vacuo*.

REFERENCES

1. Lascu, I.; Gonin, P. The Catalytic Mechanism of Nucleoside Diphosphate Kinases. *J. Bioenerg. Biomembr.* **2000**, *32*, 237-246.
2. Biggs, J.; Hersperger, E.; Steeg, P. S.; Liotta, L. A.; Shearn, A. A *Drosophila* Gene that Is Homologous to a Mammalian Gene Associated with Tumor Metastasis Codes for a Nucleoside Diphosphate Kinase. *Cell* **1990**, *63*, 933-940.
3. Rosengard, A. M.; Krutzsch, H. C.; Shearn, A.; Biggs, J. R.; Barker, E.; Margulies, I. M. K.; Richter King, C.; Liotta, L. A.; Steeg, P. S. Reduced Nm23/Awd Protein in Tumor Metastasis and Aberrant *Drosophila* Development. *Nature* **1989**, *342*, 177-180.
4. De La Rosa, A.; Williams, R. L.; Steeg, P. S. Nm23/Nucleoside Diphosphate Kinases: Toward a Structural and Biochemical Understanding of Its Biological Functions. *BioEssays* **1995**, *17*, 53-62.
5. Leone, A.; Flatow, U.; Richter King, C.; Sandeen, M.-A.; Margulies, I. M. K.; Liotta, L. A.; Steeg, P. S. Reduced Tumor Incidence, Metastatic Potential, and Cytokine Responsiveness of *nm3*-Transfected Melanoma Cells. *Cell* **1991**, *65*, 25-35.
6. Lacombe, M. L.; Sastre-Garau, X.; Lascu, I.; Vonica, A.; Wallet, V.; Thiery, J. P.; Véron, M. Overexpression of Nucleoside Diphosphate Kinase (Nm23) in Solid Tumours. *Eur. J. Cancer* **1991**, *27*, 1302-1307.

7. Steeg, P. S.; De La Rosa, A.; Flatow, U.; MacDonald, N. J.; Benedict, M.; Leone, A. *Nm23 and Breast Cancer Metastasis. Breast Cancer Res. Treat.* **1993**, *25*, 175-187.
8. Chang, C. L.; Zhu, X.-X.; Thoraval, D. H.; Ungar, D.; Rawwas, J.; Hora, N.; Strahler, J. R.; Hanash, S. M.; Radany, E. *nm23-H1 Mutation in Neuroblastoma. Nature* **1994**, *370*, 335-336.
9. Keim, D.; Hailat, N.; Melhem, R.; Zhu, X. X.; Lascu, I.; Véron, M.; Strahler, J.; Hanash, S. M. Proliferation-Related Expression of p19/nm23 Nucleoside Diphosphate Kinase. *J. Clin. Invest.* **1992**, *89*, 919-924.
10. Yokoyama, A.; Okabe-Kado, J.; Sakashita, A.; Maseki, N.; Kaneko, Y.; Hino, K.; Tomoyasu, S.; Tsuruoka, N.; Kasukabe, T.; Honma, Y. Differentiation Inhibitory Factor *nm23* as a New Prognostic Factor in Acute Monocytic Leukemia. *Blood* **1996**, *88*, 3555-3561.
11. Stahl, J. A.; Leone, A.; Rosengard, A. M.; Porter, L.; Richter King, C.; Steeg, P. S. Identification of a Second Human *nm23* Gene, *nm23-H2*. *Cancer Res.* **1991**, *51*, 445-449.
12. Postel, E. H.; Berberich, S. J.; Flint, S. J.; Ferrone, C. A. Human *c-myc* Factor PuF Identified as *nm23-H2* Nucleoside Diphosphate Kinase, a Candidate Suppressor of Tumor Metastasis. *Science* **1993**, *261*, 478-480.
13. Marcu, K. B.; Bossone, S. A.; Patel, A. J. *myc* Function and Regulation. *Annu. Rev. Biochem.* **1992**, *61*, 809-860.

14. Agou, F.; Raveh, S.; Véron, M. The Binding Mode of Human Nucleoside Diphosphate Kinase B to Single-Strand DNA. *J. Bioenerg. Biomembr.* **2000**, *32*, 285-292.
15. Zhang, L.; Zhou, W.; Velculescu, V. E.; Kern, S. E.; Hruban, R. H.; Hamilton, S. R.; Vogelstein, B.; Kinzler, K. W. Gene Expression Profiles in Normal and Cancer Cells. *Science* **1997**, *276*, 1268-1272.
16. Lascu, I.; Giartosio, A.; Ransac, S.; Erent, M. Quaternary Structure of Nucleoside Diphosphate Kinases. *J. Bioenerg. Biomembr.* **2000**, *32*, 227-236.
17. Janin, J.; Dumas, C.; Moréra, S.; Xu, Y.; Meyer, P.; Chiadmi, M.; Cherfils, J. Three-Dimensional Structure of Nucleoside Diphosphate Kinase. *J. Bioenerg. Biomembr.* **2000**, *32*, 215-225.
18. Moréra, S.; Lascu, I.; Dumas, C.; LeBras, G.; Briozzo, P.; Véron, M.; Janin, J. Adenosine 5'-Diphosphate Binding and the Active Site of Nucleoside Diphosphate Kinase. *Biochemistry* **1994**, *33*, 459-467.
19. The figure was generated by Dr. Jonathan Parrish from the corresponding PDB file (1NDP) using MOLMOL (see Koradi, R.; Billeter, M.; Wüthrich, K. MOLMOL: A Program for Display and Analysis of Macromolecular Structures. *J. Mol. Graphics* **1996**, *14*, 51) and rendered using PovRay v3.6.
20. Hama, H.; Almaula, N.; Lerner, C. G.; Inouye, S.; Inouye, M. Nucleoside Diphosphate Kinase From *Escherichia coli*; Its Overproduction and Sequence Comparison with Eukaryotic Enzymes. *Gene* **1991**, *105*, 31-36.

21. Dumas, C.; Lascu, I.; Moréra, S.; Glaser, P.; Fourme, R.; Wallet, V.; Lacombe, M.-L.; Véron, M.; Janin, J. X-Ray Structure of Nucleoside Diphosphate Kinase. *EMBO J.* **1992**, *11*, 3203-3208.
22. Cherfils, J.; Moréra, S.; Lascu, I.; Véron, M.; Janin, J. X-Ray Structure of Nucleoside Diphosphate Kinase Complexed with Thymidine Diphosphate and Mg^{2+} at 2-Å Resolution. *Biochemistry* **1994**, *33*, 9062-9069.
23. Moréra, S.; Lascu, I.; Xu, Y. W.; Lacombe, M.-L.; LeBras, G.; Janin, J. X-Ray Structure of Human Nucleoside Diphosphate Kinase B Complexed with GDP at 2 Å Resolution. *Structure* **1995** *3*, 1307-1314.
24. Kuby, S. A.; Fleming, G.; Alber, T.; Richardson, D.; Takeneka, H.; Hamada, M. Studies on Yeast Nucleoside Triphosphate-Nucleoside Diphosphate Transphosphorylase (Nucleoside Diphosphokinase). 4. Steady-State Kinetic Properties with Thymidine Nucleotides (Including 3'-Azido-3'-Deoxythymidine Analogs). *Enzyme* **1991**, *45*, 1-13.
25. Bourdais, J.; Biondi, R.; Sarfati, S.; Guerreiro, C.; Lascu, I.; Janin, J.; Véron, M. Cellular Phosphorylation of Anti-HIV Nucleosides. *J. Biol. Chem.* **1996**, *271*, 7887-7890.
26. Schneider, B.; Xu, Y. W.; Sellam, O.; Sarfati, R.; Janin, J.; Véron, M.; Deville-Bonne, D. Pre-Steady State of Reaction of Nucleoside Diphosphate Kinase with Anti-HIV Nucleotides. *J. Biol. Chem.* **1998**, *273*, 11491-11497.
27. Strelkov, S. V.; Perisic, O.; Webb, P. A.; Williams, R. L. The 1.9 Å Crystal Structure of a Nucleoside Diphosphate Kinase Complex with Adenosine 3',5'-Cyclic

- Monophosphate: Evidence for Competitive Inhibition. *J. Mol. Biol.* **1995**, *249*, 665-674.
28. Schneider, B.; Xu, Y. W.; Janin, J.; Véron, M.; Deville-Bonne, D. 3'-Phosphorylated Nucleotides Are Tight Binding Inhibitors of Nucleoside Diphosphate Kinase Activity. *J. Biol. Chem.* **1998**, *273*, 28773-28778.
29. Klaassen, C. D.; Boles, J. W. The Importance of 3'-Phosphoadenosine 5'-Phosphosulfate (PAPS) in the Regulation of Sulfation. *FASEB J.* **1997**, *11*, 404-418.
30. Saeki, T.; Hori, M.; Umezawa, H. Kinetic Studies on the Inhibition of Nucleoside Diphosphate Kinase by Desdanine. *J. Biochem.* **1974**, *76*, 623-629.
31. Lascu, I.; Pop, R. D.; Porumb, H.; Presecan, E.; Proinov, I. Pig Heart Nucleosidediphosphate Kinase. Phosphorylation and Interaction with Cibacron Blue 3GA. *Eur. J. Biochem.* **1983**, *135*, 497-503.
32. Hemmerich, S.; Yarden, Y.; Pecht, I. A Cromoglycate Binding Protein From Rat Mast Cells of a Leukemia Line Is a Nucleoside Diphosphate Kinase. *Biochemistry* **1992**, *31*, 4574-4579.
33. Martin, M. W.; O'Sullivan, A. J.; Gomperts, B. D. Inhibition by Cromoglycate and Some Flavonoids of Nucleoside Diphosphate Kinase and of Exocytosis From Permeabilized Mast Cells. *Br. J. Pharmacol.* **1995**, *115*, (1080-1086).
34. Engel, R. Phosphonates as Analogues of Natural Phosphates. *Chem. Rev.* **1977**, *77*, 349-367.
35. Berkowitz, D. B.; Maiti, G.; Charette, B. D.; Dreis, C. D.; MacDonald, R. G. Mono- and Bivalent Ligands Bearing Mannose 6-Phosphate (M6P) Surrogates: Targeting the M6P/Insulin-Like Growth Factor II Receptor. *Org. Lett.* **2004**, *6*, 4921-4924.

36. Ghosh, P.; Dahms, N.; Kornfeld, S. Mannose 6-Phosphate Receptors: New Twists in the Tale. *Nat. Rev. Mol. Cell Biol.* **2003**, *4*, 202-213.
37. Tuck, K.; Saldanha, S. A.; Birch, L. M.; Smith, A. G.; Abell, C. The Design and Synthesis of Inhibitors of Pantothenate Synthase. *Org. Biomol. Chem.* **2006**, *4*, 3598-3610.
38. Vannada, J.; Bennett, E. M.; Wilson, D. J.; Boshoff, H. I.; Barry, I., C. E.; Aldrich, C. C. Design, Synthesis, and Biological Evaluation of β -Ketosulfonamide Adenylation Inhibitors as Potential Antitubercular Agents. *Org. Lett.* **2006**, *8*, 4707-4710.
39. Vergne, A. F.; Walz, A. J.; Miller, M. J. Iron Chelators From Mycobacteria (1954-1999) and Potential Therapeutic Applications. *Nat. Prod. Rep.* **2000**, *17*, 99-116.
40. Krithika, R.; Marathe, U.; Saxena, P.; Ansari, M. Z.; Mohanty, D.; Gokhale, R. S. A. Genetic Locus Required for Iron Acquisition in *Mycobacterium tuberculosis*. *Proc. Natl. Acad. Sci. U. S. A.* **2006**, *103*, 2069-2074.
41. Jeanjean, A.; Garcia, M.; Leydet, A.; Montero, J.-L.; Morère, A. Synthesis and Receptor Binding Affinity of Carboxylate Analogues of the Mannose 6-Phosphate Recognition Marker. *Bioorg. Med. Chem.* **2006**, *14*, 3575-3582.
42. Burke, J., T. R.; Lee, K. Phosphotyrosyl Mimetics in the Development of Signal Transduction Inhibitors. *Acc. Chem. Res.* **2003**, *36*, 426-433.
43. Larsen, S. D.; Barf, T.; Liljebris, C.; May, P. D.; Ogg, D.; O'Sullivan, T. J.; Palazuk, B. J.; Schostarez, H. J.; Stevens, F. C.; Bleasdale, J. E. Synthesis and Biological Activity of a Novel Class of Small Molecular Weight Peptidomimetic Competitive Inhibitors of Protein Tyrosine Phosphatase 1B. *J. Med. Chem.* **2002**, *45*, 598-622.

44. Gao, Y.; Luo, J.; Yao, Z.-J.; Guo, R.; Zou, H.; Kelley, J.; Voigt, J. H.; Yang, D.; Burke, J., T. R. Inhibition of Grb2 SH2 Domain Binding by Non-Phosphate-Containing Ligands. 2. 4-(2-Malonyl)phenylalanine as a Potent Phosphotyrosyl Mimetic. *J. Med. Chem.* **2000**, *43*, 911-920.
45. Fisher, J. E.; Rogers, M. J.; Halasy, J. M.; Luckman, S. P.; Hughes, D. E.; Masarachia, P. J.; Wesolowski, G.; Russell, R. G. G.; Rodan, G. A.; Reszka, A. A. Alendronate Mechanism of Action: Geranylgeraniol, an Intermediate in the Mevalonate Pathway, Prevents Inhibition of Osteoclast Formation, Bone Resorption, and Kinase Activation *in vivo*. *Proc. Natl. Acad. Sci. U. S. A.* **1999**, *96*, 133-138.
46. Bergstrom, J. D.; Bostedor, R. G.; Masarachia, P. J.; Reszka, A. A.; Rodan, G. Alendronate Is a Specific, Nanomolar Inhibitor of Farnesyl Diphosphate Synthase. *Arch. Biochem. Biophys.* **2000**, *373*, 231-241.
47. Tanner, M. E. The Enzymes of Sialic Acid Biosynthesis. *Bioorg. Chem.* **2005**, *33*, 216-228.
48. Harpaz, N.; Schacter, H. Control of Glycoprotein Synthesis. Processing of Asparagine-Linked Oligosaccharides by One or More Rat Liver Golgi α -D-Mannosidases Dependent on the Prior Action of UDP-N-Acetylglucosamine: α -D-Mannoside β 2-N-Acetylglucosaminyltransferase I. *J. Biol. Chem.* **1980**, *255*, 4894-4902.
49. Sarkar, M.; Hull, E.; Nishikawa, Y.; Simpson, R. J.; Moritz, R. L.; Dunn, R.; Schachter, H. Molecular Cloning and Expression of cDNA Encoding the Enzyme That Controls Conversion of High-Mannose to Hybrid and Complex N-Glycans:

- UDP-*N*-Acetylglucosamine: α -3-D-Mannoside β -1,2-*N*-Acetylglucosaminyltransferase I. *Proc. Natl. Acad. Sci. U. S. A.* **1991**, *88*, 234-238.
50. Munro, C. A.; Gow, N. A. R. Chitin Synthesis in Human Pathogenic Fungi. *Med. Mycol.* **2001**, *39*, 41-53.
51. Kimura, K.; Bugg, T. D. H. Recent Advances in Antimicrobial Nucleoside Antibiotics Targeting Cell Wall Biosynthesis. *Nat. Prod. Rep.* **2003**, *20*, 252-273.
52. Stolz, F.; Reiner, M.; Reutter, W.; Schmidt, R. R. Novel UDP-Glycol Derivatives as Transition State Analogue Inhibitors of UDP-GlcNAc 2-Epimerase. *J. Org. Chem.* **2004**, *69*, 665-679.
53. Gordon, R. D.; Sivarajah, P.; Satkunarajah, M.; Ma, D.; Tarling, C. A.; Vitzu, D.; Withers, S. G.; Rini, J. M. X-ray Crystal Structures of Rabbit *N*-Acetylglucosaminyltransferase in Complex With Donor Substrate Analogues. *J. Mol. Biol.* **2006**, *360*, 67-79.
54. Chang, R.; Vo, T.-T.; Finney, N. S. Synthesis of the *CI*-Phosphonate Analogue of UDP-GlcNAc. *Carbohydr. Res.* **2006**, *341*, 1998-2004.
55. Heifetz, A.; Keeman, R. W.; Elbein, A. D. Mechanism of Action of Tunicamycin on the UDP-GlcNAc:Dolichyl-Phosphate GlcNAc-1-Phosphate Transferase. *Biochemistry* **1979**, *18*, 2186-2192.
56. Wang, R.; Steensma, D. H.; Takaoka, Y.; Yun, J. W.; Kajimoto, T.; Wong, C.-H. A Search for Pyrophosphate Mimics for the Development of Substrates and Inhibitors of Glycosyltransferases. *Bioorg. Med. Chem.* **1997**, *5*, 661-672.

57. Ballell, L.; Young, R. J.; Field, R. A. Synthesis and Evaluation of Mimetics of UDP and UDP- α -D-Galactose, dTDP and dTDP- α -D-glucose with Monosaccharides Replacing the Key Pyrophosphate Unit. *Org. Biomol. Chem.* **2005**, *3*, 1109-1115.
58. Singh, S. B.; Zink, D. L.; Liesch, J. M.; Goetz, M. A.; Jenkins, R. G.; Nallin-Omstead, M.; Silverman, K. C.; Bills, G. F.; Mosley, R. T.; Gibbs, J. B.; Albers-Schonberg, G.; Lingham, R. B. Isolation and Structure of Chaetomelic Acids A and B from *Chaetomella acutiseta*: Farnesyl Pyrophosphate Mimic Inhibitors of Ras Farnesyl-Protein Transferase. *Tetrahedron* **1993**, *49*, 5917-5926.
59. Lingham, R. B.; Silverman, K. C.; Bills, G. F.; Cascales, C.; Sanchez, M.; Jenkins, R. G.; Gartner, S. E.; Martin, I.; Diez, M. T.; Pelaéz, F.; Mochales, S.; Kong, Y.-L.; Burg, R. W.; Meinz, M. S.; Huang, L.; Nallin-Omstead, M.; Mosser, S. D.; Schaber, M. D.; Omer, C. A.; Pompliano, D. L.; Gibbs, J. B.; Singh, S. B. *Chaetomella acutiseta* Produces Chaetomelic Acids A and B which Are Reversible Inhibitors of Farnesyl-Protein Transferase. *Appl. Microbiol. Biotechnol.* **1993**, *40*, 370-374.
60. Singh, S. B.; Jayasuriya, H.; Silverman, K. C.; Bonfiglio, C. A.; Williamson, J. M.; Lingham, R. B. Efficient Syntheses, Human and Yeast Farnesyl-Protein Transferase Inhibitory Activities of Chaetomelic Acids and Analogues. *Bioorg. Med. Chem.* **2000**, *8*, 571-580.
61. Ratemi, E. S.; Dolence, J. M.; Poulter, C. D.; Vederas, J. C., Synthesis of Protein Farnesyltransferase and Protein Geranylgeranyltransferase Inhibitors: Rapid Access to Chaetomelic Acid A and Its Analogues. *J. Org. Chem.* **1996**, *61*, 6296-6301.

62. Mau, C. J. D.; Garneau, S.; Scholte, A. A.; Van Fleet, J. E.; Vederas, J. C.; Cornish, K. Protein Farnesyltransferase Inhibitors Interfere With Farnesyl Diphosphate Binding by Rubber Transferase. *Eur. J. Biochem.* **2003**, *270*, 3939-3945.
63. Singh, S. B.; Liesch, J. M.; Lingham, R. B.; Goetz, M. A.; Gibbs, J. B. Actinoplanic Acid A: A Macrocyclic Polycarboxylic Acid which Is a Potent Inhibitor of Ras Farnesyl-Protein Transferase. *J. Am. Chem. Soc.* **1994**, *116*, 11606-11607.
64. Silverman, K. C.; Cascales, C.; Genilloud, O.; Sigmund, J. M.; Gartner, S. E.; Koch, G. E.; Gagliardi, M. M.; Heimbuch, B. K.; Nallin-Omstead, M.; Sanchez, M.; Diez, M. T.; Martin, I.; Garrity, G. M.; Hirsch, C. F.; Gibbs, J. B.; Singh, S. B.; Lingham, R. B. Actinoplanic Acids A and B as Novel Inhibitors of Farnesyl Transferase. *Appl. Microbiol. Biotechnol.* **1995**, *43*, 610-616.
65. Singh, S. B.; Liesch, J. M.; Lingham, R. B.; Silverman, K. C.; Sigmund, J. M.; Goetz, M. A. Structure, Chemistry, and Biology of Actinoplanic Acids: Potent Inhibitors of Ras Farnesyl-Protein Transferase. *J. Org. Chem.* **1995**, *60*, 7896-7901.
66. Cheng, X.-C.; Kihara, T.; Kusakabe, H.; Magae, J.; Kobayashi, Y.; Fang, R.-P.; Ni, Z.-F.; Shen, Y.-C.; Ko, K.; Yamaguchi, I.; Isono, K. A New Antibiotic, Tautomycin. *J. Antibiot.* **1987**, *40*, 907-909.
67. Ubukata, M.; Cheng, X.-C.; Isono, K. The Structure of Tautomycin, a Regulator of Eukaryotic Cell Growth. *J. Chem. Soc., Chem. Commun.* **1990**, 244-246.
68. Ubukata, M.; Cheng, X.-C.; Isobe, M.; Isono, K. Absolute Configuration of Tautomycin, a Protein Phosphatase Inhibitor from a Streptomycete. *J. Chem. Soc., Perkin Trans. 1* **1993**, 617-624.

69. Gallego, M.; Virshup, D. M. Protein Serine/Threonine Phosphatases: Life, Death, and Sleeping. *Curr. Op. Cell Biol.* **2005**, *17*, 197-202.
70. Sugiyama, Y.; Ohtani, I. I.; Isobe, M.; Takai, A.; Ubukata, M.; Isono, K. Molecular Shape Analysis and Activity of Tautomycin, a Protein Phosphatase Inhibitor. *Bioorg. Med. Chem. Lett.* **1996**, *6*, 3-8.
71. Sheppeck, I., J. E.; Liu, W.; Chamberlin, A. R. Total Synthesis of the Serine/Threonine-Specific Protein Phosphatase Inhibitor Tautomycin. *J. Org. Chem.* **1997**, *62*, 387-398.
72. Li, Y.-M.; Casida, J. E. Cantharidin-Binding Protein: Identification as Protein Phosphatase 2A. *Proc. Natl. Acad. Sci. U. S. A.* **1992**, *89*, 11867-11870.
73. Honkanen, R. E. Cantharidin, Another Natural Toxin that Inhibits the Activity of Serine/Threonine Protein Phosphatases Types 1 and 2A. *FEBS Lett.* **1993**, *330*, 283-286.
74. Baba, Y.; Hirukawa, N.; Tanohira, N.; Sodeoka, M. Structure-Based Design of a Highly Selective Catalytic Site-Directed Inhibitor of Ser/Thr Protein Phosphatases 2B (Calcineurin). *J. Am. Chem. Soc.* **2003**, *125*, 9740-9749.
75. Dabrah, T. T.; Harwood, H. J.; Huang, L. H.; Jankovich, N. D.; Kaneko, T.; Li, J.-C.; Lindsey, S.; Moshier, P. M.; Subashi, T. A.; Therrien, M.; Watts, P. C. CP-225,917 and CP-263,114, Novel Ras Farnesylation Inhibitors from an Unidentified Fungus. 1. Taxonomy, Fermentation, Isolation, and Biochemical Properties. *J. Antibiot.* **1997**, *50*, 1-7.

76. Dabrah, T. T.; Kaneko, T.; Masefski, J., W.; Whipple, E. B. CP-225,917 and CP-263,114: Novel Ras Farnesylation Inhibitors from an Unidentified Fungus. 2. Structure Elucidation. *J. Am. Chem. Soc.* **1997**, *119*, 1594-1598.
77. Tansey, T. R.; Shechter, I. Structure and Regulation of Mammalian Squalene Synthase. *Biochim. Biophys. Acta* **2000**, *1529*, 49-62.
78. Watanabe, S.; Hirai, H.; Kambara, T.; Kojima, Y.; Nishida, H.; Sugiura, A.; Yamauchi, Y.; Yoshikawa, N.; Harwood, J., H. J.; Huang, L. H.; Kojima, N. CJ-13,981 and CJ-13,982, New Squalene Synthase Inhibitors. *J. Antibiot.* **2001**, *54*, 10025-11030.
79. Koert, U. Total Syntheses of Zaragozic Acid. *Angew. Chem. Int. Ed. Engl.* **1995**, *34*, 773-778.
80. Lindsey, S.; Harwood, J., H. J. Inhibition of Mammalian Squalene Synthetase Activity by Zaragozic Acid A Is a Result of Competitive Inhibition Followed by Mechanism-Based Irreversible Inactivation. *J. Biol. Chem.* **1995**, *270*, 9083-9096.
81. Scholte, A. A.; Eubanks, L. M.; Poulter, C. D.; Vederas, J. C. Synthesis and Biological Activity of Isopentenyl Diphosphate Analogues. *Bioorg. Med. Chem.* **2004**, *12*, 763-770.
82. Garneau, S.; Qiao, L.; Chen, L.; Walker, S.; Vederas, J. C. Synthesis of Mono- and Disaccharide Analogs of Moenomycin and Lipid II for Inhibition of Transglycosylase Activity of Penicillin-Binding Protein 1b. *Bioorg. Med. Chem.* **2004**, *12*, 6473-6494.
83. Lu, X.; Zhang, C.; Xu, Z. Reactions of Electron-Deficient Alkynes and Allenes Under Phosphine Catalysis. *Acc. Chem. Res.* **2001**, *34*, 535-544.

84. Volkov, A. N.; Volkova, K. A. α,β -Acetylenic Acids and their Derivatives in Reactions with Hydrogen Sulfide and Thiols. *Russ. J. Gen. Chem.* **2004**, *74*, 350-367.
85. Kamimura, A. Recent Developments on the Michael Addition of Sulfur and Selenium Nucleophiles. *J. Synth. Org. Chem. Jpn.* **2004**, *62*, 705-715.
86. Yamamoto, Y.; Yatagai, H.; Maruyama, K. Stereocontrolled *cis* Addition of Organocopper Reagents RCuBr'_3 to α,β -Acetylenic Carbonyl Compounds. *J. Org. Chem.* **1979**, *44*, 1744-1746.
87. Nishiyama, H.; Sasaki, M.; Itoh, K. Stereoselective Addition of Readily Available Organocopper Reagents to Dimethyl Acetylene Dicarboxylate. *Chem. Lett.* **1981**, 905-908.
88. Mongrain, C.; Gaudreault, R. C. Synthesis of Mono and Disubstituted Maleic Anhydrides from Di-*tert*-Butyl Acetylene Dicarboxylate. *Synth. Commun.* **1990**, *20*, 2491-2500.
89. Chapdelaine, M. J.; Hulce, M. Tandem Vicinal Difunctionalization: β -Addition to α,β -Unsaturated Carbonyl Substrates Followed by α -Functionalization. *Org. React.* **1990**, *38*, 225-654.
90. Kennedy, J. W. J.; Hall, D. G. Lewis Acid Catalyzed Allylboration: Discovery, Optimization, and Application to the Formation of Stereogenic Quaternary Carbon Centers. *J. Org. Chem.* **2004**, *69*, 4412-4428.
91. Inanaga, J.; Baba, Y.; Hanamoto, T. Organic Synthesis with Trialkylphosphine Catalysts. Conjugate Addition of Alcohols to α,β -Unsaturated Alkynic Acid Esters. *Chem. Lett.* **1993**, 241-244.

92. Paintner, F. F.; Metz, M.; Bauschke, G. A New, General Entry to 3,5-Unsubstituted 4-*O*-Alkyl Tetramates. *Synthesis* **2002**, 869-874.
93. Wabnitz, T. C.; Spencer, J. B. A General Brønsted Acid-Catalyzed Hetero-Michael Addition of Nitrogen, Oxygen, and Sulfur Nucleophiles. *Org. Lett.* **2003**, 5, 2141-2144.
94. Shaw, M. A.; Tebby, J. C.; Ward, R. S.; Williams, D. H. Reactions of Phosphines with Acetylenes. Part VI. 2-Phosphoniaethanesulfonate Betaines. The Sulfonation of Vinyl Phosphonium Salts. *J. Chem. Soc. (C)* **1968**, 2795-2799.
95. Lowe, G.; Ridley, D. D. Synthesis of β -Lactams by Photolytic Wolff Rearrangement. *J. Chem. Soc. Perkin Trans. 1* **1973**, 2024-2029.
96. Quartey, E. G. K.; Peters, J. A.; van Belkum, H.; Anthonsen, T., LaIII-Induced Addition of Tetrahydrofurfuryl Alcohol, Tetrahydropyran-2-ylmethanol, D-Gluconate, Methanol, and Ethanol to Maleate. *Acta Chem. Scand.* **1996**, 50, 825-831.
97. Mitsunobu, O. The Use of Diethyl Azodicarboxylate and Triphenylphosphine in Synthesis and Transformation of Natural Products. *Synthesis* **1981**, 1-28.
98. Pignot, M.; Pljevaljic, G.; Weinhold, E. Efficient Synthesis of *S*-Adenosyl-L-Homocysteine Natural Product Analogues and their Use to Elucidate the Structural Determinant for Cofactor Binding of the DNA Methyltransferase M *Hha*I. *Eur. J. Org. Chem.* **2000**, 549-555.
99. Wallace, O. B.; Springer, D. M. Mild, Selective Deprotection of Thioacetates using Sodium Thiomethoxide. *Tetrahedron Lett.* **1998**, 39, 2693-2694.

100. Journet, M.; Rouillard, A.; Cai, D.; Larsen, R. D. Double Radical Cyclization/ β -Fragmentation of Acyclic ω -Yne Vinyl Sulfides. Synthesis of 3-Vinyldihydrothiophene and Dihydropyran Derivatives. A New Example of a 5-*endo-trig* Radical Cyclization. *J. Org. Chem.* **1997**, *62*, 8630-8631.
101. Hedaya, E.; Theodoropoulos, S. The Preparation and Reactions of Stable Phosphorus Ylides Derived From Maleic Anhydrides, Maleimides or Isomaleimides. *Tetrahedron* **1968**, *24*, 2241-2254.
102. Frigerio, M.; Santagostino, M.; Sputore, S. A User-Friendly Entry to 2-Iodoxybenzoic Acid (IBX). *J. Org. Chem.* **1999**, *64*, 4537-4538.
103. Lerner, C.; Masjost, B.; Ruf, A.; Gramlich, V.; Jakob-Roetne, R.; Zürcher, G.; Borroni, E.; Diederich, F. Bisubstrate Inhibitors for the Enzyme Catechol-*O*-Methyltransferase (COMT): Influence of Inhibitor Preorganization and Linker Length Between the Two Substrate Moieties on Binding Affinity. *Org. Biomol. Chem.* **2003**, *1*, 42-49.
104. Hayakawa, H.; Haraguchi, K.; Tanaka, H.; Miyasaka, T., Direct C-8 Lithiation of Naturally-Occurring Purine Nucleosides. A Simple Method for the Synthesis of 8-Carbon-Substituted Purine Nucleosides. *Chem. Pharm. Bull.* **1987**, *35*, 72-79.
105. Fraser, R. R.; Mansour, T. S. Acidity Measurements with Lithiated Amines: Steric Reduction and Electronic Enhancement of Acidity. *J. Org. Chem.* **1984**, *49*, 3442-3443.
106. Menzel, K.; Fu, G. C. Room-Temperature Stille Cross-Couplings of Alkenyltin Reagents and Functionalized Alkyl Bromides that Possess β Hydrogens. *J. Am. Chem. Soc.* **2003**, *125*, 3718-3719.

107. Rossi, R.; Carpita, A.; Cossi, P. New Stereoselective Syntheses of Stereodefined 2-Substituted Alkyl 2-Alkenoates and their Applications. *Tetrahedron* **1992**, *48*, 8801-8824.
108. Zhang, H. X.; Guibé, F.; Balavoine, G. Palladium Catalyzed Hydrostannation of Alkynes and Palladium-Catalyzed Hydrostannolysis of Propargyl or Propargyloxycarbonyl Derivatives of Various Functional Groups. *Tetrahedron Lett.* **1988**, *29*, 619-622.
109. Leusink, A. J.; Budding, H. A.; Marsman, J. W. Studies in Group 4 Organometallic Chemistry. 24. Structure of Products Obtained in Hydrostannation of Ethynes. *J. Organomet. Chem.* **1967**, *9*, 285-291.
110. Mee, S. P. H.; Lee, V.; Baldwin, J. E. Stille Coupling Made Easier - The Synergistic Effect of Copper(I) Salts and the Fluoride Ion. *Angew. Chem. Int. Ed.* **2004**, *43*, 1132-1136.
111. Farina, V.; Krishnamurthy, V.; Scott, W. J. The Stille Reaction. *Org. React.* **1997**, *50*, 1-652.
112. Knochel, P.; Singer, R. D. Preparation and Reactions of Polyfunctional Organozinc Reagents in Organic Synthesis. *Chem. Rev.* **1993**, *93*, 2117-2188.
113. Knochel, P.; Yeh, M. C. P.; Berk, S. C.; Talbert, J. Synthesis and Reactivity Toward Acyl Chlorides and Enones of the New Highly Functionalized Copper Reagents R₂Cu(CN)ZnI. *J. Org. Chem.* **1988**, *53*, 2390-2392.
114. Retherford, C.; Chou, T.-S.; Schelkum, R. M.; Knochel, P. Preparation and Reactivity of β -Zinc Copper Enolates. *Tetrahedron Lett.* **1990**, *31*, 1833-1836.

115. Knoess, H. P.; Furlong, M. T.; Rozema, M. J.; Knochel, P. Preparation and Reactions of Zinc and Copper Organometallics Bearing Acidic Hydrogens. *J. Org. Chem.* **1991**, *56*, 5974-5978.
116. Rieke, R. D.; Li, P. T.-J.; Burns, T. P.; Uhm, S. T. Preparation of Highly Reactive Metal Powders. A New Procedure for the Preparation of Highly Reactive Zinc and Magnesium Metal Powders. *J. Org. Chem.* **1981**, *46*, 4323-4324.
117. Erdik, E. Use of Activation Methods for Organozinc Reagents. *Tetrahedron* **1987**, *43*, 2203-2212.
118. Feldhues, M.; Schäfer, H. J. Selective Mixed Coupling of Carboxylic Acids (I). - Electrolysis, Thermolysis, and Photolysis of Unsymmetrical Diacyl Peroxides with Acyclic and Cyclic Alkyl Groups. *Tetrahedron* **1985**, *41*, 4195-4212.
119. Feldhues, M.; Schäfer, H. J. Selective Mixed Coupling of Carboxylic Acids (II). - Photolysis of Unsymmetrical Diacylperoxides with Alkenyl-, Halo-, Keto-, Carboxyl-Groups and a Chiral α -Carbon. Comparison with the Mixed Kolbe Electrolysis. *Tetrahedron* **1985**, *41*, 4213-4235.
120. Feldhues, M.; Schäfer, H. J. Selective Coupling of Carboxylic Acids - III. Synthesis of Cyclopentadecanone from Cyclic Tetraacyl Diperoxides. *Tetrahedron* **1986**, *42*, 1285-1290.
121. Lomölder, R.; Schäfer, H. J. Low-Temperature Photolysis of Peracetylated Dodecanoyl Peroxides of Tartaric Acid and D-Gluconic Acid in the Solid State - A Diastereoselective Radical Coupling. *Angew. Chem. Int. Ed.* **1987**, *26*, 1253-1254.

122. Spantulescu, M. D.; Jain, R. P.; Derksen, D. J.; Vederas, J. C. Photolysis of Diacyl Peroxides: A Radical-Based Approach for the Synthesis of Functionalized Amino Acids. *Org. Lett.* **2003**, *5*, 2963-2965.
123. Jain, R. P.; Vederas, J. C. Synthesis of β -Cyclopropylalanines by Photolysis of Diacyl Peroxides. *Org. Lett.* **2003**, *5*, 4669-4672.
124. Veysoglu, T.; Mitscher, L. A.; Swayze, J. K. A Convenient Method for the Control of Selective Ozonizations of Olefins. *Synthesis* **1980**, 807-810.
125. Kar, A.; Argade, N. P. A Facile Access to Natural and Unnatural Dialkylsubstituted Maleic Anhydrides. *Tetrahedron* **2003**, *59*, 2991-2998.
126. Murray, R. W.; Agarwal, S. K. Ozonolysis of Some Tetrasubstituted Ethylenes. *J. Org. Chem.* **1985**, *50*, 4698-4702.
127. Dussault, P.; Sahli, A. 2-Methoxyprop-2-yl Hydroperoxide: A Convenient Reagent for the Synthesis of Hydroperoxides and Peracids. *J. Org. Chem.* **1992**, *57*, 1009-1012.
128. Schreier, W. J.; Schrader, T. E.; Koller, F. O.; Gilch, P.; Crespo-Hernández, C. E.; Swaminathan, V. N.; Carell, T.; Zinth, W.; Kohler, B. Thymine Dimerization in DNA Is an Ultrafast Photoreaction. *Science* **2007**, *315*, 625-629.
129. Grubbs, R. H. Olefin Metathesis. *Tetrahedron* **2004**, *60*, 7117-7140.
130. Astruc, D. The Metathesis Reactions: From a Historical Perspective to Recent Developments. *New J. Chem.* **2006**, *29*, 42-56.
131. Chatterjee, A. K.; Choi, T.-L.; Sanders, D. P.; Grubbs, R. H. A General Model for Selectivity in Olefin Cross Metathesis. *J. Am. Chem. Soc.* **2003**, *125*, 11360-11370.

132. Sajiki, H.; Kuno, H.; Hirota, K. Suppression Effect of the Pd/C-Catalyzed Hydrogenolysis of a Phenolic Benzyl Protective Group by the Addition of Nitrogen-Containing Bases. *Tetrahedron Lett.* **1998**, *39*, 7127-7130.
133. Dzubeck, V.; Schneider, J. P. One-Pot Conversion of Benzyl Carbamates into Fluorenylmethyl Carbamates. *Tetrahedron Lett.* **2000**, *41*, 9953-9956.
134. Alder, V. K.; Brachel, H. V. Beiträge Zur Kenntnis Der En-Synthese. *Justus. Liebigs. Ann. Chem.* **1962**, *651*, 141-153.
135. Osborn, J. A.; Jardine, F. H.; Young, J. F.; Wilkinson, G. The Preparation and Properties of Tris(triphenylphosphine)halogenorhodium(I) and Some Reactions Thereof Including Catalytic Homogeneous Hydrogenation of Olefins and Acetylenes and their Derivatives. *J. Chem. Soc (A)* **1966**, 1711-1732.
136. Crabtree, R. H.; Morris, G. E., Some Diolefin Complexes of Iridium(I) and a *trans*-Influence Series for the Complexes [IrCl(cod)L]. *J. Organomet. Chem.* **1977**, *135*, 395-403.
137. Hoveyda, A. H.; Evans, D. A.; Fu, G. C. Substrate-Directable Chemical Reactions. *Chem. Rev.* **1993**, *93*, 1307-1370.
138. Moppett, C. E.; Sutherland, J. K. The Biosynthesis of Glauconic Acid: C9 Precursors. *Chem. Commun.* **1966**, 772-773.
139. Huff, R. K.; Moppett, C. E.; Sutherland, J. K. A Stereoselective Synthesis of Substituted Maleic Esters by Use of Phosphonates. *J. Chem. Soc. (C)* **1968**, 2725-2726.

140. Boudreau, M. A.; Vederas, J. C. Synthesis and Biological Evaluation of Nucleoside Dicarboxylates as Potential Mimics of Nucleoside Diphosphates. *Org. Biomol. Chem.* **2007**, *5*, 627-635.
141. Stach, H.; Huggenberg, W.; Hesse, M. Synthese von 2-Hydroxy-3-methyl-2-hexen-4-olid. *Helv. Chim. Acta* **1987**, *70*, 369-374.
142. Macritchie, J. A.; Silcock, A.; Willis, C. L. Enantioselective Synthesis of Unsaturated α -Hydroxy Acids. *Tetrahedron: Asymm.* **1997**, *8*, 3895-3902.
143. Czernecki, S.; Georgoulis, C.; Provelenghiou, C., Nouvelle Methode de Benzylolation D'hydroxyles Glucidiques Encombrés. *Tetrahedron Lett.* **1976**, 3535-3536.
144. Massoudi, H. H.; Cantacuzene, D.; Wakselman, C.; Bouthier de le Tour, C. Synthesis of the *cis* and *trans*-Isomers of Homoaconitic and Fluorohomoaconitic Acid. *Synthesis* **1983**, 1010-1012.
145. Kezdi, M.; Kiss, L.; Bojan, O.; Pavel, T.; Bârzu, O. 8-Bromoinosine 5'-Diphosphate, a Suitable Phosphate Acceptor of Nucleosidediphosphate Kinase. *Anal. Biochem.* **1976**, *76*, 361-364.
146. Xu, Y.; Moréra, S.; Janin, J.; Cherfils, J. AlF_3 Mimics the Transition State of Protein Phosphorylation in the Crystal Structure of Nucleoside Diphosphate Kinase and MgADP. *Proc. Natl. Acad. Sci. U. S. A.* **1997**, *94*, 3579-3583.
147. Yan, H.; Tsai, M. D. Nucleoside Monophosphate Kinases: Structure, Mechanism, and Substrate Specificity. *Adv. Enzymol. Relat. Areas Mol. Biol.* **1999**, *73*, 103-133.

148. Fukuchi, T.; Nikawa, J.; Kimura, N.; Watanabe, K. Isolation, Overexpression and Disruption of a *Saccharomyces cerevisiae* YNK Gene Encoding Nucleoside Diphosphate Kinase. *Gene* **1993**, *129*, 141-146.
149. Briozzo, P.; Evrin, C.; Meyer, P.; Assairi, L.; Joly, N.; Bârzu, O.; Gilles, A.-M. Structure of *Escherichia coli* UMP Kinase Differs from That of Other Nucleoside Monophosphate Kinases and Sheds New Light on Enzyme Regulation. *J. Biol. Chem.* **2005**, *280*, 25533-25540.
150. Alekshun, M. N.; Levy, S. B. Molecular Mechanisms of Antibacterial Multidrug Resistance. *Cell* **2007**, *128*, 1037-1050.
151. Cotter, P. D.; Hill, C.; Ross, R. P. Bacteriocins: Developing Innate Immunity for Food. *Nature Rev. Microbiology* **2005**, *3*, 777-788.
152. Nieto Lozano, J. C.; Nissen-Meyer, J.; Sletten, K.; Pelaz, C.; Nes, I. F. Purification and Amino Acid Sequence of a Bacteriocin Produced by *Pediococcus acidilactici*. *J. Gen. Microbiol.* **1992**, *138*, 1985-1990.
153. Henderson, J. T.; Chopko, A. L.; van Wassenaar, P. D. Purification and Primary Structure of Pediocin PA-1 Produced by *Pediococcus acidilactici* PAC-10. *Arch. Biochem. Biophys.* **1992**, *295*, 5-12.
154. Fimland, G.; Johnsen, L.; Dalhus, B.; Nissen-Meyer, J. Pediocin-Like Antimicrobial Peptides (Class IIa Bacteriocins) and Their Immunity Proteins: Biosynthesis, Structure, and Mode of Action. *J. Pept. Sci.* **2005**, *11*, 688-696.
155. Drider, D.; Fimland, G.; Héchard, Y.; McMullen, L. M.; Prévost, H. The Continuing Story of Class IIa Bacteriocins. *Microbiol. Mol. Biol. Rev.* **2006**, *70*, 564-582.

156. Hastings, J. W.; Sailer, M.; Johnson, K.; Roy, K. L.; Vederas, J. C.; Stiles, M. E. Characterization of Leucocin A-UAL 187 and Cloning of the Bacteriocin Gene from *Leuconostoc gelidum*. *J. Bacteriol.* **1991**, *173*, 7491-7500.
157. Marugg, J. D.; Gonzalez, C. F.; Kunka, B. S.; Ledebuer, A. M.; Pucci, M. J.; Toonen, M. Y.; Walker, S. A.; Zoetmulder, L. C. M.; Vandenberg, P. A. Cloning, Expression, and Nucleotide Sequence of Genes Involved in Production of Pediocin PA-1, a Bacteriocin from *Pediococcus acidilactici* Pac 1.0. *Appl. Environ. Microbiol.* **1992**, *58*, 2360-2367.
158. Cintas, L. M.; Casaus, P.; Havarstein, L.; Hernandez, P. E.; Nes, I. F. Biochemical and Genetic Characterization of Enterocin P, a Novel Sec-Dependent Bacteriocin from *Enterococcus faecium* P13 with a Broad Antimicrobial Spectrum. *Appl. Environ. Microbiol.* **1997**, *63*, 4321-4330.
159. Tichaczek, P. S.; Vogel, R. F.; Hammes, W. P. Cloning and Sequencing of *sakP* Encoding Sakacin-P, the Bacteriocin Produced by *Lactobacillus sake* Lth-673. *Microbiology* **1994**, *140*, 361-367.
160. Fleury, Y.; Dayem, M. A.; Montagne, J. J.; Chaboisseau, E.; LeCaer, J. P.; Nicolas, P.; Delfour, A. Covalent Structure, Synthesis, and Structure-Function Studies of Mesentericin Y 10537, a Defensive Peptide from Gram-Positive Bacteria *Leuconostoc mesenteroides*. *J. Biol. Chem.* **1996**, *271*, 14421-14429.
161. Quadri, L. E. N.; Sailer, M.; Roy, K. L.; Vederas, J. C.; Stiles, M. E. Chemical and Genetic Characterization of Bacteriocins Produced by *Carnobacterium piscicola* Lv17b. *J. Biol. Chem.* **1994**, *269*, 12204-12211.

162. Tichaczek, P. S.; Vogel, R. F.; Hammes, W. P. Cloning and Sequencing of *curA* Encoding Curvacin-A, the Bacteriocin Produced by *Lactobacillus curvatus* Lth1174. *Arch. Microbiol.* **1993**, *160*, 279-283.
163. Métivier, A.; Pilet, M. F.; Dousset, X.; Sorokine, O.; Anglade, P.; Zagorec, M.; Piard, J. C.; Marion, D.; Cenatiempo, Y.; Fremaux, C. Divercin V41, a New Bacteriocin with Two Disulphide Bonds Produced by *Carnobacterium divergens* V41: Primary Structure and Genomic Organization. *Microbiology* **1998**, *144*, 2837-2844.
164. Le Marrec, C.; Hyronimus, B.; Bressollier, P.; Verneuil, B.; Urdaci, M. C. Biochemical and Genetic Characterization of Coagulin, a New Antilisterial Bacteriocin in the Pediocin Family of Bacteriocins, Produced by *Bacillus coagulans* I4. *Appl. Environ. Microbiol.* **2000**, *66*, 5213-5220.
165. Fregeau Gallagher, N. L.; Sailer, M.; Niemczura, W. P.; Nakashima, T. T.; Stiles, M. E.; Vederas, J. C. Three-Dimensional Structure of Leucocin A in Trifluoroethanol and Dodecylphosphocholine Micelles: Spatial Location of Residues Critical for Biological Activity in Type IIa Bacteriocins from Lactic Acid Bacteria. *Biochemistry* **1997**, *36*, 15062-15072.
166. Kazazik, M.; Nissen-Meyer, J.; Fimland, G. Mutational Analysis of the Role of Charged Residues in Target-Cell Binding, Potency and Specificity of the Pediocin-Like Bacteriocin Sakacin P. *Microbiology* **2002**, *148*, 2019-2027.
167. Chen, Y.; Ludescher, R. D.; Montville, T. J. Electrostatic Interactions, but Not the YGNGV Consensus Motif, Govern the Binding of Pediocin PA-1 and its Fragments to Phospholipid Vesicles. *Appl. Environ. Microbiol.* **1997**, *63*, 4770-4777.

168. Wang, Y.; Henz, M. E.; Fregeau Gallagher, N. L.; Chai, S.; Gibbs, A. C.; Yan, L. Z.; Stiles, M. E.; Wishart, D. S.; Vederas, J. C. Solution Structure of Carnobacteriocin B2 and Implications for Structure-Activity Relationships Among Type IIa Bacteriocins from Lactic Acid Bacteria. *Biochemistry* **1999**, *38*, 15438-15447.
169. Uteng, M.; Hauge, H. H.; Markwick, P. R. L.; Fimland, G.; Mantzilas, D.; Nissen-Meyer, J.; Muhle-Goll, C. Three-Dimensional Structure in Lipid Micelles of the Pediocin-Like Antimicrobial Peptide Sakacin P and a Sakacin P Variant that is Structurally Stabilized by an Inserted C-Terminal Disulfide Bridge. *Biochemistry* **2003**, *42*, 11417-11426.
170. Kaur, K.; Andrew, L. C.; Wishart, D. S.; Vederas, J. C. Dynamic Relationships Among Type IIa Bacteriocins: Temperature Effects on Antimicrobial Activity and on Structure of the C-Terminal Amphipathic α Helix as a Receptor-Binding Region. *Biochemistry* **2004**, *43*, 9009-9020.
171. Sprules, T.; Kawulka, K. E.; Gibbs, A. C.; Wishart, D. S.; Vederas, J. C. NMR Solution Structure of the Precursor for Carnobacteriocin B2, an Antimicrobial Peptide From *Carnobacterium piscicola*. *Eur. J. Biochem.* **2004**, *271*, 1748-1756.
172. Fimland, G.; Pirneskoski, J.; Kaewsrichan, J.; Arimatti, J.; Kristiansen, P. E.; Kinnunen, P. K. J.; Nissen-Meyer, J. Mutational Analysis and Membrane-Interactions of the β -Sheet-Like N-Terminal Domain of the Pediocin-Like Antimicrobial Peptide Sakacin P. *Biochim. Biophys. Acta* **2006**, *1764*, 1132-1140.

173. Fimland, G.; Eijsink, V. G. H.; Nissen-Meyer, J. Mutational Analysis of the Role of Tryptophan Residues in an Antimicrobial Peptide. *Biochemistry* **2002**, *41*, 9508-9515.
174. Miller, K. W.; Schamber, R.; Osmanagaoglu, O.; Ray, B. Isolation and Characterization of Pediocin AcH Chimeric Protein Mutants with Altered Bactericidal Activity. *Appl. Environ. Microbiol.* **1998**, *64*, 1997-2005.
175. Miller, K. W.; Schamber, R.; Chen, Y.; Ray, B. Production of Active Chimeric Pediocin AcH in *Escherichia coli* in the Absence of Processing and Secretion Genes from the *Pediococcus pap* Operon. *Appl. Environ. Microbiol.* **1998**, *64*, 14-20.
176. Bennik, M. H. J.; Vanloo, B.; Brasseur, R.; Corris, L. G. M.; Smid, E. J. A Novel Bacteriocin with a YGNGV Motif From Vegetable-Associated *Enterococcus mundtii*: Full Characterization and Interaction With Target Organisms. *Biochim. Biophys. Acta* **1998**, *1373*, 47-58.
177. Chikindas, M. L.; García-Garcerá, M. J.; Driessen, A. J. M.; Ledebøer, A. M.; Nissen-Meyer, J.; Nes, I. F.; Abee, T.; Konings, W. N.; Venema, G. Pediocin PA-1, a Bacteriocin From *Pediococcus acidilactici* PAC1.0, Forms Hydrophilic Pores in the Cytoplasmic Membrane of Target Cells. *Appl. Environ. Microbiol.* **1993**, *59*, 3577-3584.
178. Chen, Y.; Shapira, R.; Eisenstein, M.; Montville, T. J. Functional Characterization of Pediocin PA-1 Binding to Liposomes in the Absence of a Protein Receptor and Its Relationship to Predicted Tertiary Structure. *Appl. Environ. Microbiol.* **1997**, *63*, 524-531.

179. Montville, T. J.; Chen, Y. Mechanistic Action of Pediocin and Nisin: Recent Progress and Unresolved Questions. *Appl. Microbiol. Biotechnol.* **1998**, *50*, 511-519.
180. Herranz, C.; Chen, Y.; Chung, H. C.; Cintas, L. M.; Hernández, P. E.; Montville, T. J.; Chikindas, M. L. Enterocin P Selectively Dissipates the Membrane Potential of *Enterococcus faecium* T136. *Appl. Environ. Microbiol.* **2001**, *67*, 1689-1692.
181. Herranz, C.; Cintas, L. M.; Hernández, P. E.; Moll, G. N.; Driessen, A. J. Enterocin P Causes Potassium Ion Efflux From *Enterococcus faecium* T136 Cells. *Antimicrob. Agents Chemother.* **2001**, *45*, 901-904.
182. Fimland, G.; Johnsen, L.; Axelsson, L.; Brurberg, M. B.; Nes, I. F.; Eijsink, V. G. H.; Nissen-Meyer, J. A C-Terminal Disulfide Bridge in Pediocin-Like Bacteriocins Renders Bacteriocin Activity Less Temperature Dependent and Is a Major Determinant of the Antimicrobial Spectrum. *J. Bacteriol.* **2000**, *182*, 2643-2648.
183. Killian, J. A.; von Heijne, G. How Proteins Adapt to a Water-Membrane Interface. *Trends Biochem. Sci.* **2000**, *25*, 429-434.
184. Fimland, G.; Blingsmo, O. R.; Sletten, K.; Jung, G.; Nes, I. F.; Nissen-Meyer, J. New Biologically Active Hybrid Bacteriocins Constructed by Combining Regions from Various Pediocin-Like Bacteriocins: the C-Terminal Region Is Important for Determining Specificity. *Appl. Environ. Microbiol.* **1996**, *62*, 3313-3318.
185. Johnsen, L.; Fimland, G.; Nissen-Meyer, J. The C-Terminal Domain of Pediocin-Like Antimicrobial Peptides (Class IIa Bacteriocins) Is Involved in Specific Recognition of the C-Terminal Part of Cognate Immunity Proteins and in Determining the Antimicrobial Spectrum. *J. Biol. Chem.* **2005**, *280*, 9243-9250.

186. Yan, L. Z.; Gibbs, A. C.; Stiles, M. E.; Wishart, D. S.; Vederas, J. C. Analogues of Bacteriocins: Antimicrobial Specificity and Interactions of Leucocin A with Its Enantiomer, Carnobacteriocin B2, and Truncated Derivatives. *J. Med. Chem.* **2000**, *43*, 4579-4581.
187. Fimland, G.; Jack, R.; Jung, G.; Nes, I. F.; Nissen-Meyer, J. The Bactericidal Activity of Pediocin PA-1 Is Specifically Inhibited by a 15-mer Fragment that Spans the Bacteriocin from the Center Toward the C Terminus. *Appl. Environ. Microbiol.* **1998**, *64*, 5057-5060.
188. Dalet, K.; Cenatiempo, Y.; Cossart, P.; Héchard, Y. A σ^{54} -Dependent PTS Permease of the Mannose Family is Responsible for Sensitivity of *Listeria monocytogenes* to Mesentericin Y105. *Microbiology* **2001**, *147*, 3263-3269.
189. Ramnath, M.; Arous, S.; Gravesen, A.; Hastings, J. W.; Héchard, Y. Expression of *mptC* of *Listeria monocytogenes* Induces Sensitivity to Class IIa Bacteriocins in *Lactococcus lactis*. *Microbiology* **2004**, *150*, 2663-2668.
190. Héchard, Y.; Pelletier, C.; Cenatiempo, Y.; Frère, J. Analysis of σ^{54} -Dependent Genes in *Enterococcus faecalis*: a Mannose Permease (EII(Man)) Is Involved in Sensitivity to a Bacteriocin, Mesentericin Y105. *Microbiology* **2001**, *147*, 1575-1580.
191. Xue, J.; Hunter, I.; Steinmetz, T.; Peters, A.; Ray, B.; Miller, K. W. Novel Activator of Mannose-Specific Phosphotransferase System Permease Expression in *Listeria innocua*, Identified by Screening for Pediocin AcH Resistance. *Appl. Environ. Microbiol.* **2005**, *71*, 1283-1290.

192. Ramnath, M.; Beukes, M.; Tamura, K.; Hastings, J. W. Absence of a Putative Mannose-Specific Phosphotransferase System Enzyme IIAB Component in a Leucocin-A-Resistant Strain of *Listeria monocytogenes*, as Shown by Two-Dimensional Sodium Dodecyl Sulfate-Polyacrylamide Gel Electrophoresis. *Appl. Environ. Microbiol.* **2000**, *66*, 3098-3101.
193. Postma, P. W.; Lengeler, J. W.; Jacobson, G. R. Phosphoenolpyruvate:Carbohydrate Phosphotransferase Systems of Bacteria. *Microbiol. Rev.* **1993**, *57*, 543-594.
194. Diep, D. B.; Skaugen, M.; Salehian, Z.; Holo, H.; Nes, I. F. Common Mechanisms of Target Cell Recognition and Immunity for Class II Bacteriocins. *Proc. Natl. Acad. Sci.* **2007**, *104*, 2384-2389.
195. Morisset, D.; Berjeaud, J. M.; Marion, D.; Lacombe, C.; Frère, J. Mutational Analysis of Mesentericin Y105, an Anti-*Listeria* Bacteriocin, For Determination of Impact on Bactericidal Activity, *in vitro* Secondary Structure, and Membrane Interaction. *Appl. Environ. Microbiol.* **2004**, *70*, 4672-4680.
196. Castano, S.; Desbat, B.; Delfour, A.; Dumas, J. M.; da Silva, A.; Dufourcq, J. Study of Structure and Orientation of Mesentericin Y105, a Bacteriocin From Gram-Positive *Leuconostoc mesenteroides*, and Its Trp-Substituted Analogues in Phospholipid Environments. *Biochim. Biophys. Acta* **2005**, *1668*, 87-98.
197. Tominaga, T.; Hatakeyama, Y. Determination of Essential and Variable Residues in Pediocin PA-1 by NNK Scanning. *Appl. Environ. Microbiol.* **2006**, *72*, 1141-1147.
198. Derksen, D. J.; Stymiest, J. L.; Vederas, J. C. Antimicrobial Leucocin Analogues with a Disulfide Bridge Replaced by a Carbocycle or by Noncovalent Interactions of Allyl Glycine Residues. *J. Am. Chem. Soc.* **2006**, *128*, 14252-14253.

199. Stymiest, J. L.; Mitchell, B. F.; Wong, S.; Vederas, J. C. Synthesis of Biologically Active Dicarba Analogues of the Peptide Hormone Oxytocin Using Ring-Closing Metathesis. *Org. Lett.* **2003**, *5*, 47-49.
200. Stymiest, J. L.; Mitchell, B. F.; Wong, S.; Vederas, J. C. Synthesis of Oxytocin Analogues with Replacement of Sulfur by Carbon Gives Potent Antagonists with Increased Stability. *J. Org. Chem.* **2005**, *70*, 7799-7809.
201. Pattabiraman, V. R.; Stymiest, J. L.; Derksen, D. J.; Martin, N. I.; Vederas, J. C. Multiple On-Resin Olefin Metathesis to Form Ring-Expanded Analogues of the Lantibiotic Peptide, Lacticin 3147 A2. *Org. Lett.* **2007**, *9*, 699-702.
202. Ghalit, N.; Rijkers, D. T. S.; Liskamp, R. M. J. Alkene- and Alkyne-Bridged Mimics of Nisin as Potential Peptide-Based Antibiotics. *J. Mol. Catal. A-Chem* **2006**, *254*, 68-77.
203. Ghalit, N.; Kemmink, J.; Hilbers, H. W.; Versluis, C.; Rijkers, D. T. S.; Liskamp, R. M. J. Step-Wise and Pre-Organization Induced Synthesis of a Crossed Alkene-Bridged Nisin Z DE-Ring Mimic by Ring-Closing Metathesis. *Org. Biomol. Chem.* **2007**, *5*, 924-934.
204. Haack, T.; Mutter, M. Serine Derived Oxazolidines as Secondary Structure Disrupting, Solubilizing Building Blocks in Peptide Synthesis. *Tetrahedron Lett.* **1992**, *33*, 1589-1592.
205. Mutter, M.; Nefzi, A.; Sato, T.; Sun, X.; Wahl, F.; Wohr, T. Pseudo-Prolines (Ψ pro) for Accessing Inaccessible Peptides. *Pept. Res.* **1995**, *8*, 145-153.
206. *Novabiochem Catalog 2006-2007*. Calbiochem-Novabiochem Inc.: San Diego, CA.

207. Hutchinson, E. G.; Thornton, J. M. A Revised Set of Potentials for β -Turn Formation in Proteins. *Protein Sci.* **1994**, *3*, 2207-2216.
208. Perrin, D. D.; Armarego, W. L. F. *Purification of Laboratory Chemicals*. 3 ed.; Pergamon Press: New York, **1993**.
209. Vogel, A., *Vogel's Textbook of Practical Organic Chemistry*. 4 ed.; J. Wiley & Sons Inc.: New York, **1978**.
210. Still, W. C.; Kahn, M.; Mitra, A. Rapid Chromatographic Technique for Preparative Separations with Moderate Resolution. *J. Am. Chem. Soc.* **1978**, *95*, 1328-1333.
211. Baddiley, J.; Jamieson, G. A. Synthesis of *S*-5'-Deoxyadenosine-5'-Homocysteine, a Product from Enzymic Methylations Involving Active Methionine *J. Chem. Soc.* **1955**, 1085-1089.
212. Corey, E. J.; Samuelsson, B. One-Step Conversion of Primary Alcohols in the Carbohydrate Series to the Corresponding Carboxylic *tert*-Butyl Esters. *J. Org. Chem.* **1984**, *49*, 4735-4735.
213. More, J. D.; Finney, N. S. A Simple and Advantageous Protocol for the Oxidation of Alcohols with *o*-iodoxybenzoic acid (IBX). *Org. Lett.* **2002**, *4*, 3001-3003.
214. Matsuda, A.; Ueda, T. Synthesis of 8,6'-Cyclo-6'-Deoxyhexofuranosyladenines: Adenosines Fixed in an Anti-conformation (Nucleosides and Nucleotides. LXVI). *Chem. Pharm. Bull.* **1986**, *34*, 1573-1578.
215. Ti, G. S.; Gaffney, B. L.; Jones, R. A. Transient Protection: Efficient One-Flask Syntheses of Protected Nucleosides. *J. Am. Chem. Soc.* **1982**, *104*, 1316-1319.

216. Wnuk, S. F.; Ro, B.-O.; Valdez, C. A.; Lewandowska, E.; Valdez, N. X.; Sacasa, P. R.; Yin, D.; Zhang, J.; Borchardt, R. T.; De Clercq, E. Sugar-Modified Conjugated Diene Analogues of Adenosine and Uridine: Synthesis, Interaction with *S*-Adenosyl-L-Homocysteine Hydrolase, and Antiviral and Cytostatic Effects. *J. Med. Chem.* **2002**, *45*, 2651-2658.
217. Hollman, J.; Schlimme, E. Darstellung und Konformationszuordnung Einiger 5'-Homologer Adenosinderivate. *Liebigs Ann. Chem.* **1984**, 98-107.
218. Ubukata, M.; Isono, K. Total Synthesis of Nucleoside Antibiotic, Ascamycin. *Tetrahedron Lett.* **1986**, *27*, 3907-3908.
219. Quintard, J.-P.; Pereyre, M. Réactions D-hydrures de Triorganoétain avec des Systèmes Conjugés. III. Cas des Esteres et Nitriles α -Acétyléniques en Présence de Méthanol. *J. Organomet. Chem.* **1972**, *42*, 75-93.
220. Camps, F.; Coll, J.; Moretó, J. M.; Torras, J. Studies for Control of the Ni(CO)₄-Promoted Carbonylative Cycloaddition of Allyl Halides and Acetylenes. *J. Org. Chem.* **1989**, *54*, 1969-1978.
221. Baldwin, J. E.; Beyeler, A.; Cox, R. J.; Keats, C.; Pritchard, G. J.; Adlington, R. M.; Watkin, D. J. Reinvestigation of the Dimerisation Process Forming Isoglaucanic Acid. *Tetrahedron* **1999**, *55*, 7363-7374.
222. Wuts, P. G. An Expedient Procedure for the Purification of the CuBr CH₃SCH₃ Complex. *Synth. Commun.* **1981**, *11*, 139-140.
223. Tronchet, J. M. J.; Valero, M. J. Recherche d'Analogues de Nucléosides à Activité Antivirale. *Helv. Chim. Acta.* **1979**, *62*, 2788-2792.

224. Wnuk, S. F.; Robbins, M. J. Nucleic Acid Related Compounds. 78.
Stereocontrolled Syntheses of 6'(E and Z)-Halovinyl Analogues From Uridine-Derived Vinylsulfones via Vinyltin Intermediates. *Can. J. Chem.* **1993**, *71*, 192-198.
225. Trafelet, H.; Stulz, E.; Leumann, C. Synthesis of (5'S)-5'-C-Alkyl-2'-Deoxynucleosides. *Helv. Chim. Acta* **2001**, *84*, 87-105.
226. Aoki, S.; Mikami, K.; Terada, M.; Nakai, T. Enantio- and Diastereoselective Catalysis of Addition Reaction of Allylic Silanes and Stannanes to Glyoxylates by Binaphthol-derived Titanium Complex. *Tetrahedron* **1993**, *49*, 1783-1792.
227. Hook, J. M. A Simple and Efficient Synthesis of Ethyl and Methyl Glyoxylate. *Synth. Commun.* **1984**, *14*, 83-87.
228. Venneri, P. C.; Warkentin, J. Reaction of Dimethoxycarbene with Strained Cyclic Carbonyl Compounds. *Can. J. Chem.* **2000**, *78*, 1194-1203.
229. Tagg, J. R.; Dajani, A. S.; Wannamaker, L. W. Bacteriocins of Gram-positive Bacteria. *Bacteriol. Rev.* **1976**, *40*, 722-756.
230. Wang, S.-S. *p*-Alkoxybenzyl Alcohol Resin and *p*-Alkoxybenzyloxycarbonylhydrazide Resin for Solid Phase Synthesis of Protected Peptide Fragments. *J. Am. Chem. Soc.* **1973**, *95*, 1328-1333.
231. Barlos, K.; Gatos, D.; Kallitsis, J.; Papaphotiu, G.; Sotiriu, P.; Wenqing, Y.; Schäfer, W. Darstellung Geschützter Peptid-Fragmente Unter Einsatz Substituierter Triphenylmethyl-harze. *Tetrahedron Lett.* **1989**, *30*, 3943-3946.
232. Kaiser, E.; Colecott, R. L.; Bossinger, C. D. Color Test for Detection of Free Terminal Amino Groups in the Solid-Phase Synthesis of Peptides. *Anal. Biochem.* **1970**, *34*, 595-598.

233. Mills, J. S.; White, R.; Gough, L. J. The chemical composition of Baltic amber.
Chemical Geology, **1984**, *47*, 15-39.
234. Zinkel, D. F.; Magee, T. V. Resin acids of *Pinus ponderosa* needles.
Phytochemistry, **1991**, *30*, 845-848.
235. Hasegawa, S.; Hirose, Y. Diterpenes from the seed of *Sciadopitys verticillata*.
Phytochemistry, **1985**, *24*, 2041-2046.